



Norwegian University of Life Sciences  
Faculty of Veterinary Medicine

Philosophiae Doctor (PhD)  
Thesis 2022:26

# **Housing of laboratory mice in a natural habitat – influence on immune system, gut microbiota, and colorectal cancer development**

Oppstalling av laboratoriemus i et naturlig  
habitat – virkning på immunsystem, tarm-  
mikrobiota og utvikling av kolorektal kreft

Henriette Arnesen



# Housing of laboratory mice in a natural habitat – influence on immune system, gut microbiota, and colorectal cancer development

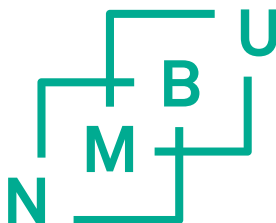
Oppstalling av laboratoriemus i et naturlig habitat -  
virkning på immunsystem, tarmmikrobiota og utvikling av  
kolorektal kreft

Philosophiae Doctor (PhD) Thesis

**Henriette Arnesen**

Norwegian University of Life Sciences  
Faculty of Veterinary Medicine

Ås 2021



Thesis number 2022:26  
ISSN 1894-6402  
ISBN 978-82-575-1874-5

© Henriette Arnesen 2021

Series of dissertations at the  
Norwegian University of Life Sciences (NMBU)

Thesis number 2022:26

ISSN 1894-6402

ISBN 978-82-575-1874-5

All rights reserved.

Illustrations by Henriette Arnesen, unless otherwise stated.

Printed by Andvord Grafisk AS

# Table of Contents

---

Acknowledgements .....	i
Abbreviations .....	iii
List of Papers .....	iv
Summary .....	v
Sammendrag (Summary in Norwegian) .....	vi
1. Introduction .....	1
1.1. The Immune System .....	1
1.1.1 Innate Immunity .....	2
1.1.2 Adaptive Immunity .....	4
1.1.3 Tolerance .....	7
1.2. The Gastrointestinal Tract.....	8
1.2.1 Anatomy and Physiology of the Intestines.....	9
1.2.2 Microbial Colonizers of the Gut .....	11
1.2.3 Gut Mucosal Immunity .....	13
1.2.4 Host and Gut Microbe Crosstalk.....	18
1.2.5 The “Hygiene Hypothesis” and its Relatives.....	22
1.3. Colorectal Cancer .....	23
1.3.1 Colorectal Carcinogenesis.....	24
1.3.2 Cancer Immunology.....	26
1.3.3 Colorectal Cancer and The Gut Microbiota .....	28
1.4. Mice as Model Organisms .....	30
1.4.1 Mouse Models of Colorectal Cancer .....	32
1.4.2 Mice Versus Humans .....	33
1.4.3 Modelling Free-living Mice .....	35
1.5. Knowledge Gaps .....	38
2. Aims of the Study .....	39
3. Summaries of Papers.....	40
4. Discussion .....	45

4.1.	Methodological Considerations .....	45
4.1.1	Ethical Reflections.....	45
4.1.2	Mouse Pen Setups and Maintenance .....	45
4.1.3	Microbial Community Analyses.....	47
4.1.4	Immunophenotyping .....	51
4.1.5	Induction and Detection of CRC .....	53
4.1.6	Analysis of SCFAs in Feces.....	56
4.1.7	RNA sequencing.....	57
4.2.	General Discussion.....	58
5.	Main Conclusions.....	67
6.	Future Perspectives.....	68
7.	References .....	69
8.	Enclosed Papers I-IV.....	89

# Acknowledgements

---

This study was conducted at the Department of Preclinical Sciences and Pathology and Department of Chemistry, Biotechnology and Food Science at the Norwegian University of Life Sciences (NMBU) during the period of 2018-2021.

First of all, I would like to thank my supervisors for motivating, guiding and inspiring me during these years. Preben Boysen, thank you for your optimism, for teaching me that there is always a way, for always having your door open to my questions and concerns, and for introducing me to so many interesting people along the way. Harald Carlsen, thank you for every advice and for always finding time for interesting discussions. Jan Erik Paulsen, thank you for your encouragements and for readily sharing your knowledge. I really appreciate the opportunity to work with you and participate in development of the feralized mice model, and I look forward to following the continuation.

I have been privileged to have met and collaborated with so many brilliant people along the way. From all of you, I have learnt so much more than what comes to terms in this thesis. A great thanks to past and previous members of the nutrition and biomedicine group at KBM and immunology group at VET for creating such a great work environment, both socially and academically. A special thanks to Lars Fredrik Moen, Sergio Rocha, Anne Mari Herfindal and Dimitrios Papoutsis for always helping out and lightening up long and tiresome days. Anne Mari, I have really appreciated our innumerable coffee breaks and discussions about the smallest and largest of things! A great thanks to Grethe M. Johansen for all the invaluable help in the lab and good talks these past few years. Mette H. B. Müller, thank you for your contagious enthusiasm and for supporting me in the most chaotic times. Siv K. Bøhn, thank you for making the nutrition and biomedicine research group such a positive place to be for everyone. I would also like to thank all co-authors of the papers encompassed by this thesis for their expert contributions and sharing of knowledge. This thesis would not have been possible without the efforts of all of you. A huge thanks to Tom Hitch and colleagues in the Functional Microbiome research group at RWTH Aachen, for introducing me to a world of microbiota analyses and taking good care of me while facing Germany. I am also grateful to the staff and animals at Ramme gaard and the Livestock Production Research Centre for supplying us with material for the mouse pens, which was crucial to make my experiment work.

A massive thanks to my amazing family and friends who have supported me through my every struggle and success. Where I am today, and my every accomplishment, is owed to you. Mom, our endless conversations about everything and nothing always keeps me going, and I cannot imagine what I would do without you and your advice. Dad and Kristin, thank you for always being there – I am so grateful that you support me no matter what. Cheers to Camilla, Magnus and their respective crews in Drammen and Horten, and to Ines, Haris and the family in Mysen. To my good friends for keeping me down to earth. Ida and Milla, thanks for all the fun these past years. And last, but not least, I am incredibly grateful for the love and patience of my remarkable partner and best friend Raisa. Thank you for reminding me which day it is, for feeding me every time I forget, for standing by me, and for always being my biggest fan. I love you!

Oslo, Nov. 2021

Liv Henriette Arnesen



# Abbreviations

---

## A

ACF	Aberrant crypt foci
AOM	Azoxymethane
<i>APC/Apc</i>	Adenomatous polyposis coli gene (human/mouse)
APC	Antigen presenting cell

## B

B6	C57BL/6 (black6) mouse strain
----	-------------------------------

## C

CD	Cluster of differentiation
CRC	Colorectal cancer
CTL	Cytotoxic T cell (CD8 <sup>+</sup> T cells)

## D

DC	Dendritic cell
DSS	Dextran sodium sulfate

## F

FMT	Fecal microbiota transfer
FcR	Fc receptor

## G

GALT	Gut-associated lymphoid tissue
GF	Germ-free
GI	Gastrointestinal

## I

IBD	Inflammatory bowel disease
IEC	Intestinal epithelial cell
IFN	Interferon
IL	Interleukin
ILP	Isolated lymphoid follicle
Ig	Immunoglobulin
i.p.	Intraperitoneal

## K

KLRG1	Killer cell lectin-like receptor G1
-------	-------------------------------------

## M

MDSC	Myeloid-derived suppressor cell
MHC	Major histocompatibility complex
Min/+	Multiple intestinal neoplasia
mLN	Mesenteric lymph node

## N

NK	Natural killer
----	----------------

## O

OTU	Operational taxonomic unit
-----	----------------------------

## P

PP	Peyer's patch
PRR	Pattern recognition receptor

## S

s.c.	Subcutaneous
SCFA	Short-chain fatty acid
SFB	Segmented filamentous bacteria
SI	Small intestine
sIgA	Secretory immunoglobulin A
SPF	Specific pathogen free
SPL	Spleen

## T

Th	T helper cell (CD4 <sup>+</sup> T cells)
T <sub>CM</sub>	Central memory T cell
TCR	T cell receptor
T <sub>EM</sub>	Effector memory T cell
TGF	Transforming growth factor
TLR	Toll-like receptor
TNF	Tumor necrosis factor
Treg	Regulatory T cell
T <sub>RM</sub>	Tissue-resident memory T cell

# List of Papers

---

## PAPER I

*A Model System for Feralizing Laboratory Mice in Large Farmyard-Like Pens*

Henriette Arnesen, Linn Emilie Knutsen, Bente Wabakken Hognestad, Grethe Marie Johansen, Mats Bemark, Oliver Pabst, Anne Kristine Storset and Preben Boysen

Front Microbiol 2021;11(3413).

<https://doi.org/10.3389/fmicb.2020.615661>

## PAPER II

*Induction of colorectal carcinogenesis in the C57BL/6J and A/J mouse strains with a reduced DSS dose in the AOM/DSS model*

Henriette Arnesen, Mette Helen Bjørge Müller, Mona Aleksandersen, Gunn Charlotte Østby, Harald Carlsen, Jan Erik Paulsen and Preben Boysen

Lab Anim Res 2021;37(1):19.

<https://doi.org/10.1186/s42826-021-00096-y>

## PAPER III

*Naturalizing laboratory mice by housing in a farmyard-type habitat confers protection against colorectal carcinogenesis*

Henriette Arnesen, Thomas C. A. Hitch, Christina Steppeler, Mette Helen Bjørge Müller, Linn Emilie Knutsen, Gjermund Gunnes, Inga Leena Angell, Ida Ormaasen, Knut Rudi, Jan Erik Paulsen, Thomas Clavel, Harald Carlsen and Preben Boysen

Gut Microbes 2021;13(1):1993581.

<https://doi.org/10.1080/19490976.2021.1993581>

## PAPER IV

*Profiling of colonic mucosa transcriptome and mucus layer in mice feralized in a farmyard-like habitat*

Henriette Arnesen, Turhan Markussen, George Birchenough, Gunnar C. Hansson, Harald Carlsen and Preben Boysen

*Manuscript.*

## Summary

---

The natural habitat for the house mouse is on the ground, typically close to humans and their livestock and hence surrounded by a rich microbial diversity that throughout evolutionary history has driven the adaptation of the house mouse. It is thus paradoxical that almost without exception, experimental disease studies using this mammalian model take place in perfect isolation from the outer microbial world. The end goal for preclinical research, humans, rarely live in microbial isolation, although lifestyles can arguably be said to vary on a scale. To develop a preclinical model that better resemble realistic lifestyles of mammals, we have established a system where laboratory mice are raised under a full set of environmental conditions present in a typical farmyard habitat for the house mouse. We call the process feralization, and the first paper covered by this thesis show the resulting mammal display more functionally mature states of immune cells and a diverse gut microbiota, likely surpassing conventional laboratory mice in resembling responses of free-living mice.

Furthermore, we demonstrated the use of this animal modelling approach that recapitulates realistic disease responses in a naturalized mammal. We first established a protocol of the AOM/DSS model for colorectal cancer (CRC) induction in mice using a lower-than-usual dose of DSS that is presented in paper II. In paper III, we employed the AOM/DSS model, as well as a previously established genetic Min/+ model of CRC, in a feralization system. We showed that the mice feralized in a farmyard-type habitat were protected against colorectal carcinogenesis compared to conventionally reared laboratory mice. Moreover, our feralization model allows for full control of the timing of microbial exposure. We took advantage of this by including groups of mice that were either born in the farmyard habitat or introduced to it in later life, demonstrating that neonatal microbial exposure was not essential for the CRC protection. The findings were supported by changes in gut microbiota profiles, as well as immunophenotypes indicative of antigenic experience in the feralized mice.

In currently unpublished work, we aimed to narrow in on mechanisms for the protective effects conveyed by feralization in the intestines. Assays investigating mucus layer properties showed no differences following feralization, yet a few genes in the colon mucosa related to barrier function were found to be significantly upregulated between feralized and conventional laboratory mice. Further assessments are needed to elaborate on the mechanisms underlying the beneficial effects of feralization.

## Sammendrag (Summary in Norwegian)

---

Det naturlige habitatet for husmus er typisk nær mennesker og deres husdyr, og husmusa er gjennom evolusjon tilpasset et slikt rikt mikrobielt levemiljø. Det er derfor paradoksalt at eksperimentelle studier der mus brukes for å studere sykdomsmekanismer, omtrent uten unntak foregår i perfekt isolasjon fra den ytre, mikrobielle verden. Målet for prekliniske studier ved bruk av forsøksmus er typisk å overføre funnene til relevans for mennesker, men mennesker lever sjeldent i mikrobiell isolasjon, selv om individuelle livsstiler varierer stort. For å utvikle en preklinisk musemodell som mer realistisk representerer naturlige livstiler hos pattedyr, har vi etablert et system der laboratoriemus fostres opp i en mer naturlig situasjon, der habitatet deres er beriket med elementer som er til stede i et typisk gårdsmiljø. Vi har kalt denne prosessen «feralisering», og den første artikkelen som omfattes av denne avhandlingen demonstrerer at de «feraliserte» musene viser tegn til mer funksjonelt modne immunceller og en rikere tarmmikrobiota sammenliknet med laboratoriemus oppstallet under tradisjonelle, rene forhold.

Videre har vi demonstrert bruken av feraliserings-systemet som kan benyttes til å studere realistiske sykdomsresponser i et naturalisert pattedyr. Først etablerte vi en protokoll for kjemisk induksjon av kolorektalkreft hos mus, ved å bruke en lavere-enn-normal dose av DSS i en AOM/DSS modell. Dette arbeidet er presentert i artikkel II. I artikkel III benyttet vi AOM/DSS modellen, så vel som en tidligere etablert genetisk Min/+ musemodell for kolorektalkreft, i feraliserings-systemet. Vi demonstrerte at musene som ble feralisert i et naturalistisk gårdsmiljø var beskyttet mot tykktarmskreft, sammenliknet med laboratoriemus oppstallet under tradisjonelle, rene forhold. Videre tillater feraliserings-systemet full kontroll av timingen for mikrobiell eksponering. Vi utnyttet dette ved å inkludere en gruppe av mus som enten var født i gårdsmiljøet, eller introdusert dit senere i livet. Med dette viste vi at neonatal mikrobiell eksponering ikke var essensiell for beskyttelse mot kolorektal kreft. Funnene ble støttet av endringer i tarmmikrobiotaprofiler, samt immunofenotyper som kan indikere at de har blitt eksponert for antigener.

I nåværende upublisert arbeid hadde vi som mål å undersøke mulige mekanismer for hvordan feralisering i et gårdsmiljø kunne gi beskyttelse mot kolorektal kreft. Undersøkelser av slimlaget i tarm viste ingen forskjeller etter feralisering. Likevel var det none få gener i tykktarmsslimhinnen relatert til barrierefunksjon som var oppregulert i feraliserte mus sammenliknet med konvensjonelt oppstallede laboratoriemus. Videre undersøkelser er nødvendig for å kunne utdype mer når det gjelder mekanismene bak feraliserings beskyttende effekt.

# 1. Introduction

## 1.1. The Immune System

The immune system in mammals is organized in two branches, namely innate and adaptive immunity, encompassing a network of organs, cells and molecules that cooperate to protect the body against potentially dangerous agents. All immune cells are generated from multipotent stem cells in the bone marrow. The granulocytes, mast cells, erythrocytes and platelets are derived from myeloid progenitor cells, while lymphocytes derive from lymphoid progenitors. The myeloid cells develop and mature while circulating in blood and lymph or residing in tissues. The development of lymphocytes occurs in the primary lymphoid organs, while activation finds place in secondary lymphoid organs. B cells develop in the bone marrow and exits into lymph as immature B cells that mature in the spleen, while T cells develop and mature in the thymus (**Figure 1A**) (1).

The innate immune system is the first line of defense and include relatively unpecific responses that occur before more specific, adaptive responses have time to develop. The innate immune mechanisms aid in elimination of damaged cells and tissue repair, as well as guiding the adaptive immune responses. The adaptive immunity is specific in the regard that specific pathogens are recognized and targeted. Moreover, adaptive immunity harbor memory potential, meaning the components of the adaptive immune system can recall previously encountered threats to better fight them the next time around (**Figure 1B**).

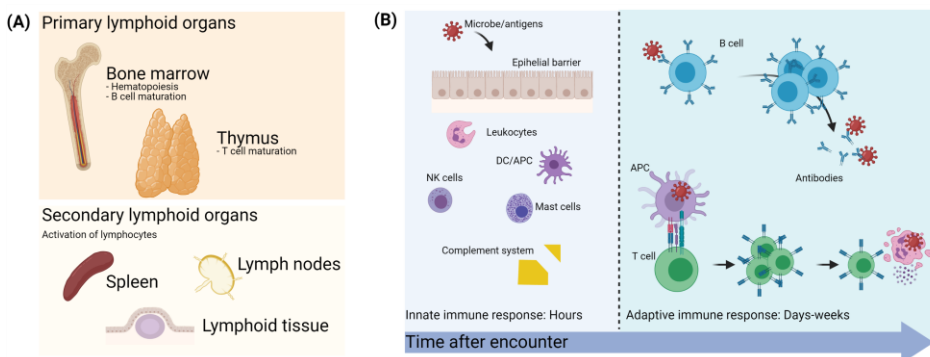


**Figure 1:** Overview of the mammalian immune system. **(A)** Lymphoid organs. **(B)** Innate and adaptive immune responses to threats. Adapted from (1). Created with biorender.com.

Lymph nodes are secondary lymphoid organs organized to ensure interaction of immune cells and antigens transported in lymph necessary for proper immune functions. The spleen is the largest secondary lymphoid organ, and it is directly connected to the circulation. Because it lacks afferent lymphatic, substances can only enter via the blood. The spleen is responsible for systemic filtering of damaged erythrocytes and function as a secondary lymphoid organ for the circulatory system, in which naïve and memory lymphocytes can be activated in response to antigen (2). Since lymphatic vessels eventually empty lymph into the blood, the spleen serves as a chief organ governing systemic immunity, and it is thus of great interest in immunological studies. The spleen holds various populations of immune cells that have been mobilized from the spleen to other tissues or vice versa (3).

### 1.1.1 Innate Immunity

The innate immune system consists of physical and chemical barriers that creates an immediate host protection against environmental insults. These include skin, mucosal membranes, low pH, antimicrobial peptides, and secreted immunoglobulins. Moreover, the innate immune system comprises the complement system and various cells that can sense the presence of pathogens and elicit targeted responses to eradicate the danger. Prominent among these cells are macrophages, neutrophil granulocytes, and dendritic cells (DCs), that have in common the expression of pattern recognition receptors (PRRs) that recognize pathogen-associated molecular patterns (PAMPs) or damage-associated molecular patterns (DAMPs). PAMPs can be components of bacterial cell walls, foreign DNA or RNA, while DAMPs are components of the host's cells that are released during cell damage or cell death. Dependent on type of PRR, recognition of PAMPs/DAMPs will lead to phagocytosis and/or activation of pro-inflammatory mechanisms via induced expression of cytokines, i.e. signaling molecules, as well as endothelial adhesion molecules that together enhance phagocytic activity and recruit additional immune cells to the site (1, 4). The primary role of DCs is to provide a link between the innate and adaptive immune system by presenting foreign antigens to adaptive immune cells (naïve helper T cells, see section 1.1.2).

In addition to being involved in the body's first line of defense, the innate immune cells serve as a bridge to activation of the adaptive immune system. NK cells are cytotoxic cells whose major function is killing of infected cells via

release of perforins and granzymes. As a part of the innate immune response against e.g. a virus, NK cells release an important cytokine, interferon (IFN)- $\gamma$ , that promote phagocytosis of the infected cell by macrophages, and potentiate adaptive T cell responses (1). The ability of NK cells to potentiate adaptive immune cell responses highlight that they function at the interface between innate and adaptive immunity. NK cells recognize cells that lack normal expression of self-proteins (MHC class I proteins; described in section 1.1.2) and can thus distinguish infected or abnormal cells from healthy cells. The activation and function of the NK cell depend on the synergistic signals from a repertoire of activating and inhibitory Ig-like and C-type lectin receptors expressed by the cell (5). Killer cell lectin-like receptor G1 (KLRG1) is an inhibitory receptor expressed by terminally mature NK cells, thought to serve as a mechanism to inhibit further NK cell expansion and effector functions (6). During maturation, NK cells upregulate CD11b, which is important in adhesion and migration of the cells to inflammatory sites, and downregulate CD27, which is a co-stimulatory receptor that regulates survival and enhance activation (7-9).

Macrophages are phagocytes that are seeded during embryonic development or derived from circulating blood monocytes. A simple classification of macrophages is based on whether they are activated in a classical or alternative manner. Classical macrophage activation occurs via contact-mediated signals and IFN- $\gamma$  produced by Th1 cells (described in section 1.1.2), and/or via stimulation of Toll-like receptors (TLRs; a type of PRR). Classical activated macrophages, commonly termed M1 macrophages, have a pro-inflammatory phenotype. Their main actions include production of reactive oxygen species (ROS) and lysosomal enzymes that enhance killing, and secretion of inflammatory cytokines such as tumor necrosis factor (TNF)- $\alpha$  and interleukins (IL)-1 and -12 that provide a positive feedback loop with differentiation of additional Th1 cells. Alternative macrophage activation is mediated by IL-4 and IL-13 produced by Th2 cells (described in section 1.1.2). The alternatively activated macrophages, commonly named M2 macrophages, are involved in tissue repair and production of anti-inflammatory cytokines, such as IL-10 (1, 10). Later studies have shown that macrophages have much more diverse and overlapping phenotypes (10).

It was long thought that immunological memory was an exclusive feature for adaptive immunity. However, recent year's investigations in numerous organisms have shown that prior microbial exposure can also train innate

immune cells, e.g. NK cells, to exhibit memory and mediate resistance to secondary challenges (11, 12). Such long-term adaptation and modification of innate immune cells have been termed “trained immunity”. The mechanisms behind this concept is yet to be discovered, but it involves epigenetic and metabolic alterations leading to functional reprogramming of the innate immune cells (13). Epigenetics is defined as heritable alterations in gene expression that do not involve permanent change in DNA.

### 1.1.2 Adaptive Immunity

Adaptive immunity can be distinguished into a cellular and a humoral arm. The cellular immunity is mediated by phagocytes, T cells, and the release of signal molecules, namely cytokines and chemokines, in response to antigen encounter. Naïve T cells recirculate through blood, lymphatic vessels and secondary lymphoid organs in search of activating antigen. Naïve T cells depend on interaction with antigen-presenting cells (APCs) to develop into an activated, functionally mature state. The APCs can be DCs, macrophages or B cells. Three sequential signals are required for activation, differentiation, and proliferation of a T cell. First, the TCR complex with CD4 or CD8 co-receptor expressed must recognize an antigen displayed on the major histocompatibility complex (MHC) molecules on cell surfaces. Two types of MHC molecules exist: MHC class I and II. The MHCs has similar function, namely to present antigens to immune cells, but they obtain antigens from different sources and present them to different types of T cells. MHC class I are expressed on all nucleated cells and present cytosolic antigens to CD8<sup>+</sup> T cells, while MHC class II are only expressed on so-called professional APCs and present extracellular antigens to CD4<sup>+</sup> T cells. The second activation signal is mediated by co-stimulatory molecules on APCs and co-receptors on the T cell that supports survival and differentiation of the T cell. The third signal involves cytokines present in the local milieu that represent the local situation. The balance of cytokines guides the T cell activation and contributes to determining the functional direction of the T cell according to what type of responses are needed (1).

The CD4<sup>+</sup> population of T cells are also called T helper (Th) cells, revealing their function related to “helping out” other cells. The most characterized subsets of Th cells are Th1, Th2 and Th17, each with a distinct profile of cytokine-secretion and functional properties. Th1 and Th2 cells are mutually



exclusive, meaning that the differentiation of one reinforces continued differentiation of one while also inhibiting the differentiation of the other. Th1 enhances cell-mediated responses, typically against intracellular bacteria and protozoa. Th1 differentiation is triggered by IL-12 and IFN- $\gamma$ , and the effector cytokines IL-12 and IFN- $\gamma$  can activate macrophages and CD8<sup>+</sup> T cells. Th2 cells stimulate IgE-, mast cell- and eosinophil-mediated reactions that serve to eliminate helminth infections. Th2 differentiation is induced by IL-4, which is also an Th2 effector cytokine. IL-13 is another Th2 effector cytokine. IL-4 and IL-13 can e.g. increase mucus production in mucosal tissues and enhance release of cytotoxic granules from eosinophils. Th17 differentiation is induced by IL-6 and transforming growth factor (TGF)- $\beta$ , while IL-23 is important for survival (1). Th17 cells enhance neutrophil recruitment and activation. Moreover, they are important in defense against extracellular bacteria and fungi (1, 14), and the characteristic cytokines produced by Th17 cells include IL-17, IL-22 and IL-26 (14). Th17 cells have great plasticity capabilities, and can become dual IL-17 and IFN- $\gamma$  producers, or they can convert into Th1-like cells producing IFN- $\gamma$ , dependent on the cytokine milieu (15).

The CD8<sup>+</sup> T cells are also called cytotoxic T lymphocytes (CTLs), disclosing their primary function, which is to kill target cells. For strong and efficient activation of CTLs, cytokine production and potentiation of APCs by Th cells are necessary (16). CTLs can kill target cells via two mechanisms. The main mechanism is killing mediated by perforin and granzyme release. The second mechanism is killing via Fas receptor-Fas ligand interaction. Fas receptor is a “death receptor” that upon activation by Fas ligand expressed on CTLs induce a cascade resulting in activation of caspases and apoptosis of the cell expressing the Fas receptor. CTLs also produce IFN- $\gamma$  that further enhance phagocytic clearance of pathogens (1).

In recent years it has become clear that populations of T cells can have functional “memory” properties. The memory T cells can respond to persistent presences of pathogens and viruses and offer protective immunity against reinfection. Th and CTL cells can be divided into effector and memory subsets dependent on expression patterns of surface molecules. Expression of CD62L and/or CCR7 has been reported to hallmark a central memory phenotype ( $T_{CM}$ ) while a lack of expression of these homing molecules designates a “effector memory” phenotype ( $T_{EM}$ ) in blood and spleen (17). The original model was that  $T_{EM}$  were an intermediate cell type transitioning from

effector cell to memory cell,  $T_{CM}$  (17). However, the picture is complex, with T cell memory being highly heterogeneous, and memory populations covering a wide range of functions, including effector functions and durability (18). The majority of CTLs in non-lymphoid tissue are non-recirculating tissue resident memory cells ( $T_{RM}$ ) (19), and that these cells do not circulate have large implications for how they participate in immune responses. Along with the efficient network of recirculation of lymphocytes, the embedding of memory T cells to tissues where they can be maintained allows for longer-term surveillance over specific exposed regions where the cells will be available immediately in case of a local defense breach (18, 19). The precise functions of  $T_{RMS}$  are still not fully elucidated, but appear to include patrolling non-lymphoid tissues for antigen, rapid initiation of immune response by communication with other immune cells as well as direct killing, which may play important roles in tumor control (19). In a recent study, Wijeyesinghe *et al.* (20) demonstrated that a portion of  $T_{RMS}$  slowly join the blood circulation and give rise to blood-borne  $T_{EMS}$ .

The humoral arm of adaptive immunity involves responses mediated by antibodies. The other key lymphocyte, namely the B cell, is responsible for antibody production. Naïve B cells recirculate between blood and secondary lymphoid tissues throughout the body. The recirculation of naïve B cells enhances their likelihood of meeting and responding to microbial antigens at different sites. A naïve B cell is characterized by expression of the immunoglobulin isotypes M and D (IgM and IgD) on its surface. B cells are activated in secondary lymphoid organs by recognition of antigen, and full B cell activation requires additional stimuli, that may be T cell-dependent or -independent. In T cell-dependent activation, the B cell receives co-stimulatory signals from Th cells. In T cell-independent activation of B cells involves other stimuli for B cell activation, such as cytokine signaling, that the antigen has been opsonized, or by binding complement factors (1).

The activated B cell will proliferate and differentiate into plasmablasts, memory B cells, and plasma cells that produce and secrete antibodies. Plasmablasts are short-lived antibody-secreting cells produced early in an infection. Plasma cells are long-lived antibody-secreting cells, and their antibodies have higher affinity towards the target antigen than those produced by plasmablasts. Dependent on stimuli upon activation, the B cell undergo class switching, which is a mechanism of changing the type of antibody produced. The antibody isotypes produced can be IgG, IgA, IgE or IgM. Only one type of antibody is produced per plasmablast or plasma cell.

The antibodies can neutralize the threat by blocking its entrance into tissues, block binding of microbe or toxins to cells and cellular receptors. Moreover, antibodies can potentiate innate immune mechanisms to eliminate the threat through opsonization. When a threat, e.g. a microbe, is coated with bound antibodies, it is opsonized. The opsonized microbe can then bind to Fc receptors (FcR) expressed on the surface of various immune cells, such as phagocytes, B cells and NK cells. Upon binding, the FcR signals activate the cell which then exert its actions in eliminating the threat (1).

### 1.1.3 Tolerance

To avoid immune responses directed against self-antigens on own cells, as well as harmless antigens such as food antigens and commensal gut microbiota, tolerance mechanisms are crucial. Central tolerance occurs in the primary lymphoid organs and ensures that immune cells can discriminate self from non-self, while peripheral tolerance occurs in the secondary lymphoid organs and prevents over-reactivity of the immune cells against various environmental entities. From an evolutionary perspective, tolerance mechanisms are thought to allow organisms to adapt to antigenic stimuli that will consistently be present, instead of expending considerable resources fighting it off repeatedly (1).

The establishment of peripheral tolerance is characterized by an expansion of immunosuppressive cells known as regulatory T cells (Tregs) that constrain inflammatory responses. In terms of discovery the Treg is a relatively young cell type. That some immune cells had suppressive features was suggested in the 1970s, but it was not until the identification of the transcription factor Foxp3 as a unique identifier of Tregs in 2003 (21-23) that the Tregs were truly acknowledged. While the exact mechanisms for Foxp3 is not yet established, this transcription factor orchestrate gene expression required for Treg differentiation and function via various mechanisms (24). The Tregs limit excessive immune responses and ensures tolerance to self, food and commensal microbial antigens via several mechanisms, including direct suppression of pro-inflammatory cells via secretion of anti-inflammatory IL-10 and TGF- $\beta$  cytokines, and indirect blocking activation of other T cells via suppression of APC activity (25).

Tregs develop from naïve CD4<sup>+</sup> cells in thymus or in peripheral tissue, giving rise to tTregs and pTregs, respectively. Both subsets require TGF- $\beta$ , retinoic acid and IL-2 signaling for their development (26, 27). The distinct roles of tTregs and pTregs are still debated, but it is becoming widely accepted that the site of origin reflects the functions of these cells, such as that tTregs recognize self-peptides while pTregs recognize foreign peptides derived from exogenous sources (26-28). Specific molecular markers of human tTregs and pTregs has not yet been discovered. However, high expression of the nuclear protein Helios and the cell surface protein neuropilin 1 (NRP1) in mice Tregs has been associated with a thymic origin, while lack of expression of these proteins has been associated with pTregs (29-31). A less studied immunosuppressive B cell type called regulatory B cells has been identified in humans and mice and have also been shown to inhibit Th1 and Th17 effector responses and promote generation of Tregs (32).

A newly identified population of immature myeloid cells called myeloid-derived suppressor cells (MDSCs), are characterized by their ability to suppress immune responses. However, the MDSCs have been shown to arise as a consequence of pathological myeloid cell activation and expand during inflammatory disease, infections and cancers (33). In mice, two MDSC phenotypes have been identified, distinguished in monocytic or granulocytic MDSCs that resemble monocytes and neutrophils, respectively. As opposed to classical activation of myeloid cells via PRR activation and mobilization of neutrophils and monocytes from the bone marrow, a persistent presence of growth factors and inflammatory signals leads to pathological activation driving MDSC development (33).

## 1.2. The Gastrointestinal Tract

The mammalian gastrointestinal (GI) system consists of a hollow tract spanning from the mouth to the anus along with accessory glands and organs including the liver, pancreas, and gall bladder. The GI tract is divided into compartments separated by sphincters, namely the buccal cavity, esophagus, stomach, small intestine (SI) and large intestine. The primary functions of the GI system are digestion and absorption of nutrients and electrolytes, maintenance of water homeostasis, as well as trafficking of macromolecular antigens and exclusion of pathogens. The anatomy of the GI wall is highly organized to support these functions (34, 35).

### 1.2.1 Anatomy and Physiology of the Intestines

The SI encompasses three segments, namely the duodenum, jejunum and ileum (36). The duodenum is the first SI segment, largely responsible for continuing digestion of chyme expelled by the stomach. The duodenum receives digestive enzymes from the pancreas and bile from the gallbladder, aiding in the digestion process. Nutrient absorption occurs in the jejunum primarily. The final SI segment, the ileum, is responsible for absorption of vitamin B12 and the reabsorption of conjugated bile salts for recycling via the enterohepatic circulation (37-40). The large intestine includes the caecum, appendix, colon, rectum and anus. In humans, the colon can be divided into four segments: descending colon, ascending colon, transverse colon, and sigmoid colon (36). The colon's functions include reabsorption of fluids, and processing and elimination of waste products from the body (41, 42).

Albeit the anatomy of the GI wall varies along its length, a layered structure of mucosa, submucosa, *muscularis propria*, and an outer layer of fibrous connective tissue is common to all segments (**Figure 2**). The mucosa consists of a luminal monolayer of columnar intestinal epithelial cells (IECs), a loose connective tissue known as the lamina propria, and a thin layer of smooth muscle layer called the *muscularis mucosae*. The mucosa contains capillaries, enteric neurons, lymphatic tissue, immune cells, and muscle cells (34). The main functions of the mucosa are to transport and absorb nutrients, keep tissues moist and protect the body from foreign particles and pathogens (43). The submucosa supports the mucosa and joins into the *muscularis propria*, which is responsible for peristaltic gut movement that moves luminal content along the GI tract and ultimately to excretion from the body via feces. Dependent on the necessity for movement or fixation of the area, the outermost layer of the GI tract is an epithelial membrane (serosa) or a loose connective tissue (adventitia) (34).

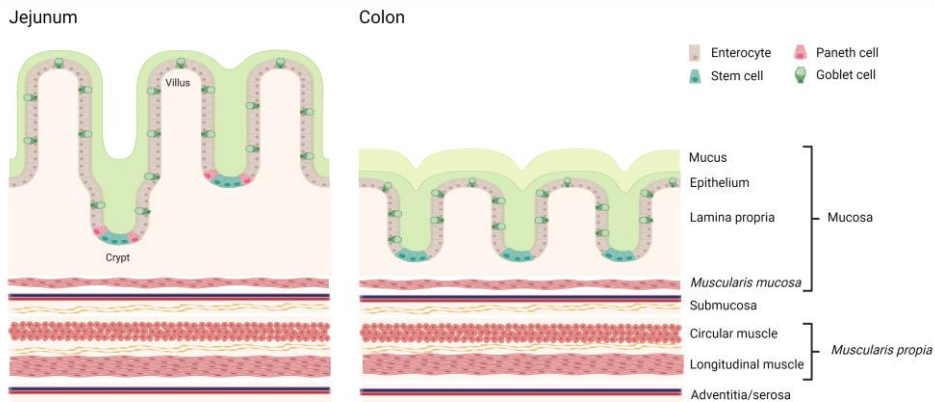


**Figure 2:** Organization of the intestinal wall. Inspired by (34). Created with biorender.com.

The mucosal monolayer of intestinal epithelium allows for secretion and absorption along the GI tract. The main absorption of nutrients, water, electrolytes occur in the intestines, and thus, the intestinal surface area is amplified by several mechanisms. In both SI and colon, crypts are formed by invaginations of mucosa. In SI, where nutrient absorption occurs, IECs also form villi, which is finger-like structures extend into lumen (**Figure 2**) (34). The major cell type of the intestinal epithelium are absorptive epithelial cells known as enterocytes. The IECs also include stem cells, Paneth cells, Goblet cells and enteroendocrine cells all with specialized functions. Stem cells and Paneth cells reside in the base of the crypts, while Goblet cells are scattered along the intestinal epithelium. Stem cells are undifferentiated cells that continuously self-renew by dividing and differentiate into specialized cells as they migrate upwards from the crypts (44). Goblet cells and Paneth cells are described in more detail in section 1.2.3.

The intercellular space between IECs is occupied with cell-cell junctions, which are protein structures anchoring the IECs together. Four main types of cell-cell junctions have been characterized, namely tight junctions, adhering junctions, gap junctions and desmosomes. These protein complexes provide means for selective paracellular permeability of nutritional solutes and water while bacteria and food antigens are restricted. Thus, the cell-cell junctions make up essential components of the intestinal barrier (45).

### 1.2.2 Microbial Colonizers of the Gut

Mammals hosts a complex and diverse ecosystem of microorganisms that reside on or within tissues and bodily fluids, collectively known as the *microbiota*. To capture the concept of the sum of microbes and their genomes, as well as the environmental interaction with the host organism, the term *microbiome* is often used. The microbiota includes bacteria, fungi, protozoa and viruses, and covers almost every surface of the human body: the skin, oral cavity, airways, and particularly the GI tract. Over its evolutionary history, the mammalian host has co-evolved with the microbiota to form a symbiotic relationship fundamental for host fitness. The microbiota has major impact on host metabolism and development of organ systems, including the immune system (46-48). The term holobiont refers to a host and its associated communities of microorganisms i.e. its microbiota (49). Mammals arose some 3 billion years after bacterial life appeared and 1 billion years after the first eukaryotic cells originated. Thus, it is likely that a relationship with microbiota existed already when the mammals first appeared, and that the host-microbe interactions has continued to shape the evolution of both parties (50).

The bacterial portion of the microbiota is the most extensively studied, likely due to the available techniques developed for relative quantification of bacteria. Phylogeny is the study of the evolutionary development of groups of organisms based on shared genetic and anatomical characteristics, and phylogenetic trees are widely used to systematize relationship between different bacterial species. High-throughput sequencing technologies utilize phylogenetics, by distinguishing bacteria based on their DNA. The 16S rRNA gene is the most widely used marker for profiling of bacterial communities because it contains both variable regions allowing to distinguish between different species, and conserved regions enabling suitable primer design (51). The 16S rRNA gene encodes prokaryotic small 30S subunit of the 70S ribosomal complex in most bacteria and archaea, and the evolutionary conservation of the 16S rRNA gene imply it has a crucial role in survival. The gene sequence consists of nine highly conserved regions, V1-V9, flanked by conserved sequences (52), and 16S rRNA-based genotyping protocols employ primers that only bind one variable region, or span two variable regions.

From a host's perspective, bacteria can be classified according to their pathogenicity. Pathogenic bacteria are bacteria that can cause disease.

Commensal bacteria, also called commensals, may produce neutral or beneficial effects for the host by e.g. inhibiting growth of pathogenic bacteria. Commensal bacteria can also be opportunistic, meaning they are usually harmless, but could cause disease under certain circumstances. The classification, nomenclature and identification of bacteria are described in their taxonomy. After kingdom, phylum is the highest taxonomic level. After phylum follows class, order, family, genus, and finally the specific bacterial species. For example, the full lineage for the human gut bacteria *Escheria coli* is: Bacteria (kingdom), Proteobacteria (phylum), Gammaproteobacteria (class), Enterobacterales (order), *Enterobacteriaceae* (family), *Escherichia* (genus), *Escheria coli* (species).

The microbiota can be separated into subsections according to location. The gut comprises the by far largest density of microorganisms and is consequently broadly studied. Because the GI tract is the primary point of contact between the microorganisms and the host's immune system, it is no mystery that the gut microbiota plays important roles in immunity and health. The gut microbiota composition varies along the GI tract, with increasing numbers and diversity from the stomach to the colon (53, 54). The GI tract provide a wide range of conditions for microbial growth, since the segments differ with respect to pH, nutrient flow, bile salts etc., and thus present a variety of niches for specialized microbiota (46).

The gut microbiota is acquired and influenced by both vertical and horizontal transmission from maternal and environmental sources, respectively (55, 56). Microbial encounters in early life play a key role for the establishment of a stable gut microbiota and immune system development, and the timeframe in which stable microbial colonization take place is called the "window of opportunity" (57, 58). The gut microbiota of a newborn is transiently dominated by *Staphylococcus* and *Enterobacteriaceae*, while *Bifidobacterium* spp. dominates in early infancy. The infant microbiota continues to develop through childhood, and the introduction of solid foods causes shifts towards a diverse adult-type gut microbiota characterized by bacteria in the Firmicutes and Bacteroidetes phyla. The infant's gut microbiota develops until it reaches a stable adult microbiota (59), which is mainly colonized by bacteria within the five phyla Bacteroidetes, Firmicutes, Actinobacteria, Proteobacteria and Verrucomicrobia (54). The gut microbiota assembly in early life has the potential to influence host susceptibility to disease in alter life (57, 58).



Recent evidence supports that microbial exposure occurs already *in utero* (59), yet the largest share of GI colonization is generally believed to happen after birth (60). The mode of delivery strongly influences the infant gut microbiome. Caesarian-section (C-section)-delivered children are not directly and immediately exposed to maternal microbes as vaginally delivered children are. Children delivered by C-section are more likely to colonize microorganisms present in the hospital environment, on the mother's skin or on the hospital staff (61). Comparisons of gut microbiota composition in 7-year old children showed significant differences between the children born by C-section and vaginal delivery, indicating persistent effects of delivery mode (62).

### 1.2.3 Gut Mucosal Immunity

The hollow GI tract is a continuous mucosal tissue in constant contact with the outside world. Only a single layer of intestinal epithelium separates the internal from the external environment, making the intestines major ports of entry for potentially harmful agents. The gut immune system is specialized to cope with the task of being permeable for nutrients, protect towards harmful agents, as well as tolerate the harmless. This is crucial for securing the gut homeostasis, that is a balanced internal environment that maintain optimal conditions for tissue specific functions.

The gut immune system is composed of multiple barriers and lymphoid tissues. In the stomach, low pH enabled by HCl-secreting parietal cells generates a chemical barrier and decrease the number of viable microorganisms to reach the intestines. Along the intestines, several barriers prevent contact between luminal content, the epithelial wall and underlying tissue. These barriers are ensured by several specialized cells, such as the Goblet cells and Paneth cells, producing and secreting mucus and antimicrobial peptides, respectively. Goblet cells are widespread along the GI tract, producing mucus composed of large glycoproteins known as mucins. The composition and thickness of mucus covering IECs differ between the SI and colon, reflecting the functions and properties of these intestinal segments. The SI (except for the distal ileum) has limited bacterial exposure and needs to allow for nutrient absorption. The SI holds a single, porous mucus layer that is loosely organized and unattached to the epithelium, allowing for movement of the loose mucus with bound bacteria to the colon

(43). The colonic lining is covered by an inner, dense layer and an outer loose layer of mucus. The colon is stably colonized with a complex microbiota that play several important roles in health (see section 1.2.4). The inner colonic mucus layer is firmly anchored to the IECs and does not allow bacteria to penetrate (although there are some exceptions, see section 1.2.4), while the outer layer is unattached and allows for bacterial penetration (43).

The mucus layer is continuously renewing and is crucial to prevent bacterial overgrowth and proximity between IECs and luminal bacteria. Mucus release can be stimulated by Goblet cells sensing potential pathogens, and increased mucus production leads to potential pathogens being physically flushed out of the body (63). Tight junctions between IECs also physically restrict paracellular passage of bacteria and luminal content. Production of antimicrobial peptides, mainly by Paneth cells along the SI, provides an additional chemical barrier. The antimicrobial peptides are secreted into the GI lumen where they form pores on microbial membranes and ensures killing of microorganisms before they can come close to the epithelium (64). Secretory IgA (sIgA) is also an important contributor to intestinal barrier function. IgA is the dominating isotype produced and secreted by plasma cells in mucosal tissues as described later in this section. IgA is transcytosed across the epithelium by a polymeric immunoglobulin receptor. During transcytosis, the receptor is cleaved, yet leaving a part of it called the secretory component associated with IgA, resulting in sIgA being released. The secretory component allows for binding to mucins and thus retaining the sIgA in mucus. SIgA protects against threats via neutralization and anchoring of microbes to the mucus, restricting their access to the epithelium, and has limited ability to induce inflammation compared to other immunoglobulins (65, 66). The ability of SIgA to prevent pathogenic access to the epithelium is commonly termed “immune exclusion”, and agglutination is critical for such protection. SIgA agglutinate pathogens, making clumps in mucus that can be removed via peristalsis and excretion in feces. Classical agglutination, in which random collisions of sIgA and target bacteria expressing antigen specific for the sIgA find place, relies on a high density of pathogens. At lower densities, it has been demonstrated that sIgA generate large clumps by a different mechanism called “enchained growth”. SIgA can cross-link dividing bacterial cells and prevent them from separating, and hence remove them via peristalsis and excretion (67).

Between IECs, a population of T cells called intraepithelial lymphocytes (IELs), are located. The IELs are long-lived effector cells that patrol the intestinal mucosal tissue and rapidly release cytokines upon antigen encounter. Although the antigen recognition and mechanism of action of the various IEL lineages are poorly defined, they likely play important roles in maintenance of intestinal barrier integrity (68).

The adaptive branch of the gut immune system is commonly divided into inductive sites and effector sites. The inductive sites encompass the gut-associated lymphoid tissue (GALT) and mesenteric lymph nodes (mLNs), which is where naïve lymphocytes are first activated by antigens. Naïve lymphocytes continuously move through blood, lymphatic vessels, secondary lymphoid organs, and non-lymphoid organs until they are activated. The GALT includes Peyer's patches (PPs) and isolated lymphoid follicles (ILFs). Following activation by antigen, the lymphocytes express a distinct set of receptors targeting them for their effector site destination. The gut effector sites encompass the lamina propria, where activated elicit their functions.

IECs and immune cells in lamina propria are equipped with numerous types of PRRs, enabling them to recognize molecular structures on microorganisms and other potentially harmful agents coming near the epithelium. Once activated PRRs can, dependent on type and location, secrete cytokines resulting in recruitment of immune cells and induction of immune responses to eliminate the threat (69). TLRs are perhaps the most widely studied PRRs, particularly in the gut. Dependent on cell type on which they are expressed, the TLRs have unique roles in balancing defense and tolerance responses at the gut mucosal interface. TLRs expressed on IECs play important roles in maintenance of the epithelial barrier function (70). For example, colonic goblet cells in mice have been shown to recognize TLR ligands and consequently provoke secretion of the Muc2 mucin, improving the colonic mucus layer (63).

Intestinal macrophages are abundant throughout the GI tract, mostly located in lamina propria. The intestinal macrophages do not fit into the M1/M2 classification, since they express hallmarks of both subtypes. Importantly, intestinal macrophages do not induce classic pro-inflammatory responses (71). As blood monocytes enter the lamina propria, they undergo a gradual phenotypic differentiation and acquisition of typical intestinal macrophage functions such as production of IL-10, decreased production of IL-6, enhanced

phagocytic activity and hyporesponsiveness to TLR stimulation (10). Following exposure and engulfing of bacteria, the intestinal macrophages do not induce inflammation and impair homeostasis, enabling them to act as efficient “silent” scavengers (72). Moreover, intestinal macrophages can via their IL-10 production facilitate expansion of local Tregs and thus suppression of other T cell activity (10, 72).

Before lymphocytes can be activated and adaptive immune responses occur, antigens must enter the tissue from the intestinal lumen. The PPs and ILPs do not have afferent lymphatics, and thus induction of adaptive immune responses relies on continuous sampling of antigens from the intestinal lumen along the GI tract. The transport of antigens across the intestinal epithelium and presentation of these antigens to the mucosal immune cells can occur via several routes (**Figure 3**). The simplest form of antigen sampling is via paracellular leakage. Moreover, DCs residing in the LP can extend into the lumen and capture antigens (73). Microfold (M) cells are specialized cells for sampling of larger antigens, including bacteria, which are taken up by underlying APCs for presentation to naïve T cells (1, 74). Moreover, goblet cell-associated antigen passages (GAPs) is another pathway for antigen sampling in the SI (75). The APCs receive and present their antigen to T cells, either in the GALT, or after migration to mLNs. Lymphocytes are activated and given receptors for return to the gut effector sites, namely gut-homing receptors. They then return via the blood to elicit their effector function in lamina propria.

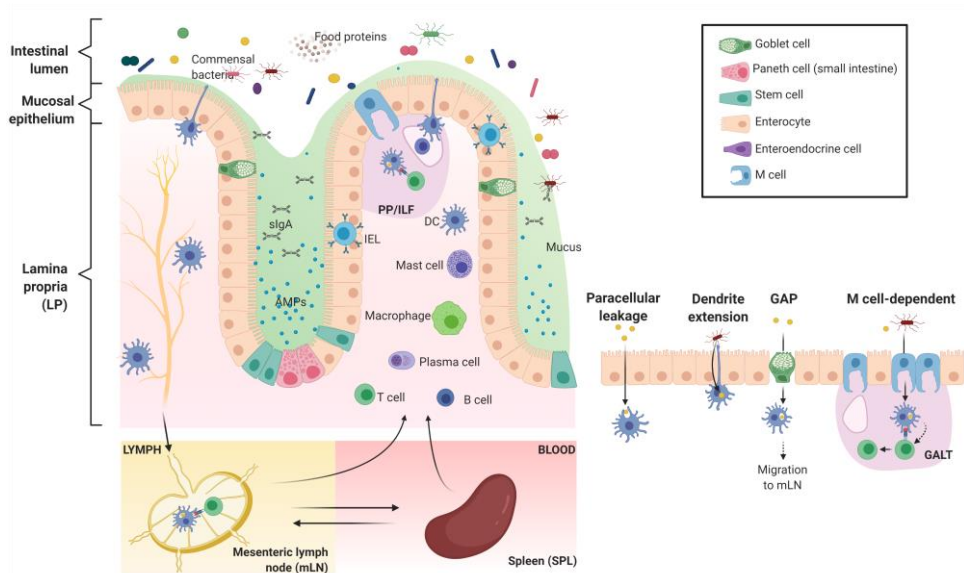


**Figure 3:** Overview of the GI immune system. Inspired by (1), (76), (64) and (77). GAP, goblet cell-associated antigen passage; IEL, intraepithelial lymphocyte; ILF, isolated lymphoid follicle (in colon); PP, Peyer’s patch (in SI); sIgA, secretory immunoglobulin A. Created with biorender.com.

The gut mucosa harbors abundant and dynamic populations of Tregs and Th17 cells, reflecting the need to tolerate harmless agents and attack potential threats, respectively. Under steady state, this remarkable balance ensures intestinal homeostasis, partly through the dual role of TGF- $\beta$  in inducing both Tregs and Th17. Both tTregs and pTregs are present in the intestine, although available evidence suggests that tolerance towards the commensal bacteria, as well as dietary antigens, are mainly mediated by pTregs. Moreover, differentiation of pTregs in the gut is thought to direct CD4<sup>+</sup> T cells away from differentiation into other pro-inflammatory Th states (28). Signals and stimuli generated by the gut microbiota and immune responses to the gut microbes mediates the Th17/Treg balance. The interaction between gut microbiota and host immune system is further elaborated in section 1.2.4.

The production of IgA begins with activation of B cells in GALT, with PPs as the principal IgA-inductive sites (78). The activation can be independent or dependent on Th cell help, of which the latter leads to differentiation of long-lived plasma cells and production of high affinity IgA antibodies. The cytokines produced by the Th cells, particularly TGF- $\beta$ , contributes greatly to the class switching in B cells from producing IgM and IgD as naïve B cells, to

acquire the expression of IgA as activated B cells (78). As mentioned previously in the current section, the IgA-mediated immunity is a non-inflammatory defense contributing to avoid unnecessary inflammation in the gut (1, 66). IgA can both inhibit and facilitate growth and fitness of gut microbes as further described in section 1.2.4.

#### 1.2.4 Host and Gut Microbe Crosstalk

Numerous factors can potentially shape the gut microbiota during the host lifespan (**Figure 4**), with the perhaps most apparent and widely studied being the diet. Studies in both humans and mice have shown large implications of diet on gut microbiota composition, yet the functional consequences for both microbes and host are largely unknown (79).

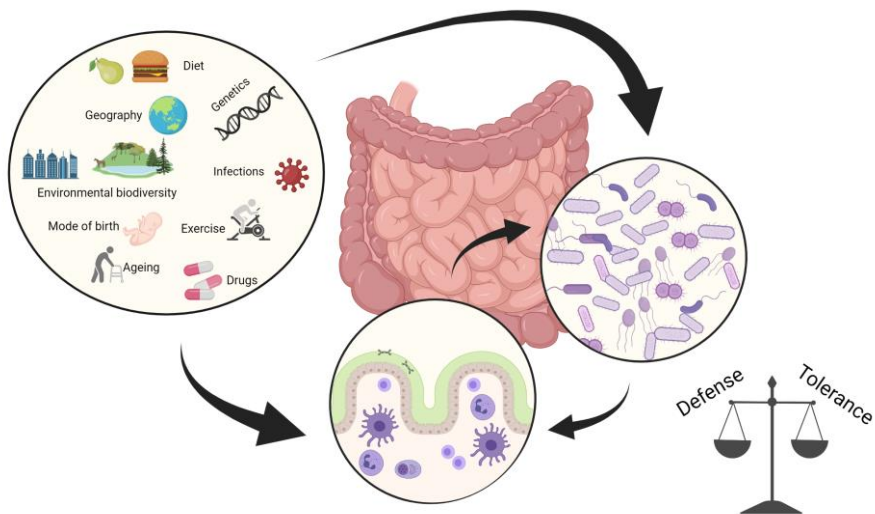


**Figure 4:** The relationship between host and gut microbiota relationship with influencing factors. Created with biorender.com

A meta-study from 2018 showed that interventions with dietary fibers, especially fructans and galactooligosaccharides were found to increase the fecal relative abundance of *Bifidobacterium* spp. and *Lactobacillus* spp. in humans (80). Dietary fiber has long been considered beneficial with respect to gut microbiota composition, at least in part because they are substrates for short-chain fatty acid (SCFA) producing bacteria (81, 82). SCFAs are end-products of fermentation of dietary fibers and resistant starch by gut

microbiota, and the main SCFAs produced in both human and mice gut are acetate, propionate and butyrate. The SCFAs can contribute to regulation of immune function by activating free fatty acid receptors (FFARs) on the epithelial and immune cells, bringing about modulation of enzymatic activity and transcriptional regulation (83). The role of SCFAs, particularly butyrate, in regulating the Treg pool has received much attention. The mechanism for this is thought to involve the inhibition of histone deacetylase enzymes (HDACs) that leads to enhanced histone acetylation in the *Foxp3* locus and increased expression of this transcription factor (84, 85). The main producers of butyrate in both human and mouse gut belong to the phylum Firmicutes, such as *Roseburia* spp., *Eubacterium* spp. (86) and *Faecalibacterium prausnitzii* (87). These species can produce butyrate via fermentation of carbohydrates, utilization of acetate as energy source for the production through so-called “cross-feeding”, or both (88, 89).

Compelling evidence show that dietary fat can also influence the gut microbiota composition, and that this crosstalk may account for some of the disease conditions associated with high-fat diets (90). A possible mechanism linking dietary fat to gut microbiota is the secretion of bile acids. Bile acids are synthesized in the liver as conjugated primary bile acids that are secreted into the intestinal lumen in response to dietary fat consumption. A recent study demonstrated that a bile acid-supplemented diet shifted mouse gut microbiota to a similar composition as seen in mice fed a high fat diet (91). A considerable body of evidence show that bile acids are involved in regulation of metabolic as well as inflammatory responses (92). A fraction of the primary bile acids is metabolized in the intestinal lumen by gut bacteria into secondary bile acids. This metabolism influences the availability and activities of bile acids and thus, both primary and secondary bile acids are, in company with SCFAs, receiving attention with respect to gut microbiota modulation and colon homeostasis (93).

Although short-term changes in diet have demonstrated alterations in gut microbiota composition, such changes are transient if the subjects return to their habitual lifestyle (94). Dietary patterns correspond with gut microbial composition when viewing cross-sectional studies across populations (95). Thus, long-term dietary patterns are likely more important than short-term changes in shaping an individual’s microbiota profile. An extensive longitudinal study from 2013 indicated that 60 % of all bacterial strains within an individual persisted for 5 years (96). This study emphasizes the

resilience of the established gut microbiota to intestinal perturbations. A resilient microbiota will return to its original state after being exposed to perturbations, while a non-resilient microbiota will shift to an altered state. The colonic crypts, as well as the human appendix and mouse caecum, are protected regions of the GI tract, and it is hypothesized they may serve a reservoir role, harboring a diverse microbial community that can repopulate the lumen after environmental insults (54). However, unhealthy gut microbiota states may also be resilient, possibly predisposing the individual for diseases (97).

Apart from diet, environmental factors influencing the gut microbiota includes infections, medications and age (46), as well as the surrounding environment (98). Exposure to soil microbes, house dust and decaying plants has been shown to increase diversity of the gut microbiota in mice (99). In a recent study, the microbiota of mice born in various soil environments was assessed over time, showing that environmental microbes colonized the mouse gut, and that the environmental microbes from the birthplace persisted in the mouse gut over time (100). Moreover, children in a nature-oriented daycare where they were exposed to a high microbial biodiversity environment exhibited a changed gut microbiota profile with increased diversity and enrichment of Gammaproteobacteria (phylum Proteobacteria) (101). The same research group also found higher relative abundances of *Faecalibacterium* and *Ruminococcaceae* (both phylum Firmicutes) in elderly individuals having a diverse yard vegetation around their homes compared to those living in an urban area (102).

The gut microbiota interacts with host cells to regulate several physiological processes, such as energy harvest, metabolism, and immune response. The ability of microbes to set the immunological tone of tissues requires tonic sensing of microbes and complex feedback loops between innate and adaptive components of the immune system. We are only just beginning to understand this intricate communication, but it is obvious that the gut microbiota and host immunity has profound connections (103).

The importance of gut microbiota in shaping the host immune system is apparent in studies of antibiotic-treated mice and germ-free (GF) mice lacking microbiotas partly or completely, respectively. GF mice show an underdeveloped immune system and impaired responses to pathogens (104). Moreover, GF mice have an increased penetrability of their inner colonic mucus layer, as well as absent Th17 cells, both of which could be restored



upon microbial colonization (105-107). Memory phenotypes of CTLs require stimuli from microbiota, demonstrated by CD8<sup>+</sup> T cells in GF mice showing no transition into memory cells (108). Additionally, when transferred into GF mice, *in vitro* antigen activated CD8<sup>+</sup> T cells has failed to transition into long-lived memory cells characterized by high CD69 and CD44 expression and intermediate CD62L and CXCR1 expression (108). Administration of broad-spectrum antibiotic to mice has been shown to cause an hyperactivation of intestinal macrophages, increased Th1 responses cells and increased susceptibility to infections (109). In humans, evidence associates the use of antibiotics during childhood with the development of various immune-mediated diseases, including inflammatory bowel diseases (IBDs) (110).

Through killing, competing for resources and physical space, as well as production of metabolites that have inhibitory effects on other bacteria, the gut microbiota is in constant battle. The continuous competition between gut bacteria leads to commensal bacteria inhibiting colonization and overgrowth of new and often pathogenic bacteria, what is known as “colonization resistance” (111, 112). The host mucus layer and secretion of antimicrobial peptides are fundamental features for keeping the gut microbiota compartmentalized. Moreover, the continuous interaction between various innate and adaptive immune cells and the gut microbiota enables generation of microbiota-specific responses. TLRs are involved in regulation of the host commensal microbes and maintenance of tissue integrity. Polysaccharide A (PSA) produced by *Bacteroides fragilis* (phylum Bacteroidetes) is an example of a well-studied molecule shown to promote host immune system modulation (113). PSA is recognized by TLR2/TLR1 that, in cooperation with a C-type lectin PRR called Dectin-1, ultimately leads to expression of anti-inflammatory genes (114). *Bacteroides fragilis* binding to IgA has been shown to promote long-term maintenance of this species in the gut microbiota in mice (115), demonstrating that IgA has a dual role in both inhibiting and promoting gut bacterial growth.

Segmented filamentous bacteria (SFB) (phylum Firmicutes) have long been shown to stimulate functional maturation of T and B cells and induce an increase in small intestinal Th17 responses (116). These bacteria are one of few unique non-pathogenic bacteria that penetrate the mucus layer. Adherence of intestinal microbes to the IECs has been characterized as a mechanism utilized by SFB, as well as pathogens such *Citribacter rodentium* and *Escherichia coli* (both phylum Proteobacteria), to induce Th17 responses

(106). Thus, rather than recognition of released microbial components or metabolites such as SCFAs, the gut mucosal immune system can mount Th17 responses through recognition of physical interactions with microbes. More recently, it has been demonstrated that the intestine harbors Th17 cells that exhibit different functions dependent on which bacteria activates them. The Th17 cells activated by SFB are non-inflammatory, while those induced by *C. rodentium* release inflammatory cytokines (117).

A lingering enigma is whether, and which, changes in gut microbiota composition are beneficial or not for the host. Most findings in microbiota research relates to if the composition is advantageous or disadvantageous for a specific condition or phenotype. Clinical observations in both human and animals have associated dysregulation of the gut microbiota and immune system crosstalk to a spectrum of illnesses, including metabolic disorders, allergies, autoimmunity, as well as IBDs and colorectal cancer (CRC) (103). However, given the intimate bidirectional communication between gut microbiota and host immune system, determination of cause and effect is rather challenging.

### 1.2.5 The “Hygiene Hypothesis” and its Relatives

The “hygiene hypothesis” was first postulated by David P. Strachan in the late 1980s, who stated that allergic diseases were less common in children from large families, where they were likely to be more exposed to infectious agents through their relations (118). Hygiene itself may not explain the observed differences, and reforms of the “hygiene hypothesis” have been suggested because of the inappropriate focus on cleanliness which was not supported by evidence that modern cleaning habits had reduced microbial exposure. Refinements of the hypothesis include the “old friends hypothesis” proposed by Rook *et al.*, emphasizing that it was not merely infectious agents that was interesting, but rather that microbes we have co-evolved with are considered “friends” by the immune system (119, 120). The “old friends hypothesis” highlight that the lack of, or changed, microbial exposure was likely what caused the increased incidence of allergies and chronic inflammatory diseases. New concepts include the “biodiversity hypothesis”, stating that loss of biodiversity leads to immune dysfunction and disease (121, 122).

Common for all these hypotheses is the idea that contact with natural elements and microbes promotes health via stimulation and priming of the immune system. The hypotheses are backed up by epidemiological studies demonstrating that children exposed to high microbial biodiversity environments harbor different microbiomes and enhanced immune regulation than urban children (101), and are less susceptible to diseases such as asthma and allergies (122-124). Comparisons of Amish and Hutterite children in the U.S. showed significantly reduced prevalence of asthma and allergies in the Amish children, accompanied by profound differences in their immune profiles (125). Moreover, dust from the homes of these children were used in an experimental mouse model of asthma, showing that the dust from Amish, but not Hutterite, homes significantly reduced hyperreactivity of the airways. Amish and Hutterite populations live similar lifestyle except for their farming practices, where the Amish follow traditional farming practices and Hutterite employ industrialized practice (125). Additionally, farmers have reduced risk of certain types of cancer (126). A connection between decreased environmental biodiversity accompanying an urban living and increased risk for IBDs has also been suggested (127, 128). Still, despite widespread interest in the “hygiene hypothesis” and its relatives, only a handful of experimental studies in animal models exist to date. Among these studies, Olszak *et al.* demonstrated neonatal, but not adult, recolonization of GF mice with microbiota from conventional lab mice protected them from colitis and asthma sensitivity (129). More recent studies have demonstrated that mice exposed to biodiverse soil show shift in their gut microbiota, reduced anxiety (130) and alleviated Th2-driven inflammation related to allergic responses in a murine asthma model (131). Moreover, protection from allergen-induced skin contact hypersensitivity was seen in mice exposed to a farm environment by being placed in a cattle barn (132).

### 1.3. Colorectal Cancer

Cancer is a group of diseases involving uncontrolled cell growth that infiltrate and destroy normal tissue and has the potential to spread throughout the body. Colorectal cancer (CRC) is, with over 1.9 million new cases diagnosed worldwide in 2020, the third most frequently diagnosed malignancy in men and second most common cancer in women (133, 134). The incidence and mortality rate of CRC correlate with the adoption of a western lifestyle, and

rates remain among the highest in highly developed countries (135). In Norway, as well as Europe as a whole, CRC was in 2020 the second most common cause of cancer deaths (136).

CRC is a multifactorial disease that usually progress slowly, and the risk for CRC development increases with age. Neoplasia is the process that forms a neoplasm, i.e. a type of abnormal growth of cells. Most CRCs are malignant neoplasms developing from glandular epithelial cells of the colon and rectum, called adenocarcinomas (137). The majority of CRC cases arise sporadically through acquired somatic and epigenetic anomalies largely attributable to potentially modifiable environmental factors (138). A minority of CRC cases are attributed to hereditary cancer syndromes caused by germline mutations in susceptibility genes, such as familial adenomatous polyposis (FAP) in which the patient harbors mutations of the *APC* gene (137, 138).

### 1.3.1 Colorectal Carcinogenesis

The initial changes in colorectal carcinogenesis generally involve formation of hyperplastic and dysplastic crypts that in turn proliferate to form microadenomas giving rise to adenomatous polyps, carcinoma, and ultimately invasive cancer (139, 140). The initial cancerous alterations take place in the stem cells that reside in the base of the crypts. Aberrant crypt foci (ACF) are morphological alterations of the colonic crypts that are considered the earliest identifiable lesions in the colorectal carcinogenesis (141). ACFs have been identified as precursor of the dysplasia-carcinoma sequence in patients with ulcerative colitis (142) and is a widely used biomarker of colorectal carcinogenesis in rodent models of CRC (see section 1.4.1 and 4.1.5).

Progressive accumulation of genetic and epigenetic alterations leads to the transformation of normal glandular epithelial cells into invasive cancer. A multistep model of colorectal tumorigenesis named the adenoma-carcinoma sequence was proposed by Vogelstein and Fearon in 1990 (143). This model described the stepwise pattern of mutational activation of oncogenes and inactivation of tumor-suppressor genes that accompanies the transformation of normal colorectal epithelium to adenomatous polyps and ultimately invasive and metastatic carcinoma. Since its early description, a body of research has supported and elaborated on this well-established paradigm (**Figure 5**).

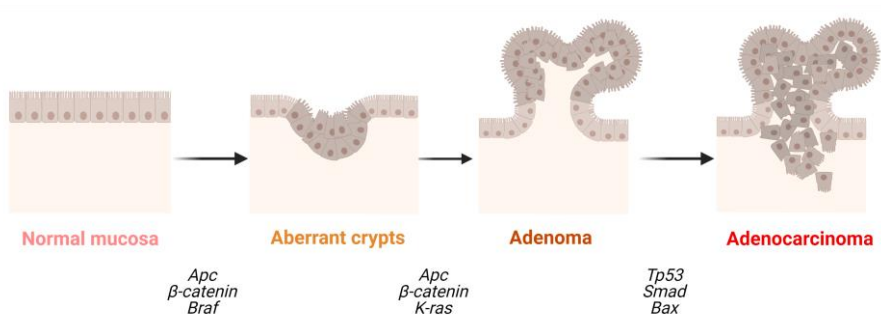


**Figure 5:** The adenoma-carcinoma sequence; initiation and progression of sporadic CRC with commonly mutated oncogenes and tumor-suppressor genes in each phase. Inspired by (139, 140, 144). Created with biorender.com.

The tumor-suppressor gene *APC* is the most commonly mutated gene in CRCs, and this gene is an important part of the canonical Wnt signaling pathway. The Wnt signaling pathways are involved in maintenance of intestinal homeostasis by regulating cell proliferation, migration, differentiation, and death. Normally, in proliferating cells, Wnt causes an accumulation of  $\beta$ -catenin in the cytoplasm that eventually translocate into the cell nucleus where it acts as transcription factor for Wnt target genes, such as *CCND1* (Cyclin D1) and *MYC* (c-Myc) involved in proliferation. When cells are differentiated, the Wnt signaling ceases. In the absence of Wnt signaling, the *APC* proteins build a complex serving to bind  $\beta$ -catenin and target it for degradation. Thus, *APC* prevents the  $\beta$ -catenin accumulation and translocation. In CRC, *APC* loss-of-function usually occurs early in the pathogenesis, and results in increased activity in the canonical Wnt pathway, with disrupted  $\beta$ -catenin degradation.  $\beta$ -catenin accumulates and leads to increased cell proliferation (145, 146).

Somatic mutations of *APC* have been reported in the majority of sporadic colorectal tumors (146, 147). However, CRC tumors are one of the malignancies with the highest mutational burden (148), and the molecular pathways are far from characterized. For example, some CRCs have increased  $\beta$ -catenin due to mutations of the  $\beta$ -catenin gene (*CTNNB1*) itself, that blocks its own cessation, or mutations in other genes with similar functions as *APC*. Progression of carcinogenesis is ensured by accumulation of mutations in additional tumor-suppressor genes, such as *TP53*, *SMAD* and *KRAS* (146).

Several molecular pathways of colorectal carcinogenesis have been defined. The most common pathway involves chromosomal instability (CIN), which is identified in about 85 % of sporadic CRC in humans (149). CIN involves changes in chromosome number and structure resulting from losses or gains of chromosomal segments, loss of heterozygosity (LOH) and chromosomal arrangements (150). Microsatellite instability (MSI) is seen in about 15 % of sporadic CRC and results from mutations in DNA mismatch repair (MMR) genes that cause instability within microsatellite regions, i.e. regions with short repetitive gene sequences (151). Various epigenetic instability phenotypes in CRC have also been characterized, such as CpG island methylation phenotype (CIMP) involving gene silencing due to hypermethylation of CpG islands found in promoter regions of gene throughout the genome (152, 153).

The types of epi-/genetic instabilities are commonly used to define subgroups of CRCs. However, reports have indicated the presence of CIN, MSI, as well as CIMP and other epigenetic instabilities could be overlapping, blurring the lines for exact definition (146). For example, MSI is not necessarily a result of mutation of MMR genes themselves but can be a consequence of epigenetic silencing of the *MLH1* gene by hypermethylation of its promoter (154). Still, tumors are composed of cell populations with different properties, and such intra-tumoral heterogeneity is also reflected in the epigenetic alterations which vary substantially between cells dependent on location in the tumor (155). New technologies, such as various single cell sequencing techniques and spatial profiling have enabled investigation of single cell genetic and epigenomic signatures across tumors and adjacent tissues that is valuable for the expansion of our pathophysiological knowledge of CRC.

### 1.3.2 Cancer Immunology

The term immunosurveillance refers to the immune system recognition and demolition of pre-cancerous or cancerous cells. Tumors may express various tumor antigens that are recognized by the immune system and induce immune responses. However, tumor cells often escape immune-mediated destruction by immunoediting of their tumor antigens or surface molecules, rendering them undetectable (156). The continuous crosstalk between the immune system and tumor cells could be considered an arms race with three

possible outcomes; tumor elimination, equilibrium where the tumor is kept in check, or that the tumor escapes the immune control.

The principal and most characterized mechanism for immune protection against cancers is killing of tumor cells by CTLs. The CTLs recognize tumor antigens presented on MHC class I via their TCR. Studies have shown a correlation between the infiltration of T cells, and specifically CTLs, into the tumor microenvironment and better prognosis in several types of cancers, including melanoma and CRC (157). Robust priming of CTLs primarily occur in in tumor-draining lymph nodes. However, most tumor cells do not express the co-stimulators needed to initiate T cell responses or the class II MHC molecules needed to stimulate Th cells that promote the differentiation of CTLs. Thus, CTL responses specific for tumor antigens may require cross-presentation of the tumor antigens by antigen-presenting cells (APCs), meaning that an APC ingest tumor cells or tumor antigens, process them intracellularly to peptides that can be displayed bound to MHC class I molecules for CTL recognition. The APCs carry the tumor antigens to lymph nodes and colocalize with naïve T cells. The APCs also express co-stimulators, and these or Th cells that are activated at the same time provide the signals needed for differentiation of naïve CD8<sup>+</sup> T cells into tumor specific CTLs. Once effector CTLs are generated, they are able to recognize and kill the tumor cells in any tissue, without a requirement for co-stimulation (1).

A characterized strategy for cancer cells to escape immune control is by expressing surface molecules that interact with inhibition receptors on immune cells, e.g. PD-L1 that interact with PD-1 on the T cell surface, causing inhibition of the T cell response. By blocking such interactions, what is known as “checkpoint inhibition”, T cell responses are enabled, which allows for attack of the cancer cells (158). The 2018 Nobel prize in physiology and medicine went to the discoverers of the principle of checkpoint inhibition, which one type of immunotherapy now used to treat various cancers (159).

NK cells are highly capable of killing many types of tumor cells and may contribute to immune surveillance against cancer. NK cells may be activated to kill tumor cells coated with anti-tumor antibodies by antibody-dependent cell-mediated cytotoxicity. Moreover, MHC class I expressing cells are readily recognized and killed by CTLs. Thus, some tumors lose expression of MHC class I molecules as a result of selection. This loss of MHC class I molecules make tumors particularly good targets for NK cells, since lack of MHC class I

binding to inhibitory receptors on NK cells lead to NK cell mediated killing of the target cell (160).

In healthy tissues, Tregs are important in conveying immunological tolerance to self and to harmless agents passing the GI tract. However, in malignancies like cancer, Tregs have been shown to hinder the development of anti-tumor immunity by creating a immunosuppressive microenvironment (161). The immunosuppressive activity of Tregs on e.g. CTLs, inhibit the killing of cancerous cells. This is advantageous for the tumor, and tumors themselves sometimes induce Tregs by producing TGF- $\beta$  (162).

In human CRC, stronger expression of genes encoding of Th1 response (such as *IFNG*), CD8<sup>+</sup> T cell pathways, and extensive intratumoral infiltration of NK cells have been associated with good prognosis. In contrast, high levels of MDSCs have been correlated with advanced tumor stage and metastasis, and higher proportions of Th17 cells secreting IL-17, IL-21 and TNF- $\alpha$  has been found in tumors and blood of CRC patients relative to healthy controls (163).

### 1.3.3 Colorectal Cancer and The Gut Microbiota

While the causes of CRC are unknown, numerous risk factors have been characterized. Inflammation is a well-established driver of colorectal carcinogenesis, and individuals with IBDs such as ulcerative colitis and Crohn's disease have substantially increased risk of CRC (138, 164). The inflammation-driven type of CRC is commonly termed colitis-associated CRC and is characterized by chronic overt inflammation that contributes to a favorable tumor microenvironment and thus stimulate carcinogenesis.

Mechanisms and pathways by which exaggerated inflammation leads to tumor formation is not fully elucidated and remains the focus of extensive ongoing research. However, a widely accepted theory is that disruption of the epithelial barrier leads to influx of normally compartmentalized luminal microorganisms into the tissue. The luminal microorganisms may activate untimely innate and adaptive immune responses as well as oxidative stress (165). Oxidative stress, inflicted by the impaired production of reactive oxygen species (ROS) and the counteractive effects of antioxidants, can mediate genomic instability and DNA damage that in turn may cause mutations and initiation of cell transformation and cancer (166). The breakdown of barrier integrity increase the exposure of colonocytes to the



luminal agents (165). Enhanced IEC permeability and tumor formation has been reported in mice deficient in PRR-associated genes, such as *Nod1*, *Nod2* and *Ripk2* (167, 168), emphasizing the importance of defense mechanisms and IEC function in preventing carcinogenesis.

For spontaneous, non-hereditary CRC, widely acknowledged risk factors include a low-fiber high-fat diet, obesity, smoking, alcohol intake and a sedentary lifestyle (137), all of which are associated with a western lifestyle. The negative effects of these factors on CRC development may in part be inflicted via inflammatory, metabolic, or gut physiological mechanisms. For example, a high-fiber diet is associated with a reduced risk of CRC (169). A low intake of fiber has been shown to promote expansion of colonic mucus-degrading bacteria and promote aggressive colitis following infection with the enteric pathogen *C. rodentium* in mice (170). Fiber in the diet improves gut motility and decreases the stool transit time (171) and thus limiting the time potential carcinogens can stay in the intestines and affect the epithelium. Moreover, as described in section 1.2.4, dietary fiber is fermented by gut-residing bacteria to SCFAs that are important immunomodulatory molecules.

Several of the mechanisms involved in colorectal carcinogenesis, such as immune regulation and inflammation, are closely linked to the gut microbiota (172). Studies from as early as the 1960 and 70s demonstrated that GF rodents administered carcinogens developed less cancer relative to conventional rats and thus supported a role for microbes in CRC development (173). Perturbing the microbiota with various combinations of antibiotics have been shown to influence colonic tumor count in mice subjected to chemical induction of CRC, and tumor number can be predicted from the microbiota at both start and end of the model (174).

Microbiota modulation by exposure to microbially diverse environments in everyday life may convey beneficial traits with respect to disease, which may be reflected in a higher incidence of IBDs in developed than developing countries (175). Surely, Western microbiomes are less diverse than non-Western microbiomes (176), and given the increased risk for CRC in individuals with IBDs, it can be hypothesized that exposure to environmental microbes and previous infections may also influence the risk for CRC.

In various mechanistic and association studies, specific bacteria have been individually linked to CRC. In mice, various *Lactobacillus* spp. (phylum Firmicutes) has been reported to be predictive of a light tumor burden, and reduction of GI inflammation (174). *Bifidobacterium* spp. (phylum Actinobacteria) have also been shown to confer anti-cancer effects (177).

*Lachnospiraceae* (phylum Firmicutes), Clostridiales (phylum Firmicutes), Proteobacteria, *Alistipes* spp. (phylum Bacteroidetes) and *Aneroplasma* spp. (phylum Tenericutes) are all examples of taxa for which high relative abundance has been associated with increased tumor burden in mice (174). *B. fragilis* has been shown to inhibit colorectal tumor formation in mice, a protective role that was dependent on PSA production and TLR2 signaling (178). In humans, compelling evidence supports a role of human *Fusobacterium nucleatum* (phylum Fusobacteria) in colorectal carcinogenesis. *F. nucleatum* has been shown to directly inhibit NK cell-mediated killing of tumors (179), and when engrafted into mice, *F. nucleatum* isolated from human feces was shown to activate TLR4 signaling to promote tumor development (180, 181).

Although strong evidence of single bacteria playing important roles in CRC is available, recent studies have accentuated that the total bacterial community rather than single bacterial species are likely the determinant for beneficial or adverse effects of perturbances (182). The term “dysbiosis” has often been used with respect to impaired microbiota associated with various diseases, yet the definition of “dysbiosis” is unclear. A “dysbiotic” microbiota has been interpreted as a “Anna Karenina principle” (183), stating that an impairment in any one of a vast number of factors in a healthy microbiota can lead to it becoming unhealthy, paralleling Leo Tolstoy’s famous quote “all happy families look alike; each unhappy family is unhappy in its own way”. Identification of effects of single bacteria in various health and disease settings is valuable for mechanistic insights in microbiome research. Yet, when taking a step back to overlook the currently available research on different microbe-host interactions and the various roles one bacterial strain can have, we can certainly understand that this is a multidimensional picture we must carefully consider when drawing conclusions.

## 1.4. Mice as Model Organisms

The mouse is the dominant model organism for the study of human biology, due to their anatomical, physiological, and genetic similarities. Studies in mice allow manipulation and monitoring of biological processes in an organismal setting, and the approach of utilize information obtained from studying mice to understand similar processes in humans has been vivid for decades. Advantages of rodents over other research animals include their small size, easy maintenance in large numbers, short life cycle, and high breeding

efficiency. Additionally, the use of rodents is advantageous with respect to the genetic information available. The mouse genome was sequenced in 2002 (184), making genetical modifications in mice rather easy to achieve, and a wide array of disease models in mice are readily available.

Today, the murine strains employed in research belong to the common house mouse (*Mus musculus*) species, derived from domesticated Asian or European mice that were developed as pets as early as 1200 BCE (185). In USA, Abbie E.C. Lathrop began breeding mice in the early 1900s. Her mice were originally intended for pets, but soon she also supplied mice to numerous researchers. Moreover, she conducted mice experiments herself (186). Miss Lathrop's business grew, and she started inbreeding to separate her mice from wild mice. These inbred mice are the ancestors of the most widely used strain in research, C57BL/6, also called black-6 (B6) (185). Inbreeding of mice refers to mating closely related animals to bring about standardized, known genotypic backgrounds. Inbred mice are the most widely used in biomedical research. However, outbred mice that are bred to maximize genetic variance, are also available and can be useful to study the genetic basis of complex disease phenotypes (187).

When used in research, mice are typically housed in cages of a single, small, open space. To stimulate species-specific behavior, research mice must be supplied environmental enrichments such as nesting material and toys (188). Albeit with inconsistencies between studies, environmental enrichments are found beneficial with respect to anxiety, stress, and general well-being (189-191). Therefore, laboratory mice are usually offered enrichments such as nesting material, hiding structures, and running wheels.

Moreover, research mice are housed under strict hygiene levels, with the most commonly being specific pathogen free (SPF) facilities, in which the mice are demonstrated free of a specified list of pathogens. Albeit some variation between breeding facilities, the list includes a selection of common pathogens associated with disease in mice, such as mouse parvovirus, *Salmonella* spp., *Helicobacter* spp. and protozoa (192, 193). GF mice, as previously mentioned, are free of all microorganisms, while gnotobiotic mice are typically GF mice that have been engrafted with one or more defined non-pathogenic microorganisms.

### 1.4.1 Mouse Models of Colorectal Cancer

Mouse models that mimic the initiation and progression of CRC are of great importance to study causes and mechanisms. Genetic models such as the Min/+ (multiple intestinal neoplasia) mice harboring a mutant allele of the murine *Apc* gene (see section 1.3.1) are widely used (194). Originally, Min/+ mice were bred on a B6 background. However, they have been shown to develop more small intestinal lesions than colonic. Min/+ mice on a A/J background have been shown to develop colonic lesions (195). Other genetically modified mice harbor alternative *Apc* mutations, or less commonly, various mutations in e.g. *Kras*, *p53* or *Braf* genes (196).

Another approach to study CRC in mice is via chemical induction, such as administration of the specific colorectal pro-carcinogens dimethylhydrazine (DMH) and its metabolite azoxymethane (AOM) (194). AOM is converted to methylazocymethanol (MAM) following metabolism by CYP2E1. MAM is a highly reactive alkylating species that generate O<sup>6</sup> methylguanine adducts in DNA resulting in mutation accumulation and induction of carcinogenesis (194, 197, 198). A model involving a combinatory treatment with AOM and dextran sulfate sodium (DSS) salt, called the AOM/DSS model, was developed to mimic human colitis-associated CRC (199). DSS is a negatively charged, sulphated polysaccharide that inflict colonic epithelial damage and promote colorectal carcinogenesis (200-203). The AOM/DSS model has emerged to become one of the most frequently used models to study inflammation-associated colorectal carcinogenesis in rodents (194, 204-206). With the DSS treatment, the AOM/DSS model is inarguably driven by inflammation, yet inflammation is also a driving factor in the Min/+ models. Administration of DSS to conventional B6 Min/+ mice promotes the intestinal carcinogenesis, highlighting the interplay between *Apc* inactivation and inflammation (207, 208).

More direct models for CRC include orthotopic injection of cancer cell lines or implantation of patient-derived xenografts into mice that are usually immunodeficient (196). These approaches allow for easier control and monitoring than the abovementioned methods of spontaneous or chemically induced CRC. However, given that the cancerous cells have not developed in the host, these models are less suitable for studying early carcinogenesis as well as genetic and molecular events leading up to the cancer formation.

## 1.4.2 Mice Versus Humans

The aim of studying laboratory mice is typically to translate the findings to humans. However, there are both genetic and physiological differences between mice and humans that must be taken into consideration when extrapolating findings from mice studies to human relevance.

Albeit the structure and functions of the GI system is highly conserved in mammals, interspecies variations surely do exist. The average ratio of intestinal surface area and body surface area is similar between humans and mice, but the ratio differs over different intestinal segments, highlighting evolutionary adaptation to different diets. Compared to humans, mice have a much longer colon relative to their SI length, and an enlarged caecum, which reflects the need for fermentation of plant materials and extraction of nutrients from the higher proportion of indigestible food components in their diet (209). The mouse caecum provides storage for these fiber-rich plant foods while gut bacteria metabolize them. Mice frequently eat feces, known as coprophagy, and thus recycle nutrients and microorganisms. Such recirculation rarely occurs in humans, and the small human caecum with an anatomical structure similar to that of the colon holds no clear role (185, 210). The human gut also includes a distinct appendix, while the mouse appendix is hardly separated from the caecum (185).

The gut microbiota composition in mice and humans has been found to be substantially different. B6 mice have demonstrated lower Firmicutes/Bacteroidetes ratio than humans, and is dominated by *Muribaculaceae* (earlier designated *S24-7* (211)) (phylum Bacteroidetes) and *Clostridiaceae* (phylum Firmicutes) (212). Based on published 16S rRNA gene datasets, Nguyen *et al.* conducted a meta-analysis of mouse and human fecal microbiota back in 2015, showing 79 genera overlapping (210). The taxonomic overlap between mouse and human microbiomes has been estimated to only 4 %. However, about 95 % of the functional annotations were common between the mouse and human datasets, indicating a significant functional overlap (213). These findings suggest that the mouse and human microbiome may consist of different species with shared functions. This is supported by fecal microbiota transfers (FMTs) from human to mice showing that mice require a mouse-specific microbiota for immune maturation and regulation (214, 215).

Regarding the immune system, several differences between the two species have been characterized, likely in due to divergent species-specific evolutionary pressure. The overall structure of the mouse and human immune system is similar, albeit some organizational differences such as different architecture of T and B cell zones in the spleen has been presented (2). The balance of lymphocytes and neutrophils are quite different, with lymphocytes dominating mouse blood, while human blood is neutrophil-rich (216). Moreover, differences in FcR expression, Ig isotypes, and expression costimulatory receptors on T cells between mice and humans have been characterized (216). The types of NK cell receptors used by humans and mice to recognize HLA/MHC class I also differ, where humans use KIRs and mice use lectin-like receptors of the Ly49 family (217). Investigation of immune cell lineage-specific gene expression profiles in mice and humans show that while most of the orthologs are conserved, some hundred genes show clearly divergent expression (218).

The discrepancies between human and mouse immune responses has led to the development of humanized mice. Humanized mice are typically immunodeficient mice that have received functional human cells or organs (219). Humanized mice serve as surrogates of a human immune system and have emerged to become a valuable tool to circumvent the fact that experiments in mice rely on the mouse immune system which is not always representative for human responses (220). However, a fair question is whether we can expect human immune cells to exhibit normal activity in a mouse environment. Although the mouse being immunodeficient, there is a continuous need to identify human-specific factors that may be required for optimal human cell differentiation and function. Last, we know that most studies in mice are conducted on inbred mice that lack genetic diversity that we know human populations have, and outbred mice are suggested to better reflect such individual natural genetic variance (187, 221).

The functional consequences of the species-specific differences are still unclear, yet we do know they exist. Infamous examples of such include the numerous drug development trials working excellent in mice, while failing tremendously in the subsequent human clinical trials (222, 223). Seok *et al.* conducted a systematic comparison of genomic responses between human inflammatory diseases and mouse models, finding that gene expression and signaling responses to inflammatory stress in mouse studies correlate poorly with human conditions as well as one another (224). Apart from genetic and

physiological differences between mice and men, the poor correlation and unsuccessful translation to bedside practice could also be explained by the distance between conditions the laboratory mice and humans are studied in. Humans are studied in their natural setting, exposed to microbes and infections, while laboratory mice are almost exclusively studied in settings far removed from their natural way of life.

### 1.4.3 Modelling Free-living Mice

The common house mouse is one species in the genus *Mus* and includes four *M. musculus* subspecies: *M. musculus musculus*, *M. musculus domesticus*, *M. musculus castaneus* and *M. musculus bactrianus* (225). *M. musculus musculus* and *M. musculus domesticus* are the dominant subspecies in East and West Europe, respectively, with hybrid zones where they abut (226). The house mice thrive in a variety of habitats, but they are typically found near human dwellings, such as farm buildings, sheds and garages (225, 226). Through evolution in their natural habitats they have, as humans, been exposed to a vast microbial load from the environment.

The environmental stimuli have undoubtedly set an evolutionary imprint on the house mouse physiology. Given that the environment explains the majority of the human immunophenotype (227-229), there is no surprise if this is also the case for mice. Surely, studies of various strains of wild mice have demonstrated that their immune system show signs of a primed phenotype, indicative of more effective responses to threats compared to conventionally housed laboratory mice (230-233). For instance, significantly higher levels of effector memory CD4<sup>+</sup> and CD8<sup>+</sup> T cells as well as KLRG1<sup>+</sup> CD8<sup>+</sup> T cells has been reported in both wild mice sampled in Minnesota, USA (234), and *M. m. domesticus* captured around United Kingdom (230) compared to laboratory mice. The differences are likely brought about by a blend of genetics, bystander infections and microbiome, and a few recent studies have demonstrated substantial differences between wild and laboratory mouse microbiomes (235, 236).

Although there are relatively few studies of wild mice microbiology and immunology published to date, and the species studied varies greatly, they have shown that wild mice harbor a diverse microbiome, including a complex mycobiome, virome, and parasitome (235-237). The wild mouse microbiotas

that have been characterized up till now are generally much more diverse than the laboratory mouse microbiota and characterized by higher relative abundance of Proteobacteria (235, 236). The presence of *Helicobacter* spp. has also been frequently reported in wild mice (235, 236, 238, 239), suggesting it is a natural component of a wild mouse microbiome. Wild mice microbiomes has also demonstrated significant inter-individual heterogeneity (240) and clear seasonal variation (241).

In contrast, the majority of laboratory mice studied in research are deprived of natural stimuli. Engraftment of minimal or specific microbial communities in gnotobiotic and germ-free mice have been widely employed for studies of gut microbiota in health and disease (242-244). The Schaedler flora (245) and OligoMM<sup>12</sup> (243) are examples of defined consortia that have served, and continue to serve, as valuable tools for studying the mechanistic basis of how microbes influence the host (246). However, as mentioned in section 1.2.4, the immune system of GF mice is underdeveloped, and while engraftment of defined microbial consortia allows for controlled composition of microbiotas, this methodology most likely lack important contributions from known and unknown interspecies interactions.

The laboratory mice are known to have a more restricted microbiota variation compared to their wild relatives. Given the “reproducibility crisis”, encompassing that scientific studies are problematic to reproduce (247), this serves as a good argument to abandon the variability of wild mice. Yet, numerous known and unknown factors can modify the gut microbiota of laboratory mice, including diet, mode of delivery and medicinal use, such factors include water source, housing density, type of bedding and type of cage (248, 249). This emphasize that the laboratory mouse microbiota is perhaps not as restricted as we think. Importantly, both inter- and intra-facility variability in the laboratory mice microbiome is enough to alter the outcomes in disease models (249-251).

The increased awareness of the tandem function of gut microbes and host immune system convey concerns over the potential bias introduced by the hygienic housing on the microbiota and immune system, and their downstream effect on disease modelling in mice (252, 253). A growing body of research has highlighted that conventional laboratory mice may be too far removed from their natural, microbially rich habitat to accurately recapitulate the immunological responses of free-living mammals.



Consequently, several approaches to study the laboratory mice in more natural situations have emerged, aiming to generate mouse models that better reflect realistic immune responses that may improve the translatability to human relevance (254-257). Currently, developed approaches to such naturalization of laboratory mice range from controlled sequentially infections with a combination of pathogens to alter immunity (258), naturalization of the laboratory mouse microbiome directly via FMTs from wild mice (235) or transfer of laboratory mouse embryos to wild mice generating “wildlings” (236), to more holistic strategies with co-housing (234) and re-wilding (259, 260).

Up until now, these studies have shown that by co-housing with pet store-bought mice, laboratory mice approach immunophenotypes found in wild mice and adult humans (234), with increased numbers and frequencies of circulating neutrophils and monocytes, as well as enhanced expression of TLR2 and TLR4 on circulating cells (261). Analyses of immune phenotypes based on RNA sequencing of various tissues revealed that the expression profile in spleens of “wildlings” clustered closer to that of wild mice than laboratory mice (236). For the gut immune profile, about 50 % of the wildlings clustered with the wild mice, while the other 50 % clustered with laboratory mice (236). In laboratory mice that had been re-wilded by housing in outdoor enclosures, an expansion of granulocytes, increased maturation of lymphocytes and higher levels of cytokines secreted from their immune cells upon stimuli was observed (259).

A handful of studies have assessed the performance of naturalized mice in disease modelling compared to laboratory mice. Laboratory mice co-housed with pet-shop mice have increased resistance to *Listeria monocytogenes* infection (261), and transfer of fecal microbiota from wild mice to laboratory mice confer improved outcome of both viral influenza A infection and CRC (235). Rosshart *et al.* (236) took a step further and tested the translational value of “wildlings” by studying their response to treatments that had previously failed upon transition from mouse trials to clinical trials in humans. Interestingly, the experiments in these laboratory mice born to wild mice mothers have mirrored findings from human clinical trials more accurately than conventionally reared laboratory mice (236).

## 1.5. Knowledge Gaps

Experimental disease studies in mice usually take place in perfect isolation from the outer microbially diverse world, far away from the mammal they are aiming to model, namely humans. This aspect has raised concerns over the translatability of findings from studies of hygienic, immunologically naïve laboratory mice to human relevance. The last few years, various approaches to bring laboratory mice closer to a natural setting with diverse microbial exposure while keeping the traceable genetics has emerged. A handful of studies have aimed for such naturalization of laboratory mice, either by microbiota transfer, co-housing with wild mice, or housing in an outdoor natural environment. Common for the naturalized laboratory mice are shifts in gut microbiomes, improved immunity, and altered disease outcomes. A couple of studies have also indicated that naturalized mice better mimic responses of humans. These findings underline the need for, and use of, research mice adapted to a more natural situation in disease modelling for improving translatability to human responses.

Additionally, the traditional reductionist approach of mice studies, searching for single factors contributing to a given physiological process or disease outcome, has certainly brought a vast amount of knowledge. However, while studies of humans are conducted in their natural situation, research mice are removed from theirs. There is a lack of novel model systems to study laboratory mice in a real-world setting and by such means move closer towards the environmental conditions of humans. Such naturalization systems need to be described and characterized with respect to effects on immunological parameters and disease modelling in the mice.

Among diseases largely influenced by environmental factors we find CRC, and diet has been given a lot of attention in studying the etiology of CRC development. However, epidemiological findings indicate the surrounding environment itself can reduce the risk of IBD and thus influence CRC risk, in concordance with variants of the “hygiene hypothesis”. Cleaner environments may protect us against infections, but paradoxically also make us vulnerable to lifestyle diseases as well as novel infections. The surrounding environment includes some of the first colonizers of our gut and continues to shape the gut microbiota composition throughout life. However, the lack of studies addressing the impact of the outer environmental setting on CRC is likely due to lack of suitable models – an issue naturalization models may potentially contribute to resolve.

## 2. Aims of the Study

---

To develop a preclinical mouse model that more realistically represents a natural mammalian lifestyle, we have established a system where laboratory mice are raised under a full set of environmental conditions present in a naturalistic, farmyard-type habitat. We call this process feralization, and in this project, the main aim was to explore the model system for feralization of laboratory mice with respect to influence on immune system, gut microbiota, and CRC development.

### Objectives:

- Characterize how various setups of feralization may influence immune and gut microbiota profiles.
- Establish a procedure for chemical induction of CRC in B6 mice by AOM and DSS administration.
- Assess if feralization influences neoplastic development in the mouse colon.
- Evaluate the role of feralization timing and thus microbial encounter (early versus later in life).
- Generate hypotheses of potential underlying protective mechanisms conferred by feralization.

### 3. Summaries of Papers

---

#### **Paper I**

##### *A Model System for Feralizing Laboratory mice in Large Farmyard-Like Pens*

In this paper, we presented a naturalistic housing system for laboratory mice reflecting a natural habitat. The housing system consisted of indoor enclosures, or pens, containing farmyard-like environmental material such as soil, fecal droppings from farm animals, and plant materials.

This paper covers three experiments. First, adult male and female B6 mice were feralized in the farmyard-like pens together with wild-caught feral mice. The feral mice carried antibodies for certain pathogens that was transferred to the feralized mice. Moreover, parasites were detected in both feral and feralized mice, while the control B6 mice housed under SPF conditions tested negative for all tested pathogens and parasites. The terminal gut microbiota from this trial was presented in a previous paper by Lindner *et al.* (262) and thus not included in this paper. Briefly, the gut microbiota profile of the feralized mice approached that of feral mice, distinctly separated from the SPF mice. In the second experiment, juvenile female B6 mice were feralized in the farmyard-like pens in the presence of female feral mice. Analysis of the gut microbiota profiles in this experiment largely mirrored the findings from experiment 1, with feralized mice approaching a feral-like profile and increased alpha diversity measures.

Assessment of cellular phenotypes in both experiment 1 and 2 revealed that the feral mice showed immunophenotypes indicative of antigenic experience and immune training, such as consistently higher levels of effector and central memory T cells, and KLRG1 expression on NK cells. Multivariate analysis of immune parameters from experiment 2 showed the feralized mice clustered in the direction of feral mice. Measurements of antibody isotypes showed an elevation of IgE, IgG2a and IgG2b, but not IgA, in serum of feralized mice. These findings were consistent with findings from the feral mice. However, the IgA concentration was clearly elevated in feral mice while no difference was detected between feralized and SPF mice.

The feralized mice in experiment 1 and 2 were fed a seed diet, as opposed to a regular chow diet that was fed the SPF mice. We therefore included a third experiment in this paper to assess the contributions of the different diets to

gut microbiota and immunophenotypes. We observed shifts in the gut microbiota of the seed-fed mice fed the seed diet in the direction of what was seen in the feralized mice. Yet, we observed no differences between the seed fed and chow fed mice with respect to immunophenotypes. This suggests the alterations in immunophenotypes seen in feralized mice were driven by other stimuli, or other components of the microbiota, than those conferred by the diet.

This model system represents a naturalistic experimental setting, while still allowing for experiments with mice of well-known inbred backgrounds. The setup for this model system is adaptable to the study purpose, such as the inclusion or exclusion of wild mice as co-habitants, as well as different environmental material and pen sizes. We suggest this model system can be a valuable complement to conventional SPF and GF laboratory mice studies.

## **Paper II**

*Induction of colorectal carcinogenesis in the C57BL/6J and A/J mouse strains with a reduced DSS dose in the AOM/DSS model*

Paper II encompass the AOM/DSS model for induction of inflammation-associated CRC in mice. Searching literature for adequate protocols for CRC-induction in mice revealed that the employed regimens of AOM/DSS vary greatly between studies, and commonly involve high ( $\geq 2$  %) doses of DSS under various time spans. Previous experiences with the use of DSS in our lab has shown that giving doses  $>1$  % to mice most often inflict severe colitis and accordingly adverse symptoms in the animals. The combination of AOM and numerous treatments with high doses of DSS is thus likely to bring about advanced disease, which has also been reported previously. This may prove unnecessary for several study purposes. Some reports show tumorigenic effect of smaller doses of DSS. Additionally, the use of preneoplastic lesions as an outcome measure instead of solid tumors has been suggested to relieve animal suffering (263). Various preneoplastic lesions with different features have been characterized in rodents, and ACFs are preneoplastic lesions that has been well-characterized in mice previously (195, 264, 265).

For the abovementioned reasons, with the study summarized in paper II, our aim was to evaluate if an AOM/DSS model involving a single dose of AOM and a lowered (1 %) DSS dose could induce CRC and detectable preneoplastic

lesions in two mouse strains, namely the B6 and A/J, representing two extremes with respect to AOM susceptibility (266) (267). With this study, we demonstrated that an AOM/DSS model involving a single dose of AOM and a lowered dose DSS was adequate to induce preneoplastic lesions in our facility. The outcome measures included ACFs assessed by microscopy and pathohistological classification of morphological changes.

Although several papers on various dose regimens in the AOM/DSS model has been published previously, none included all factors we were interested in. Particularly, we were interested in the assessment of ACFs by use of a low dose DSS in B6, which has been shown less susceptible to AOM and reliant on the DSS treatment for carcinogenesis to occur. Thus, the findings in this paper may also be of interest to other researchers planning to employ the AOM/DSS model. However, we stress that responses to AOM and DSS may vary greatly among facilities. Based on the findings from this experiment, we proceeded with using a regimen of one AOM injection and 1 % DSS treatment for the AOM/DSS trial covered by paper III.

### **Paper III**

*Naturalizing laboratory mice by housing in a farmyard-type habitat confers protection against colorectal carcinogenesis*

Based on the findings from paper I, we wanted to study whether a naturalistic environment itself was enough for immune priming and gut microbiota shifts. If so, we wanted to see what this meant in disease models. CRC is a disease with a tangible phenotypic outcome that is easily detectable. Moreover, epidemiological data indicates a high biodiversity environment may reduce CRC risk in humans. We therefore wanted to conduct experiments looking at how feralization influenced the CRC development. In paper III, we conducted two independent experiments using two different mice models of CRC.

In the first experiment we employed male A/J Min/+ mice, which spontaneously develop CRC in due to lack of one functional allele of the *Apc* gene. The A/J Min/+ mice were developed to better resemble CRC than Min/+ mice on a B6 background (195, 265) and has been frequently used for CRC research at NBMU (264, 268). Adult A/J Min/+ mice, and wild-type control mice, all males, were feralized or kept under conventional laboratory conditions for 7-9 weeks before they were euthanized. We found significantly

fewer lesions in the colons of feralized Min/+ mice than laboratory Min/+ mice.

In the second experiment, we employed the AOM/DSS model, i.e. a chemical induction model of inflammation-associated CRC, using the protocol we examined in paper II. We bred laboratory mice in the naturalistic conditions, and thus they were feralized from birth. Additionally, we included a group of late feralized mice that were born in the laboratory and relocated to the naturalistic environment after weaning. After CRC induction, we found significantly smaller lesions in the feralized mice than the laboratory mice. Moreover, in contrast to the conventionally reared laboratory mice, the feralized mouse gut microbiota structure remained stable and resistant to the mutagen- and colitis induced neoplasia. The feralized mice also exhibited signs of a more functionally mature immunophenotype, indicated by increased expression of NK and T cell maturation markers, and a more potent IFN- $\gamma$  T cell response to stimuli. The late feralized group matched the early feralized group with respect gut microbiota but showed a disease phenotype in between that of early feralized and laboratory mice, yet more alike the former. This suggests that the timing of microbial encounter had some effect yet was not crucial for conferring protection against CRC.

Taken together, we show that laboratory mice feralized in a farmyard-type habitat were protected against colorectal carcinogenesis. With this study we demonstrate the utility of the feralization model that recapitulates realistic disease responses in a naturalized mammal.

## **Paper IV**

*Profiling of colonic mucosa transcriptome and mucus layer in mice feralized in a farmyard-like habitat (Manuscript)*

Following the experiments presented in paper III, we hypothesized that the CRC protection could be explained, at least in part, by changes in the local intestinal barrier function prior to the cancer induction. Thus, with this study, we aimed to address the potential effects of feralization on intestinal barrier function that could be further pursued for deciphering of the protective mechanisms of feralization seen in paper III. The feralized mice included in paper IV were males from the same study as described in paper III, feralized from birth (in absence of feral mice). After weaning these male mice were kept

in cages enriched with farmyard material. In healthy feralized and conventionally reared laboratory mice, we measured mucus layer properties, gene expression locally in the colon, and microbiota profiling of caecum.

Mucus measurements were conducted by collaborators in the Mucin biology research group at University of Gothenburg that developed these methods (269, 270). We did not find significant differences in mucus layer properties between feralized and laboratory mice. This was rather surprising, as mucus layer is guided by microbiota, and a less penetrable mucus layer has been reported in feral mice compared to laboratory mice previously (271).

RNA sequencing was conducted on colonic mucosal scrapings from the distal part of the mouse colons. Using acknowledged statistical methods for RNA sequencing data, we identified relatively few differentially expressed genes between feralized and laboratory mice. A closer look at the genes upregulated in feralized mice showed genes encoding two major colonic mucus proteins important in mucus structure and attachment. These findings indicate that there may be differences in feralized mice mucus although we did not observe differences in the mucus growth or penetrability. Moreover, the gene encoding Intelectin1 (*Itln1*), a protein that aggregate bacteria, was also upregulated in feralized mice.

Last, minimal differences in cecal microbiota composition was detected between the feralized and laboratory mice. In conclusion, these data suggests that the observed beneficial effects of feralization may involve improved structure of colonic mucus and enhanced bacterial defense. However, from our analyses we cannot distinguish whether gene expression in single cell populations differed, and for a definite conclusion future studies should also address other parts of the intestines and employ more targeted approaches.



## 4. Discussion

---

### 4.1. Methodological Considerations

#### 4.1.1 Ethical Reflections

All the animal experiments were approved by the Norwegian Animal Research Authority. The studies were conducted at Section for Experimental Biomedicine, Faculty of Veterinary Medicine, NMBU, Oslo, or the Faculty for Chemistry, Biotechnology and Food Science, NMBU, Ås, in accordance with local and national regulations for laboratory animal experiments. The animal facilities were licensed by the Norwegian Food Safety Authority, with the FOTS IDs stated in the individual papers. The health of the animals was monitored following a program recommended by the Federation of European Laboratory Animal Science Association (FELASA)<sup>1</sup>.

Moreover, in the CRC experiments described in paper II and III, the animals were monitored closely for any disease symptoms or signs of distress. Humane endpoints were defined as body weight loss >15 %, rectal bleeding defined as blood around anus sustained over two subsequent days, a complete bulging of distal colon out of rectum, and/or severely under-conditioned appearance and behavior. The study presented in paper II was conducted to evaluate if we could use lower doses of chemicals in the AOM/DSS induction model for CRC, producing less severe disease in the animals. With this experiment we offer a refinement to future studies employing this CRC model by minimizing pain and distress in the animals. The feralization system itself represent a refinement in that a naturalistic housing enables natural behavior in the mice, which likely contributes to minimizing distress and improve their welfare.

#### 4.1.2 Mouse Pen Setups and Maintenance

The experiments described in paper I and the A/J Min/+ mice experiment reported in paper III was conducted in re-built pig pens at Faculty of Veterinary Medicine, NMBU, Oslo. Later, permanent mouse pens were established at the Faculty for Chemistry, Biotechnology and Food Science, NMBU, Ås, and these were used in the AOM/DSS experiment of paper III. The

---

<sup>1</sup> [www.felasa.eu](http://www.felasa.eu)

setup, environmental sources and maintenance differed between these two mouse pen versions (**Figure 6**), which must be taken into consideration when interpreting the findings of the presented studies.

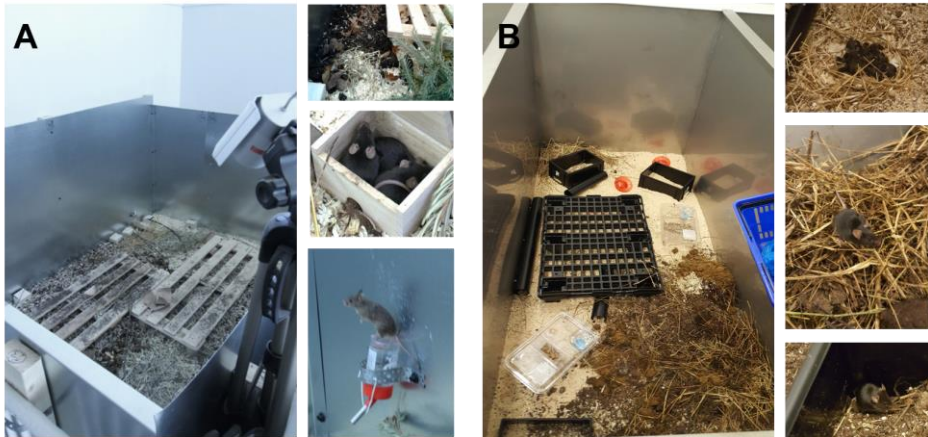


**Figure 6:** Pictures of feralized mice and mouse pens versions 1 (A) and 2 (B).

Version 1, reported in paper I and the Min/+ trial of paper III, involved escape-proofing of pig pens with sheets of galvanized steel, each pen measuring  $2.0 \times 2.5 \times 1.25$  m (W x D x H) on concrete floor. Pens were enriched with wood shavings, organic garden soil, compost, twigs, hay and fecal content from farmed pigs, cows and horses from Department of Production Animal Clinical Science (Prodmed) at NMBU. Oat and carrot sprouts were planted occasionally to provide fresh plants as would be encountered in a farmyard. Wooden pallets were used as stepping platforms for personnel to avoid disturbing the habitats or crushing animals, also contributing to environmental complexity and shelter. Standard nipples drinking bottles provided water. Small wooden boxes were provided for nesting and sheltering.

Version 2, reported in the AOM/DSS trial of paper III and IV, involved specially designed mouse pens constructed of galvanized steel plates, measuring  $1.10 \times 2.40 \times 1.20$  m (W x D x H). A base layer of dried woodchip bedding (primarily Norway spruce, but pine tree (*Pinus sylvestris*) may have appeared) was laid down and enriched with organic soil (Plantasjen, Norway), straw, and fecal content from farmed pigs, cows, horses, and poultry, originating from an organic farm located in Eastern Norway. Every two weeks during the experiments, fresh farm animal fecal content, always from the same source, was added to maintain a naturalistic situation.

In paper III and IV, mice also were housed in laboratory cages enriched with farmyard material from the mouse pens (version 2). In paper III, these mice were used as control groups for the enlarged space the mouse pens represent, while in paper IV they comprised the feralized group.

#### 4.1.3 Microbial Community Analyses

High-throughput 16S rRNA gene sequencing is a much used and cost-effective method for phylogenetic studies of bacteria, and this method was selected for identification and relative quantification of different gut bacteria in our studies. The rapid expansion of microbiota studies has brought about readily available protocols, technologies, and analysis software. The earliest technology was the 454 platform developed by Roche, based on pyrosequencing. This platform was discontinued in 2016 but is still used, although the Illumina platform has largely taken over. Both procedures involve the fragmentation of sample DNA, and generation of a library of DNA (16S rRNA gene; see section 1.2.2) fragments with bound adapters. In 454 pyrosequencing, the clonal expansion of DNA occurs by emulsion PCR on the surfaces of DNA capture beads. The beads are then deposited in wells of a sequencing chip, and in the sequencer, sequencing reagents including labeled nucleotides (dNTPs) are flushed across the plate. Addition of dNTPs to the DNA strand generates a chemiluminescent signal that is detected. The strength of the signal is proportional to the number of dNTPs incorporated in a single flush (272). In Illumina sequencing, the amplification of DNA occurs by bridge PCR on flow cells, on which clusters of identical DNA fragments are generated. Fluorescently labeled dNTPs are added, one by one, onto the DNA fragments. With each dNTP incorporation, the fluorescent dye is imaged to identify the base. The sequence of base pairs generated from sequencing one DNA fragment is known as a read. The DNA fragments can be sequenced from one or both ends, which is referred to as single and paired end sequencing, respectively. Paired end generates twice the number of reads compared to single end and enables more accurate consensus sequences when the forward and reverse reads are assembled.

In the experiments presented in paper I, 454 pyrosequencing on the Genome Sequencer FLX system (Roche) was conducted for consistency with a previously published paper that included gut microbiota data from experiment 1 (262). Comparisons of Illumina and Roche 454 show they are

both reliable for assessment of genetic diversity within samples (273). However, because of the discontinuation of 454, Illumina technology is now preferred, which is why sequencing with MiSeq was conducted for the later experiments covered in paper III and IV. Moreover, the choice of variable regions to target is most often based on in-house established protocols, which was also the reason for our choice of V1-V3 region (paper I) and V3-V4 region (paper III and IV).

Apart from different sequencing technologies, a wide array of platforms is available for the processing and interpretation of 16S rRNA gene amplicon data. Of the most common ones can be mentioned QIIME, mothur and DADA2. In recent years, user-friendly platforms such as the Integrated Microbial Next Generation Sequencing (IMNGS) (274) has been developed, which was used in the processing of data presented in papers I, III and IV. The platforms employ different strategies and programming language, but common for all are filtering of noise and problematic sequences, assemblance and alignment of reads, clustering of Operational Taxonomic Units (OTUs) or Amplicon Sequence Variants (ASVs) and taxonomy assignment.

While OTU clustering seeks to collect similar sequences in a consensus sequence, the ASV approach attempts to do the rather opposite, by determining exact sequences that are most likely “real” and filtering sequences that are highly likely to be errors. Because the ASVs are exact sequences, they could provide more precise identification of microbes (275). Yet, ASVs do not replace the relevance of OTUs, which is still widely used for microbiome profiling purposes. OTUs are groups of undistinguishable 16S rRNA gene sequences. A clustering of OTUs at 97 % sequence similarity has long been considered standard, since a dissimilarity threshold 3 % can distinguish bacteria at species level (276). In our analyses, we complied with the traditional 97 % cutoff. However, an update to 99 % similarity clustering has more recently been suggested (277), which could have improved our data resolution, yet would have required a different processing and another set of precautions, such as data inflation.

The different processing platforms employ different strategies for generation of OTUs from sequence data. IMNGS is based on the UPARSE approach for OTU construction, which has shown better performance than QIIME, AmpliconNoise (AN) and mothur with respect to biological sequence reconstruction accuracy (278). UPARSE constructs OTUs completely *de novo*,

meaning the reads are clustered based on sequence similarities only, without any reference database. Benefits of a *de novo* approach is that discoveries are not limited by a reference and thus information is not thrown away. However, the drawbacks are that it takes longer time and requires powerful computers and servers. *De novo* clustering has been shown superior to reference-based methods with respect to variation in diversity indices across 16S rRNA databases for taxonomic assignments (279).

Integrated in IMNGS is OTU clustering at 97 % sequence similarity, and assignment of taxonomy using the RDP database over known 16S sequences (280). Taxonomies were assigned at an 80 % similarity level, meaning at the taxonomic level where the OTU sequence and the database sequence are >80 % similar. In paper I and III, the taxonomy was based on the RDP database implemented in the IMNGS version available at the time. When going in depth on single OTUs, the OTU sequences were checked with the EzBiocloud database which is a reputable database for identifying sequences at genus or species level (279). For paper IV, an updated version of IMNGS was used, involving the use of SILVA database for taxonomical assignment instead of RDP.

The statistical analyses of 16S rRNA gene amplicon data in paper I, III and IV was conducted using Rhea<sup>2</sup>, which is a series of R scripts designed to accept IMNGS output (281). A simple normalization was chosen for the analyses presented in the mentioned papers, as opposed to rarefying that is an often-used normalization approach. Rarefaction has been criticized for several reasons, such as omitting valid data and adding uncertainty because of the randomness in rarefaction (282). With the simple normalization we can keep as much of the data as possible. Moreover, only data with relative abundance  $\geq 0.25$  % and prevalence of  $\geq 30$  % in at least one of the groups that were compared were included in the statistical analyses. The reasons for applying these cutoffs were to eliminate noise and focusing the analysis on taxa that are likely to be of the highest biological relevance.

To describe the microbiota community structure, both diversity and composition measures are used. The abundance of bacterial taxa relative to the total detected bacterial content is used to describe the composition. Recent years, determination of absolute abundance of bacteria has gained attention (283, 284), yet the established framework for relative abundance is

---

<sup>2</sup> Available from <https://github.com/Lagkouvardos/Rhea>

still the dominating metric for microbiota profiling. Diversity is a descriptive measure for the variety of the microbiota composition. *Alpha*-diversity is a measure of variety within a community, i.e. within a sample. *Alpha*-diversity measures summarize the community structure based on number of species (richness), how close in numbers each species in the sample is (evenness), or a combination of the two. A commonly used *Alpha*-diversity metric is the Shannon diversity index, which takes into consideration both the richness and evenness. However, given their non-linearity, *alpha*-diversity indices are not all intuitive. Effective numbers are suggested to give linearity to the indices and thus be useful in comparing *Alpha*-diversity measures across experiments (285, 286). Briefly, effective diversity is the number of equally abundant species that would give any value of a given index.

Another important diversity measure is the *Beta*-diversity, which designate the variation of microbial composition between communities, i.e. between samples. *Beta*-diversity can be calculated in several ways, but common for all is the calculation of distance, or dissimilarity, matrices. The two simplest metrics are the Bray-Curtis dissimilarity, in which differences in abundance between the samples are calculated, and the Jaccard distance, which is solely based on the presence or absence of species and do not involve abundance information. UniFrac is a distance metric in which sequence distances are calculated based on a phylogenetic tree, and thus takes into consideration the phylogenetic similarities between species when calculating how different to communities are. UniFrac can be unweighted, meaning the measure is purely based on sequence distances, or weighted, meaning the branch lengths of the phylogenetic tree are weighed by relative abundance so that both sequence and abundance information is included. Unweighted and weighted UniFrac are sensitive to rare and dominant species, respectively. Therefore, a balanced version, called generalized UniFrac, unified the unweighted and weighted UniFrac in a single framework (287), which was the distance metric we chose for *Beta*-diversity analyses in the papers I, III and IV.

General drawbacks with 16S rRNA gene amplicon sequencing is that only DNA is detected, meaning we cannot distinguish between dead or alive bacteria. A recent study showed that only 1/3 of the reads from 16S rRNA gene amplicon sequencing were generated from the live bacteria, while the remaining bacteria were injured or dead (288). Moreover, fecal samples are typically used as a proxy for the gut microbiota, particularly in humans, where sampling directly from the intestine is often unfeasible. This strategy offers

advantages such as non-invasive repetitive sampling allowing for longitudinal studies of one individual and is the preferred sample in time-course studies in mice, while caecum and intestinal tissues can be collected *postmortem*. However, given the different conditions along the GI tract, it is to be expected that the microbial composition vary dependent on sample type. It has been reported that fecal microbiota profile is much different from mucosa-associated microbiota in both humans and mice (289-291), and that mouse cecal and fecal microbiota differs in both composition and function (292).

Generally, comparisons of data obtained from 16S rRNA gene amplicon sequencing between studies should be made with caution, as different protocols and analysis pipelines may result in nonconform data. The rapidly evolving technologies, methods and database updates should also be taken into consideration. Lastly, it is important to acknowledge that the microbiome consists of much more than bacteria. We did not assess fungi, viruses, nor parasites beyond the test panels in any of the experiments encompassed by this thesis. This would have required more advanced and costly metagenomic analyses, such as shotgun sequencing, that we simply did not have the resources for at the time. Fungal load was attempted assessed in our samples by collaborators, but the DNA extraction method used for 16S rRNA gene amplicon sequencing of our samples provided no signal for primers targeting the Internal Transcribed Spacer (ITS) region of fungal DNA.

#### 4.1.4 Immunophenotyping

Immunophenotyping based on multicolor flow cytometry is a sensitive method for quick and accurate detection of presence or absence of molecules on or inside cells based on light scattering and fluorescence emission occurring when a laser light hits single cells moving in a stream. Thus, we can identify immune cells based on their characteristics (phenotype), such as size, shape, complexity, and type of molecules present on or inside the cells. Briefly, the procedure for immunophenotyping involves isolation of cells from tissues which are then incubated with fluorescently labeled probes that bind the molecules of interest (293). The relative amount of the particular molecule can then be measured by determining the amount of fluorescence emitted.

Most often, the probes are fluorochrome-labeled antibodies specific for a cell surface or cytoplasmic molecule, which was also the case for the

immunophenotyping presented in paper I and III. Monoclonal antibodies are produced by a single clone of B cells recognizing only a particular epitope on the antigen. Since all antibodies bind to the same antigen epitope, they produce substantially cleaner data as opposed to polyclonal antibodies which is a heterogeneous mixture of antibodies produced by various B cell clones recognizing various epitopes of the same antigen. The target molecules, also called markers, can be proteins which alone or in combination designates a specific type of immune cell. For example, CD45, known as the common leukocyte antigen, is an important anchor marker used to identify the leukocyte population in a cell suspension. Staining cells with CD45 as well as with CD3, which is expressed on T cells, enables the study of the T cell population specifically.

To design a multicolor flow cytometry panel, where multiple fluorochrome-labeled markers are included to characterize cellular populations of interest, some critical information must be known. The lasers of the flow cytometer must be known, since only fluorochromes that are excited by the corresponding wavelength of light from the lasers can be used in the panel. Moreover, the cell populations, antigens and fluorochromes must be identified. For low or unknown antigen expression and/or low cell populations, brighter fluorochromes should be used. On the contrary, dimmer fluorochromes should be used for high antigen expression and/or high cell populations. The spectral overlap should be minimized by choosing fluorochromes that do not overlap, yet this may not be possible for all antibodies of interest and thus compensation can be used to control the effects in the analyses.

To obtain reliable results from the flow cytometry analyses, several controls should be included, such as live/dead markers to only include live cells, single-stained positive controls for setting the compensation, and fluorescence minus one (FMO) controls to define positive populations. Unstained cells and/or isotype controls should also be included to define negative populations, cell size and granularity. Isotype controls are antibodies of the same isotype as the antibody specific to the target, but that lacks specificity to the target. To avoid non-specific binding, antibodies should be titrated and Fc blocking reagents should be used in cells with high content of Fc receptors, e.g. phagocytic cells (294).



To characterize cells based on their expressed molecules, which molecules to look for must be known and antibodies targeting them must be available and validated. General challenges with flow cytometry-based methods lies within the development and validation. The staining protocols used in paper I and III was developed and optimized in our lab in collaboration with the 3i immunophenotyping project<sup>3</sup>. Limitations in our studies include that we did not determine absolute cell numbers that would have required the use of known concentrations of fluorescent beads. Immunophenotyping of organs perceptibly requires euthanasia of the animals and thus we cannot follow individual mice over time. We conducted immunophenotyping at the end of the trials and thus the data represent a snapshot of how the immune cells look after feralization.

#### 4.1.5 Induction and Detection of CRC

In experiments presented in paper II and III, we employed the most common mouse models of CRC, namely the Min/+ mice and the AOM/DSS induction model. The choice of A/J Min/+ mice over B6 Min/+ mice was based the previous studies indicating that A/J Min/+ mice are a better model of CRC, while B6 Min/+ mice develop most lesion in the SI (195, 265).

CRC was also chemically induced by AOM/DSS treatment in wild-type mice. AOM was chosen over its precursor DMH, because of previous reports indicating enhanced potency and stability in solution (295). In previous studies employing AOM/DSS models, AOM is injected subcutaneously (s.c.) or intraperitoneally (i.p.). In paper II and III, we chose the s.c. route for two reasons; first, this inflicts less trauma to the animal, as the needle only needs to penetrate the skin. Second, this represents a more physiological route compared to i.p. However, the choice of this route may contribute to a later onset CRC, since the absorption of chemicals are slower when administered s.c. compared to i.p.

A variety of preneoplastic lesions reported to be involved in the initiation of colorectal tumorigenesis are used as biomarkers of colorectal carcinogenesis in research. The preneoplastic lesions characterized in rodents include aberrant crypt foci (ACF) (296), flat aberrant crypt foci (flat ACF) (297, 298), mucin-depleted foci (MDF) (299) and  $\beta$ -catenin accumulated crypts (BCAC)

---

<sup>3</sup> <https://www.immunophenotype.org/>

(300), that may partly overlap (301). Our choice of assessing ACFs were largely based on their easy detection, and that ACFs have been shown useful as a CRC biomarker in human populations (302-304) (**Figure 7A**).

A/J Min/+ mice have been shown to exclusively develop flat ACFs, while classical ACFs are observed upon AOM treatment in both Min/+ and wild-type mice (297, 305). Flat ACFs, but not classical ACFs, have been characterized as fast-growing crypts that reliably advances to tumors (298, 305). Grounded in this information, we cannot preclude if lesions in A/J and B6 wild-type mice are different from each other. Along these lines, we cannot state whether the protection conferred by the feralization against carcinogenesis presented in paper III was a consequence of enhanced induction of classical slow-progressing ACFs rather than flat fast-progressing ACFs, or due to inhibited progression of flat ACFs to tumors. However, an exposition of the inhibitory mechanisms in the different CRC pathogeneses was beyond the scope of the studies, yet the observed differences in protective traits conferred by feralization in the different models of CRC postures an interesting subject for further mechanistic investigation.

To investigate epithelial changes in the colon cross-sections we proceeded with histopathological assessment of the tissue (**Figure 7B**) using the following criteria: hyperplasia/dysplasia, adenoma (tumor restricted to the mucosa) or carcinoma (tumor with distinct infiltrative growth through the mucosa into the submucosa). All histopathological analyses were conducted blindly by trained pathologists. Paper II revealed that few adenomas developed in the AOM/DSS-treated B6 mice, indicative of very early phase CRC. In the AOM/DSS trial presented in paper III, adenomas were detected in all B6 mice but one in the late feralized group. The differences likely lie in the duration of the two trials, as well as the fact they were conducted in different animal facilities.

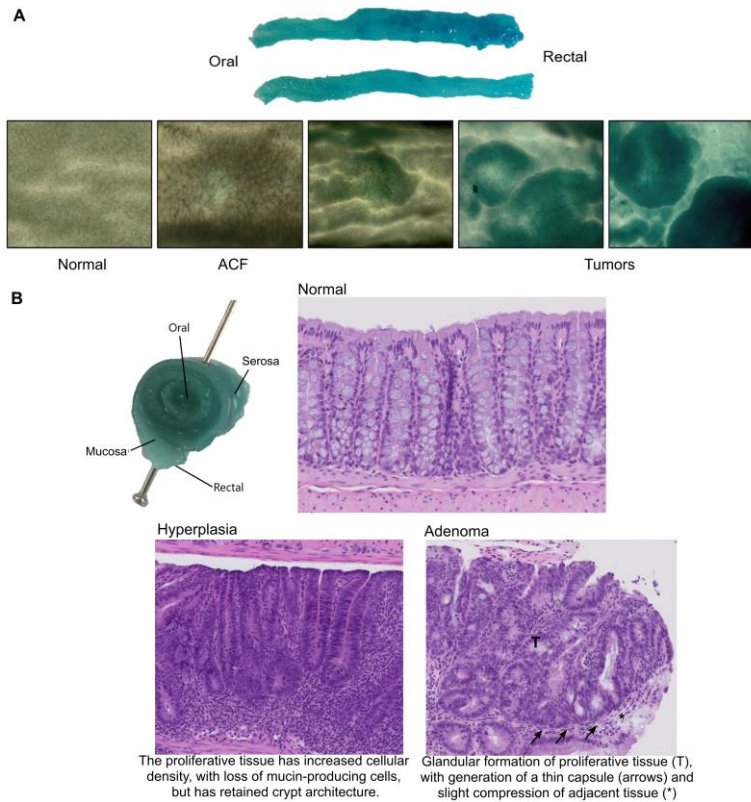


**Figure 7:** Classification of colonic lesions by surface microscopy (**A**) and histopathology (**B**). Modified reprint from paper III (Supplementary figure 8).

Previous studies have shown that colonic flat ACFs in A/J Min/+ mice develop into carcinomas over time (195). ACFs are not fully committed to neoplasia, and previous studies have indicated the risk for ACFs developing into tumors differs depend on mouse strains, with A/J mice considered at high risk (306). In our studies, we did not conduct molecular nor genetic features of the lesions. Thus, based on the scoring of lesions and histopathological assessments alone, we cannot know lesions detected in the AOM/DSS-treated wild-type A/J mice and wild-type B6 mice of paper II and paper III would advance into carcinomas with time, nor if the malignancy differed between groups. Moreover, we cannot conclude on carcinogenic mechanisms that potentially lie behind the group differences.

#### 4.1.6 Analysis of SCFAs in Feces

Quantitative detection of SCFAs can be done in different media and with different techniques. The most common are feces and serum, by use of chromatography methods. We chose to analyze our samples with a gas chromatograph (GC) coupled to a flame ionizing detector (FID). This method had been established at NMBU and used for SCFA detection in mouse feces previously (307).

The principle of gas chromatography is to separate analytes before detecting them. The components of GC include a long column arranged in a coil, a stationary phase and a mobile phase. Components in the sample travels along the column in the mobile phase (carrier gas). The different components of the sample travels with different speed, which reflects their affinity for the stationary and mobile phases. The interaction of molecules with the phases depends on their volatility, meaning their ability to change form from solid or liquid to vapor, which again depends on their molecular weight and intermolecular bonds. The less volatile compounds interact more with the stationary phase and thus move slower, while the more volatile compounds interact more with the mobile phase and move more easily along the column.

At the end of the column is a detector which detects the sample, of which a common one is FID, involving ionization of the compounds when they reach a flame. The released electrons are detected by electrodes over the flame. When a molecule is detected, a peak is shown at the retention time on the chromatogram. At last, the peaks produced in a sample is compared to peaks produced by known standard solutions for each SCFA. Thus, prior to a GC run, the system must be calibrated with standards that contain known concentrations of the SCFAs we want to investigate.

In general, GC-FID is a recommended method for SCFA analysis in feces (308). However, an important note is that fecal SCFAs represent the excreted SCFAs, while SCFAs are normally absorbed by IECs in a healthy colon (81). Thus, fecal SCFAs only reflect a fraction of the SCFAs produced but left unabsorbed, and numerous factors influencing the production and absorption of SCFAs can affect the finding. In paper III, we did not have data of water content in the feces samples subjected to SCFA analysis, which could have affected the results. Although we have no indications that the feralized mice had more watery feces than laboratory mice, using dry feces weight should be considered in future assessment of SCFAs.

#### 4.1.7 RNA sequencing

RNA sequencing (RNA-seq) is a technique which uses next-generation sequencing to reveal the presence of RNA in biological samples at a given moment. RNA-seq can be used to investigate all types of RNA, such as messengerRNA (mRNA), ribosomal RNA (rRNA), microRNA (miRNA) and transferRNA (tRNA). Commonly, researchers are only interested in the expressed genes and thus the mRNA only, which was what we studied in the colonic mucosa in paper IV. This involves a procedure to select only RNA with 3' polyadenylated (poly(A)) tails. In eukaryotes, the addition of poly(A) tails is a part of the process in which mRNA matures for translation, and thus poly(A) selection yields only the mRNA we are interested in, rejecting the other types of RNA that exist in the total RNA pool (309, 310).

The principle of RNA-seq is much the same as for the 16S rRNA gene sequencing. However, the start material is RNA as opposed to DNA for 16S rRNA gene sequencing, and some features of RNA are distinct and require attention in preparation of the sequencing library. Illumina sequencing technology is based on DNA amplification and thus needs a DNA, not RNA, template. Moreover, RNA is longer than DNA, and sequencers often have size limitations preventing them from accommodating many RNA transcripts. The library preparation procedures vary, but the key steps are always the same and include chopping of RNA strands into fragments before converting them to DNA. Then, RNA-DNA hybrids are generated, and dsDNA is synthesized. To keep track of the directionality of the original RNA, we must distinguish the two strands in the dsDNA. Different kits do this differently, but the principle is to tag one of the strands to be digested, leaving a final library where the DNA strand is the reverse complement of the RNA that we started with. This represents an opposing strand specific library because the direction of the sequences is the opposite of the original transcript. Libraries can be same strand specific or non-directional, or opposite strand specific (310).

A common pipeline for processing of RNA-seq data is trimming off adapters and, if necessary, trim sequences to a given quality. This leaves the high-quality, adapter-free parts of the reads, that can be aligned against a reference genome to figure out where the reads came from in the genome (309). Several aligners are available, but when working with organisms that have RNA splicing, such as mice and humans, a splicing-aware aligner must be used.

Splicing leads to reads spanning exon-exon junctions, which cannot be aligned to a reference genome directly. Splicing-aware aligners align unspliced reads first, and then use different strategies to detect splice junctions. In analysis of the RNA-seq data presented in paper IV, we used HISAT2, which is a *de novo* splice-aware aligner, that do not just detect splice junctions already known and available in databases but allows for detection of new splice junctions (311).

To visualize and analyze the mapped RNA-seq data, we used the SeqMonk<sup>4</sup> tool. We quantitated the data on gene level, i.e. counted the number of reads that overlapped with exons for each gene, leaving a number for the expression of that particular gene in a given sample. Normalization of the data is conducted to account for e.g. sequencing depth and gene length, ensuring differences in expression are not just in due to differences in the total number of reads. Along the way, quality checks are performed to ensure everything goes as planned. The last step in handling RNA-seq data is the statistical analysis and interpretation, where identification of differentially expressed genes (DEGs) is most often the goal. Many algorithms have been developed specifically for the purpose of identifying DEGs from RNA-seq data, a popular one being DESeq2 that estimates expression values for each gene in each sample and then calculates differential expression (309, 312).

As with targeted 16S rRNA gene amplicon sequencing, the DNA can be sequenced in a single end or paired end mode. However, the mouse genome is fully sequenced and can be used as a reference for alignment of the RNA-seq reads. Therefore, while paired end RNA-seq enables discoveries of unknown transcripts or novel splice isoforms, such discovery applications were not the purpose of our study and thus single end was considered sufficient.

## 4.2. General Discussion

Animal models have been developed with aims to minimize factors contributing to variance in human trials. Yet, there is still a reproducibility crisis in animal research (247), where experiments do not let reproduce when put to the test by independent researchers. Another challenge in animal

---

<sup>4</sup> Available from <https://www.bioinformatics.babraham.ac.uk/projects/seqmonk/>

research is the potential bias introduced by the hygienic housing on disease modeling in mice, which may explain the often-unsuccessful translatability of findings from preclinical mouse experiments to human relevance. Thus, a debate lies in whether we should consider embracing the variance to a greater extent also in animal trials, or if we should attempt to control it even more. The latter idea may be the easiest to imagine, for example by microbiota standardization. Moreover, the advancement of alternatives to *in vivo* mouse models such as organoids and lab-on-chip technologies could eventually be important in studying complex interactions difficult to perform and determine causality *in vivo* (313). However, *in vivo* models are still the most widely used tactic to study processes in whole organismal settings. By developing naturalized mice models we could enable both control and relevance, because the different systems can be combined. Our feralization model join a small club of naturalized mouse models, all with their own benefits and limitations. The strategies for naturalizing laboratory mice could be placed on a scale of relevance and control of mouse experiments, ranging from germ-free mice to wild mice (**Figure 8**). Common for them all is the aim of ultimately minimizing the chasm between basic and applied research.

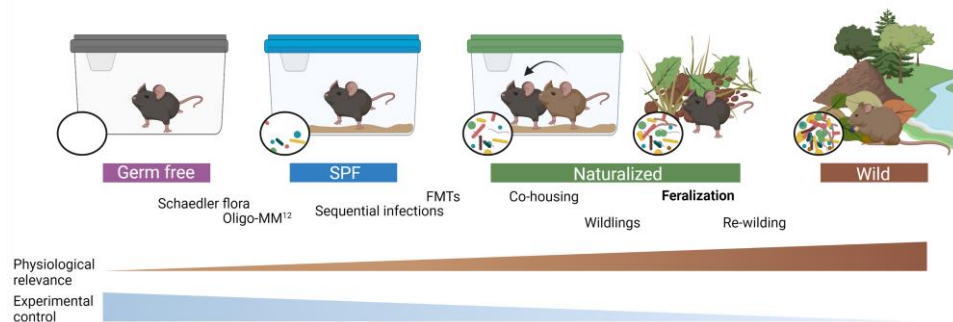


**Figure 8.** Mouse microbial exposure models. Inspired by (256), (261) and (314). Created with biorender.com.

That the microbiota influences the immune system is well-established, and the studies by Rosshart *et al.* showed us that naturalization of laboratory mouse microbiota led to protection against infection and mirrored wild mice immune gene expression profile (235, 236). Yet, the FMT from wild to laboratory mice solely reflect the influence of gut microbiota but neglects potential influence of and interaction with factors in the environment, such as microbiotas elsewhere than in the gut, continuous antigenic experience and

natural behavioral opportunities. Moreover, the general challenges with FMT are that methodological uncertainties exist in almost every step. The handling of fecal material, mode and repetitions of administration play essential roles in the resulting colonization of the recipient gut. Thus, upon transfer of wild mouse microbiota to laboratory mice one cannot be certain that 1. the entire microbial community is in fact transferred, nor 2. the full transferred community is colonized in the recipient gut. The wildlings approach, as well as co-housing, captures not just gut microbiota but microbiota at other locations. However, it is still only microbiota that is naturalized.

An approach to naturalize the laboratory mouse immune system directly is sequential infections and thus construction of exposure histories as shown by Reese *et al.* (258). By such approach, the laboratory mouse immune system is primed and has been shown to better reflect immune system of pet-shop mice and humans. Moreover, they show altered response to vaccines compared to conventional SPF mice, suggesting their potential beneficial use in preclinical investigation for more successful translation (254, 256). However, which combinations of microbes and infectious agents to choose to represent the exposure histories and antigenic experience of wild mice is challenging. Moreover, the exact microorganisms that bring about the best immunological match between mice and human immune systems is far from unraveled.

The two abovementioned approaches are more reductionist strategies to naturalize laboratory mice involving manipulation of microbiotas or antigenic experience directly. Other approaches move towards realism, so that interactive and additive effects of various environmental variables can be studied in a holistic fashion. Our feralization model includes environmental aspects by housing in a full set of natural environmental factors which also allows for species-specific behavior. With this model we can study mice in a naturalistic setting that likely better resembles the situation of a free-living mammal. However, our environment is simulated. We must expect that immunological impact of wilderness go beyond antigenic experience, with neuroendocrine connections, complex behavioral requirements that comes with wild living, and seasonal variation. Temperature have long been known to profoundly influence research mice metabolism, physiology, and immunity (315). Moreover, light-dark cycles influence the type and magnitude of immune responses in the mice because of circadian rhythmical variation in immune cell function and trafficking (257). Additionally, stress and availability of nutritional elements are also likely to influence immune



responses (316). Re-wilding of mice includes these wilderness influences and thus, re-wilding surpasses our model with respect to a full natural environment and maximization of relevance to real-world mammals. However, the high risk of spreading genetically modified mice, chemicals or potential toxins to the surroundings, restricts what kind of experiments can be conducted in a re-wilding system.

An apparent query would be why we do not just study wild mice instead of making such effort in creating naturalized models. This would likely provide us with immunocompetent mice harboring robust microbiotas, but at the expense of genetic homogeneity that the inbred mouse strains inherit, the possibilities for genetic manipulation, as well as control of important variables such as age and nutrition. Moreover, the ethical aspect of studying wild animals should not be circumvented. Therefore, the naturalized mice could be regarded as a bridge between the artificial and the wild, as **Figure 8** emphasize. However, a discussion of whether outbred research mice should be chosen over inbred mice could be raised, though introducing both genetic and environmental variance would necessitate a tremendous number of animals to ensure sufficient power.

The concept of causality comprise that one factor contributes to the effect. The FMT approaches to naturalization can to a larger degree claim causality of studied factors than the other approaches. With studies of feralized mice, as well as re-wilded mice (259, 260), we cannot escape the cons of the holistic approach. This likely leaves us closer to human trials, where variability is tremendous, at the cost of controlling individual factors. We are bringing the laboratory mice closer to a “real world” and cannot demonstrate causality of one single factor. There are numerous factors in the environmental setting of feralized mice we cannot easily control for, or at least we must consider only a few at the time. We introduce “all of them”, then remove some of the most important ones, as shown in the experiments in paper I and III, where we in the first experiments of paper I went all-in and followed up with controlling for one and one factor, such as diet and feral mouse cohabitation, in the later experiments. Yet, natural environmental materials such as soil, dirt, wood, and plant material may allow for sheltering, nesting, social and cognitive stimuli that have been reported on neurological diseases, various immune parameters, and cancers, albeit with some discrepancies between studies (189, 317). However, by testing the environmental material in both pens and

in cages in paper III, we document limited effect of physiological and behavioral consequences of the enlarged space.

Testing of specific mechanisms, drugs, or preventive measures in different systems as illustrated in **Figure 8** would likely give more robust results than solely testing in one of the systems. In our feralization model, the strength of genetically controlled mouse models persists, and studies of genetically controlled feralized mice can complement studies of conventional SPF or GF mice, as demonstrated in three previous reports (262, 318, 319). The costs and ethics of repeating experiments in different systems must be taken into consideration, yet if the resulting findings are more robust and translatable it is likely to spare both money and research animal lives. Moreover, one may find mechanisms that only exist in one environmental setting and not another. It would be interesting in itself to figure out what the environmental setting does to confer such trait.

Although we capture a holistic picture with our feralization model, we believe the microbiota is a central factor in conveying immunological priming. We studied the gut microbiota which represents the largest compartment also important in CRC, yet it is a limitation with our studies to only assess this one compartment. In paper I and III we show inconsistent gut microbiota composition of mice feralized in the two setups. This could be in due to discrepancies related to the 16S rRNA gene amplicon sequencing protocols, and divergence in the source of environmental material as discussed in sections 4.1.2 and 4.1.3.

Host-specific microbiota is essential for efficient immune maturation (214). Because the genome of laboratory strains such as B6 is closest to *M. m. domesticus* (320), the capture of *M. m. domesticus* might have had some advantages over the selected *M. m. musculus* in paper I. However, studies have shown that geographical factors shape the mouse gut microbiota to a greater extent than genotype (239, 321). In our location, *M. m. musculus* dominates, although we are situated in a hybrid zone between the two species (322). Indeed, trial and error in our group has shown that both types, and even hybrids, were caught within a short radius. In fact, this led to a genotypic discovery, as the *M. musculus* subspecies were found to carry an aberrant form of the CD94 receptor in NK cells (323). While we could have made efforts to secure *M. m. domesticus* individuals, it is doubtful that this would have altered our findings any more than other factors. The gut microbiota of both

wild mice and humans has been shown to vary dependent on location (237, 324, 325).

Proteobacteria is the most diverse of phyla, and its members includes well-known opportunistic pathogens such as *Salmonella* spp. and *E. coli*. This phylum is often reported in association with diseases in both mice and humans (326, 327). However, Proteobacteria could also be important in maintenance of a healthy microbiota. The majority of gut microbes are anaerobic, while Proteobacteria are mostly facultative or obligately anaerobic, meaning they often consume oxygen and contribute to lowering redox potential, which in turn could allow for colonization of other anaerobic bacteria. In humans, Proteobacteria has, in spite of its low abundance, been shown to contribute to much of the functional variation in the gut microbiome (328). That naturalized mice often show an enrichment of Proteobacteria species, also seen in wild mice, is indicative of this being a natural component of a wild, healthy microbiota. We saw a bloom of Proteobacteria species in feralized mice in paper I and the Min/+ trial of paper III, both of which found place in the first version of the pens and were given environmental enrichment from the same source. However, the closest species similarities showed no consistent pattern, with *Desulfovibrio vulgaris* enriched in feralized Min/+ mice, while *Helicobacter* spp. were enriched in the feralized mice of paper I. The sequence similarity was relatively low for *Desulfovibrio vulgaris*, indicating a low resolution of these data and the sequence may belong to another species. An enrichment of *Helicobacter* spp. was also detected in feces from the feralized B6 mice in paper III. *Helicobacter* spp. are included in the SPF list and were not detected in any of our laboratory mice, while it is likely a natural component of the microbiome of wild mice (231, 232, 234, 235). For their association with disease in certain mouse strains, many consider rodent *Helicobacter* species to be pathobionts. *Helicobacter* spp. is often used in immunocompromised mice such as IL-10 knock-out mice to study IBD. Yet, when colonized in wild-type B6 mice, no inflammation and only minimal changes in cytokine gene expression has been seen (329). Thus, *Helicobacter* species may not initiate inflammatory responses in immunocompetent B6 mice directly, but rather provoke inflammation initiated by other species in immunodeficient states. In paper III, the feralized B6 mice harbored *Campylobacter jejuni*, which is another species found in wild mice, although in *Mus minutus* and not *Mus musculus* (330).

The influence of feralization on *alpha*-diversity differed between the herein presented studies. The mice feralized in presence of feral mice (paper I) showed higher richness and effective Shannon counts than laboratory mice, indicating a higher diversity of species in the feralized mice. On the contrary, the mice feralized in absence of feral mice (paper III) showed a similar richness and lower effective Shannon counts than laboratory mice, indicating a gut microbiota where fewer species dominate. However, the richness and effective Shannon counts were unchanged from baseline to endpoint in feral mice (paper I), and in the mice feralized from birth (paper III). Accompanied by minimal changes in composition over time compared to the laboratory mice, these findings point towards a stability of the feral and feralized microbiome, which may be more robust to perturbances such as the CRC induction.

Despite the need to decipher roles of individual components of the gut microbiota in health and disease, recent focus has been directed towards community rather than specific bacterial species. Laboratory mice microbiota may be vulnerable as may be hypothesized for the human industrialized microbiota (331). Massive changes seen in studies with laboratory mice following interventions could perhaps be in due to their suboptimal microbiota. The laboratory mice establish gut microbes that exist in their environment. With the limited diversity of microbes in their environment and consequently little competition in colonization, the resulting microbial composition may be suboptimal and vulnerable for external perturbances. Studies have shown that wild mice microbiotas are stable over time and resilient to environmental challenges (236), which may be more comparable to humans.

We are assuming the microbes in the environment are important in CRC protection, as previous studies have implied. However, the causal driving factors for the observed CRC protection following feralization will need further mechanistic studies. Therefore, we only claim that CRC protection seen following feralization is likely connected to gut microbiota modifications yet can be in due to other factors. As mentioned in section 4.1.3, we solely assessed the bacterial portion of the gut microbiota, and we have no control over potential transkingdom interactions. Helminths, protozoa and ectoparasites were present in feralized co-housed mice in paper I but were not found in the feralized mice in paper III, indicating that the feral mice were likely the parasite source in the former study. That the feral mice were

exposed to such parasites, as well as other natural factors, for a long time would explain the enhanced immune parameters in feral mice compared to feralized mice. However, our findings suggest parasitic exposure are not essential in protection against CRC as reported in paper III.

Concerning the immune system of our feralized mice, we found higher relative numbers of CD44<sup>+</sup> CD8<sup>+</sup> T cells in lymph nodes and spleens of B6 mice feralized both in presence and absence of feral mice (papers I and III). Moreover, the higher relative numbers of KLRG1<sup>+</sup> NK cells, and mature NK cells (papers I and III), are all findings consistent with previous reports of immunophenotypes in wild and naturalized mice (231, 234). We did however also notice inconsistent findings in the immunophenotypes, such as in assessment of Tregs, where the feral mice in paper I showed a lower proportion of Foxp3<sup>+</sup> CD4<sup>+</sup> T cells, but a higher proportion of pTregs (NRP1<sup>-</sup>) in their lymph nodes, which may indicate Tregs induced in the gut mucosa (30). This was not reproduced in the feralized mice, and whether this is a “good” or “bad” thing is more challenging to determine since the Foxp3<sup>+</sup> cells are heterogenous and include cells of various functions (332). Thus, additional markers of functional Treg subsets would need assessment in future studies. An additional note is that we did not assess all the same immune parameters in papers I and III, yet of the common parameters we found overall similar immunophenotypes and response to *ex vivo* stimulation independently of the presence of feral mice.

An important inquiry is whether the altered immunophenotype and function in the feralized mice mean improved immunity. We tried to show this with respect to CRC in the trials presented in paper III. Enhanced IFN- $\gamma$ -secretion in response to stimuli was seen in feralized mice, both in paper I and III. Given the importance of CD8<sup>+</sup> T cell and NK cell responses in cancer combat, our findings suggest the maturation of these cell types and improved response could be, at least in part, responsible for the CRC protection in feralized mice.

Based on previous studies demonstrating a thicker mucus layer in feral mice (271), and that gut microbiota can shape the mucus layer composition (105, 271), we hypothesized that the protection against CRC in feralized mice could be in due to changes in the intestinal mucosal barrier including the mucus layer. The microbiota data from this study showed minimal differences between feralized and laboratory mice, which was in contrast to the findings from paper I and III. Yet, the data from paper IV were obtained from caecums

in male mice, in contrast to feces from female mice in papers I and II, meaning there are many factors influencing the microbiota composition that prevent a meaningful comparison between the papers.

We found no differences in the mucus layer and RNA sequencing of the colonic mucosal tissue revealed only a limited number of differentially expressed genes between feralized and laboratory mice. However, some of the genes upregulated in feralized mice encode the known mucus components *Fcgbp* and *Cla1* (333-335), suggesting that the mucus layer could still be enforced. Other genes encode proteins involved in bacterial defense mechanisms, such as *Itn1* (336, 337), proposing that feralized mice may have improved bacterial defense. Yet, we cannot distinguish whether gene expression in single cell populations differed across the two groups, and the data presented in paper IV point towards the necessity of conducting more specialized analyses to decipher and generate hypothesis of potential protective effects of feralization.

## 5. Main Conclusions

---

This study present and characterize a novel approach to naturalize laboratory mice by feralization in a farmyard-like habitat. Thus, this work contributes to further enable the potential of moving the conditions of research mice closer to a real-world situation that may better reflect a human situation. This work also contributes to highlighting the importance of choice of protocol, outcome measure, and focus on animal welfare in mouse disease models by reporting the usefulness of reducing the dose of DSS in the common AOM/DSS model; that detection of preneoplastic colonic lesions can be reliably detected in B6 and A/J mice while persistent severe symptoms are limited.

Feralization of B6 mice in a naturalistic farmyard-type habitat with feral mice cohabitants result in immunophenotypes indicative of antigenic experience, with higher levels of effector and central memory T cells, and KLRG1 expression on NK cells. This type of feralization also bring about a shift in gut microbiota profile from SPF-like to feral-like. Feralization in a naturalistic farmyard-type habitat, without feral cohabitants, is sufficient in shifting the gut microbiota profile of A/J Min/+ mice and wild-type B6 mice and protect them against genetic and chemically induced colorectal carcinogenesis, respectively. Upon chemical CRC induction, the feralized gut microbiota remains stable, while the laboratory gut microbiota shifts substantially. When compared to laboratory reared mice, both mice feralized from birth and later in life are protected against chemically induced CRC, downplaying the role of early microbial exposure. Last, assessment of intestinal barrier function revealed inconclusive results but suggests that an enhanced barrier could contribute to the beneficial effects of feralization, yet this hypothesis inquire further assessment.

Overall, the results of the present study facilitate further investigations into naturalized mice models in general, and the use of the feralization model in particular.

## 6. Future Perspectives

---

We have established a model framework for naturalizing laboratory mice in a farmyard-like habitat and demonstrated the utility of such approach in CRC disease models. However, many questions remain unanswered.

The possibilities for employing the feralization model are endless, but an important future perspective is to determine a best practice of the feralization system. The establishment of the feralization system is finished, but the characterization has only just begun. To establish the most appropriate use of the feralization system, additional factors and aspects need characterization. Till now, we have seen that laboratory mice feralized in presence and absence of feral mice show signs of more primed and mature immune cells accompanied by gut microbiota shifts. However, the relative contributions of mouse-specific and environment-specific factors remains to be deciphered. Moreover, contributions of other microbiota components than the bacterial, such as fungi and archaea, needs assessment.

We believe that the feralization model and other naturalization models can be used in combination with traditional reductionist studies in search of both accuracy in reflecting true responses and precision in determining biological mechanisms. However, we only rely on previous reports of naturalized mice better resembling humans than conventionally housed laboratory mice. Validation of results from trials with feralized mice with findings and data from human trials should be conducted to describe how well they translate. A similar retrospective bench-to-bedside strategy as employed by Rosshart *et al.* (236) would be an elegant continuation of the work with characterization of the feralization model.

Down the line, future studies should aim to combine feralization and more reductionist studies to unravel the mechanisms by which feralization may reduce susceptibility to CRC and potential implications in improving the translational value of immunotherapeutic studies. We have focused on T and NK cells, but as much as there are populations of these cells we have not yet assessed, there are also many other immune cell types that play important roles that should be investigated in the future. Moreover, paper IV reveals that future studies should address various intestinal regions and assess specific intestinal cells populations. Assessment of epigenetic modifications associated with immune training would also be an interesting outlook.



## 7. References

---

1. Abbas A, Lichtman A, Pillai S. Cellular and molecular immunology. 9th ed. Philadelphia: Elsevier; 2018.
2. Lewis SM, Williams A, Eisenbarth SC. Structure and function of the immune system in the spleen. *Sci Immunol*. 2019;4(33):eaau6085.
3. Bronte V, Pittet MJ. The spleen in local and systemic regulation of immunity. *Immunity*. 2013;39(5):806-18.
4. Amarante-Mendes GP, Adjemian S, Branco LM, et al. Pattern Recognition Receptors and the Host Cell Death Molecular Machinery. *Front Immunol*. 2018;9(2379).
5. Long EO, Kim HS, Liu D, et al. Controlling natural killer cell responses: integration of signals for activation and inhibition. *Annu Rev Immunol*. 2013;31:227-58.
6. Huntington ND, Tabarias H, Fairfax K, et al. NK cell maturation and peripheral homeostasis is associated with KLRG1 up-regulation. *J Immunol*. 2007;178(8):4764-70.
7. Goh W, Huntington ND. Regulation of Murine Natural Killer Cell Development. *Front Immunol*. 2017;8(130).
8. Nabekura T, Lanier LL. Tracking the fate of antigen-specific versus cytokine-activated natural killer cells after cytomegalovirus infection. *J Exp Med*. 2016;213(12):2745-58.
9. Fu B, Wang F, Sun R, et al. CD11b and CD27 reflect distinct population and functional specialization in human natural killer cells. *Immunology*. 2011;133(3):350-9.
10. Na YR, Stakenborg M, Seok SH, et al. Macrophages in intestinal inflammation and resolution: a potential therapeutic target in IBD. *Nat Rev Gastroenterol Hepatol*. 2019;16(9):531-43.
11. Netea MG, Joosten LA, Latz E, et al. Trained immunity: A program of innate immune memory in health and disease. *Science*. 2016;352(6284).
12. Netea MG, Quintin J, van der Meer JW. Trained immunity: a memory for innate host defense. *Cell Host Microbe*. 2011;9(5):355-61.
13. Netea MG, Domínguez-Andrés J, Barreiro LB, et al. Defining trained immunity and its role in health and disease. *Nat Rev Immunol*. 2020;20(6):375-88.
14. Geginat J, Paroni M, Maglie S, et al. Plasticity of Human CD4 T Cell Subsets. *Front Immunol*. 2014;5(630).
15. Chewing JH, Weaver CT. Development and Survival of Th17 Cells within the Intestines: The Influence of Microbiome- and Diet-Derived Signals. *J Immunol*. 2014;193(10):4769-77.
16. Zhang N, Bevan Michael J. CD8+ T Cells: Foot Soldiers of the Immune System. *Immunity*. 2011;35(2):161-8.
17. Wherry EJ, Teichgraber V, Becker TC, et al. Lineage relationship and protective immunity of memory CD8 T cell subsets. *Nat Immunol*. 2003;4(3):225-34.
18. Jameson SC, Masopust D. Understanding Subset Diversity in T Cell Memory. *Immunity*. 2018;48(2):214-26.
19. Masopust D, Soerens AG. Tissue-Resident T Cells and Other Resident Leukocytes. *Annu Rev Immunol*. 2019;37:521-46.

20. Wijeyesinghe S, Beura LK, Pierson MJ, et al. Expansile residence decentralizes immune homeostasis. *Nature*. 2021;592(7854):457-62.
21. Fontenot JD, Gavin MA, Rudensky AY. Foxp3 programs the development and function of CD4+CD25+ regulatory T cells. *Nat Immunol*. 2003;4(4):330-6.
22. Khattri R, Cox T, Yasayko SA, et al. An essential role for Scurfin in CD4+CD25+ T regulatory cells. *Nat Immunol*. 2003;4(4):337-42.
23. Hori S, Nomura T, Sakaguchi S. Control of regulatory T cell development by the transcription factor Foxp3. *Science*. 2003;299(5609):1057-61.
24. Kitagawa Y, Ohkura N, Sakaguchi S. Molecular Determinants of Regulatory T Cell Development: The Essential Roles of Epigenetic Changes. *Front Immunol*. 2013;4(106).
25. Shevach EM. Mechanisms of Foxp3+ T Regulatory Cell-Mediated Suppression. *Immunity*. 2009;30(5):636-45.
26. Tanoue T, Atarashi K, Honda K. Development and maintenance of intestinal regulatory T cells. *Nat Rev Immunol*. 2016;16(5):295-309.
27. Shevryev D, Tereshchenko V. Treg Heterogeneity, Function, and Homeostasis. *Front Immunol*. 2020;10(3100).
28. Savage PA, Klawon DEJ, Miller CH. Regulatory T Cell Development. *Annu Rev Immunol*. 2020;38(1):421-53.
29. Singh K, Hjort M, Thorvaldson L, et al. Concomitant analysis of Helios and Neuropilin-1 as a marker to detect thymic derived regulatory T cells in naïve mice. *Sci Rep*. 2015;5:7767.
30. Weiss JM, Bilate AM, Gobert M, et al. Neuropilin 1 is expressed on thymus-derived natural regulatory T cells, but not mucosa-generated induced Foxp3+ T reg cells. *J Exp Med*. 2012;209(10):1723-42.
31. Yadav M, Stephan S, Bluestone JA. Peripherally induced tregs - role in immune homeostasis and autoimmunity. *Front Immunol*. 2013;4:232.
32. Alhabbab RY, Nova-Lamperti E, Aravena O, et al. Regulatory B cells: Development, phenotypes, functions, and role in transplantation. *Immunol Rev*. 2019;292(1):164-79.
33. Veglia F, Sanseviero E, Gabrilovich DI. Myeloid-derived suppressor cells in the era of increasing myeloid cell diversity. *Nat Rev Immunol*. 2021;21(8):485-98.
34. Binder HJ. Organization of the gastrointestinal system. In: Boron WF, Boulpaep EL. *Medical physiology: A cellular and molecular approach*. 2nd ed. Philadelphia, United States: Saunders/Elsevier; 2012.
35. Barrett KE. Functional Anatomy of the GI Tract and Organs Draining into It. In *Gastrointestinal Physiology, 2e*. New York, NY: The McGraw-Hill Companies; 2014.
36. Moore KL, Dalley AF, Agur AMR. Chapter 2 Abdomen. In *Clinically Oriented Anatomy*. 6th ed. Philadelphia, USA: Wolters Kluwer Health/Lippincott Williams & Wilkins; 2010.
37. Binder HJ, Reuben A. Nutrient digestion and absorption. In: Boron WF, Boulpaep EL. *Medical physiology: A cellular and molecular approach*. 2nd ed. Philadelphia, United States: Saunders/Elsevier; 2012.
38. Barrett KE. Bile Formation and Secretion. In *Gastrointestinal Physiology, 2e*. New York, NY: The McGraw-Hill Companies; 2014.

39. Suchy FJ. Hepatobiliary function. In: Boron WF, Boulpaep EL. *Medical physiology: A cellular and molecular approach*. 2nd ed. Philadelphia, United States: Saunders/Elsevier; 2012.
40. Barrett KE. Carbohydrate, Protein, and Water-Soluble Vitamin Assimilation. In *Gastrointestinal Physiology, 2e*. New York, NY: The McGraw-Hill Companies; 2014.
41. Barrett KE. Water and Electrolyte Absorption and Secretion. In *Gastrointestinal Physiology, 2e*. New York, NY: The McGraw-Hill Companies; 2014.
42. Binder HJ. Intestinal fluid and electrolyte movement. In: Boron WF, Boulpaep EL. *Medical physiology: A cellular and molecular approach*. 2nd ed. Philadelphia, United States: Saunders/Elsevier; 2012.
43. Johansson MEV, Sjövall H, Hansson GC. The gastrointestinal mucus system in health and disease. *Nat Rev Gastroenterol Hepatol*. 2013;10(6):352-61.
44. Flier LGvd, Clevers H. Stem Cells, Self-Renewal, and Differentiation in the Intestinal Epithelium. *Annu Rev Physiol*. 2009;71(1):241-60.
45. Garcia M, Nelson W, Chavez N. Cell-Cell Junctions Organize Structural and Signaling Networks. *Cold Spring Harb Perspect Biol*. 2018;10(4):a029181.
46. Koren O, Ley RE. The human intestinal microbiota and microbiome. In: Podolsky DK, Camilleri M, Fitz JG, Kalloo AN, Shanahan F, Wang TC. *Yamada's Textbook of Gastroenterology*. 6th ed: John Wiley & Sons, Ltd.; 2016.
47. Foster KR, Schluter J, Coyte KZ, et al. The evolution of the host microbiome as an ecosystem on a leash. *Nature*. 2017;548(7665):43-51.
48. Rook G, Backhed F, Levin BR, et al. Evolution, human-microbe interactions, and life history plasticity. *Lancet*. 2017;390(10093):521-30.
49. Simon J-C, Marchesi JR, Mougel C, et al. Host-microbiota interactions: from holobiont theory to analysis. *Microbiome*. 2019;7(1):5.
50. McFall-Ngai M, Hadfield MG, Bosch TCG, et al. Animals in a bacterial world, a new imperative for the life sciences. *Proc Natl Acad Sci U S A*. 2013;110(9):3229-36.
51. Tringe SG, Hugenholtz P. A renaissance for the pioneering 16S rRNA gene. *Curr Opin Microbiol*. 2008;11(5):442-6.
52. Neefs JM, Van de Peer Y, De Rijk P, et al. Compilation of small ribosomal subunit RNA structures. *Nucleic Acids Res*. 1993;21(13):3025-49.
53. Sender R, Fuchs S, Milo R. Revised Estimates for the Number of Human and Bacteria Cells in the Body. *PLoS Biol*. 2016;14(8):e1002533.
54. Donaldson GP, Lee SM, Mazmanian SK. Gut biogeography of the bacterial microbiota. *Nat Rev Microbiol*. 2016;14(1):20-32.
55. Moeller AH, Suzuki TA, Phifer-Rixey M, et al. Transmission modes of the mammalian gut microbiota. *Science*. 2018;362(6413):453-7.
56. Hornef MW, Torow N. 'Layered immunity' and the 'neonatal window of opportunity' - timed succession of non-redundant phases to establish mucosal host-microbial homeostasis after birth. *Immunology*. 2020;159(1):15-25.
57. Arrieta MC, Stiemsma LT, Amenyogbe N, et al. The intestinal microbiome in early life: health and disease. *Front Immunol*. 2014;5:427.
58. Gensollen T, Iyer SS, Kasper DL, et al. How colonization by microbiota in early life shapes the immune system. *Science*. 2016;352(6285):539-44.

59. Tanaka M, Nakayama J. Development of the gut microbiota in infancy and its impact on health in later life. *Allergol Int.* 2017;66(4):515-22.
60. Gomez de Agüero M, Ganal-Vonarburg SC, Fuhrer T, et al. The maternal microbiota drives early postnatal innate immune development. *Science.* 2016;351(6279):1296-302.
61. Milani C, Duranti S, Bottacini F, et al. The First Microbial Colonizers of the Human Gut: Composition, Activities, and Health Implications of the Infant Gut Microbiota. *Microbiology and Molecular Biology Reviews.* 2017;81(4).
62. Salminen S, Gibson GR, McCartney AL, et al. Influence of mode of delivery on gut microbiota composition in seven year old children. *Gut.* 2004;53(9):1388-9.
63. Birchenough GM, Nyström EE, Johansson ME, et al. A sentinel goblet cell guards the colonic crypt by triggering Nlrp6-dependent Muc2 secretion. *Science.* 2016;352(6293):1535-42.
64. Mowat AM, Agace WW. Regional specialization within the intestinal immune system. *Nat Rev Immunol.* 2014;14:667.
65. Russell MW, Kilian M, Mantis NJ, et al. Chapter 21 - Biological Activities of IgA. In: Mestecky J, Strober W, Russell MW, Kelsall BL, Cheroutre H, Lambrecht BN. *Mucosal Immunology (Fourth Edition).* Boston: Academic Press; 2015. p. 429-54.
66. Jahnsen FL, Bækkevold ES, Hov JR, et al. Do Long-Lived Plasma Cells Maintain a Healthy Microbiota in the Gut? *Trends Immunol.* 2018;39(3):196-208.
67. Hoces D, Arnoldini M, Diard M, et al. Growing, evolving and sticking in a flowing environment: understanding IgA interactions with bacteria in the gut. *Immunology.* 2020;159(1):52-62.
68. McDonald BD, Jabri B, Bendelac A. Diverse developmental pathways of intestinal intraepithelial lymphocytes. *Nat Rev Immunol.* 2018;18(8):514-25.
69. Goto Y. Epithelial Cells as a Transmitter of Signals From Commensal Bacteria and Host Immune Cells. *Front Immunol.* 2019;10(2057).
70. Burgueño JF, Abreu MT. Epithelial Toll-like receptors and their role in gut homeostasis and disease. *Nat Rev Gastroenterol Hepatol.* 2020;17(5):263-78.
71. Bain CC, Mowat AM. Macrophages in intestinal homeostasis and inflammation. *Immunol Rev.* 2014;260(1):102-17.
72. Wang S, Ye Q, Zeng X, et al. Functions of Macrophages in the Maintenance of Intestinal Homeostasis. *J Immunol Res.* 2019;2019:1512969.
73. Niess JH, Brand S, Gu X, et al. CX3CR1-mediated dendritic cell access to the intestinal lumen and bacterial clearance. *Science.* 2005;307(5707):254-8.
74. Mabbott NA, Donaldson DS, Ohno H, et al. Microfold (M) cells: important immunosurveillance posts in the intestinal epithelium. *Mucosal Immunology.* 2013;6(4):666-77.
75. Knoop KA, McDonald KG, McCrate S, et al. Microbial sensing by goblet cells controls immune surveillance of luminal antigens in the colon. *Mucosal Immunology.* 2015;8(1):198-210.
76. Brown EM, Sadarangani M, Finlay BB. The role of the immune system in governing host-microbe interactions in the intestine. *Nat Immunol.* 2013;14(7):660-7.
77. Mowat AM. To respond or not to respond - a personal perspective of intestinal tolerance. *Nat Rev Immunol.* 2018;18(6):405-15.

78. Lycke NY, Bemark M. The regulation of gut mucosal IgA B-cell responses: recent developments. *Mucosal Immunol.* 2017;10(6):1361-74.
79. Rinninella E, Cintoni M, Raoul P, et al. Food Components and Dietary Habits: Keys for a Healthy Gut Microbiota Composition. *Nutrients.* 2019;11(10):2393.
80. So D, Whelan K, Rossi M, et al. Dietary fiber intervention on gut microbiota composition in healthy adults: a systematic review and meta-analysis. *Am J Clin Nutr.* 2018;107(6):965-83.
81. den Besten G, van Eunen K, Groen AK, et al. The role of short-chain fatty acids in the interplay between diet, gut microbiota, and host energy metabolism. *J Lipid Res.* 2013;54(9):2325-40.
82. O'Keefe SJ. Diet, microorganisms and their metabolites, and colon cancer. *Nat Rev Gastroenterol Hepatol.* 2016;13(12):691-706.
83. Corrêa-Oliveira R, Fachi JL, Vieira A, et al. Regulation of immune cell function by short-chain fatty acids. *Clin Transl Immunology.* 2016;5(4):e73-e.
84. Furusawa Y, Obata Y, Fukuda S, et al. Commensal microbe-derived butyrate induces the differentiation of colonic regulatory T cells. *Nature.* 2013;504(7480):446-50.
85. Smith PM, Howitt MR, Panikov N, et al. The Microbial Metabolites, Short-Chain Fatty Acids, Regulate Colonic Treg Cell Homeostasis. *Science.* 2013;341(6145):569-73.
86. Louis P, Young P, Holtrop G, et al. Diversity of human colonic butyrate-producing bacteria revealed by analysis of the butyryl-CoA:acetate CoA-transferase gene. *Environ Microbiol.* 2010;12(2):304-14.
87. Duncan SH, Holtrop G, Lobley GE, et al. Contribution of acetate to butyrate formation by human faecal bacteria. *Br J Nutr.* 2004;91(6):915-23.
88. Louis P, Flint HJ. Diversity, metabolism and microbial ecology of butyrate-producing bacteria from the human large intestine. *FEMS Microbiol Lett.* 2009;294(1):1-8.
89. Louis P, Flint HJ. Formation of propionate and butyrate by the human colonic microbiota. *Environ Microbiol.* 2017;19(1):29-41.
90. Mokkala K, Houttu N, Cansev T, et al. Interactions of dietary fat with the gut microbiota: Evaluation of mechanisms and metabolic consequences. *Clinical Nutrition.* 2020;39(4):994-1018.
91. Zheng X, Huang F, Zhao A, et al. Bile acid is a significant host factor shaping the gut microbiome of diet-induced obese mice. *BMC Biol.* 2017;15(1):120.
92. de Aguiar Vallim Thomas Q, Tarling Elizabeth J, Edwards Peter A. Pleiotropic Roles of Bile Acids in Metabolism. *Cell Metabolism.* 2013;17(5):657-69.
93. Zeng H, Umar S, Rust B, et al. Secondary Bile Acids and Short Chain Fatty Acids in the Colon: A Focus on Colonic Microbiome, Cell Proliferation, Inflammation, and Cancer. *Int J Mol Sci.* 2019;20(5).
94. David LA, Materna AC, Friedman J, et al. Host lifestyle affects human microbiota on daily timescales. *Genome Biol.* 2014;15(7):R89.
95. Wu GD, Chen J, Hoffmann C, et al. Linking long-term dietary patterns with gut microbial enterotypes. *Science.* 2011;334(6052):105-8.
96. Faith JJ, Guruge JL, Charbonneau M, et al. The Long-Term Stability of the Human Gut Microbiota. *Science.* 2013;341(6141):1237439.

97. Fassarella M, Blaak EE, Penders J, et al. Gut microbiome stability and resilience: elucidating the response to perturbations in order to modulate gut health. *Gut*. 2021;70(3):595-605.
98. Tasnim N, Abulizi N, Pither J, et al. Linking the Gut Microbial Ecosystem with the Environment: Does Gut Health Depend on Where We Live? *Front Microbiol*. 2017;8(1935).
99. Zhou D, Zhang H, Bai Z, et al. Exposure to soil, house dust and decaying plants increases gut microbial diversity and decreases serum immunoglobulin E levels in BALB/c mice. *Environ Microbiol*. 2016;18(5):1326-37.
100. Liu W, Sun Z, Ma C, et al. Exposure to soil environments during earlier life stages is distinguishable in the gut microbiome of adult mice. *Gut Microbes*. 2021;13(1):1830699.
101. Roslund MI, Puhakka R, Grönroos M, et al. Biodiversity intervention enhances immune regulation and health-associated commensal microbiota among daycare children. *Sci Adv*. 2020;6(42):eaba2578.
102. Parajuli A, Hui N, Puhakka R, et al. Yard vegetation is associated with gut microbiota composition. *Sci Total Environ*. 2020;713:136707.
103. Zheng D, Liwinski T, Elinav E. Interaction between microbiota and immunity in health and disease. *Cell Research*. 2020;30(6):492-506.
104. Round JL, Mazmanian SK. The gut microbiota shapes intestinal immune responses during health and disease. *Nat Rev Immunol*. 2009;9(5):313-23.
105. Johansson ME, Jakobsson HE, Holmén-Larsson J, et al. Normalization of Host Intestinal Mucus Layers Requires Long-Term Microbial Colonization. *Cell Host Microbe*. 2015;18(5):582-92.
106. Atarashi K, Tanoue T, Ando M, et al. Th17 Cell Induction by Adhesion of Microbes to Intestinal Epithelial Cells. *Cell*. 2015;163(2):367-80.
107. Ivanov II, Frutos RdL, Manel N, et al. Specific microbiota direct the differentiation of IL-17-producing T-helper cells in the mucosa of the small intestine. *Cell Host Microbe*. 2008;4(4):337-49.
108. Bachem A, Makhlof C, Binger KJ, et al. Microbiota-Derived Short-Chain Fatty Acids Promote the Memory Potential of Antigen-Activated CD8+ T Cells. *Immunity*. 2019;51(2):285-97.e5.
109. Scott NA, Andrusaite A, Andersen P, et al. Antibiotics induce sustained dysregulation of intestinal T cell immunity by perturbing macrophage homeostasis. *Sci Transl Med*. 2018;10(464):eaa04755.
110. Hviid A, Svanström H, Frisch M. Antibiotic use and inflammatory bowel diseases in childhood. *Gut*. 2011;60(1):49-54.
111. Pickard JM, Zeng MY, Caruso R, et al. Gut microbiota: Role in pathogen colonization, immune responses, and inflammatory disease. *Immunol Rev*. 2017;279(1):70-89.
112. Kamada N, Chen GY, Inohara N, et al. Control of pathogens and pathobionts by the gut microbiota. *Nat Immunol*. 2013;14(7):685-90.
113. Ramakrishna C, Kujawski M, Chu H, et al. *Bacteroides fragilis* polysaccharide A induces IL-10 secreting B and T cells that prevent viral encephalitis. *Nat Commun*. 2019;10(1):2153.

114. Erturk-Hasdemir D, Oh SF, Okan NA, et al. Symbionts exploit complex signaling to educate the immune system. *Proc Natl Acad Sci U S A*. 2019;116(52):26157-66.
115. Donaldson GP, Ladinsky MS, Yu KB, et al. Gut microbiota utilize immunoglobulin A for mucosal colonization. *Science*. 2018;360(6390):795-800.
116. Flannigan KL, Denning TL. Segmented filamentous bacteria-induced immune responses: a balancing act between host protection and autoimmunity. *Immunology*. 2018;154(4):537-46.
117. Omenetti S, Bussi C, Metidji A, et al. The Intestine Harbors Functionally Distinct Homeostatic Tissue-Resident and Inflammatory Th17 Cells. *Immunity*. 2019;51(1):77-89.e6.
118. Strachan DP. Hay fever, hygiene, and household size. *BMJ*. 1989;299(6710):1259-60.
119. Rook GAW, Brunet LR. Microbes, immunoregulation, and the gut. *Gut*. 2005;54(3):317-20.
120. Bloomfield SF, Rook GA, Scott EA, et al. Time to abandon the hygiene hypothesis: new perspectives on allergic disease, the human microbiome, infectious disease prevention and the role of targeted hygiene. *Perspectives in public health*. 2016;136(4):213-24.
121. von Hertzen L, Hanski I, Haahela T. Natural immunity. Biodiversity loss and inflammatory diseases are two global megatrends that might be related. *EMBO Rep*. 2011;12(11):1089-93.
122. Haahela T. A biodiversity hypothesis. *Allergy*. 2019;74(8):1445-56.
123. von Mutius E. The microbial environment and its influence on asthma prevention in early life. *J Allergy Clin Immunol*. 2016;137(3):680-9.
124. Birzele LT, Depner M, Ege MJ, et al. Environmental and mucosal microbiota and their role in childhood asthma. *Allergy*. 2017;72(1):109-19.
125. Stein MM, Hrusch CL, Gozdz J, et al. Innate Immunity and Asthma Risk in Amish and Hutterite Farm Children. *N Engl J Med*. 2016;375(5):411-21.
126. Tual S, Lemarchand C, Boulanger M, et al. Exposure to Farm Animals and Risk of Lung Cancer in the AGRICAN Cohort. *Am J Epidemiol*. 2017;186(4):463-72.
127. Soon IS, Molodecky NA, Rabi DM, et al. The relationship between urban environment and the inflammatory bowel diseases: a systematic review and meta-analysis. *BMC Gastroenterol*. 2012;12(1):51.
128. Mills JG, Brookes JD, Gellie NJC, et al. Relating Urban Biodiversity to Human Health With the 'Holobiont' Concept. *Front Microbiol*. 2019;10(550).
129. Olszak T, An D, Zeissig S, et al. Microbial exposure during early life has persistent effects on natural killer T cell function. *Science*. 2012;336(6080):489-93.
130. Liddicoat C, Sydnor H, Cando-Dumancela C, et al. Naturally-diverse airborne environmental microbial exposures modulate the gut microbiome and may provide anxiolytic benefits in mice. *Sci Total Environ*. 2020;701:134684.
131. Ottman N, Ruokolainen L, Suomalainen A, et al. Soil exposure modifies the gut microbiota and supports immune tolerance in a mouse model. *J Allergy Clin Immunol*. 2019;143(3):1198-206.e12.
132. Frossard CP, Lazarevic V, Gaïa N, et al. The farming environment protects mice from allergen-induced skin contact hypersensitivity. *Clinical & Experimental Allergy*. 2017;47(6):805-14.

133. Dekker E, Tanis PJ, Vleugels JLA, et al. Colorectal cancer. *Lancet*. 2019;394(10207):1467-80.
134. World Health Organization (WHO): International Agency for Research on Cancer. Globocan 2020: Cancer Fact Sheets — Colorectal Cancer. Available from: [https://gco.iarc.fr/today/data/factsheets/cancers/10\\_8\\_9-Colorectum-fact-sheet.pdf](https://gco.iarc.fr/today/data/factsheets/cancers/10_8_9-Colorectum-fact-sheet.pdf) [Accessed 8 Jun 2021].
135. Arnold M, Sierra MS, Laversanne M, et al. Global patterns and trends in colorectal cancer incidence and mortality. *Gut*. 2017;66(4):683-91.
136. Ferlay J, Ervik M, Lam F, et al. Global Cancer Observatory: Cancer Today. Lyon: International Agency for Research on Cancer; 2020. Available from: <https://gco.iarc.fr/today> [Accessed 8 Jun 2021].
137. Keum N, Giovannucci E. Global burden of colorectal cancer: emerging trends, risk factors and prevention strategies. *Nat Rev Gastroenterol Hepatol*. 2019;16(12):713-32.
138. Jasperson KW, Tuohy TM, Neklason DW, et al. Hereditary and familial colon cancer. *Gastroenterology*. 2010;138(6):2044-58.
139. Nguyen LH, Goel A, Chung DC. Pathways of Colorectal Carcinogenesis. *Gastroenterology*. 2020;158(2):291-302.
140. Tariq K, Ghias K. Colorectal cancer carcinogenesis: a review of mechanisms. *Cancer Biol Med*. 2016;13(1):120-35.
141. Stevens RG, Swede H, Rosenberg DW. Epidemiology of colonic aberrant crypt foci: Review and analysis of existing studies. *Cancer Lett*. 2007;252(2):171-83.
142. Kukitsu T, Takayama T, Miyanishi K, et al. Aberrant Crypt Foci as Precursors of the Dysplasia-Carcinoma Sequence in Patients with Ulcerative Colitis. *Clin Cancer Res*. 2008;14(1):48-54.
143. Fearon ER, Vogelstein B. A genetic model for colorectal tumorigenesis. *Cell*. 1990;61(5):759-67.
144. Brennan CA, Garrett WS. Gut Microbiota, Inflammation, and Colorectal Cancer. *Annu Rev Microbiol*. 2016;70:395-411.
145. Gregorieff A, Clevers H. Wnt signaling in the intestinal epithelium: from endoderm to cancer. *Genes Dev*. 2005;19(8):877-90.
146. Margalit O, DuBois RN. Neoplasia of the gastrointestinal tract (Chapter 32). In: Podolsky DK, Camilleri M, Fitz JG, Kalloo AN, Shanahan F, Wang TC. *Yamada's Textbook of Gastroenterology*. 6th ed: John Wiley & Sons, Ltd.; 2016.
147. Fearnhead NS, Britton MP, Bodmer WF. The ABC of APC. *Hum Mol Genet*. 2001;10(7):721-33.
148. Muzny DM, Bainbridge MN, Chang K, et al. Comprehensive molecular characterization of human colon and rectal cancer. *Nature*. 2012;487(7407):330-7.
149. Cisyk AL, Penner-Goeke S, Lichtensztejn Z, et al. Characterizing the Prevalence of Chromosome Instability in Interval Colorectal Cancer. *Neoplasia*. 2015;17(3):306-16.
150. McGranahan N, Burrell RA, Endesfelder D, et al. Cancer chromosomal instability: therapeutic and diagnostic challenges. *EMBO Rep*. 2012;13(6):528-38.
151. Vilar E, Gruber SB. Microsatellite instability in colorectal cancer-the stable evidence. *Nat Rev Clin Oncol*. 2010;7(3):153-62.



152. Toyota M, Ahuja N, Ohe-Toyota M, et al. CpG island methylator phenotype in colorectal cancer. *Proc Natl Acad Sci U S A*. 1999;96(15):8681-6.
153. Grady WM, Carethers JM. Genomic and epigenetic instability in colorectal cancer pathogenesis. *Gastroenterology*. 2008;135(4):1079-99.
154. Herman JG, Umar A, Polyak K, et al. Incidence and functional consequences of hMLH1 promoter hypermethylation in colorectal carcinoma. *Proc Natl Acad Sci U S A*. 1998;95(12):6870-5.
155. Jung G, Hernández-Illán E, Moreira L, et al. Epigenetics of colorectal cancer: biomarker and therapeutic potential. *Nat Rev Gastroenterol Hepatol*. 2020;17(2):111-30.
156. Galon J, Bruni D. Tumor Immunology and Tumor Evolution: Intertwined Histories. *Immunity*. 2020;52(1):55-81.
157. Reiser J, Banerjee A. Effector, Memory, and Dysfunctional CD8(+) T Cell Fates in the Antitumor Immune Response. *J Immunol Res*. 2016;2016:8941260.
158. Drake CG, Lipson EJ, Brahmer JR. Breathing new life into immunotherapy: review of melanoma, lung and kidney cancer. *Nat Rev Clin Oncol*. 2014;11(1):24-37.
159. The Nobel Prize in Physiology or Medicine 2018. [Internet]. NobelPrize.org: Nobel Prize Outreach AB; [updated 24 Oct 2021; cited 25 Oct 2021]. Available from: <https://www.nobelprize.org/prizes/medicine/2018/summary/> [Accessed 25 Oct 2021].
160. Shimasaki N, Jain A, Campana D. NK cells for cancer immunotherapy. *Nat Rev Drug Discov*. 2020;19(3):200-18.
161. Togashi Y, Shitara K, Nishikawa H. Regulatory T cells in cancer immunosuppression — implications for anticancer therapy. *Nat Rev Clin Oncol*. 2019;16(6):356-71.
162. Brierie B, Moses HL. Tumour microenvironment: TGFbeta: the molecular Jekyll and Hyde of cancer. *Nat Rev Cancer*. 2006;6(7):506-20.
163. Picard E, Verschoor CP, Ma GW, et al. Relationships Between Immune Landscapes, Genetic Subtypes and Responses to Immunotherapy in Colorectal Cancer. *Front Immunol*. 2020;11(369).
164. Jess T, Rungoe C, Peyrin-Biroulet L. Risk of colorectal cancer in patients with ulcerative colitis: a meta-analysis of population-based cohort studies. *Clin Gastroenterol Hepatol*. 2012;10(6):639-45.
165. Genua F, Raghunathan V, Jenab M, et al. The Role of Gut Barrier Dysfunction and Microbiome Dysbiosis in Colorectal Cancer Development. *Front Oncol*. 2021;11:626349.
166. Schetter AJ, Heegaard NH, Harris CC. Inflammation and cancer: interweaving microRNA, free radical, cytokine and p53 pathways. *Carcinogenesis*. 2010;31(1):37-49.
167. Couturier-Maillard A, Secher T, Rehman A, et al. NOD2-mediated dysbiosis predisposes mice to transmissible colitis and colorectal cancer. *J Clin Invest*. 2013;123(2):700-11.
168. Chen GY, Shaw MH, Redondo G, et al. The innate immune receptor Nod1 protects the intestine from inflammation-induced tumorigenesis. *Cancer Res*. 2008;68(24):10060-7.
169. Ben Q, Sun Y, Chai R, et al. Dietary fiber intake reduces risk for colorectal adenoma: a meta-analysis. *Gastroenterology*. 2014;146(3):689-99.e6.

170. Desai MS, Seekatz AM, Koropatkin NM, et al. A Dietary Fiber-Deprived Gut Microbiota Degrades the Colonic Mucus Barrier and Enhances Pathogen Susceptibility. *Cell*. 2016;167(5):1339-53.e21.
171. de Vries J, Miller PE, Verbeke K. Effects of cereal fiber on bowel function: A systematic review of intervention trials. *World J Gastroenterol*. 2015;21(29):8952-63.
172. Tilg H, Adolph TE, Gerner RR, et al. The Intestinal Microbiota in Colorectal Cancer. *Cancer Cell*. 2018;33(6):954-64.
173. Wong SH, Yu J. Gut microbiota in colorectal cancer: mechanisms of action and clinical applications. *Nat Rev Gastroenterol Hepatol*. 2019;16(11):690-704.
174. Zackular JP, Baxter NT, Chen GY, et al. Manipulation of the Gut Microbiota Reveals Role in Colon Tumorigenesis. *mSphere*. 2016;1(1):e00001-15.
175. Ng SC, Bernstein CN, Vatn MH, et al. Geographical variability and environmental risk factors in inflammatory bowel disease. *Gut*. 2013;62(4):630-49.
176. Davenport ER, Sanders JG, Song SJ, et al. The human microbiome in evolution. *BMC Biol*. 2017;15(1):127.
177. Asadollahi P, Ghanavati R, Rohani M, et al. Anti-cancer effects of Bifidobacterium species in colon cancer cells and a mouse model of carcinogenesis. *PLoS One*. 2020;15(5):e0232930.
178. Lee YK, Mehrabian P, Boyajian S, et al. The Protective Role of Bacteroides fragilis in a Murine Model of Colitis-Associated Colorectal Cancer. *mSphere*. 2018;3(6).
179. Gur C, Ibrahim Y, Isaacson B, et al. Binding of the Fap2 protein of Fusobacterium nucleatum to human inhibitory receptor TIGIT protects tumors from immune cell attack. *Immunity*. 2015;42(2):344-55.
180. Yang Y, Weng W, Peng J, et al. Fusobacterium nucleatum Increases Proliferation of Colorectal Cancer Cells and Tumor Development in Mice by Activating Toll-Like Receptor 4 Signaling to Nuclear Factor- $\kappa$ B, and Up-regulating Expression of MicroRNA-21. *Gastroenterology*. 2017;152(4):851-66.e24.
181. Wu Y, Wu J, Chen T, et al. Fusobacterium nucleatum Potentiates Intestinal Tumorigenesis in Mice via a Toll-Like Receptor 4/p21-Activated Kinase 1 Cascade. *Dig Dis Sci*. 2018;63(5):1210-8.
182. Janney A, Powrie F, Mann EH. Host-microbiota maladaptation in colorectal cancer. *Nature*. 2020;585(7826):509-17.
183. Zaneveld JR, McMinds R, Vega Thurber R. Stress and stability: applying the Anna Karenina principle to animal microbiomes. *Nat Microbiol*. 2017;2(9):17121.
184. Waterston RH, Lindblad-Toh K, Birney E, et al. Initial sequencing and comparative analysis of the mouse genome. *Nature*. 2002;420(6915):520-62.
185. Hugenholtz F, de Vos WM. Mouse models for human intestinal microbiota research: a critical evaluation. *Cell Mol Life Sci*. 2018;75(1):149-60.
186. Steensma DP, Kyle RA, Shampo MA. Abbie Lathrop, the "Mouse Woman of Granby": Rodent Fancier and Accidental Genetics Pioneer. *Mayo Clin Proc*. 2010;85(11):e83.
187. Saul MC, Philip VM, Reinholdt LG, et al. High-Diversity Mouse Populations for Complex Traits. *Trends Genet*. 2019;35(7):501-14.
188. European Parliament and Council of the European Union. Directive 2010/63/EU of the European Parliament and of the Council of 22 September 2010 on the protection of animals used for scientific purposes. Strasbourg, France: Council of Europe; 2010.

189. Bailoo JD, Murphy E, Boada-Saña M, et al. Effects of Cage Enrichment on Behavior, Welfare and Outcome Variability in Female Mice. *Frontiers in Behavioral Neuroscience*. 2018;12(232).
190. Froberg-Fejko KM, Lecker JL. Going back to nature: the benefits of wood enrichment. *Lab Animal*. 2012;41(11):346-7.
191. Froberg-Fejko KM. Addressing the environmental enrichment needs of mice: thinking outside the cage. *Lab Animal*. 2008;37(11):534-5.
192. Dobson GP, Letson HL, Biroš E, et al. Specific pathogen-free (SPF) animal status as a variable in biomedical research: Have we come full circle? *EBioMedicine*. 2019;41:42-3.
193. Charles River. Mouse Models - Health Profiles. Available from: <https://www.criver.com/sites/default/files/resource-files/spf-sopf-health-profiles-charles-river-europe-mice.pdf> [Accessed 7 Jun 2021].
194. Rosenberg DW, Giardina C, Tanaka T. Mouse models for the study of colon carcinogenesis. *Carcinogenesis*. 2009;30(2):183-96.
195. Sodring M, Gunnes G, Paulsen JE. Spontaneous initiation, promotion and progression of colorectal cancer in the novel A/J Min/+ mouse. *Int J Cancer*. 2016;138(8):1936-46.
196. Bürtin F, Mullins CS, Linnebacher M. Mouse models of colorectal cancer: Past, present and future perspectives. *World J Gastroenterol*. 2020;26(13):1394-426.
197. Sohn OS, Fiala ES, Requeijo SP, et al. Differential effects of CYP2E1 status on the metabolic activation of the colon carcinogens azoxymethane and methylazoxymethanol. *Cancer Res*. 2001;61(23):8435-40.
198. Perše M, Cerar A. Morphological and molecular alterations in 1,2 dimethylhydrazine and azoxymethane induced colon carcinogenesis in rats. *J Biomed Biotechnol*. 2011;2011:473964.
199. Tanaka T, Kohno H, Suzuki R, et al. A novel inflammation-related mouse colon carcinogenesis model induced by azoxymethane and dextran sodium sulfate. *Cancer Sci*. 2003;94(11):965-73.
200. Eichele DD, Kharbanda KK. Dextran sodium sulfate colitis murine model: An indispensable tool for advancing our understanding of inflammatory bowel diseases pathogenesis. *World J Gastroenterol*. 2017;23(33):6016-29.
201. Araki Y, Mukaisyo K, Sugihara H, et al. Increased apoptosis and decreased proliferation of colonic epithelium in dextran sulfate sodium-induced colitis in mice. *Oncol Rep*. 2010;24(4):869-74.
202. Melgar S, Karlsson A, Michaëlsson E. Acute colitis induced by dextran sulfate sodium progresses to chronicity in C57BL/6 but not in BALB/c mice: correlation between symptoms and inflammation. *Am J Physiol Gastrointest Liver Physiol*. 2005;288(6):G1328-38.
203. Chassaing B, Aitken JD, Malleshappa M, et al. Dextran sulfate sodium (DSS)-induced colitis in mice. *Curr Protoc Immunol*. 2014;104:15.25.1-15.25.14.
204. Thaker AI, Shaker A, Rao MS, et al. Modeling Colitis-Associated Cancer with Azoxymethane (AOM) and Dextran Sulfate Sodium (DSS). *J Vis Exp*. 2012(67):4100.
205. De Robertis M, Massi E, Poeta ML, et al. The AOM/DSS murine model for the study of colon carcinogenesis: From pathways to diagnosis and therapy studies. *J Carcinog*. 2011;10:9.

206. Tanaka T. Development of an inflammation-associated colorectal cancer model and its application for research on carcinogenesis and chemoprevention. 2012;2012:658786.
207. Cooper HS, Everley L, Chang WC, et al. The role of mutant Apc in the development of dysplasia and cancer in the mouse model of dextran sulfate sodium-induced colitis. *Gastroenterology*. 2001;121(6):1407-16.
208. Tanaka T, Kohno H, Suzuki R, et al. Dextran sodium sulfate strongly promotes colorectal carcinogenesis in Apc(Min/+) mice: inflammatory stimuli by dextran sodium sulfate results in development of multiple colonic neoplasms. *Int J Cancer*. 2006;118(1):25-34.
209. Casteleyn C, Rekecki A, Van der Aa A, et al. Surface area assessment of the murine intestinal tract as a prerequisite for oral dose translation from mouse to man. *Lab Anim*. 2010;44(3):176-83.
210. Nguyen TLA, Vieira-Silva S, Liston A, et al. How informative is the mouse for human gut microbiota research? *Dis Models Mech*. 2015;8(1):1-16.
211. Lagkouvardos I, Lesker TR, Hitch TCA, et al. Sequence and cultivation study of Muribaculaceae reveals novel species, host preference, and functional potential of this yet undescribed family. *Microbiome*. 2019;7(1):28.
212. Nagpal R, Wang S, Solberg Woods LC, et al. Comparative Microbiome Signatures and Short-Chain Fatty Acids in Mouse, Rat, Non-human Primate, and Human Feces. *Front Microbiol*. 2018;9(2897).
213. Xiao L, Feng Q, Liang S, et al. A catalog of the mouse gut metagenome. *Nat Biotechnol*. 2015;33(10):1103-8.
214. Chung H, Pamp SJ, Hill JA, et al. Gut immune maturation depends on colonization with a host-specific microbiota. *Cell*. 2012;149(7):1578-93.
215. Lundberg R, Toft MF, Metzendorff SB, et al. Human microbiota-transplanted C57BL/6 mice and offspring display reduced establishment of key bacteria and reduced immune stimulation compared to mouse microbiota-transplantation. *Sci Rep*. 2020;10(1):7805.
216. Mestas J, Hughes CC. Of mice and not men: differences between mouse and human immunology. *J Immunol*. 2004;172(5):2731-8.
217. Sternberg-Simon M, Brodin P, Pickman Y, et al. Natural Killer Cell Inhibitory Receptor Expression in Humans and Mice: A Closer Look. *Front Immunol*. 2013;4(65).
218. Shay T, Jojic V, Zuk O, et al. Conservation and divergence in the transcriptional programs of the human and mouse immune systems. *Proc Natl Acad Sci U S A*. 2013;110(8):2946-51.
219. Walsh NC, Kenney LL, Jangalwe S, et al. Humanized Mouse Models of Clinical Disease. *Annu Rev Pathol*. 2017;12:187-215.
220. De La Rochere P, Guil-Luna S, Decaudin D, et al. Humanized Mice for the Study of Immuno-Oncology. *Trends Immunol*. 2018;39(9):748-63.
221. Chia R, Achilli F, Festing MF, et al. The origins and uses of mouse outbred stocks. *Nat Genet*. 2005;37(11):1181-6.
222. Seyhan AA. Lost in translation: the valley of death across preclinical and clinical divide – identification of problems and overcoming obstacles. *Trans Med Commun*. 2019;4(1):18.

223. Mak IW, Evaniew N, Ghert M. Lost in translation: animal models and clinical trials in cancer treatment. *Am J Transl Res*. 2014;6(2):114-8.
224. Seok J, Warren HS, Cuenca AG, et al. Genomic responses in mouse models poorly mimic human inflammatory diseases. *Proc Natl Acad Sci U S A*. 2013;110(9):3507-12.
225. Boursot P, Auffray J-C, Britton-Davidian J, et al. The Evolution of House Mice. *Annu Rev Ecol Syst*. 1993;24(1):119-52.
226. Sage RD, Atchley WR, Capanna E. House Mice as Models in Systematic Biology. *Systematic Biology*. 1993;42(4):523-61.
227. Brodin P, Jojic V, Gao T, et al. Variation in the human immune system is largely driven by non-heritable influences. *Cell*. 2015;160(1-2):37-47.
228. Brodin P, Davis MM. Human immune system variation. *Nat Rev Immunol*. 2017;17(1):21-9.
229. Kaczorowski KJ, Shekhar K, Nkulikiyimfura D, et al. Continuous immunotypes describe human immune variation and predict diverse responses. *Proc Natl Acad Sci U S A*. 2017;114(30):E6097-E106.
230. Abolins S, King EC, Lazarou L, et al. The comparative immunology of wild and laboratory mice, *Mus musculus domesticus*. *Nat Commun*. 2017;8:14811.
231. Boysen P, Eide DM, Storset AK. Natural killer cells in free-living *Mus musculus* have a primed phenotype. *Molecular Ecology*. 2011;20(23):5103-10.
232. Abolins S, Lazarou L, Weldon L, et al. The ecology of immune state in a wild mammal, *Mus musculus domesticus*. *PLoS Biol*. 2018;16(4):e2003538-e.
233. Abolins SR, Pocock MJO, Hafalla JCR, et al. Measures of immune function of wild mice, *Mus musculus*. *Molecular Ecology*. 2011;20(5):881-92.
234. Beura LK, Hamilton SE, Bi K, et al. Normalizing the environment recapitulates adult human immune traits in laboratory mice. *Nature*. 2016;532(7600):512-6.
235. Rosshart SP, Vassallo BG, Angeletti D, et al. Wild Mouse Gut Microbiota Promotes Host Fitness and Improves Disease Resistance. *Cell*. 2017;171(5):1015-28.e13.
236. Rosshart SP, Herz J, Vassallo BG, et al. Laboratory mice born to wild mice have natural microbiota and model human immune responses. *Science*. 2019;365(6452).
237. Weldon L, Abolins S, Lenzi L, et al. The Gut Microbiota of Wild Mice. *PLOS ONE*. 2015;10(8):e0134643.
238. Wasimuddin, Čížková D, Bryja J, et al. High prevalence and species diversity of *Helicobacter* spp. detected in wild house mice. *Appl Environ Microbiol*. 2012;78(22):8158-60.
239. Linnenbrink M, Wang J, Hardouin EA, et al. The role of biogeography in shaping diversity of the intestinal microbiota in house mice. *Molecular Ecology*. 2013;22(7):1904-16.
240. Baxter NT, Wan JJ, Schubert AM, et al. Intra- and interindividual variations mask interspecies variation in the microbiota of sympatric *peromyscus* populations. *Appl Environ Microbiol*. 2015;81(1):396-404.
241. Maurice CF, Cl Knowles S, Ladau J, et al. Marked seasonal variation in the wild mouse gut microbiota. *ISME J*. 2015;9(11):2423-34.

242. Walter J, Maldonado-Gomez MX, Martinez I. To engraft or not to engraft: an ecological framework for gut microbiome modulation with live microbes. *Curr Opin Biotechnol.* 2018;49:129-39.
243. Brugiroux S, Beutler M, Pfann C, et al. Genome-guided design of a defined mouse microbiota that confers colonization resistance against *Salmonella enterica* serovar Typhimurium. *Nat Microbiol.* 2016;2(2):16215.
244. Garzetti D, Brugiroux S, Bunk B, et al. High-Quality Whole-Genome Sequences of the Oligo-Mouse-Microbiota Bacterial Community. *Genome Announc.* 2017;5(42):e00758-17.
245. Wymore Brand M, Wannemuehler MJ, Phillips GJ, et al. The Altered Schaedler Flora: Continued Applications of a Defined Murine Microbial Community. *ILAR J.* 2015;56(2):169-78.
246. Eberl C, Ring D, Münch PC, et al. Reproducible Colonization of Germ-Free Mice With the Oligo-Mouse-Microbiota in Different Animal Facilities. *Front Microbiol.* 2020;10(2999).
247. Begley CG, Ioannidis JP. Reproducibility in science: improving the standard for basic and preclinical research. *Circ Res.* 2015;116(1):116-26.
248. Franklin CL, Ericsson AC. Microbiota and reproducibility of rodent models. *Lab Anim (NY).* 2017;46(4):114-22.
249. Rausch P, Basic M, Batra A, et al. Analysis of factors contributing to variation in the C57BL/6J fecal microbiota across German animal facilities. *Int J Med Microbiol.* 2016;306(5):343-55.
250. Roy U, Galvez EJC, Iljazovic A, et al. Distinct Microbial Communities Trigger Colitis Development upon Intestinal Barrier Damage via Innate or Adaptive Immune Cells. *Cell Rep.* 2017;21(4):994-1008.
251. Leystra AA, Clapper ML. Gut Microbiota Influences Experimental Outcomes in Mouse Models of Colorectal Cancer. *Genes.* 2019;10(11):900.
252. Masopust D, Sivula CP, Jameson SC. Of Mice, Dirty Mice, and Men: Using Mice To Understand Human Immunology. *J Immunol.* 2017;199(2):383-8.
253. Ericsson AC, Montonye DR, Smith CR, et al. Modeling a Superorganism - Considerations Regarding the Use of "Dirty" Mice in Biomedical Research. *Yale J Biol Med.* 2017;90(3):361-71.
254. Tao L, Reese TA. Making Mouse Models That Reflect Human Immune Responses. *Trends Immunol.* 2017;38(3):181-93.
255. Huggins MA, Jameson SC, Hamilton SE. Embracing microbial exposure in mouse research. *J Leukoc Biol.* 2019;105(1):73-9.
256. Hamilton SE, Badovinac VP, Beura LK, et al. New Insights into the Immune System Using Dirty Mice. *J Immunol.* 2020;205(1):3-11.
257. Graham AL. Naturalizing mouse models for immunology. *Nat Immunol.* 2021;22(2):111-7.
258. Reese TA, Bi K, Kambal A, et al. Sequential Infection with Common Pathogens Promotes Human-like Immune Gene Expression and Altered Vaccine Response. *Cell Host Microbe.* 2016;19(5):713-9.

259. Yeung F, Chen Y-H, Lin J-D, et al. Altered Immunity of Laboratory Mice in the Natural Environment Is Associated with Fungal Colonization. *Cell Host Microbe*. 2020;27(5):809-22.e6.
260. Leung JM, Budischak SA, Chung The H, et al. Rapid environmental effects on gut nematode susceptibility in rewilded mice. *PLoS Biol*. 2018;16(3):e2004108.
261. Huggins MA, Sjaastad FV, Pierson M, et al. Microbial Exposure Enhances Immunity to Pathogens Recognized by TLR2 but Increases Susceptibility to Cytokine Storm through TLR4 Sensitization. *Cell Rep*. 2019;28(7):1729-43.e5.
262. Lindner C, Thomsen I, Wahl B, et al. Diversification of memory B cells drives the continuous adaptation of secretory antibodies to gut microbiota. *Nat Immunol*. 2015;16(8):880-8.
263. Suzui M, Morioka T, Yoshimi N. Colon preneoplastic lesions in animal models. *J Toxicol Pathol*. 2013;26(4):335-41.
264. Steppeler C, Sødrring M, Paulsen JE. Colorectal Carcinogenesis in the A/J Min/+ Mouse Model is Inhibited by Hemin, Independently of Dietary Fat Content and Fecal Lipid Peroxidation Rate. *BMC Cancer*. 2016;16(1):832.
265. Sødrring M, Gunnes G, Paulsen JE. Detection and Characterization of Flat Aberrant Crypt Foci (Flat ACF) in the Novel A/J Min/+ Mouse. *Anticancer Res*. 2016;36(6):2745-50.
266. Suzuki R, Kohno H, Sugie S, et al. Strain differences in the susceptibility to azoxymethane and dextran sodium sulfate-induced colon carcinogenesis in mice. *Carcinogenesis*. 2006;27(1):162-9.
267. Nambiar PR, Girnun G, Lillo NA, et al. Preliminary analysis of azoxymethane induced colon tumors in inbred mice commonly used as transgenic/knockout progenitors. *Int J Oncol*. 2003;22(1):145-50.
268. Johanson SM, Swann JR, Umu Ö CO, et al. Maternal exposure to a human relevant mixture of persistent organic pollutants reduces colorectal carcinogenesis in A/J Min/+ mice. *Chemosphere*. 2020;252:126484.
269. Gustafsson JK, Ermund A, Johansson MEV, et al. An ex vivo method for studying mucus formation, properties, and thickness in human colonic biopsies and mouse small and large intestinal explants. *Am J Physiol Gastrointest Liver Physiol*. 2012;302(4):G430-G8.
270. Volk JK, Nyström EEL, van der Post S, et al. The Nlrp6 inflammasome is not required for baseline colonic inner mucus layer formation or function. *J Exp Med*. 2019;216(11):2602-18.
271. Jakobsson HE, Rodriguez-Pineiro AM, Schutte A, et al. The composition of the gut microbiota shapes the colon mucus barrier. *EMBO Rep*. 2015;16(2):164-77.
272. Metzker ML. Sequencing technologies — the next generation. *Nat Rev Genet*. 2010;11(1):31-46.
273. Luo C, Tsementzi D, Kyrpides N, et al. Direct Comparisons of Illumina vs. Roche 454 Sequencing Technologies on the Same Microbial Community DNA Sample. *PLOS ONE*. 2012;7(2):e30087.
274. Lagkouvardos I, Joseph D, Kapfhammer M, et al. IMNGS: A comprehensive open resource of processed 16S rRNA microbial profiles for ecology and diversity studies. *Sci Rep*. 2016;6:33721.

275. Caruso V, Song X, Asquith M, et al. Performance of Microbiome Sequence Inference Methods in Environments with Varying Biomass. *mSystems*. 2019;4(1).
276. Stackebrandt E, Goebel BM. Taxonomic Note: A Place for DNA-DNA Reassociation and 16S rRNA Sequence Analysis in the Present Species Definition in Bacteriology. *Int J Syst Bacteriol*. 1994;44(4):846-9.
277. Edgar RC. Updating the 97% identity threshold for 16S ribosomal RNA OTUs. *Bioinformatics*. 2018;34(14):2371-5.
278. Edgar RC. UPARSE: highly accurate OTU sequences from microbial amplicon reads. *Nat Methods*. 2013;10(10):996-8.
279. Park S-C, Won S. Evaluation of 16S rRNA Databases for Taxonomic Assignments Using Mock Community. *Genomics Inform*. 2018;16(4):e24-e.
280. Wang Q, Garrity GM, Tiedje JM, et al. Naive Bayesian classifier for rapid assignment of rRNA sequences into the new bacterial taxonomy. *Appl Environ Microbiol*. 2007;73(16):5261-7.
281. Lagkouvardos I, Fischer S, Kumar N, et al. Rhea: a transparent and modular R pipeline for microbial profiling based on 16S rRNA gene amplicons. *PeerJ*. 2017;5:e2836.
282. McMurdie PJ, Holmes S. Waste Not, Want Not: Why Rarefying Microbiome Data Is Inadmissible. *PLoS Computational Biology*. 2014;10(4):e1003531.
283. Vandeputte D, Kathagen G, D'Hoe K, et al. Quantitative microbiome profiling links gut community variation to microbial load. *Nature*. 2017;551(7681):507-11.
284. Barlow JT, Bogatyrev SR, Ismagilov RF. A quantitative sequencing framework for absolute abundance measurements of mucosal and luminal microbial communities. *Nat Commun*. 2020;11(1):2590.
285. Jost L. Entropy and diversity. *Oikos*. 2006;113(2):363-75.
286. Jost L. Partitioning diversity into independent alpha and beta components. *Ecology*. 2007;88(10):2427-39.
287. Chen J, Bittinger K, Charlson ES, et al. Associating microbiome composition with environmental covariates using generalized UniFrac distances. *Bioinformatics*. 2012;28(16):2106-13.
288. Bellali S, Lagier J-C, Million M, et al. Running after ghosts: are dead bacteria the dark matter of the human gut microbiota? *Gut Microbes*. 2021;13(1):1897208.
289. Rangel I, Sundin J, Fuentes S, et al. The relationship between faecal-associated and mucosal-associated microbiota in irritable bowel syndrome patients and healthy subjects. *Aliment Pharm Ther*. 2015;42(10):1211-21.
290. Ringel Y, Maharshak N, Ringel-Kulka T, et al. High throughput sequencing reveals distinct microbial populations within the mucosal and luminal niches in healthy individuals. *Gut Microbes*. 2015;6(3):173-81.
291. Tap J, Derrien M, Törnblom H, et al. Identification of an Intestinal Microbiota Signature Associated With Severity of Irritable Bowel Syndrome. *Gastroenterology*. 2017;152(1):111-23.e8.
292. Tanca A, Manghina V, Fraumene C, et al. Metaproteogenomics Reveals Taxonomic and Functional Changes between Cecal and Fecal Microbiota in Mouse. *Front Microbiol*. 2017;8(391).
293. Adan A, Alizada G, Kiraz Y, et al. Flow cytometry: basic principles and applications. *Critical Reviews in Biotechnology*. 2017;37(2):163-76.



294. Hulspas R, O'Gorman MRG, Wood BL, et al. Considerations for the control of background fluorescence in clinical flow cytometry. *Cytometry Part B: Clinical Cytometry*. 2009;76B(6):355-64.
295. Neufert C, Becker C, Neurath MF. An inducible mouse model of colon carcinogenesis for the analysis of sporadic and inflammation-driven tumor progression. *Nat Protoc*. 2007;2(8):1998-2004.
296. Bird RP. Observation and quantification of aberrant crypts in the murine colon treated with a colon carcinogen: preliminary findings. *Cancer Lett*. 1987;37(2):147-51.
297. Paulsen JE, Namork E, Steffensen IL, et al. Identification and quantification of aberrant crypt foci in the colon of Min mice--a murine model of familial adenomatous polyposis. *Scand J Gastroenterol*. 2000;35(5):534-9.
298. Paulsen JE, Løberg EM, Olstørn HB, et al. Flat dysplastic aberrant crypt foci are related to tumorigenesis in the colon of azoxymethane-treated rat. *Cancer Res*. 2005;65(1):121-9.
299. Caderni G, Femia AP, Giannini A, et al. Identification of mucin-depleted foci in the unsectioned colon of azoxymethane-treated rats: correlation with carcinogenesis. *Cancer Res*. 2003;63(10):2388-92.
300. Yamada Y, Yoshimi N, Hirose Y, et al. Frequent  $\beta$ -Catenin Gene Mutations and Accumulations of the Protein in the Putative Preneoplastic Lesions Lacking Macroscopic Aberrant Crypt Foci Appearance, in Rat Colon Carcinogenesis. *Cancer Res*. 2000;60(13):3323-7.
301. Femia AP, Paulsen JE, Dolara P, et al. Correspondence between flat aberrant crypt foci and mucin-depleted foci in rodent colon carcinogenesis. *Anticancer Res*. 2008;28(6a):3771-5.
302. Kowalczyk M, Orłowski M, Klepacki Ł, et al. Rectal aberrant crypt foci (ACF) as a predictor of benign and malignant neoplastic lesions in the large intestine. *BMC Cancer*. 2020;20(1):133.
303. Sakai E, Takahashi H, Kato S, et al. Investigation of the prevalence and number of aberrant crypt foci associated with human colorectal neoplasm. *Cancer Epidemiol Biomarkers Prev*. 2011;20(9):1918-24.
304. Ohkubo H, Takahashi H, Yamada E, et al. Natural history of human aberrant crypt foci and correlation with risk factors for colorectal cancer. *Oncol Rep*. 2012;27(5):1475-80.
305. Paulsen JE, Steffensen IL, Loberg EM, et al. Qualitative and quantitative relationship between dysplastic aberrant crypt foci and tumorigenesis in the Min/+ mouse colon. *Cancer Res*. 2001;61(13):5010-5.
306. Nambiar PR, Nakanishi M, Gupta R, et al. Genetic signatures of high- and low-risk aberrant crypt foci in a mouse model of sporadic colon cancer. *Cancer Res*. 2004;64(18):6394-401.
307. Andreassen M, Rudi K, Angell IL, et al. Allergen Immunization Induces Major Changes in Microbiota Composition and Short-Chain Fatty Acid Production in Different Gut Segments in a Mouse Model of Lupine Food Allergy. *Int Arch Allergy Immunol*. 2018;177(4):311-23.
308. Primec M, Mičetić-Turk D, Langerholc T. Analysis of short-chain fatty acids in human feces: A scoping review. *Analytical Biochemistry*. 2017;526:9-21.

309. Conesa A, Madrigal P, Tarazona S, et al. A survey of best practices for RNA-seq data analysis. *Genome Biol.* 2016;17(1):13.
310. Lowe R, Shirley N, Bleackley M, et al. Transcriptomics technologies. *PLoS computational biology.* 2017;13(5):e1005457-e.
311. Kim D, Paggi JM, Park C, et al. Graph-based genome alignment and genotyping with HISAT2 and HISAT-genotype. *Nat Biotechnol.* 2019;37(8):907-15.
312. Love MI, Huber W, Anders S. Moderated estimation of fold change and dispersion for RNA-seq data with DESeq2. *Genome Biol.* 2014;15(12):550.
313. Glowacki RWP, Engelhart MJ, Ahern PP. Controlled Complexity: Optimized Systems to Study the Role of the Gut Microbiome in Host Physiology. *Front Microbiol.* 2021;12(2690).
314. Kuypers M, Despot T, Mallevaey T. Dirty mice join the immunologist's toolkit. *Microb Infect.* 2021:104817.
315. Fischer AW, Cannon B, Nedergaard J. Optimal housing temperatures for mice to mimic the thermal environment of humans: An experimental study. *Mol Metab.* 2018;7:161-70.
316. Viney M, Riley EM. The Immunology of Wild Rodents: Current Status and Future Prospects. *Front Immunol.* 2017;8:1481-.
317. Westwood JA, Darcy PK, Kershaw MH. Environmental enrichment does not impact on tumor growth in mice. *F1000Res.* 2013;2:140.
318. Monin L, Ushakov DS, Arnesen H, et al.  $\gamma\delta$  T cells compose a developmentally regulated intrauterine population and protect against vaginal candidiasis. *Mucosal Immunology.* 2020;13(6):969-81.
319. Yeh Y-W, Chaudhuri AS, Zhou L, et al. Mast Cells Are Identified in the Lung Parenchyma of Wild Mice, Which Can Be Recapitulated in Naturalized Laboratory Mice. *Front Immunol.* 2021;12(3816).
320. Yang H, Bell TA, Churchill GA, et al. On the subspecific origin of the laboratory mouse. *Nature Genetics.* 2007;39(9):1100-7.
321. Kreisinger J, Cížková D, Vohánka J, et al. Gastrointestinal microbiota of wild and inbred individuals of two house mouse subspecies assessed using high-throughput parallel pyrosequencing. *Mol Ecol.* 2014;23(20):5048-60.
322. Jones EP, Van Der Kooij J, Solheim R, et al. Norwegian house mice (*Mus musculus musculus*/domesticus): distributions, routes of colonization and patterns of hybridization. *Molecular Ecology.* 2010;19(23):5252-64.
323. Knutsen LE, Dissen E, Saether PC, et al. Evidence of functional Cd94 polymorphism in a free-living house mouse population. *Immunogenetics.* 2019;71(4):321-33.
324. Suzuki TA, Worobey M. Geographical variation of human gut microbial composition. *Biology letters.* 2014;10(2):20131037-.
325. Yatsunenkov T, Rey FE, Manary MJ, et al. Human gut microbiome viewed across age and geography. *Nature.* 2012;486(7402):222-7.
326. Litvak Y, Byndloss MX, Tsolis RM, et al. Dysbiotic Proteobacteria expansion: a microbial signature of epithelial dysfunction. *Curr Opin Microbiol.* 2017;39:1-6.
327. Shin N-R, Whon TW, Bae J-W. Proteobacteria: microbial signature of dysbiosis in gut microbiota. *Trends in Biotechnology.* 2015;33(9):496-503.

328. Bradley PH, Pollard KS. Proteobacteria explain significant functional variability in the human gut microbiome. *Microbiome*. 2017;5(1):36.
329. Myles MH, Dieckgraefe BK, Criley JM, et al. Characterization of cecal gene expression in a differentially susceptible mouse model of bacterial-induced inflammatory bowel disease. *Inflamm Bowel Dis*. 2007;13(7):822-36.
330. Song H, Kim J, Guk J-H, et al. Metagenomic Analysis of the Gut Microbiota of Wild Mice, a Newly Identified Reservoir of *Campylobacter*. *Frontiers in Cellular and Infection Microbiology*. 2021;10(909).
331. Sonnenburg JL, Sonnenburg ED. Vulnerability of the industrialized microbiota. *Science*. 2019;366(6464).
332. Tanaka A, Sakaguchi S. Regulatory T cells in cancer immunotherapy. *Cell Research*. 2017;27(1):109-18.
333. Johansson ME, Thomsson KA, Hansson GC. Proteomic analyses of the two mucus layers of the colon barrier reveal that their main component, the Muc2 mucin, is strongly bound to the Fcgbp protein. *J Proteome Res*. 2009;8(7):3549-57.
334. Johansson MEV, Phillipson M, Petersson J, et al. The inner of the two Muc2 mucin-dependent mucus layers in colon is devoid of bacteria. *Proc Natl Acad Sci U S A*. 2008;105(39):15064-9.
335. Nyström EEL, Arike L, Ehrencrona E, et al. Calcium-activated chloride channel regulator 1 (CLCA1) forms non-covalent oligomers in colonic mucus and has mucin 2-processing properties. *J Biol Chem*. 2019;294(45):17075-89.
336. Almalki F, Nonnecke EB, Castillo PA, et al. Extensive variation in the intelectin gene family in laboratory and wild mouse strains. *Sci Rep*. 2021;11(1):15548.
337. Nonnecke EB, Castillo PA, Dugan AE, et al. Human intelectin-1 (ITLN1) genetic variation and intestinal expression. *Sci Rep*. 2021;11(1):12889.



## 8. Enclosed Papers I-IV

---



# Paper I

I







# A Model System for Feralizing Laboratory Mice in Large Farmyard-Like Pens

Henriette Arnesen<sup>1,2</sup>, Linn Emilie Knutsen<sup>1</sup>, Bente Wabakken Hognestad<sup>1</sup>, Grethe Marie Johansen<sup>1</sup>, Mats Bemark<sup>3,4</sup>, Oliver Pabst<sup>5</sup>, Anne Kristine Storset<sup>1</sup> and Preben Boysen<sup>1\*</sup>

<sup>1</sup> Faculty of Veterinary Medicine, Norwegian University of Life Sciences, Oslo, Norway, <sup>2</sup> Faculty of Chemistry, Biotechnology and Food Science, Norwegian University of Life Sciences, Aas, Norway, <sup>3</sup> Department of Microbiology and Immunology, Institute of Biomedicine, Sahlgrenska Academy, University of Gothenburg, Gothenburg, Sweden, <sup>4</sup> Region Västra Götaland, Sahlgrenska University Hospital, Department of Clinical Immunology and Transfusion Medicine, Gothenburg, Sweden, <sup>5</sup> Institute of Molecular Medicine, RWTH Aachen University, Aachen, Germany

Laboratory mice are typically housed under extremely clean laboratory conditions, far removed from the natural lifestyle of a free-living mouse. There is a risk that this isolation from real-life conditions may lead to poor translatability and misinterpretation of results. We and others have shown that feral mice as well as laboratory mice exposed to naturalistic environments harbor a more diverse gut microbiota and display an activated immunological phenotype compared to hygienic laboratory mice. We here describe a naturalistic indoors housing system for mice, representing a farmyard-type habitat typical for house mice. Large open pens were installed with soil and domestic animal feces, creating a highly diverse microbial environment and providing space and complexity allowing for natural behavior. Laboratory C57BL/6 mice were co-housed in this system together with wild-caught feral mice, included as a source of murine microbionts. We found that mice feralized in this manner displayed a gut microbiota structure similar to their feral cohabitants, such as higher relative content of Firmicutes and enrichment of Proteobacteria. Furthermore, the immunophenotype of feralized mice approached that of feral mice, with elevated levels of memory T-cells and late-stage NK cells compared to laboratory-housed control mice, indicating antigenic experience and immune training. The dietary elements presented in the mouse pens could only moderately explain changes in microbial colonization, and none of the immunological changes. In conclusion, this system enables various types of studies using genetically controlled mice on the background of adaptation to a high diversity microbial environment and a lifestyle natural for the species.

**Keywords:** animal model, mice, feral mice, feralized mice, trained immunity, immune experience, gut microbiota, naturalistic environment

## INTRODUCTION

The common habitat for the house mouse (*Mus musculus*) is on the ground, typically close to larger animals like humans and their livestock, and the genetic basis for all research mice evolved in such environments (Boursot et al., 1993). Colonization by a host-specific microbiota is necessary to develop essential parts of the mucosal immune system in mice (Cebra, 1999; Chung et al., 2012),

## OPEN ACCESS

### Edited by:

Jean-François Brugère,  
Université Clermont Auvergne, France

### Reviewed by:

Henning Seedorf,  
Temasek Life Sciences Laboratory,  
Singapore  
Stephan Rosshart,  
University of Freiburg Medical Center,  
Germany

### \*Correspondence:

Preben Boysen  
preben.boysen@nmbu.no

### Specialty section:

This article was submitted to  
Microbial Symbioses,  
a section of the journal  
Frontiers in Microbiology

**Received:** 09 October 2020

**Accepted:** 09 December 2020

**Published:** 11 January 2021

### Citation:

Arnesen H, Knutsen LE,  
Hognestad BW, Johansen GM,  
Bemark M, Pabst O, Storset AK and  
Boysen P (2021) A Model System  
for Feralizing Laboratory Mice in Large  
Farmyard-Like Pens.  
Front. Microbiol. 11:615661.  
doi: 10.3389/fmicb.2020.615661

and expression of effector- as well as tolerance-associated immune genes are upregulated following microbial colonization (El Aidy et al., 2012). Nevertheless, mice are usually studied under strictly hygienic laboratory conditions. Hence, concerns have been raised whether hygienically raised laboratory (lab) mice will reach a level of immune maturation that fully recapitulates the immune response in a mammal (Tao and Reese, 2017). Large variations in microbiota and cellular composition of the gut mucosa have been observed between animal facilities, accompanied by different immune phenotypes and experimental performance (Ivanov et al., 2009; Kriegel et al., 2011; Jakobsson et al., 2015; Rausch et al., 2016; Franklin and Ericsson, 2017). Thus, an artificial between-lab variability may have replaced natural variability in the course of comprehensible efforts to standardize the world's most used animal model.

Theories have postulated that a modernized lifestyle has led to a loss of proximity to a diverse range of microbes and parasites, thus removing balancing factors in the immune homeostasis, which may explain an increase of inflammatory diseases and cancer (Hunter, 2020). A major current research field addresses how colonizing microbes, including bacteria, parasites and even viruses, may affect the immune system to generate a lasting and general protection from various diseases. Beyond specific immunity, recent evidence shows how innate immune cells may undergo long-lasting reprogramming following microbial challenges, sometimes referred to as trained immunity (Oh et al., 2014; Honda and Littman, 2016; Netea et al., 2020). Adaptive immune cells may also be primed in a similar manner (Muraille and Goriely, 2017). The concept of immune training has been associated with enhancement of immune responses to vaccines and infections as well as to anti-inflammatory actions (Quinn et al., 2019). The outcome of immune training for a particular disease may thus point in either direction and needs to be explored empirically in organisms exposed to diverse microbial cues.

This background gives a rationale to develop animal models reflecting more realistic ecological contexts (Flies and Wild Comparative Immunology Consortium, 2020). In contrast to the widespread use of hygienically raised inbred mice, studies investigating the microbiota and immunity of mice under more naturalistic conditions have only recently emerged. We and others have demonstrated that feral (wild-caught) mice had an immunological steady state different from lab mice (Devalapalli et al., 2006; Abolins et al., 2011, 2017, 2018), as well as a thicker mucus layer in the gut (Jakobsson et al., 2015). In an effort to decipher the impact of environment, one study found profound changes in the immune system of inbred mice following co-housing with "dirty" pet store mice, approaching

phenotypes found in feral mouse as well as adult humans (Beura et al., 2016). In another, pre-infection of inbred mice with selected common mouse pathogens resulted in stronger vaccine responses (Reese et al., 2016). Furthermore, by transplanting feral mouse feces (Rosshart et al., 2017) or by transferring microbiota vertically from feral surrogate mothers (Rosshart et al., 2019), "wildling" lab mice were shown to develop a trained immune system and increased protection against disease. The latter study demonstrated the translational gain by using naturalized mice, as wildling mice behaved immunologically human-like in two clinical settings where conventional lab mice had failed to predict the response. Another study showed that the provision of soil heaps in mice cages modified the gut microbiota and repressed Th2-driven inflammation, in support of the "hygiene hypothesis" (Ottman et al., 2019). However, in all the studies mentioned above, lab mice remained in conventional cages, with limitations of space and behavioral opportunities relative to a wild house mouse lifestyle. A recently described model where mice were kept in large outdoor enclosures, showed altered microbiota, a shift toward Th1-type immunity and an increased susceptibility to helminth infection (Leung et al., 2018; Lin et al., 2020; Yeung et al., 2020). While offering a habitat clearly representing wild conditions, this setup allows limited surveillance of the animals and may prove inaccessible for most researchers.

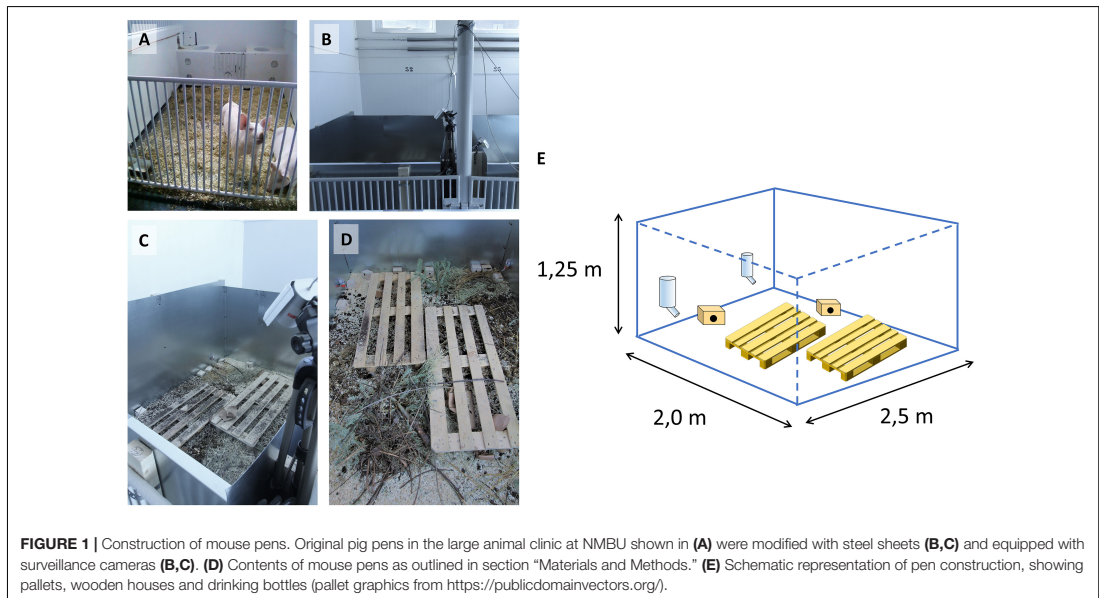
We present a naturalistic environment housing system for mice consisting of large indoor enclosures (pens) containing farmyard-like elements such as fecal content from farm animals, soil and plant materials, with spatial living conditions reflecting a natural habitat. In a set of experiments, C57BL/6 mice were feralized under these conditions in the presence of feral house mice, serving as a natural source of mouse microbes, including pathogens and parasites. We show that feralization lead to a significant conversion of the gut microbiota composition, and to immunological parameters associated with antigenic experience and immune training.

## MATERIALS AND METHODS

### Animals and Experimental Design

A mouse pen housing system was designed at The Norwegian University of Life Sciences (NMBU) by escape-proofing pig pens with sheets of galvanized steel, each pen measuring 2.0 × 2.5 × 1.25 m (WxDxH) on concrete floor (Figures 1A–E and Supplementary Video S1). Pens were enriched with wood shavings, organic garden soil, compost, twigs, hay and fecal content from pigs, cows and horses. Oat and carrot sprouts were planted occasionally to provide fresh plants as would be encountered in a farmyard. Wooden pallets were used as stepping platforms for personnel to avoid disturbing the habitats or crushing animals, also contributing to environmental complexity and shelter. Standard nipped drinking bottles provided water. Small wooden boxes were provided for nesting and sheltering. In Experiment (Exp.) 1, surveillance cameras with infrared sensors were used for continuous monitoring.

**Abbreviations:** B6, C57BL/6 inbred mouse strain; CM T-cell, Central memory T-cell; EM T-cell, Effector memory T-cell; Exp. 1/Exp. 2, Experiment 1/Experiment 2; Fzd, Feralized (here: female) B6 mice; Fzd<sup>F</sup>, B6 females feralized in the presence of female feral mice; Fzd<sup>M</sup>, B6 females feralized in the presence of male feral mice; Ig, Immunoglobulin; IL, Interleukin; IVC, Individually ventilated cage; KLRG1, Killer cell lectin-like receptor subfamily G member 1; NRP-1, Neuropilin-1; OTU, Operational taxonomic unit; PCA, Principal component analysis; PLN, Peripherial lymph node; pTreg, Peripherally induced regulatory T-cell; Rm1, Rat and Mouse No.1 diet (T<sup>M</sup> of Special Diet Services); SPE, Specific pathogen-free; Treg, Regulatory T-cell.



Following purchase, C57BL/6N (B6) specific pathogen-free (SPF) mice (Charles River/Scanbur, Norway) were acclimatized for 1 week in individually ventilated cages (IVCs) under SPF conditions at NMBU. Feral house mice were captured in domestic animal farms in south-eastern Norway by overnight deployment of Ugglan Special No1 live traps (Grahnbab, Gnosjö, Sweden), equipped with wood shavings, fresh fruit and peanut butter as bait, as previously described (Boysen et al., 2011). Representatives of these catches were subtyped as *Mus musculus* ssp. *musculus*, with a minor contribution of ssp. *domesticus* as reported previously (Knutsen et al., 2019). The ages of feral mice could not be determined, but only visibly adult individuals were included. Mice were individually marked using ear punch or microchip injected subcutaneously (Nonatec Lutronic, Rodange, Luxembourg). Feral and B6 mice were released simultaneously into pens.

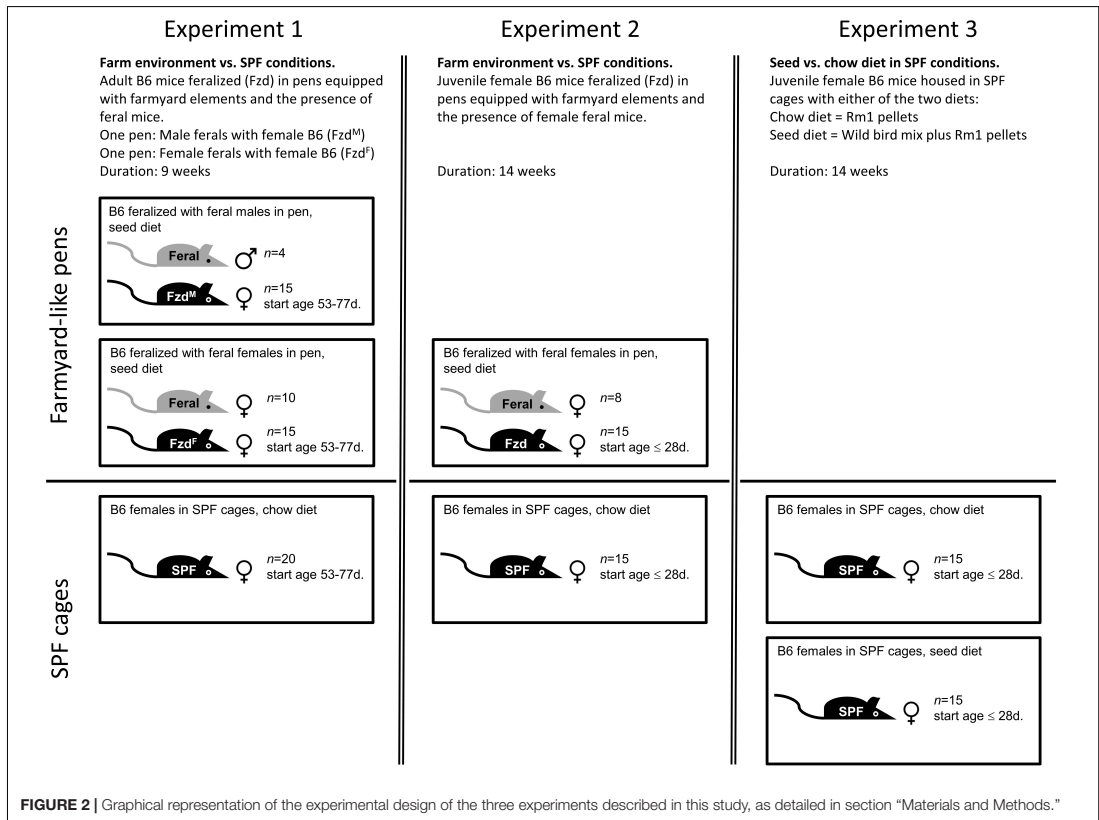
Experiments and housing design were approved by the National Animal Research Authority in Norway (FOTS 4788, 6801, and 8080). Feral mice capture was approved by The Norwegian Directorate for Nature Management (2012/693 and 2014/7215).

In Exp. 1 (Figure 2), female B6 mice aged 53–77 days were feralized by housing in pens together with feral mice for 9 weeks, divided into two subgroups: In one pen, 15 female B6 mice were co-housed with 10 female feral mice (Fzd<sup>F</sup>; feralized with feral females). In a second pen, 15 female B6 mice were co-housed with 4 male feral mice (Fzd<sup>M</sup>; feralized with feral males). Fzd<sup>M</sup> mice produced several litters of hybrid offspring excluded from the study. To provide a diet reflecting food sources in a natural setting, we provided an unprocessed wild bird seed mix consisting of sunflower seeds (25%), sorghum

(25%), oat (25%), and wheat (25%) (Wild bird mix, Plantasjen, Köping, Sweden), mixed with standard “chow” pellets (Rm1, Special Diet Services, United Kingdom/Scanbur, Norway) *ad lib* on the ground (see **Supplementary Table S1** for nutrient composition.) In addition, pen mice had access to a variation of plant material, including dried hay, spruce twigs collected outdoors, and occasional fresh lettuce, carrots and fruits. 20 female B6 mice of the same cohort were housed in cages under SPF conditions as controls, receiving standard chow diet only, to maintain typical lab conditions.

In Exp. 2 (Figure 2), 15 female B6 mice aged 28 days were feralized in mouse pens with 8 female adult feral mice for 14 weeks (Fzd), while 15 B6 females were kept in cages as SPF controls. Feeding regimen as described above. As the feralized mice were fed a natural diet in the previous experiments, we designed Exp. 3 (Figure 2) to assess the effects of the major dietary sources of the previous two experiments, carried out in IVCs under conventional lab conditions. 30 female B6 mice (source, age and gender as in Exp. 2) were housed for 14 weeks in cages of 5 mice per cage. The animals were randomized into two groups receiving either chow or a combinatory diet of chow and seed mix (the latter hereafter referred to as seed group for simplicity).

The mice were exposed to human caretakers in the pens on a daily basis, but direct handling was minimized, and mice were not re-captured until termination of the experiment. Only mice that were clinically healthy condition at termination were included in the studies. All mice were euthanized by neck dislocation, followed by immediate exsanguination by cardiac puncture, weighing and measuring, and dissection of sample tissues.



## Isolation of Cells and Serum

Cells harvested from tissues using a GentleMACS dissociator and mouse Spleen Dissociation Kit (Miltenyi Biotech, Bergisch Gladbach, Germany) according to the manufacturer's instructions. Splenic suspensions were briefly treated with  $\text{NH}_4\text{Cl}$  solution to lyse erythrocytes. Single-cell suspensions were prepared using a  $70\ \mu\text{m}$  cell strainer (BD Biosciences) and concentrations standardized after counting using a Countess automated cell counter (Thermo Fisher Scientific). Serum was isolated from blood following centrifugation of clotted whole blood at  $3,000\ \text{g}$  for 5 min.

## Microbial Community Analyses

For microbial community analyses, fecal pellets were flash frozen in liquid  $\text{N}_2$  after collection and stored at  $-80^\circ\text{C}$ . DNA extraction, library preparation and 16S rDNA 454 pyrosequencing were conducted as described previously (Lindner et al., 2015). Briefly, DNA was isolated and purified with QIAamp DNA Stool Mini Kit (Qiagen) according to manufacturer's manual. Libraries were generated with a primer set covering the V1–V3 regions of the 16S rRNA gene (8F/541R). 16S rRNA gene amplicons were purified by gel electrophoresis followed by gel

extraction (QIAquick Gel Extraction kit, Qiagen). Amplicons were prepared with the GS FLX Titanium SV emPCR kit (Lib-A) for 454 pyrosequencing on the Genome Sequencer FLX system (Roche) according to manufacturer's instructions. In Exp. 2 and 3, feces was collected from all individuals at baseline ( $t_0$ ) and termination following 14 weeks of feralization ( $t_1$ ).

Raw reads were processed using the Integrated Microbial Next Generation Sequencing (IMNGS) pipeline (Lagkouvardos et al., 2016) based on the UPARSE approach. Briefly, sequences were demultiplexed, trimmed to the first base with a quality score  $> 3$  and paired. Sequences with  $> 1000$  nucleotides and assembled reads with expected error of  $> 3$  were excluded from the analyses (Exp. 2, USEARCH 8.0; Exp. 3, USEARCH 8.1) (Edgar, 2010). Remaining reads were trimmed by 10 nucleotides at forward and reverse end. The presence of chimeras was tested with UCHIME (Edgar et al., 2011). Operational taxonomic units (OTUs) were clustered at 97% sequence similarity (Edgar, 2010) (Exp. 2, USEARCH 8.0; Exp. 3, USEARCH 8.1), and only those with a relative abundance of  $> 0.50\%$  (Exp. 2) or  $> 0.25\%$  (Exp. 3) in at least one sample were kept. Taxonomies were assigned at 80% confidence level with the RDP classifier (Wang et al., 2007) (version 2.11, training set 15). Sequences were aligned with

MUSCLE (Edgar, 2004) and trees were generated with Fasttree (Price et al., 2010). In Exp. 2 the analyzed dataset included 1,207,683 quality- and chimera-checked sequences ranging from 6,527 to 48,172 per sample, representing a total of 338 OTUs. One individual in the Fzd group was excluded from analyses due to abnormally high sequence depth (152,009). In Exp. 3 the analyzed dataset included 3,481,304 quality- and chimera-checked sequences ranging from 39,504 to 131,663 per sample, representing a total of 220 OTUs. Sequencing files from Exp. 2 and Exp. 3 are deposited to the Sequence Read Archive and are available under the accession number PRJNA668303.

## Flow Cytometry and *in vitro* T-Cell Stimulation

Immunophenotyping was carried out by incubating single-cell suspensions in phosphate-buffered saline (PBS) with 0.5% bovine serum albumin and 10 mM Na<sub>3</sub> on ice. After FcR-blocking with anti-CD32/16 antibody (eBioscience), cells were stained with Live/Dead Fixable Yellow Dead Cell Stain Kit (Thermo Fisher Scientific) followed by incubation with combinations of monoclonal antibodies as listed in **Supplementary Table S2**. For intracytoplasmic staining, cells were treated with Intracellular Fixation and Permeabilization Buffer Set, or with Foxp3/Transcription Factor Staining Buffer Set for intranuclear antigens (both eBioscience), according to the manufacturer's instructions. Fluorescence levels were measured using a Gallios 3-laser flow cytometer and analyzed using Kaluza 1.2 software (Beckman Coulter). Cells were gated as shown in **Supplementary Figure S1**, using single cell staining, omission of antibodies and matched isotypes as controls. For stimulation assays, splenocytes were cultured at concentration of  $2 \times 10^6$  cells/ml together with Dynabeads Mouse T-Activator CD3/CD28 (Thermo Fisher Scientific) at a 1:1 ratio, in RPMI (Gibco) l-glutamine supplemented with 60 µg/ml penicillin, 100 µg/ml streptomycin, 1 mM sodium pyruvate, 50 µM 2-mercaptoethanol, non-essential amino acids (all Gibco/Invitrogen), 10% fetal calf serum (PAA) and 30 U/ml recombinant murine (rm)IL-2 (eBioscience) for 48 h. Brefeldin A (10 µg/ml; Sigma) was added 4 h before harvesting, followed by immunophenotyping.

## Multiplex Assays

Cytokines were measured in serum using the following multiplex assays: Bio-Plex Pro Mouse Cytokine 8-plex panel (#M60000007A) supplemented with IL-6 and IL-17A singleplex, Bio-Plex Pro™ TGF-β 3-plex Assay (#171W4001M) (Bio-Rad), or ProcartaPlex Th1/Th2/Th9/Th17/Th22/Treg Cytokine 17-Plex Mouse Panel (EPX170-26087-901) (Thermo Fisher Scientific). Antibody subclasses were measured using ProcartaPlex Mouse Antibody Isotyping 7-plex panel (EPX070-20815-901). In all cases the analyses were carried out following the manufacturers' instructions, using a Luminex 200 reader and BioPlex Manager 6.0 software (BioRad). Analysis was performed on fluorescence index (FI) values minus background, while figures show concentrations calculated from standard curve. Analytes with more than 40% data points

below limit of detection (Antweiler, 2015) were excluded from statistical evaluation.

## Statistical Analyses

Microbial profiles and composition were analyzed in the R programming environment (R version 4.0.2) (R\_Core\_Team, 2020) using Rhea (Lagkourvaros et al., 2017)<sup>1</sup>. To account for differences in sequence depth, OTU tables were first normalized by dividing each sample's reads to their total reads, then multiplication by the total reads of the smallest sample. Beta-diversity was calculated based on generalized UniFrac distances (Chen et al., 2012) and the significance of separation between groups was tested by permutational multivariate analysis of variance (PERMANOVA). Alpha-diversity was assessed based on species richness and Shannon effective diversity as described in detail in Rhea. Only taxa with a prevalence of  $\geq 30\%$  (proportion of samples positive for the given taxa) in one given group, and relative abundance  $\geq 0.25\%$  were considered for statistical testing. For analyses of differences in relative abundance between  $> 2$  groups (Exp. 2), Kruskal-Wallis Rank Sum test was performed. A significant Kruskal-Wallis test ( $p < 0.05$ ) was followed by pairwise Wilcoxon Rank Sum tests. *P*-values were corrected for multiple comparisons according to the Benjamini-Hochberg method, and adjusted *p*-values are reported. For comparisons of two groups (Exp. 3), Wilcoxon Rank Sum tests were performed directly. For analyses of differences in prevalence between groups, Fisher's exact tests were performed. Over-time analyses within groups were performed using paired Wilcoxon Signed Rank Sum tests.

In order to identify patterns of differentially abundant and prevalent OTUs in Feral and SPF mice, we conducted an indicator species analysis implemented by the *indicspecies* package (De Cáceres and Legendre, 2009) in R. The significance of the associations was determined by permutation tests followed by Benjamini-Hochberg correction of resulting *p*-values. To identify highly indicative OTUs, we included only OTUs that occurred in  $\geq 70\%$  of the mice in either the Feral or SPF group at each timepoint. For Exp. 3, an indicator species analysis was conducted in the same manner as described for Exp. 2, to identify OTUs indicative of Chow-fed or Seed-fed animals independent of timepoint. For all groups at both timepoints, the relative abundances of the identified indicator-OTUs were plotted with the *heatmap.2* function from the *gplots* package (Warnes et al., 2020) in R. The closest species related to the indicator-OTU sequences were identified with EzBioCloud (Yoon et al., 2017). See **Supplementary Table S3** for a complete list of indicator-OTUs presented in **Figure 3E** and **Supplementary Figure S4E**.

Immunological data was analyzed using log (Ln)-transformed values. Comparisons between groups were performed using the statistical applications JMP v.14 (SAS Institute Inc.) or Prism v.7 (GraphPad Software, Inc.), applying Student's *t*-test for two groups, and Tukey-Kramer's multiple comparison test for  $> 2$  groups, at alpha level 0.05, unless otherwise stated. In figures with letter indications, levels not sharing the same letter were significantly different. Multivariate analyses were

<sup>1</sup><https://github.com/Lagkourvaros/Rhea>

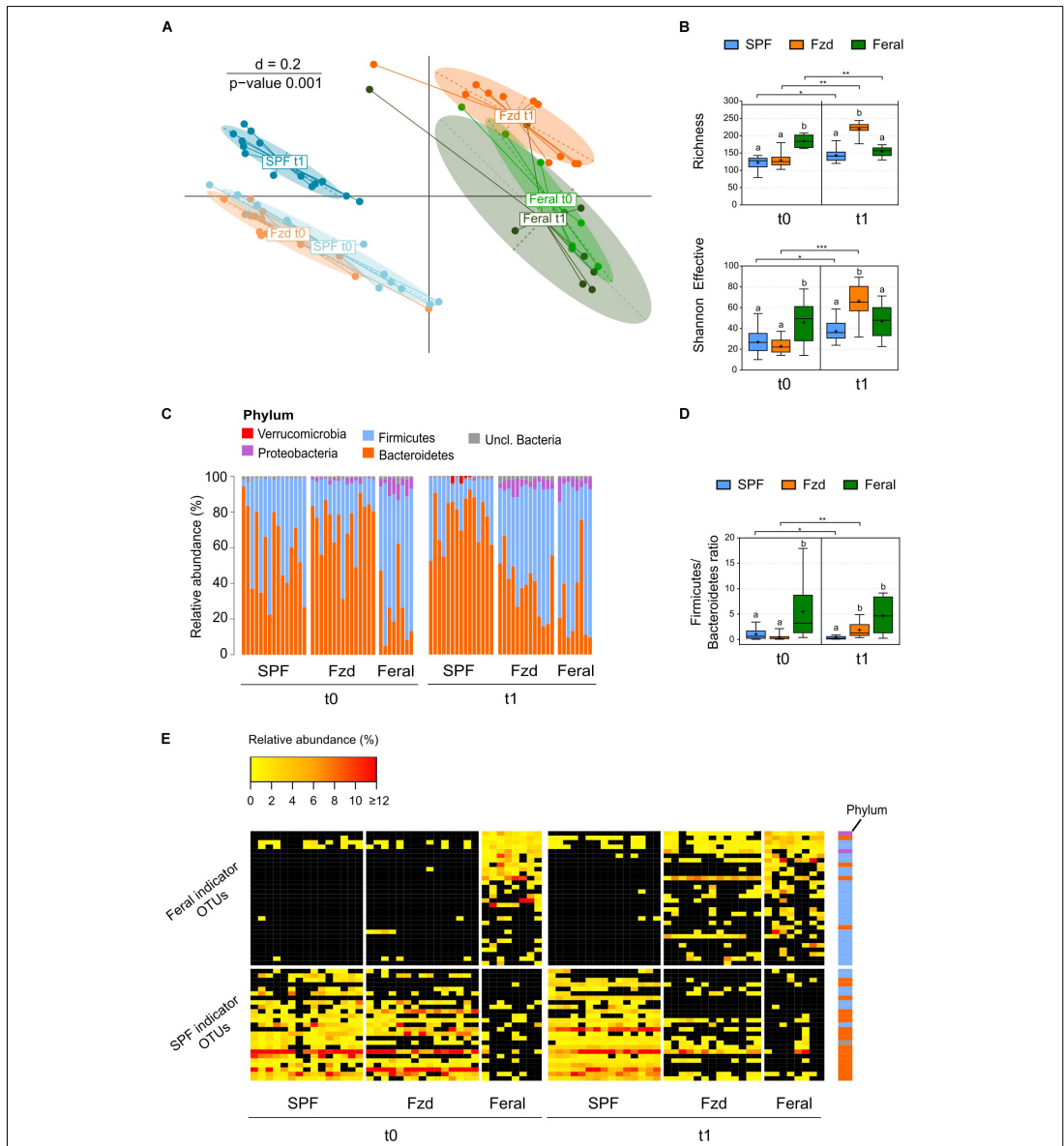


**FIGURE 3 |** Feralization lead to a gut microbiota diversity and composition converging with feral mice. Presented data is from Exp. 2. **(A)** Multi-dimensional scaling (MDS) plot of microbiota profiles for feral, feralized (Fzd) and SPF mice at baseline (t0) and termination (t1). Similarities between profiles were computed using generalized Unifrac distances. The significance of separation between groups was tested by PERMANOVA.  $d$  = dissimilarity scale. **(B)** Richness (observed OTUs) and Shannon effective diversity index. Box plots show median (line), mean (+), IQR (box) and minimum to maximum (whiskers). Asterisks designate over-time differences determined by Wilcoxon Signed-Rank Sum test. Differences between groups at each timepoint were determined by Kruskal-Wallis and Mann-Whitney  $U$ -tests. The Benjamini-Hochberg method was used to correct for multiple testing. Levels not sharing the same letter were significantly different at  $\alpha = 0.05$ .  $*p \leq 0.05$ ,  $**p \leq 0.01$ ,  $***p \leq 0.001$ . **(C)** Taxonomic binning at the rank of phylum, presented as relative abundance for each individual, with groups and timepoints indicated. **(D)** Firmicutes/Bacteroidetes ratio presented as in **(B)**. **(E)** Heatmap of relative abundance of Feral- and SPF-associated OTUs identified by indicator species analysis. Phyla of which the OTUs belong to are designated with colored squares specified in **(C)**. Relative abundances of the OTUs  $< 0.25\%$  were set to NA (black). All plots:  $n = 8$  (feral) or  $n = 13\text{--}15$  (other groups).

performed using the principal component analysis (PCA) on Correlations, and hierarchical clustering using Ward's minimum variance method in JMP on the variables listed in **Supplementary Table S4**, excluding one Fzd mouse with an incomplete data set.

## RESULTS

### Lab Mice Adapted Well to a Farmyard Habitat in the Presence of Feral Mice

Throughout Exp. 1 we closely monitored how animals performed through direct inspection and using surveillance or handheld cameras (**Supplementary Figure S2**). Feral and B6 mice were released simultaneously into the pens to avoid biased territorializing (**Supplementary Video S2**). The mice dug holes in the soil that appeared preferential for nesting rather than using wooden houses provided for this purpose (**Supplementary Video S3**). Feral and B6 mice mingled well, in both the male-female and the female-female setups. Feral mice generally reacted to human presence by hiding, re-emerged within few minutes and approached people (**Supplementary Video S4**), whilst the B6 mice were generally less shy. Feral mice quickly adapted to drinking from water bottles. However, four feral individuals were found dead with no visible signs of injuries and lack of water being a possible cause. No B6 mice died, showed visible bruises or signs of disease, except one slow-moving Fzd<sup>M</sup> female that was excluded from the study. Fzd<sup>M</sup> females mated with feral males and produced litters that were cared for in a shared dirt-hole nursing colony. However, since past or present pregnancy might confound the readouts, we chose to carry out subsequent experiments in an all-female setting. In Exp. 2 the observed behavior was similar to Exp. 1, and all introduced mice were recaptured in healthy condition.

### Feralized Mice Acquired Mouse Pathogens and a Feral-Like Gut Microbiota

Serum samples from four individuals of each mouse group in Exp. 1 were screened for antibodies against a range of pathogens. Feral mice carried antibodies for Minute virus of mice (MVM), Mouse parvovirus (MPV), Mouse Cytomegalovirus (MCMV) and, in one case, *Pasteurella pneumotropica* (*Pp*) (**Supplementary Table S5A**). Fzd<sup>M</sup> mostly seroconverted to mimic the feral mice, while only a single Fzd<sup>F</sup> mouse tested positive for one pathogen (*Pp*). SPF controls were negative for all tested agents. A gross parasitological examination of intestines with fecal content revealed the presence worms or eggs in feral and Fzd<sup>M</sup> mice, but to a less extent in Fzd<sup>F</sup> mice while negative in SPF controls (**Supplementary Table S5B**).

The terminal gut microbiota in stool samples from Fzd<sup>F</sup> mice in Exp. 1 has been reported previous (Lindner et al., 2015). Briefly, the microbiota profile of the feralized mice approached that of feral mice, including a higher relative abundance of Firmicutes and Proteobacteria, while SPF mice stood out with a separate profile. Data from Exp. 2 largely mirrored the findings of Exp. 1. At baseline, *beta*-diversity analysis demonstrated a distinct

clustering of baseline gut microbiota of the B6 mice separate from feral mice (**Figure 3A**), and *alpha*-diversity measures showed a significantly higher number of observed OTUs (richness) in feral mice compared to the Fzd and SPF groups (both  $p \leq 0.001$ ) (**Figure 3B**). At the rank of phylum, a significantly higher relative abundance of Firmicutes and lower relative abundance of Bacteroidetes was detected in feral mice compared to Fzd (both  $p \leq 0.001$ ) and SPF ( $p = 0.035$  and  $p = 0.005$ , respectively), as reflected in a higher Firmicutes/Bacteroidetes ratio (**Figures 3C,D**). Moreover, Proteobacteria abundance above cutoffs were detected in all feral mice and the majority of feralized mice, but only in one SPF individual (**Figure 3C**). In feral mice, the Proteobacteria was mainly accounted for by two OTUs with closest sequence similarity to *Helicobacter* species (*Helicobacter ganmani*, 99.6% similarity; *Helicobacter typhlonius*, 100% similarity), while in Fzd the Proteobacteria was mainly accounted for by one OTU with the closest sequence similarity to *Kiloniella laminariae* (86.3% similarity).

A clear shift in the microbiota profile was seen following feralization, in which the Fzd mice approached a Feral-like profile (**Figure 3A**). Feralization led to a dramatic increase in both richness and Shannon effective ( $p = 0.002$  and  $p \leq 0.001$ , respectively), indicating an elevated number of species representing a higher level of phylogenetic diversity (**Figure 3B**). An increase in relative abundance of Firmicutes and decrease in relative abundance of Bacteroidetes (both  $p = 0.001$ ) was observed following feralization, reflected in an increased Firmicutes/Bacteroidetes ratio ( $p = 0.005$ ) (**Figures 3C,D**). The shift following feralization was further supported by analysis of the terminal gut microbiota, in which the Fzd and feral mice demonstrated significantly higher *alpha*-diversity measures and Firmicutes/Bacteroidetes ratios, and increased relative abundances of Proteobacteria compared to the SPF mice (**Figures 3C,D**). Moreover, we conducted an Indicator Species Analysis to identify OTUs that were most indicative for Feral and SPF mice based on the probability of occurrence and abundance in these groups independent of timepoint. This algorithm was first developed by Dufrene and Legendre (1997) and has been employed previously to track persistence of OTUs in mice following environmental changes (Seedorf et al., 2014) and fecal microbiota transfer from wild to laboratory mice (Rosshart et al., 2017). Generally, the OTUs associated with Feral mice belonged to the Firmicutes phylum, while the SPF-associated OTUs were members of Bacteroidetes, mirroring the detected phylum-level differences (**Figure 3E**). Two OTUs with closest sequence similarities to *Helicobacter* species (*Helicobacter ganmani*, 99.6%; *Helicobacter typhlonius*, 100%) were identified as Feral-associated OTUs (**Figure 3E** and **Supplementary Table S3A**). By plotting the abundances of the indicator OTUs for all samples, we were able to track the Feral-associated and SPF-associated OTUs in the Fzd group over time. Prior to feralization, the Fzd and SPF groups showed overlapping patterns, with high abundance of SPF-associated and generally low abundance of Feral-associated OTUs. Following feralization, a substantial proportion of Feral-associated OTUs was detected, while only a very few SPF-associated OTUs undetected in Feral mice remained in the Fzd group at endpoint (**Figure 3E**).

Taken together, feralization led to a substantial change in gut microbiota structure, approaching the profile and composition seen in feral mice. Seropositivity to viral pathogens was detected in all feral mice, and in female feralized mice co-housed with feral males, but not in those co-housed with feral females.

## Feralization Lead to Immunophenotypes Consistent With Antigenic Experience and Immune Training

Cellular phenotypes were measured according to gating strategies shown in **Supplementary Figure S1**. In both Exp. 2 and Exp. 3, the number of T-cells and CD4<sup>+</sup> and CD8<sup>+</sup> subsets were similar in feralized and SPF mice in SPL as well as peripheral lymph nodes (PLNs) (not shown). Memory T-cells, defined as CD44<sup>+</sup>CD62L<sup>+</sup> central memory (CM) cells, or CD44<sup>+</sup>CD62L<sup>-</sup> effector memory (EM) cells were measured in the spleen and PLNs, respectively, according to the most common compartments for these subsets (Wherry et al., 2003; Stockinger et al., 2006). Feralized mice showed increased levels of CD8<sup>+</sup> T cells with an EM phenotype in the spleen (**Figures 4A,B**) as well as CM cells in the PLNs (**Figures 4C,D**). A tendency for increased proportions of EM CD4<sup>+</sup> cells was seen in the spleen of feralized mice (**Figures 4E,F**), but not for CM CD4<sup>+</sup> cells in

the PLNs (**Figures 4G,H**). Feral mice consistently had more cells displaying an EM or CM phenotype within the CD8 as well as the CD4 subsets (**Figures 4A–H**). To assess if T-cells of feralized mice had changed their potency as effector cells, we cultured splenocytes with anti-CD3/CD28 coupled beads for 48 h in the presence of IL-2 in Exp. 2. The frequency of interferon-gamma positive CD8<sup>+</sup> and to a lesser extent CD4<sup>+</sup> T-cell populations was higher in feralized mice compared to SPF mice (**Figures 5A,B**).

Regulatory T-cells (Tregs) (CD3<sup>+</sup>CD4<sup>+</sup>CD25<sup>+</sup>Foxp3<sup>+</sup>) were measured in PLNs. In Exp. 1, feralized mice had similar number of Tregs as SPF mice, while feral mice had a lower proportion (**Figure 6A**). In Exp. 2, slightly elevated Treg numbers were seen in feralized but not in feral mice (**Figure 6B**). We furthermore, assessed neuropilin-1 (NRP-1) dim or negative cells, associated with peripherally induced regulatory T-cells (pTregs), especially induced by gastrointestinal exposure (Bilate and Lafaillle, 2012). In both Exp. 1 and 2, the proportion of pTregs was slightly elevated in the feral mice, but insignificantly so in feralized mice (**Figures 6C,D**).

NK cells numbers were elevated in PLNs but not spleens of feral mice (**Figures 7A,B** and **Supplementary Figures S3A,B**), as observed previously (Boysen et al., 2011). In feralized mice NK cells tended to increase, albeit not statistically significant, in the PLNs (**Figures 7A,B**), while no differences were observed

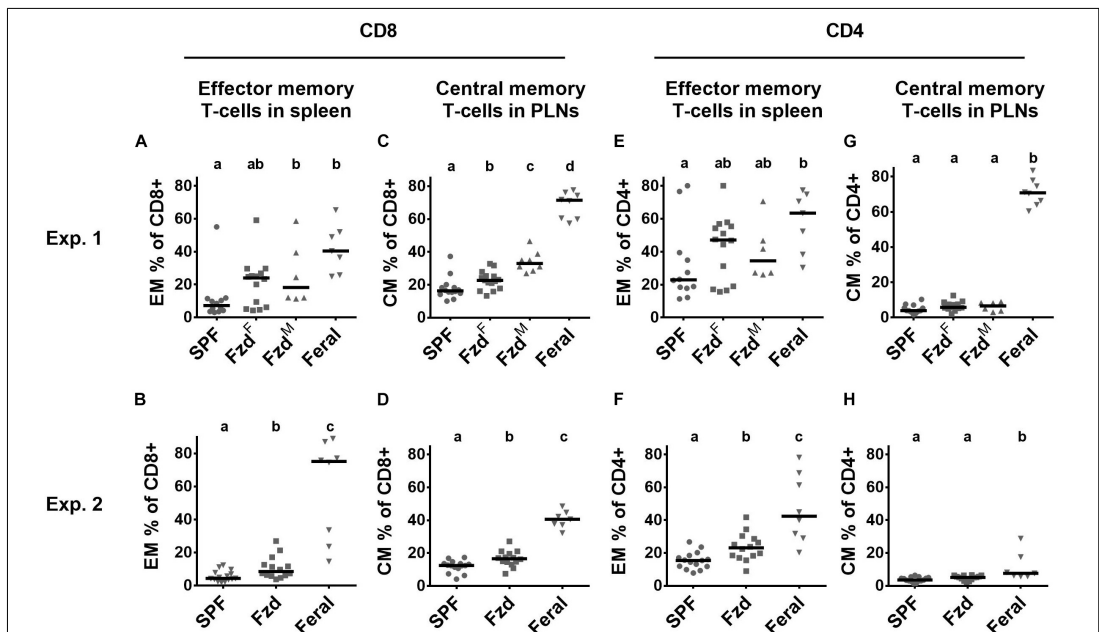
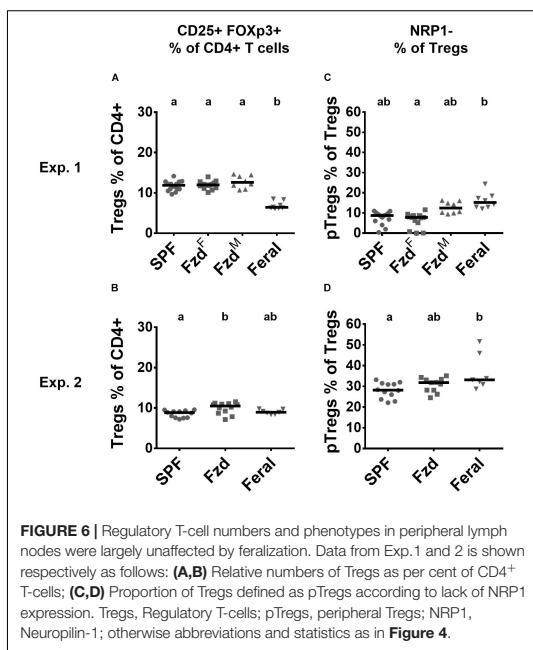
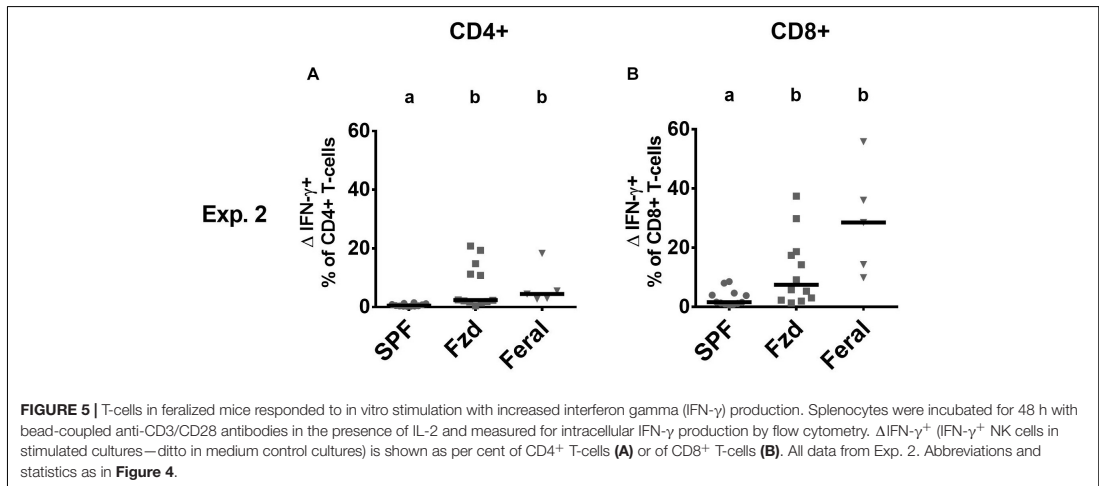


**FIGURE 4 |** Memory T-cell subsets were accumulated in feralized mice. Cellular phenotypes were measured by flow cytometry, gated as indicated in **Supplementary Figure S1**. Data from Exp. 1 and 2 is shown respectively as follows: **(A,B)** CD8<sup>+</sup> EM T-cells in spleen; **(C,D)** CD8<sup>+</sup> CM T-cells in PLNs; **(E,F)** CD4<sup>+</sup> EM T-cells in spleen; **(G,H)** CD4<sup>+</sup> CM T-cells in PLNs. PLNs, peripheral lymph nodes; Exp., Experiment; EM, Effector memory; CM, Central memory; SPF, Specific pathogen free; Fzd<sup>F</sup> or Fzd, Female B6 feralized with female feral mice; Fzd<sup>M</sup>, Female B6 feralized with male feral mice. Levels not sharing the same letter were significantly different at  $\alpha = 0.05$ .





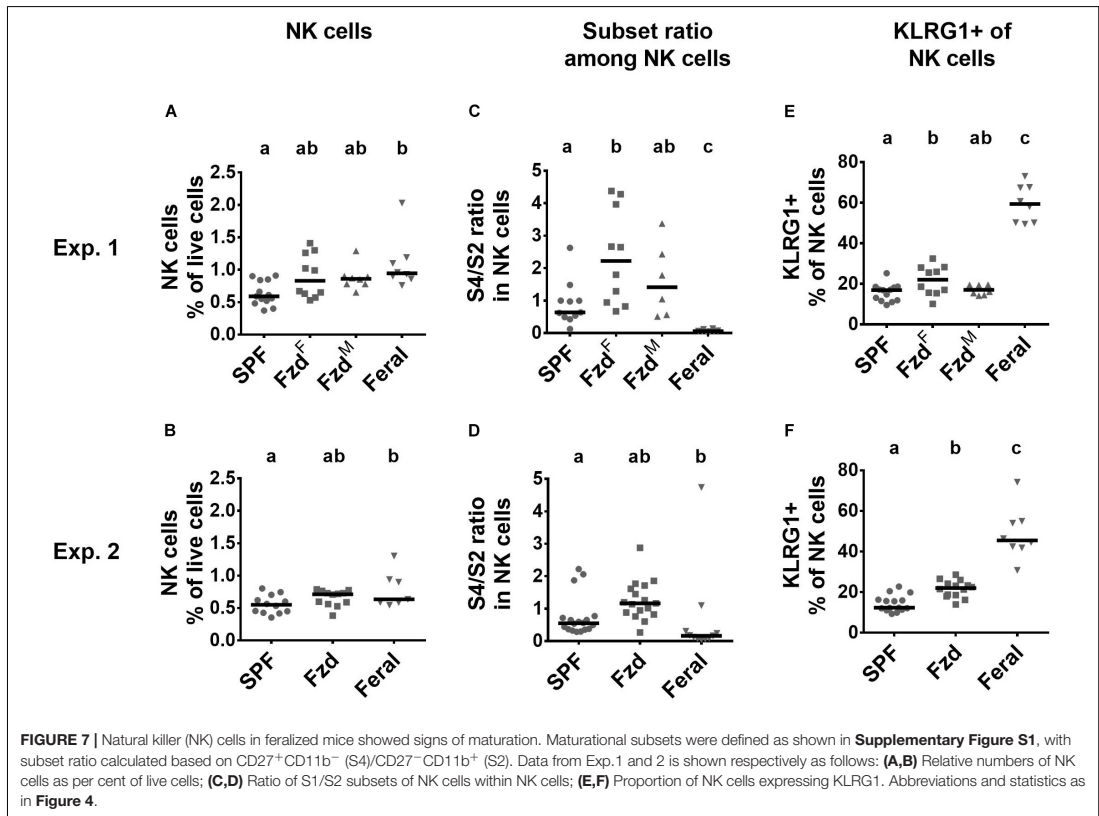
in the spleen (Supplementary Figures S3A,B). Murine NK cells can be phenotypically divided into maturation stages as early (S1) CD27<sup>-</sup>CD11b<sup>-</sup>, mid (S2) CD27<sup>+</sup>CD11b<sup>-</sup>, late (S3) CD27<sup>+</sup>CD11b<sup>+</sup>, and fully mature (S4) CD27<sup>-</sup>CD11b<sup>+</sup> stages (Chiossone et al., 2009; Abolins et al., 2017), most cells normally found within the S2–S4 categories. We found that feral mice had a decreased S4/S2 ratio in both PLNs and in spleen, as

seen previously (Boysen et al., 2011). In contrast, increased S4/S2 ratio was detected in feralized mice, most evident in the PLNs (Figures 7C,D and Supplementary Figures S3C,D). KLRG1 expression was elevated in NK cells in feral mice in PLN (Figures 7E,F) and partly in spleen (Supplementary Figures S3E,F), confirming previous observations (Boysen et al., 2011). To a lesser extent, feralized mice also had elevated KLRG1 in PLNs (Figures 7E,F), a tendency also evident in spleen (Supplementary Figures S3E,F).

Most tested serum cytokines were low and not significantly altered between groups (Figure 8). However, IL-18 was lower in the feralized and feral mice (Figure 8F). A tendency of increased TGF- $\beta$ 1 in feralized mice was noted but with high variability and not statistically confirmed (Figures 8G,H). Some additional cytokines were either not significantly altered or fell below the lower limit of detection (Supplementary Table S6).

Increased serum levels of IgE and IgG1 have previously been reported in feral mice (Devalapalli et al., 2006; Abolins et al., 2011), and in Exp. 2 we measured immunoglobulin subclasses using a multiplex assay, demonstrating that feral mice had increased serum IgA, IgE, Ig2a, Ig2b, and IgM (Figure 9). Feralized mice showed a tendency of increased IgE and IgG2b, while the remaining subclasses fell within the same range as SPF controls. IgG1 was not detected above background levels (not shown).

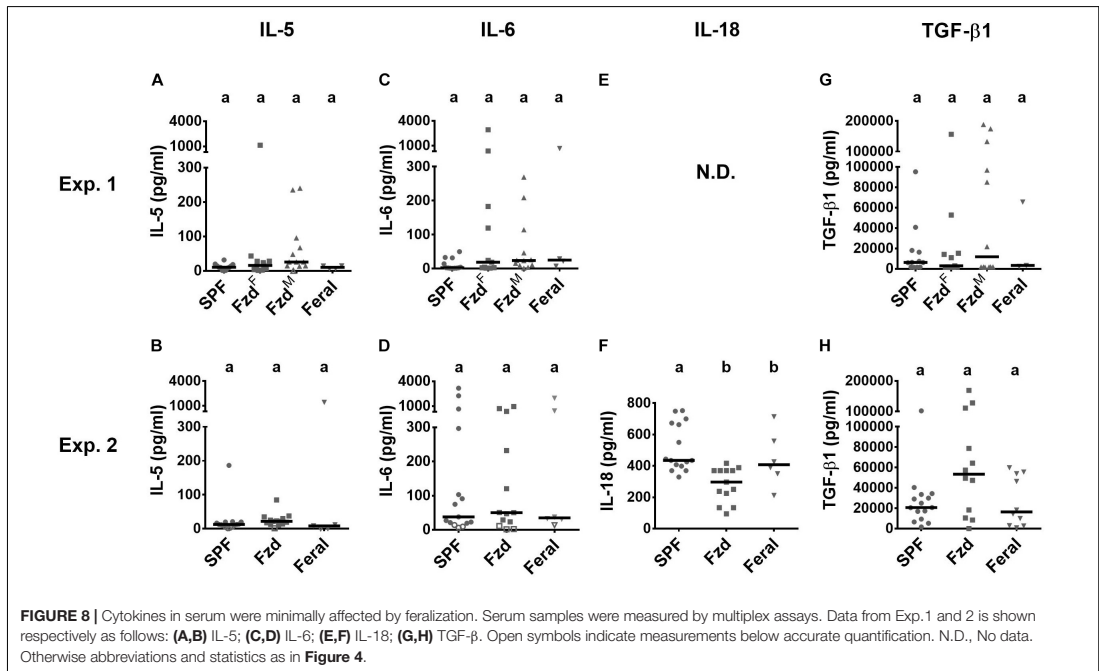
The data from Exp. 2 had a completeness that allowed multivariate analysis of immune parameters, in order to explore any co-variation undetected when assessing single parameters. A PCA analysis revealed that feralized mice grouped separately from SPF controls, in the direction of feral mice (Figure 10A), significantly different between all groups in first principal component (Prin1) but not Prin2 (Figure 10B). Likewise, a cluster analysis grouped mice from each study group separately, except a minor overlap between SPF and feralized mice (Figure 10C).



## Diet May Explain Shifts in Gut Microbiota, but Was Not Found to Drive Immunological Changes

To assess the contributions of differing diets between groups in Exp. 1 and 2 to gut microbiota and immunophenotypes, Exp. 3 was designed to incorporate the two diets in a SPF lab cage setting. Microbial profiling of feces showed a shift in microbiota composition and increased *alpha*-diversity measures on both diets, although more prominently in mice fed the seed diet compared to regular chow (**Supplementary Figures S4A,B**). At the rank of phylum, no significant changes were detected in the chow-fed animals. For the seed-fed animals, we detected a significantly decreased relative abundance of Bacteroidetes ( $p = 0.013$ ) and increased relative abundance of Firmicutes ( $p = 0.011$ ), reflected in increased Firmicutes/Bacteroidetes ratio over-time ( $p = 0.048$ ) (**Supplementary Figures S4C,D**). Similar to Exp. 2, the over-time changes were supported by analyses of the terminal gut microbiota, in which seed-fed mice demonstrated significantly higher *alpha*-diversity measures and Firmicutes/Bacteroidetes ratio compared to the chow-fed mice. However, in contrast to the findings from

Exp. 2, relative abundances of Proteobacteria were unchanged following the different diets. In the analysis of data from Exp. 3 we also conducted an indicator species analysis to identify OTUs that were most indicative for the Chow-fed and Seed-fed mice independent of timepoint. Relatively few indicator-OTUs were identified in this analysis, indicating only small differences between Chow- and Seed-fed mice at the OTU-level (**Supplementary Figure S4E** and **Supplementary Table S3B**). At baseline, prior to administration of different diets, the two groups showed overlapping patterns (**Supplementary Figure S4E**). From baseline to endpoint, Seed-fed animals showed an enrichment of several OTUs belonging to the phylum Firmicutes, mirroring the findings at phylum-level. Whilst we found changes in gut microbiota following the two diets, immunophenotyping showed no diet-induced difference in  $CD44^+$  cells in the  $CD8^+$  T-cell compartment. In the  $CD4^+$  T-cell subset, a minor increase of  $CD44^+$  cells was observed in seed-fed mice (**Supplementary Figure S5A**). In *ex vivo* CD3/CD28 stimulated splenocytes, intracellular IFN- $\gamma$  production was similar in the two diet groups in both  $CD8^+$  or  $CD4^+$  T-cells (**Supplementary Figure S5D**). Moreover, we observed no significant effect of diet on Treg



levels or pTreg proportions, NK cells or NK cells subsets (Supplementary Figures S5B,D).

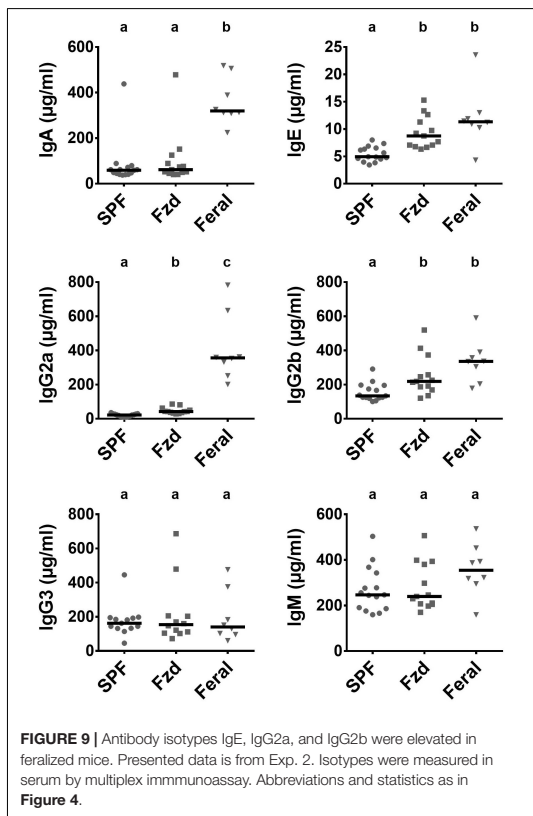
Taken together, the findings from Exp. 3 indicated that a diet similar to that given to feralized mice in Exp. 1 and 2 caused a significant shift in gut microbiota structure, yet provided no evidence for any shift in immunological parameters assignable to the diet.

## DISCUSSION

A spacious and naturalistically enriched environment meets an increasing demand to improve housing conditions to refine the experimental output from mouse models (Balcombe, 2010). Large indoor enclosures have previously been used to study house mouse behavior (Gray et al., 2000; Jensen et al., 2003, 2005; Weissbrod et al., 2013), but to our knowledge, no reports describe the microbiological and immunological phenotypes of mice reared in such enclosures enriched as a naturalistic environment. The tremendous adaptability of the house mouse implies that no single habitat is universally “natural.” Nevertheless, house mice are predominantly found in or near human dwellings, farm buildings, food stores and waste areas, and its dispersal largely follows human movements (Pocock et al., 2005). The house mouse often forms high-density territories as small as a few square meters (Selander, 1970). To set up a well-defined naturalistic scenario we constructed large pens containing essential farmyard elements through domestic animal fecal

material, soil and plants, and with wild-caught mice present as microbial donors. The aim of the current report was to observe the performance of laboratory mice housed in this model system and to observe their resulting fecal microbiota and key elements of their systemic immunity phenotype.

Feralization led to a significant shift in gut microbiota composition and increased *alpha*-diversity measures following feralization, supportive of previous reports of microbially exposed mice (Ottman et al., 2019; Liddicoat et al., 2020). We observed an enrichment of Proteobacteria in feral and feralized mice, in agreement with findings in “wildling” B6 mice born to feral mothers (Rosshart et al., 2019) as well as B6 mice co-housed with pet store mice (Huggins et al., 2019). Two OTUs associated with feral mice microbiota showed the closest similarity to *Helicobacter* species and were enriched in feralized mice. In a recent paper, *Helicobacter* species have been suggested to trigger colonic T cell responses in a context-dependent manner (Chai et al., 2017). Moreover, the higher Firmicutes/Bacteroidetes ratios in feralized and feral mice corresponds to a previous report of feral mice (Kreisinger et al., 2014), but contrasts the lower relative abundance of Firmicutes seen in fecal samples from wildlings (Rosshart et al., 2019), from B6 mice receiving fecal transfer from wild mice (Rosshart et al., 2017), as well as from soil-exposed mice (Ottman et al., 2019). However, care should be taken when interpreting between studies, as geographical factors have been shown to drive the microbiota composition to a larger extent than genotypes, including between *Mus musculus* subspecies (Linnenbrink et al., 2013; Kreisinger et al., 2014).



Notably, feral mice maintained a similar microbiota before and after pen housing in Exp. 2. Their prior microbial environment and diet is unknown, but they were caught at farms distant from the sources used for enrichment, and these findings could either indicate that the conditions we created reflected their feral situation, or that their colonized microbiota was more resilient to change compared to the SPF-derived laboratory mice.

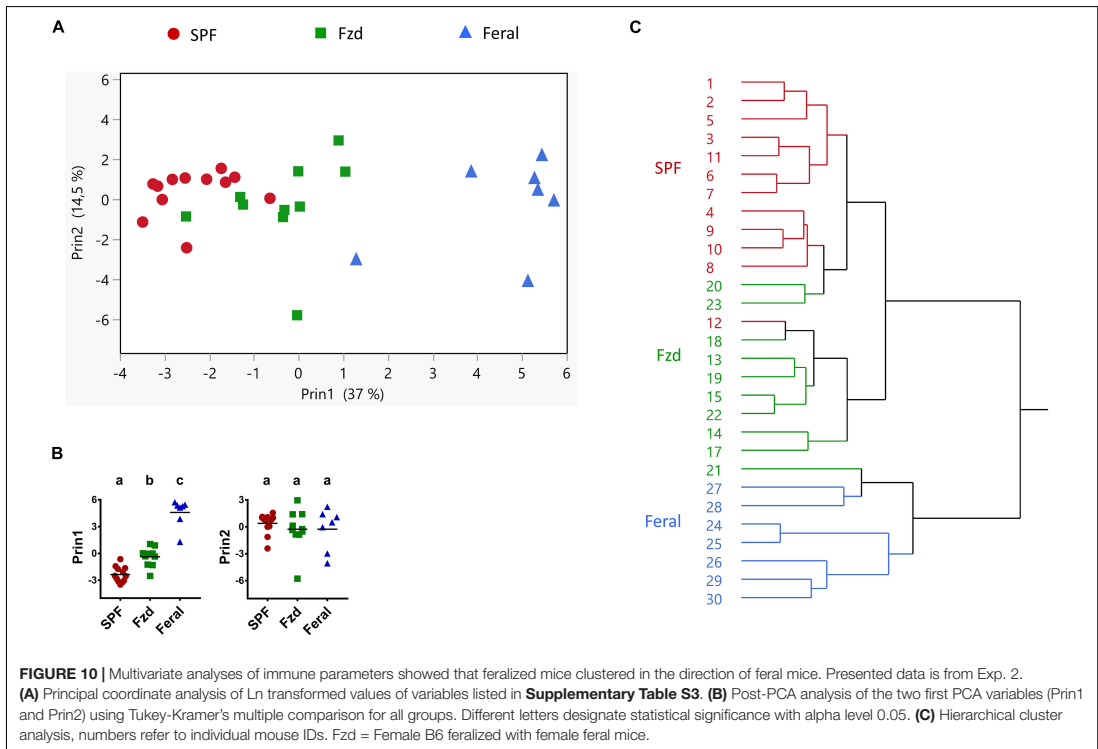
The seed-based diet offered in the naturalistic environment contained higher amounts of fiber and fat compared to the standard chow diet, both of which are groups of dietary components demonstrated to alter gut microbiota composition and influence immunity in a wide range of previous studies (Daniel et al., 2014; Trompette et al., 2014; Desai et al., 2016; Xiao et al., 2017; Las Heras et al., 2019). We therefore set up a third experiment to assess this impact in an otherwise hygienic context. Seed-fed mice had increased *alpha*-diversity and Firmicutes/Bacteroidetes ratio, suggesting a partial explanation for changes seen in the feralized mice. We did not observe differences in the investigated immune parameters following the two diets, suggesting the alterations of immunophenotypes were driven by other stimuli, or other components of the microbiota, than those conferred by diet.

A multivariate analysis showed that the combined systemic immune phenotype of feralized mice clustered distinctly from SPF mice in the direction of feral mice, albeit still closer to SPFs. For cellular measurements we concentrated on NK and T-cell phenotypes associated with maturation and memory. Feralized and feral mice had increased numbers of memory CD8<sup>+</sup> T cells, in line with report of long-lasting expansion following *in vivo* challenge (Vezys et al., 2009). Similar upregulation of memory T cells has been reported in feral and pet-store mice, in lab mice co-housed with pet-store mice and in rewilded mice (Beura et al., 2016; Abolins et al., 2017; Lin et al., 2020). Following *ex vivo* stimulation, we found that T-cells in feralized and feral mice responded more potently with IFN-gamma production compared to lab mice, similar to previous reports in feral and rewilded mice (Abolins et al., 2017; Lin et al., 2020).

We found little effect of feralization on the total Treg cell numbers, while pTregs, defined as NRP-1<sup>-</sup> Tregs (Bilate and Lafaille, 2012), showed a slightly increasing tendency, not significant in feralized but significant in feral mice. A previous study in feral mice found marginal increase in splenic Tregs (Abolins et al., 2017), while two other studies of microbially diversified lab mice found no alteration in Treg cell numbers (Frossard et al., 2017; Rosshart et al., 2019). These findings suggest that Tregs in systemic organs do not respond substantially to these types of environmental triggers.

NK cells may be activated by pathogens or primed by proinflammatory cytokines, transforming the cells into a more mature state, in many cases persisting as memory-like or trained NK cells (Nabekura and Lanier, 2016; Netea et al., 2020). In mice, trained NK cells have been found to display a mature KLRG1<sup>+</sup> and CD27<sup>-</sup>CD11b<sup>+</sup> phenotype (Nabekura and Lanier, 2016). We reproducibly found more CD27<sup>-</sup>CD11b<sup>+</sup> and KLRG1<sup>+</sup> NK cells in feralized B6 mice. Notably, as reported previously (Boysen et al., 2011; Abolins et al., 2017), feral mice had a contrasting overweight of CD27<sup>+</sup>CD11b<sup>-</sup> NK cells, yet with a high KLRG1 expression. Feral and feralized mice underwent the same microbial pressure for 2–3 months, suggesting that the CD27/CD11b discrepancy may be genetic rather than environmental. However, this aberrance is unlikely due to genetic differences amongst subspecies, as while the present mice were *M. m. musculus*-dominated, the same NK cell phenotype have been noted in feral *M. m. domesticus* mice (Abolins et al., 2017), the latter constituting the major genetic background for the B6 mouse (Yang et al., 2011). Regardless of cause, the finding emphasizes the importance of assessing genetically controlled individuals in this type of studies.

Low levels of serum cytokines were detected and these were apparently not sensitive to environmental changes, as also seen in wildlings (Rosshart et al., 2019). The observed elevation of IgE in feral and feralized mice compare with findings from other studies (Devalapalli et al., 2006; Abolins et al., 2011, 2017) and are possibly caused by the presence of parasites as were detected in Exp. 1. Besides parasites, seroconversion for pathobionts were especially evident in the Fzd<sup>M</sup> females, which made frequent intimate contacts with feral males during mating. In the all-female setup, a feral-type feral microbiota was obtained,



yet the serological results indicated that they acquired less of a pathogenic burden. These findings may suggest that relatively strong and/or frequent transmission pressure of pathobionts is needed for a mouse to reach a feral-like immunophenotype.

The scope of the presented studies was to achieve a full-scale naturalistic environment, rather than to explore underlying mechanisms, which would require multiple investigations or a substantial reduction of the very elements that create diversity. Depending on the scope, future studies may add or exclude elements, such as considering the necessity of mouse-specific microbiota obtained through the inclusion of feral mice. While the basis for environmental diversity will inevitably vary between geographical sites (Linnenbrink et al., 2013; Kreisinger et al., 2014), so does the microbiota in highly isolated conventional facilities (Rausch et al., 2016). The strength of genetically controlled model animals remains, and studies on the background of mice feralized in this manner can complement studies in conventional SPF and germ-free lab mice, as demonstrated by us in two reports (Lindner et al., 2015; Monin et al., 2020). By ensuring that environmental materials derive from the same sources throughout the experiment, and preferably between experiments, well-controlled and reproducible experiments can be achieved. A “dirty” environment as described here must in most cases be established separate from clean mouse houses, in our hands

successfully achieved in an experimental large animal facility, and later built as a separate satellite unit.

## CONCLUSION

In conclusion, we have demonstrated how laboratory mice can be feralized in large pens containing feral cohabitant mice, recapitulating a natural mouse habitat. Feralized mice reproducibly carried an altered fecal microbiota and immunophenotype in systemic immune tissues. This model system represents a refinement opportunity for various purposes, such as assessing the performance of infections, drugs or vaccines on the background of “real-world” adapted animals.

## DATA AVAILABILITY STATEMENT

The original contributions presented in the study are publicly available. This data can be found in NCBI, under accession number PRJNA668303.

## ETHICS STATEMENT

The animal study was reviewed and approved by National Animal Research Authority, Norwegian Food Safety Authority.

## AUTHOR CONTRIBUTIONS

PB and AKS designed the research. BWH and PB conducted animal Exp. 1. LEK and PB conducted animal Exp. 2 and 3. BWH, LEK, GMJ, MB, OP, and PB performed the laboratory procedures. HA and PB analyzed the data and wrote the manuscript. All authors contributed to the article and approved the submitted version.

## FUNDING

This research was funded internally at NMBU and the collaborators, microbiota analyses was supported by a grant from The Nansen Fund (Unifor, Norway).

## ACKNOWLEDGMENTS

We are indebted to Jane Hurst (University of Liverpool, United Kingdom) for valuable advice on the design of the mouse pens, the staff at Department of ProdMed at NMBU for assistance with the pen constructions and monitoring of mice (and for keeping the cat out!), the staff at ExBio (NMBU) for housing and tending of control mice, Andrew Janczak (NMBU) for lending of surveillance cameras, Teresa Hagen (NMBU, Parasitology group) for parasitological examinations, Peter O. Hofgaard (University of Oslo, Department of Immunology at Oslo University Hospital), Profs. Jan E. Paulsen and Harald Carlsen (NMBU) for advice on animal dissection and lab methods, Johanna Kabbert, Christina Petrick, Thomas Hitch (RWTH Aachen, Germany), and Anne Mari Herfindal (NMBU) for help and discussions related to the microbiota analyses.

## SUPPLEMENTARY MATERIAL

The Supplementary Material for this article can be found online at: <https://www.frontiersin.org/articles/10.3389/fmicb.2020.615661/full#supplementary-material>

**Supplementary Figure 1** | Flow cytometry gating strategies. (A) Single cell, mononuclear cells (MNC) and live cell gates. (B) NK cells defined as NKp46+CD3- cells, further defined as maturational stages S1–S4 based on CD27

and CD11b expression, or gated for the expression of KLRG1. (C) T-cells gated equivalent to above, gated as CD4+ or CD8+ and defined as Central Memory (CM; CD62L+CD44+) or Effector Memory (EM; CD62L-CD44+). (D) Regulatory T-cells, gated on CD4+ T-cells equivalent to above, defined as CD25+Foxp3+, and further gated for the expression of Neuropilin-1 (NRP1). (E) *In vitro* stimulated T-cells, cultured for 48 h in the presence of CD3/CD28 activator beads and IL-2, gated on T-cells equivalent to above and gated for the expression of interferon gamma (IFN $\gamma$ ).

**Supplementary Figure 2** | Photos from the mouse experiments carried out in the farmyard-like pens. (A) Pallet, soil, large animal feces, twigs, straw, feral mice. (B) Feral mouse peeking from water bottle. (C) Nest with B6 x feral mouse crosses. (D) B6 mice checking box (mostly used as toilets; dirt holes were preferred as nests). (E) Feral mouse. (F) Nighttime grazing on sprouts. (G) Offspring playing in box.

**Supplementary Figure 3** | Natural killer (NK) cell numbers and phenotypes in spleen, equivalent to **Figure 7**. Abbreviations and statistics as in **Figure 4**.

**Supplementary Figure 4** | Gut microbiota diversity and composition of SPF mice fed different diets. Presented data is from Exp. 3. (A) Multi-dimensional scaling (MDS) plot of microbiota profiles for seed- and chow-fed animals at baseline (t0) and termination (t1). Similarities between profiles were computed using generalized Unifrac distances. The significance of separation between groups was tested by PERMANOVA. d = dissimilarity scale. (B) Richness (observed OTUs) and Shannon effective diversity index. Box plots show median (line), mean (+), IQR (box) and minimum to maximum (whiskers). Asterisks designate over-time differences determined by Wilcoxon Signed-Rank Sum test. Letters designate differences between groups at each timepoint determined by Kruskal-Wallis and Mann-Whitney U tests. The Benjamini-Hochberg method was used to correct for multiple testing. Different letters designate statistical significance with corrected  $p \leq 0.05$ . \* $p \leq 0.05$ , \*\* $p \leq 0.01$ , \*\*\* $p \leq 0.001$ . (C) Taxonomic binning at the rank of phylum, presented as relative abundance for each individual, with groups and timepoints indicated. (D) Firmicutes/Bacteroidetes ratio presented as in (B). (E) Heatmap of relative abundances of Chow- and Seed-associated OTUs identified by indicator species analysis. Phyla of which the OTUs belong to are designated with colored squares specified in (C). Relative abundances of the OTUs < 0.25% were set to NA (black). All plots:  $n = 12$  (chow) or  $n = 13$  (seed).

**Supplementary Figure 5** | Cellular immunological phenotypes of mice in Exp. 3, corresponding to measurements in main experiments shown in **Figures 4–7**. Abbreviations and statistics as in **Figure 4**.

**Supplementary Video 1** | Mouse pen overview, wooden pallets, soil heaps with fresh domestic animal manure, straw, spruce twigs. / C57BL/6 mice in farm environment.

**Supplementary Video 2** | Release of feral (wild-caught) mouse. / First encounters between C57BL/6 and feral mice.

**Supplementary Video 3** | Feral mouse showing agile behavior, use of available space and resources.

**Supplementary Video 4** | Feral mice showing curiosity, adaptability to B6 mice and people.

## REFERENCES

- Abolins, S., King, E. C., Lazarou, L., Weldon, L., Hughes, L., Drescher, P., et al. (2017). The comparative immunology of wild and laboratory mice, *Mus musculus domesticus*. *Nat. Commun.* 8:14811. doi: 10.1038/ncomms14811
- Abolins, S., Lazarou, L., Weldon, L., Hughes, L., King, E. C., Drescher, P., et al. (2018). The ecology of immune state in a wild mammal, *Mus musculus domesticus*. *PLoS Biol.* 16:e2003538. doi: 10.1371/journal.pbio.2003538
- Abolins, S. R., Pocock, M. J., Hafalla, J. C., Riley, E. M., and Viney, M. E. (2011). Measures of immune function of wild mice, *Mus musculus*. *Mol. Ecol.* 20, 881–892. doi: 10.1111/j.1365-294x.2010.04910.x
- Antweiler, R. C. (2015). Evaluation of statistical treatments of left-censored environmental data using coincident uncensored data sets. II. Group comparisons. *Environ. Sci. Technol.* 49, 13439–13446. doi: 10.1021/acs.est.5b02385
- Balcombe, J. (2010). Laboratory rodent welfare: thinking outside the cage. *J. Appl. Anim. Welf. Sci.* 13, 77–88. doi: 10.1080/10887700903272168
- Beura, L. K., Hamilton, S. E., Bi, K., Schenkel, J. M., Odumade, O. A., Casey, K. A., et al. (2016). Normalizing the environment recapitulates adult human immune traits in laboratory mice. *Nature* 532, 512–516. doi: 10.1038/nature17655
- Bilate, A. M., and Lafaille, J. J. (2012). Induced CD4+Foxp3+ Regulatory T Cells in immune tolerance. *Annu. Rev. Immunol.* 30, 733–758. doi: 10.1146/annurev-immunol-020711-075043
- Boursot, P., Auffray, J. C., Britton-Davidian, J., and Bonhomme, F. (1993). The evolution of house mice. *Annu. Rev. Ecol. Syst.* 24, 119–152. doi: 10.1146/annurev.es.24.110193.001003

- Boysen, P., Eide, D. M., and Storset, A. K. (2011). Natural killer cells in free-living *Mus musculus* have a primed phenotype. *Mol. Ecol.* 20, 5103–5110. doi: 10.1111/j.1365-294X.2011.05269.x
- Cebra, J. J. (1999). Influences of microbiota on intestinal immune system development. *Am. J. Clin. Nutr.* 69, 1046S–1051S.
- Chai, J. N., Peng, Y., Rengarajan, S., Solomon, B. D., Ai, T. L., Shen, Z., et al. (2017). *Helicobacter* species are potent drivers of colonic T cell responses in homeostasis and inflammation. *Sci. Immunol.* 2:eaa15068. doi: 10.1126/sciimmunol.aal5068
- Chen, J., Bittinger, K., Charlson, E. S., Hoffmann, C., Lewis, J., Wu, G. D., et al. (2012). Associating microbiome composition with environmental covariates using generalized UniFrac distances. *Bioinformatics* 28, 2106–2113. doi: 10.1093/bioinformatics/bts342
- Chioccolone, L., Chaix, J., Fuseri, N., Roth, C., Vivier, E., and Walzer, T. (2009). Maturation of mouse NK cells is a 4-stage developmental program. *Blood* 113, 5488–5496. doi: 10.1182/blood-2008-10-187179
- Chung, H., Pamp, S. J., Hill, J. A., Surana, N. K., Edelman, S. M., Troy, E. B., et al. (2012). Gut immune maturation depends on colonization with a host-specific microbiota. *Cell* 149, 1578–1593. doi: 10.1016/j.cell.2012.04.037
- Daniel, H., Gholami, A. M., Berry, D., Desmarchelier, C., Hahne, H., Loh, G., et al. (2014). High-fat diet alters gut microbiota physiology in mice. *ISME J.* 8, 295–308. doi: 10.1038/ismej.2013.155
- De Cáceres, M., and Legendre, P. (2009). Associations between species and groups of sites: indices and statistical inference. *Ecology* 90, 3566–3574. doi: 10.1890/08-1823.1
- Desai, M. S., Seekatz, A. M., Koropatkin, N. M., Kamada, N., Hickey, C. A., Wolter, M., et al. (2016). A dietary fiber-deprived gut microbiota degrades the colonic mucus barrier and enhances pathogen susceptibility. *Cell* 167, 1339–1353.e21. doi: 10.1016/j.cell.2016.10.043
- Devalapalli, A. P., Leshar, A., Shieh, K., Solow, J. S., Everett, M. L., Edala, A. S., et al. (2006). Increased levels of IgE and autoactive, polyreactive IgG in wild rodents: implications for the hygiene hypothesis. *Scand. J. Immunol.* 64, 125–136. doi: 10.1111/j.1365-3083.2006.01785.x
- Dufrene, M., and Legendre, P. (1997). Species assemblages and Indicator species: the need for a flexible asymmetrical approach. *Ecol. Monogr.* 67, 345–366. doi: 10.2307/2963459
- Edgar, R. C. (2004). MUSCLE: multiple sequence alignment with high accuracy and high throughput. *Nucleic Acids Res.* 32, 1792–1797. doi: 10.1093/nar/gkh340
- Edgar, R. C. (2010). Search and clustering orders of magnitude faster than BLAST. *Bioinformatics* 26, 2460–2461. doi: 10.1093/bioinformatics/btq461
- Edgar, R. C., Haas, B. J., Clemente, J. C., Quince, C., and Knight, R. (2011). UCHIME improves sensitivity and speed of chimera detection. *Bioinformatics* 27, 2194–2200. doi: 10.1093/bioinformatics/btr381
- El Aidi, S., van Baaren, P., Derrien, M., Lindenbergh-Kortleve, D. J., Hooveld, G., Levenez, F., et al. (2012). Temporal and spatial interplay of microbiota and intestinal mucosa drive establishment of immune homeostasis in conventionalized mice. *Mucosal Immunol.* 5, 567–579. doi: 10.1038/mi.2012.32
- Flies, A. S., and Wild Comparative Immunology Consortium (2020). Rewilding immunology. *Science* 369, 37–38. doi: 10.1126/science.abb8664
- Franklin, C. L., and Ericsson, A. C. (2017). Microbiota and reproducibility of rodent models. *Lab Anim.* 46, 114–122. doi: 10.1038/labana.1222
- Frossard, C. P., Lazarevic, V., Gaia, N., Leo, S., Doras, C., Habre, W., et al. (2017). The farming environment protects mice from allergen-induced skin contact hypersensitivity. *Clin. Exp. Allergy* 47, 805–814. doi: 10.1111/cea.12905
- Gray, S. J., Jensen, S. P., and Hurst, J. L. (2000). Structural complexity of territories: preference, use of space and defence in commensal house mice, *Mus domesticus*. *Anim. Behav.* 60, 765–772. doi: 10.1006/anbe.2000.1527
- Honda, K., and Littman, D. R. (2016). The microbiota in adaptive immune homeostasis and disease. *Nature* 535, 75–84. doi: 10.1038/nature18848
- Huggins, M. A., Sjaastad, F. V., Pierson, M., Kucaba, T. A., Swanson, W., Staley, C., et al. (2019). Microbial exposure enhances immunity to pathogens recognized by TLR2 but increases susceptibility to cytokine storm through TLR4 sensitization. *Cell Rep.* 28, 1729. doi: 10.1016/j.celrep.2019.07.028
- Hunter, P. (2020). Public Health struggles to square hygiene with diversity: research on the link between microbiomes and immune function puts the “hygiene hypothesis” to rest. *EMBO Rep.* 21:e51540. doi: 10.15252/embr.202051540
- Ivanov, I. I., Atarashi, K., Manel, N., Brodie, E. L., Shima, T., Karaoz, U., et al. (2009). Induction of intestinal Th17 cells by segmented filamentous bacteria. *Cell* 139, 485–498. doi: 10.1016/j.cell.2009.09.033
- Jakobsson, H. E., Rodriguez-Pineiro, A. M., Schutte, A., Ermund, A., Boysen, P., Bemark, M., et al. (2015). The composition of the gut microbiota shapes the colon mucus barrier. *EMBO Rep.* 16, 164–177. doi: 10.15252/embr.201439263
- Jensen, S. P., Gray, S. J., and Hurst, J. L. (2003). How does habitat structure affect activity and use of space among house mice? *Anim. Behav.* 66, 239–250. doi: 10.1006/anbe.2003.2184
- Jensen, S. P., Gray, S. J., and Hurst, J. L. (2005). Excluding neighbours from territories: effects of habitat structure and resource distribution. *Anim. Behav.* 69, 785–795. doi: 10.1016/j.anbehav.2004.07.008
- Knutsen, L. E., Dissen, E., Saether, P. C., Bjornsen, E. G., Pialek, J., Storset, A. K., et al. (2019). Evidence of functional Cd94 polymorphism in a free-living house mouse population. *Immunogenetics* 71, 321–333. doi: 10.1007/s00251-018-01100-x
- Kreisinger, J., Cizkova, D., Vohanka, J., and Pialek, J. (2014). Gastrointestinal microbiota of wild and inbred individuals of two house mouse subspecies assessed using high-throughput parallel pyrosequencing. *Mol. Ecol.* 23, 5048–5060. doi: 10.1111/mec.12909
- Kriegel, M. A., Sefik, E., Hill, J. A., Wu, H. J., Benoist, C., and Mathis, D. (2011). Naturally transmitted segmented filamentous bacteria segregate with diabetes protection in nonobese diabetic mice. *Proc. Natl. Acad. Sci. U.S.A.* 108, 11548–11553. doi: 10.1073/pnas.1108924108
- Lagkouvardos, I., Fischer, S., Kumar, N., and Clavel, T. (2017). Rhea: a transparent and modular R pipeline for microbial profiling based on 16S rRNA gene amplicons. *PeerJ* 5:e2836. doi: 10.7717/peerj.2836
- Lagkouvardos, I., Joseph, D., Kapfhammer, M., Giritli, S., Horn, M., Haller, D., et al. (2016). IMNGS: a comprehensive open resource of processed 16S rRNA microbial profiles for ecology and diversity studies. *Sci. Rep.* 6:33721. doi: 10.1038/srep33721
- Las Heras, V., Clooney, A. G., Ryan, F. J., Cabrera-Rubio, R., Casey, P. G., Hueston, C. M., et al. (2019). Short-term consumption of a high-fat diet increases host susceptibility to *Listeria monocytogenes* infection. *Microbiome* 7:7. doi: 10.1186/s40168-019-0621-x
- Leung, J. M., Budischak, S. A., The, H. C., Hansen, C., Bowcutt, R., Neill, R., et al. (2018). Rapid environmental effects on gut nematode susceptibility in rewilded mice. *PLoS Biol.* 16:e2004108. doi: 10.1371/journal.pbio.2004108
- Liddicoat, C., Sydnor, H., Cando-Dumancela, C., Dresken, R., Liu, J., Gellie, N. J. C., et al. (2020). Naturally-derived airborne environmental microbial exposures modulate the gut microbiome and may provide anxiolytic benefits in mice. *Sci. Total Environ.* 701:134684. doi: 10.1016/j.scitotenv.2019.134684
- Lin, J. D., Devlin, J. C., Yeung, F., McCauley, C., Leung, J. M., Chen, Y. H., et al. (2020). Rewilding Neod 2 and Atg16l1 mutant mice uncovers genetic and environmental contributions to microbial responses and immune cell composition. *Cell Host Microbe* 27, 830–840.e4. doi: 10.1016/j.chom.2020.03.001
- Lindner, C., Thomsen, I., Wahl, B., Ugur, M., Sethi, M. K., Friedrichsen, M., et al. (2015). Diversification of memory B cells drives the continuous adaptation of secretory antibodies to gut microbiota. *Nat. Immunol.* 16, 880–888. doi: 10.1038/ni.3213
- Linnenbrink, M., Wang, J., Hardouin, E. A., Kunzel, S., Metzler, D., and Baines, J. F. (2013). The role of biogeography in shaping diversity of the intestinal microbiota in house mice. *Mol. Ecol.* 22, 1904–1916. doi: 10.1111/mec.12206
- Monin, L., Ushakov, D. S., Arnesen, H., Bah, N., Jandke, A., Munoz-Ruiz, M., et al. (2020). gamma delta T cells compose a developmentally regulated intrauterine population and protect against vaginal candidiasis. *Mucosal Immunol.* 13, 969–981. doi: 10.1038/s41385-020-0305-7
- Muraille, E., and Goriely, S. (2017). The nonspecific face of adaptive immunity. *Curr. Opin. Immunol.* 48, 38–43. doi: 10.1016/j.coi.2017.08.002
- Nabekura, T., and Lanier, L. L. (2016). Tracking the fate of antigen-specific versus cytokine-activated natural killer cells after cytomegalovirus infection. *J. Exp. Med.* 213, 2745–2758. doi: 10.1084/jem.20160726
- Netea, M. G., Dominguez-Andres, J., Barreiro, L. B., Chavakis, T., Divangahi, M., Fuchs, E., et al. (2020). Defining trained immunity and its role in health and disease. *Nat. Rev. Immunol.* 20, 375–388. doi: 10.1038/s41577-020-0285-6

- Oh, J. Z., Ravindran, R., Chassaing, B., Carvalho, F. A., Maddur, M. S., Bower, M., et al. (2014). TLR5-mediated sensing of gut microbiota is necessary for antibody responses to seasonal influenza vaccination. *Immunity* 41, 478–492. doi: 10.1016/j.immuni.2014.08.009
- Ottman, N., Ruokolainen, L., Suomalainen, A., Sinkko, H., Karisola, P., Lehtimäki, J., et al. (2019). Soil exposure modifies the gut microbiota and supports immune tolerance in a mouse model. *J. Allergy Clin. Immunol.* 143, 1198. doi: 10.1016/j.jaci.2018.06.024
- Pocock, M. J., Hauffe, H., and Searle, J. B. (2005). Dispersal in house mice. *Biol. J. Linn. Soc.* 84, 565–583. doi: 10.1111/j.1095-8312.2005.00455.x
- Price, M. N., Dehal, P. S., and Arkin, A. P. (2010). FastTree 2—approximately maximum-likelihood trees for large alignments. *PLoS One* 5:e9490. doi: 10.1371/journal.pone.0009490
- Quinn, S. M., Cunningham, K., Raverdeau, M., Walsh, R. J., Curham, L., Malara, A., et al. (2019). Anti-inflammatory trained immunity mediated by helminth products attenuates the induction of T cell-mediated autoimmune disease. *Front. Immunol.* 10:1109. doi: 10.3389/fimmu.2019.01109
- Rausch, P., Basic, M., Batra, A., Bischoff, S. C., Blaut, M., Clavel, T., et al. (2016). Analysis of factors contributing to variation in the C57BL/6J fecal microbiota across German animal facilities. *Int. J. Med. Microbiol.* 306, 343–355. doi: 10.1016/j.ijmm.2016.03.004
- Reese, T. A., Bi, K., Kambal, A., Filali-Mouhim, A., Beura, L. K., Burger, M. C., et al. (2016). Sequential infection with common pathogens promotes human-like immune gene expression and altered vaccine response. *Cell Host Microbe* 19, 713–719. doi: 10.1016/j.chom.2016.04.003
- Rosshart, S. P., Herz, J., Vassallo, B. G., Hunter, A., Wall, M. K., Badger, J. H., et al. (2019). Laboratory mice born to wild mice have natural microbiota and model human immune responses. *Science* 365:eaaw4361. doi: 10.1126/science.aaw4361
- Rosshart, S. P., Vassallo, B. G., Angeletti, D., Hutchinson, D. S., Morgan, A. P., Takeda, K., et al. (2017). Wild mouse gut microbiota promotes host fitness and improves disease resistance. *Cell* 171, 1015–1028.e13. doi: 10.1016/j.cell.2017.09.016
- R\_Core\_Team (2020). *R: A Language and Environment for Statistical Computing*. Vienna: R Foundation for Statistical Computing.
- Seedorf, H., Griffin, N. W., Ridaura, V. K., Reyes, A., Cheng, J., Rey, F. E., et al. (2014). Bacteria from diverse habitats colonize and compete in the mouse gut. *Cell* 159, 253–266. doi: 10.1016/j.cell.2014.09.008
- Selander, R. K. (1970). Behavior and genetic variation in natural populations. *Am. Zool.* 10, 53–66. doi: 10.1093/icb/10.1.53
- Stockinger, B., Bourgeois, C., and Kassiotis, G. (2006). CD4+ memory T cells: functional differentiation and homeostasis. *Immunol. Rev.* 211, 39–48. doi: 10.1111/j.0105-2896.2006.00381.x
- Tao, L., and Reese, T. A. (2017). Making mouse models that reflect human immune responses. *Trends Immunol.* 38, 181–193. doi: 10.1016/j.it.2016.12.007
- Trompette, A., Gollwitzer, E. S., Yadava, K., Sichelstiel, A. K., Sprenger, N., Ngombu, C., et al. (2014). Gut microbiota metabolism of dietary fiber influences allergic airway disease and hematopoiesis. *Nat. Med.* 20, 159–166. doi: 10.1038/nm.3444
- Vezys, V., Yates, A., Casey, K. A., Lanier, G., Ahmed, R., Antia, R., et al. (2009). Memory CD8 T-cell compartment grows in size with immunological experience. *Nature* 457, 196–199. doi: 10.1038/nature07486
- Wang, Q., Garrity, G. M., Tiedje, J. M., and Cole, J. R. (2007). Naive Bayesian classifier for rapid assignment of rRNA sequences into the new bacterial taxonomy. *Appl. Environ. Microbiol.* 73, 5261–5267. doi: 10.1128/aem.00062-07
- Warnes, G. R., Bolker, B., Bonebakker, L., Gentleman, R., Huber, W., Liaw, A., et al. (2020). Available online at: <https://CRAN.R-project.org/package=gplots> (accessed December 01, 2020).
- Weissbrod, A., Shapiro, A., Vasserman, G., Edry, L., Dayan, M., Yitzhaky, A., et al. (2013). Automated long-term tracking and social behavioural phenotyping of animal colonies within a semi-natural environment. *Nat. Commun.* 4:2018. doi: 10.1038/ncomms3018
- Wherry, E. J., Teichgräber, V., Becker, T. C., Masopust, D., Kaech, S. M., Antia, R., et al. (2003). Lineage relationship and protective immunity of memory CD8 T cell subsets. *Nat. Immunol.* 4, 225–234. doi: 10.1038/ni889
- Xiao, L., Sonne, S. B., Feng, Q., Chen, N., Xia, Z., Li, X., et al. (2017). High-fat feeding rather than obesity drives taxonomical and functional changes in the gut microbiota in mice. *Microbiome* 5:43.
- Yang, H., Wang, J. R., Didion, J. P., Buus, R. J., Bell, T. A., Welsh, C. E., et al. (2011). Subspecific origin and haplotype diversity in the laboratory mouse. *Nat. Genet.* 43, 648–655. doi: 10.1038/ng.847
- Yeung, F., Chen, Y. H., Lin, J. D., Leung, J. M., McCauley, C., Devlin, J. C., et al. (2020). Altered immunity of laboratory mice in the natural environment is associated with fungal colonization. *Cell Host Microbe* 27, 809–822.e6. doi: 10.1016/j.chom.2020.02.015
- Yoon, S. H., Ha, S. M., Kwon, S., Lim, J., Kim, Y., Seo, H., et al. (2017). Introducing EzBioCloud: a taxonomically united database of 16S rRNA gene sequences and whole-genome assemblies. *Int. J. Syst. Evol. Microbiol.* 67, 1613–1617. doi: 10.1099/ijsem.0.001755

**Conflict of Interest:** The authors declare that the research was conducted in the absence of any commercial or financial relationships that could be construed as a potential conflict of interest.

Copyright © 2021 Arnesen, Knutsen, Hognestad, Johansen, Bemark, Pabst, Storset and Boysen. This is an open-access article distributed under the terms of the Creative Commons Attribution License (CC BY). The use, distribution or reproduction in other forums is permitted, provided the original author(s) and the copyright owner(s) are credited and that the original publication in this journal is cited, in accordance with accepted academic practice. No use, distribution or reproduction is permitted which does not comply with these terms.



# Paper II



II



RESEARCH

Open Access



# Induction of colorectal carcinogenesis in the C57BL/6J and A/J mouse strains with a reduced DSS dose in the AOM/DSS model

Henriette Arnesen<sup>1,2\*</sup> , Mette Helen Bjørge Müller<sup>3</sup>, Mona Aleksandersen<sup>1</sup>, Gunn Charlotte Østby<sup>4</sup>, Harald Carlsen<sup>2</sup>, Jan Erik Paulsen<sup>3</sup> and Preben Boysen<sup>1</sup>

## Abstract

**Background:** Colorectal cancer (CRC) is one of the most frequently diagnosed cancers worldwide and thus mouse models of CRC are of significant value to study the pathogenesis. The Azoxymethane/Dextran sulfate sodium (AOM/DSS) model is a widely used, robust initiation-promotion model for chemical induction of colitis-associated CRC in rodents. However, the dosage of chemicals, treatment regimens and outcome measures vary greatly among studies employing this model. Thus, the aim of this study was to examine an AOM/DSS model involving a reduced (1%) dose of DSS for induction of carcinogenesis in A/J and C57BL/6J (B6) mice.

**Results:** We show that colonic preneoplastic lesions can be reliably detected in A/J and B6 mice by use of a AOM/DSS model involving a single injection of 10 mg/kg AOM followed by three 7-day cycles of a low-dose (1%) DSS administration. Supporting existing evidence of A/J mice exhibiting higher susceptibility to AOM than B6 mice, our AOM/DSS-treated A/J mice developed the highest number of large colonic lesions. Clinical symptoms in both strains subjected to the AOM/DSS treatment did not persist in-between treatment cycles, demonstrating that the animals tolerated the treatment well.

**Conclusions:** Our findings suggest that a reduced dose of DSS in the AOM/DSS model can be considered in future studies of early phase colorectal carcinogenesis in the A/J and B6 mouse strains using preneoplastic lesions as an outcome measure, and that such regimen may reduce the risk of early trial terminations to accommodate human endpoints. Overall, our data emphasize the importance of devoting attention towards choice of protocol, outcome measures and mouse strain in studies of CRC in mice according to the study purpose.

**Keywords:** AOM/DSS, Colorectal cancer, Mouse models, Disease models, Azoxymethane, Dextran sulfate sodium

## Background

Colorectal cancer (CRC) is the second most diagnosed cancer in women, and the third most in men worldwide [1, 2]. CRC etiology is not known, but numerous risk factors have been characterized. A minority of CRC

cases are attributed to hereditary factors, such as germline mutations in susceptibility genes, while most CRCs arise sporadically with inflammation being a well-established driver. Individuals with inflammatory bowel diseases (IBDs) such as ulcerative colitis and Crohn's disease have substantially increased risk of CRC [3, 4]. Generally, the initial changes in colorectal carcinogenesis involve formation of hyperplastic and dysplastic crypts that in turn proliferate to form microadenomas giving rise to adenomatous polyps, carcinoma and ultimately

\* Correspondence: [henriette.arnesen@nmbu.no](mailto:henriette.arnesen@nmbu.no)

<sup>1</sup>Department of Preclinical Sciences and Pathology, Faculty of Veterinary Medicine, Norwegian University of Life Sciences (NMBU), Oslo, Norway

<sup>2</sup>Faculty of Chemistry, Biotechnology and Food Science, Norwegian University of Life Sciences (NMBU), Ås, Norway

Full list of author information is available at the end of the article



© The Author(s). 2021 **Open Access** This article is licensed under a Creative Commons Attribution 4.0 International License, which permits use, sharing, adaptation, distribution and reproduction in any medium or format, as long as you give appropriate credit to the original author(s) and the source, provide a link to the Creative Commons licence, and indicate if changes were made. The images or other third party material in this article are included in the article's Creative Commons licence, unless indicated otherwise in a credit line to the material. If material is not included in the article's Creative Commons licence and your intended use is not permitted by statutory regulation or exceeds the permitted use, you will need to obtain permission directly from the copyright holder. To view a copy of this licence, visit <http://creativecommons.org/licenses/by/4.0/>. The Creative Commons Public Domain Dedication waiver (<http://creativecommons.org/publicdomain/zero/1.0/>) applies to the data made available in this article, unless otherwise stated in a credit line to the data.

invasive cancer [5–7]. A variety of preneoplastic lesions reported to be involved in the initiation of colorectal tumorigenesis are widely used as biomarkers of colorectal carcinogenesis. The preneoplastic lesions characterized in rodents include aberrant crypt foci (ACF) [8], flat aberrant crypt foci (flat ACF) [9, 10], mucin-depleted foci (MDF) [11] and  $\beta$ -catenin accumulated crypts (BCAC) [12], that may partly overlap [13].

Experimental mouse models that mimic the initiation and progression of CRC is of great importance to study causes, mechanisms and preventive agents. Genetic models such as the Min (multiple intestinal neoplasia) mice harboring a mutant allele of the murine *Apc* (adenomatous polyposis coli) gene are widely used [14]. Another approach is via chemical induction, such as administration of the specific colorectal pro-carcinogen azoxymethane (AOM) [14]. Following metabolism by CYP2E1, AOM is converted to methylazoxymethanol (MAM), a highly reactive alkylating species that generate O<sup>6</sup> methylguanine adducts in DNA resulting in mutation accumulation and induction of carcinogenesis [14–16]. A model involving a combinatory treatment with AOM and dextran sulfate sodium (DSS) salt, called the AOM/DSS model, was developed to mimic human colitis-associated CRC [17]. DSS is a heparin-like polysaccharide that inflict colonic epithelial damage, mucosal permeability and transmural inflammation in mice [18–20]. The AOM/DSS model is considered robust and reproducible, and it has emerged to become one of the most frequently used models to study inflammation-associated colorectal carcinogenesis in rodents [14, 21–23].

Commonly, AOM/DSS protocols involve one or more AOM injections followed by colitis induced by repeated cycles of 2–3% (w/v) DSS administered via drinking water [14, 17, 22]. Nevertheless, the administered doses of AOM and DSS vary greatly between studies, and there is no consensus practice for this experimental model. Tumorigenic effects of AOM combined with a low dose of DSS ( $\leq 1\%$ ) has been reported in various mouse strains [24, 25]. Yet, to our knowledge, only a few reports have since employed AOM/DSS models with DSS doses lower than 2% for the study of agents influencing colorectal carcinogenesis in mice [26–29]. Dependent on the doses and frequency of DSS administration as well as experimental timespan, AOM/DSS treatment can lead to consistent development of adenomas and adenocarcinomas [24, 26] or inconsistent tumor incidence [24, 27].

An increasing body of evidence have also emphasized high discrepancies with respect to susceptibility to DSS and AOM in different inbred mouse strains. The A/J mice has been shown to be among the most susceptible strains to AOM-induced colorectal carcinogenesis while C57BL/6J (B6) has been reported relatively resistant [25,

30, 31]. Furthermore, the B6 strain is reportedly more susceptible to DSS-induced inflammation compared to other strains [32]. Based on this knowledge, adjustments of treatment regimen for the susceptibility the mouse strain is recommended prior to design of experiments employing the AOM/DSS model.

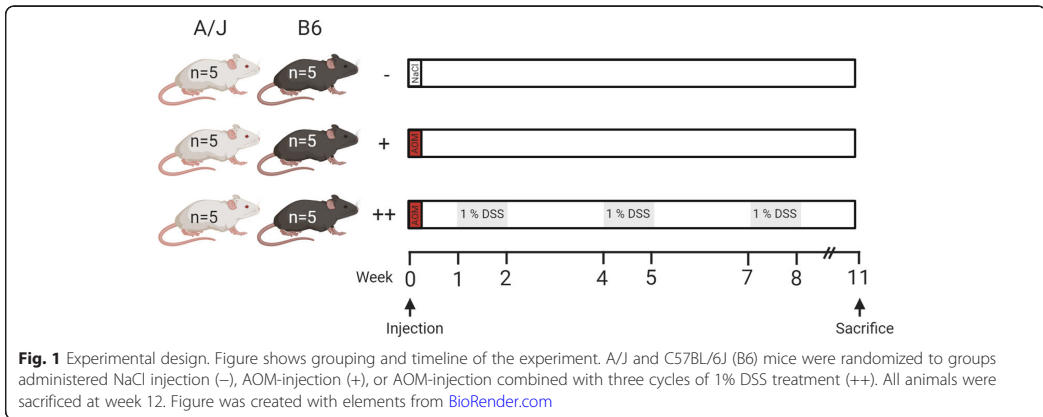
Clinical symptoms following AOM/DSS treatments are caused by colitis or advancement of cancer itself, and can include body weight loss, bloody stool and rectal bleeding, rectal prolapse, as well as early death [20, 21, 24, 33]. However, observed symptoms following treatments are often scarcely documented in studies employing AOM/DSS models. Moreover, outcome measures vary between AOM/DSS studies, with count of macroscopically visible tumors and histopathological assessment being the dominant endpoints. The use of preneoplastic lesions such as ACFs as biomarkers has been commended to minimize animal suffering in CRC experiments [34], which is in compliance with the European directive 2010/63 on the protection of animals used for scientific purposes [35].

In this study, we evaluated an AOM/DSS model involving a single injection of AOM in combination with three treatment cycles of a reduced (1%) dose of DSS for induction of carcinogenesis in colons of A/J and B6 mice, reportedly representing two extremes with respect to AOM susceptibility. We hypothesized that ACFs are reliably detected in colons of mice subjected to such treatment approach, and thus enables modelling of the induction phase of carcinogenesis while limiting adverse clinical symptoms.

## Results

### General findings and clinical evaluation

Wild-type A/J mice were administered an AOM injection, an AOM injection combined with DSS treatment, or control treatment (Fig. 1). For the AOM/DSS-treated animals, bodyweight and clinical symptoms were registered every 2nd day throughout the DSS treatment periods. Neither of these groups showed significant reduction in bodyweight loss during the DSS treatment cycles (Fig. 2A). Comparison of the bodyweight change between the AOM/DSS-treated and control groups revealed a significant interaction effect ( $p < 0.001$ ) of group and time. Pairwise comparisons showed a significantly lower bodyweight in the AOM/DSS-treated A/J mice compared to the AOM/DSS-treated B6 mice at day 56 ( $p = 0.048$ ) and 60 ( $p = 0.050$ ), and a significantly lower bodyweight in the AOM/DSS-treated B6 compared to the control B6 group at day 60 ( $p = 0.031$ ) and 62 ( $p = 0.010$ ). Intake of DSS was similar for the B6 and A/J mice, indicating differences in disease states were not biased by inconsistent DSS consumption (Fig. 2B).



Both A/J and B6 strains exhibited clinical symptoms during AOM/DSS treatment, with A/J mice showing the most prominent symptoms. The first symptoms appeared during the 2nd DSS cycle, with observed blood in feces of both A/J mice (day 36) and B6 mice (day 38) (Fig. 2C). Throughout the DSS treatment regimens, blood in feces was observed in all AOM/DSS-treated A/J individuals, while only in two B6 individuals. Rectal bleeding, defined as blood around anus, was observed in two A/J individuals at the end of the 3rd cycle of DSS treatment. Rectal bleeding was also observed in two B6 mice at the end of the 2nd and 3rd cycle of DSS treatment, respectively. All animals did, however, convalesce during the subsequent recovery periods. Appearance and behavior were normal for all animals, except one A/J individual during the 2nd DSS cycle (day 39) that convalesced during the subsequent recovery period. One individual in B6 AOM/DSS group showed signs of rectal prolapse at termination. All AOM and control treated animals appeared healthy throughout the trial, with no recorded symptoms or bodyweight loss ([S1 dataset](#)).

#### Identification of intestinal lesions

ACFs were detected in all AOM/DSS- and AOM-treated animals. Following AOM/DSS treatment, the total number, load and average size of the ACFs were similar in both B6 and A/J strains, indicating a comparable development of these preneoplastic lesions (Fig. 3A). However, the multiplicity of larger lesions categorized as tumors was significantly higher in A/J mice compared to B6 ( $p = 0.008$ ). Tumors were detected in all AOM/DSS-treated mice, and the counts ranged from 2 to 19 in B6 to 30–56 in A/J. The average size of the tumors was not significantly different between the two strains ( $p = 0.548$ ), while tumor load was significantly higher in the A/J ( $p = 0.008$ ), indicating the load was influenced by several tumors rather than a few very large (Fig. 3B).

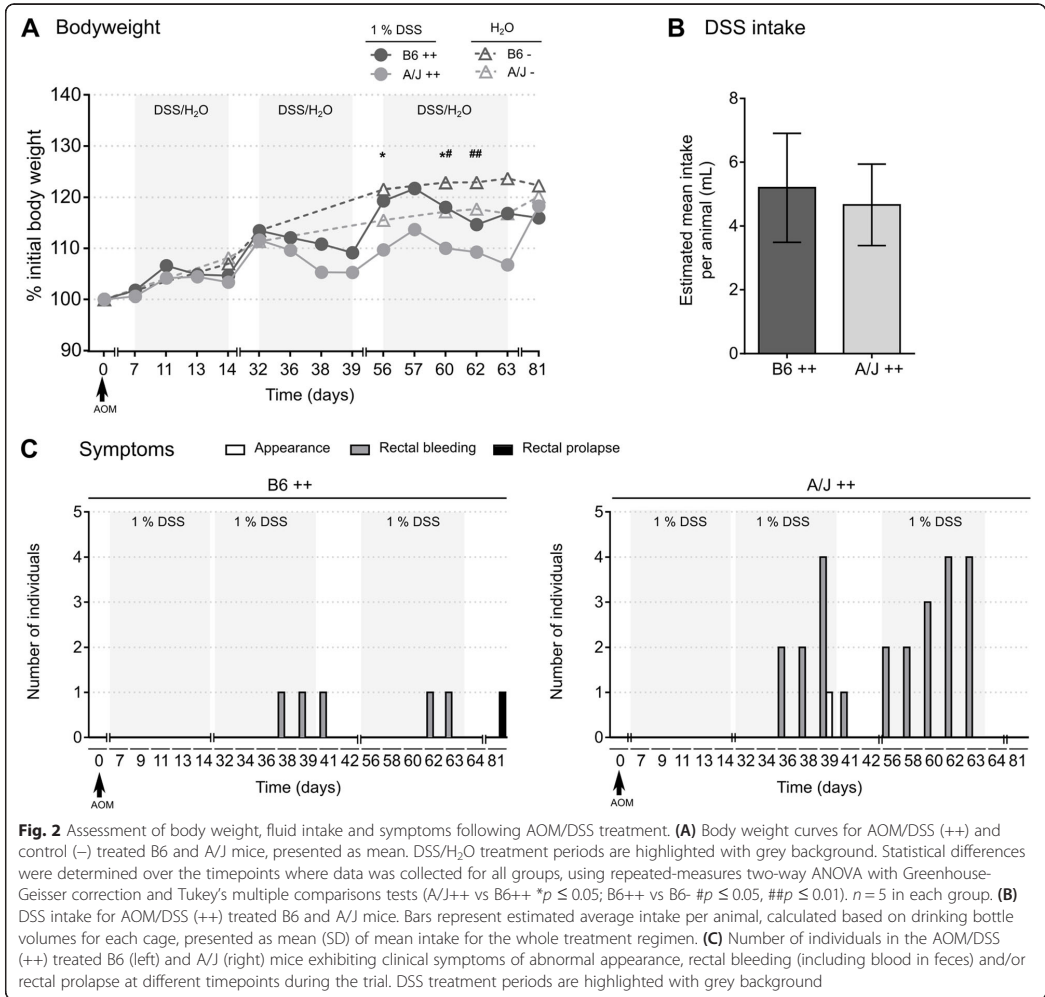
The size distribution of lesions illustrates that AOM with DSS promotion led to development of a markedly higher number of larger lesions in the A/J mice compared to B6 (Fig. 3C).

Following AOM treatment without DSS promotion, all animals of both strains developed ACFs, indicating that AOM injection alone can induce carcinogenesis in both strains. The A/J mice did, however, develop significantly higher abundance, size and load of ACFs compared to B6 (Fig. 3A). All AOM-treated A/J mice developed tumors, while no B6 mice treated with only AOM developed lesions categorized as tumors. Tumor count ranged between 1 and 20 for the AOM-treated A/J mice (Fig. 3B, C). These findings indicate that AOM without DSS promotion effectively led to development of ACFs as well as tumors in A/J mice, while this treatment was ineffective in B6 mice.

Min mice on both B6 and A/J background have been shown to also develop small intestinal lesions [36, 37]. Thus, the small intestines (SI) for all individuals were also examined and scored. For SI lesions, average counts were < 5 for both strains (Fig. 3D). Neither in the AOM/DSS-treated nor the AOM-treated groups were there significant differences in number, average size or lesion load detected between the two strains.

#### Histopathological characterization of colonic lesions

To further characterize the lesions, histopathological evaluation of colons from the two AOM/DSS-treated groups was conducted (Table 1). As a relatively high number of colonic lesions was observed in A/J mice treated with AOM only, this group was also included for histopathological assessment. Colonic lesions were classified as hyperplasia/dysplasia, adenomas or carcinomas according to morphological features as visualized in Fig. 4. Hyperplasia/dysplasia was detected in all AOM/DSS-treated mice independent of strain. For the AOM/



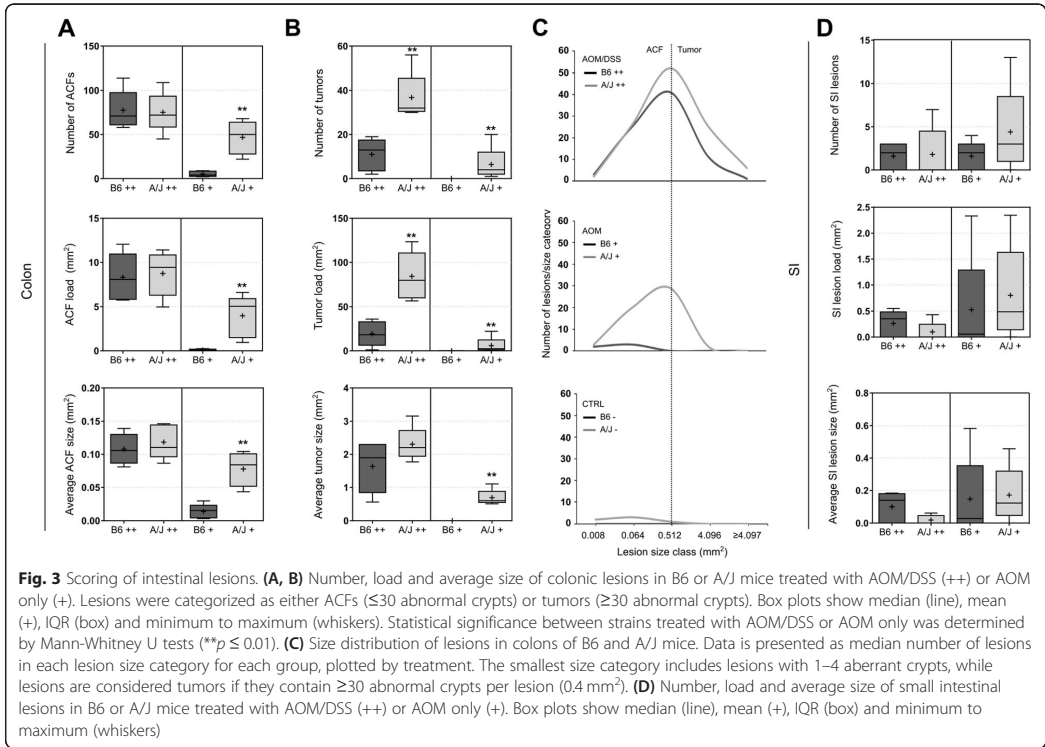
DSS-treated animals, adenomas were recorded in all A/J mice, and in 3 out of 5 B6 mice. No carcinomas were detected in any of the groups assessed. The count of both hyperplasia/dysplasia and adenomas were significantly higher in the A/J mice compared to B6 mice (both *p* = 0.008). Moreover, the size of adenomas, as shown in Fig. 4, was larger in the AOM/DSS-treated A/J mice than the AOM/DSS-treated B6 mice. For the AOM-treated A/J mice, hyperplasia/dysplasia was detected in 2 out of 5 and adenomas in only 1 out of 5 (Table 1).

Colonic lesions from B6 or A/J mice were classified as hyperplasia/dysplasia, adenomas or carcinomas. Data shows the number of individual mice in which at least one lesion within the class was detected, and mean

numbers of lesions detected within each class (mean ± SD), in the given experimental groups.

### Discussion

Since the first reports of the AOM/DSS model for induction of colorectal carcinogenesis, several variations of its implementation have been employed. Commonly used AOM/DSS models employing high doses of DSS are likely to inflict advanced disease and detrimental effects in the animals, which for many study purposes may be avoidable. For studies aiming to detect possible risk factors for, modifiers of, or chemopreventive agents that arrest the carcinogenesis, it may be advantageous to assess the early phases of CRC. To date, the majority of



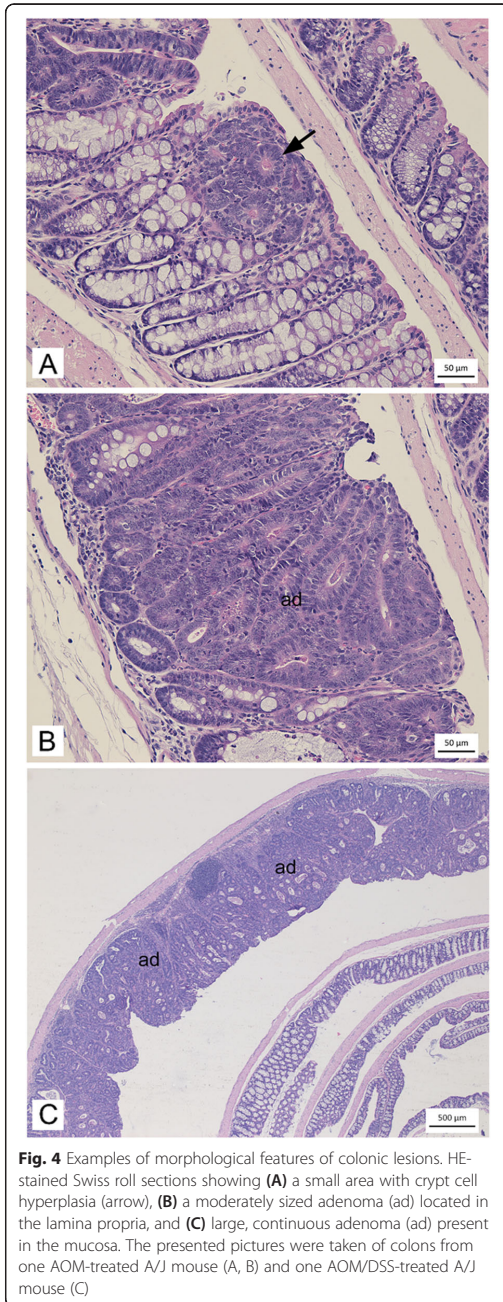
studies using the AOM/DSS model have employed DSS doses of 2% or higher [14, 17, 22, 38, 39], although previous reports have shown clear tumor-promoting effects of lower doses. Male ICR [24] and B6 mice [25] subjected to a single AOM injection (10 mg/kg, i.p) followed by a 7- or 4-day administration of 1% in drinking water showed consistent tumor development within 14 to 18 weeks after injection, respectively. A substantial number of mice in these two studies developed both adenomas and adenocarcinomas, possible due to the duration of the trials. In ICR mice, a protocol of a single i.p. injection of AOM followed by a 7-day administration of 1% DSS yielded adenomas and adenocarcinomas in all mice after 20 weeks [28].

Shorter-term experiments in which preneoplastic lesions is used as a biomarker has been advised to

minimize animal suffering in CRC experiments [34]. We show that by using an AOM/DSS model involving a single AOM injection (10 mg/kg, s.c.) followed by repeated administration ( $3 \times 7$  days) of a low dose (1%) DSS, we could consistently detect ACFs as well as hyperplasia/dysplasia in both B6 and A/J mice after 12 weeks. These findings indicate that a dosage of 1% DSS can be sufficient in the AOM/DSS model for study of early phase carcinogenesis, when using preneoplastic lesions as the outcome measure. Adenomas were detected in the majority of B6 mice and in all A/J mice subjected to our modified protocol, highlighting differential strain susceptibility to the AOM/DSS model as further discussed below. An important note is that ACFs can be distinguished into classical and flat ACFs, where classical ACFs are elevated from the mucosa. Although both flat

**Table 1** Histopathological classification of colonic lesions

	AOM/DSS (++)		A/J		AOM (+)	
	B6		A/J		A/J	
Hyperplasia/dysplasia	5/5	2.20 ± 1.64	5/5	9.80 ± 1.79	2/5	1.80 ± 3.49
Adenoma	3/5	1.00 ± 1.00	5/5	14.20 ± 2.86	1/5	1.20 ± 2.68
Carcinoma	0/5	0.00 ± 0.00	0/5	0.00 ± 0.00	0/5	0.00 ± 0.00



and classical ACFs have been detected in AOM-treated A/J mice previously, flat ACFs are reportedly most likely to develop into tumors [40]. In the current study, we could not elucidate if a higher proportion of classical ACFs rather than flat ACFs were developed in B6 compared to A/J, and whether this played a role for the progression of lesions into adenomas.

We sought to carefully assess clinical symptoms during the trial. We detected blood in feces in AOM/DSS-treated mice despite the low dose of DSS, and thus clinical symptoms were not avoided with our approach. The symptoms accompanied disease progression, as emphasized by more prevalent symptoms in the A/J mice which consistently developed adenomas and larger lesions compared to B6. A recent report on methods to assess affective state in AOM/DSS-treated B6 mice has provided extensive data on clinical symptoms throughout the trial [41]. In the study by Chartier et al., the AOM/DSS protocol involved a single injection of AOM (7.4 mg/g, i.p.) followed by three cycles of 7-day 2% DSS treatment. Although divergent from our employed protocol, the data from this previous study showed that rectal bleeding occurred at the first cycle of DSS treatment, and symptoms such as under-condition and body-weight loss were either sustained or progressed along the trial. Early symptoms including blood in feces have been shown to manifest immediately upon high-dose DSS treatment in B6 mice [20]. In our study, symptoms manifested during the 2nd cycle of DSS treatment in both strains, indicating the animal suffering can be alleviated by reduction of DSS concentration. The symptoms did not persist in-between treatment cycles, demonstrating recovery among the animals. Taken together, reducing the dose of DSS could contribute to reduced risk of early trial terminations in due to reached humane endpoints in studies employing the AOM/DSS model.

In addition to effective induction of carcinogenesis with the combinatory AOM and DSS treatment, we found that a single AOM injection induced ACF formation in A/J mice, supportive of previous studies [40, 42, 43]. On the contrary, we detected no ACFs in response to exposure of AOM alone in B6 mice, demonstrating a promotion using DSS is necessary to induce carcinogenesis in this strain. This is in agreement with previous studies in which no colonic tumors were detected in B6 mice given only AOM or only 1% DSS [25], and that A/J mice are less susceptible than B6 mice to inflammation induced by 3% DSS, yet more susceptible to the combined AOM/DSS-induced CRC [44]. Studies have investigated strain variances with respect to genetics [44, 45], gut microbiota and mucosal immune system [46–48], inflammatory response [49] and CYP-dependent metabolism [50] that may all contribute to the differential



susceptibility observed in our study as well as in previous reports.

In general, age and gender have been reported to influence the susceptibility of mice to AOM and/or DSS. Males have been shown to develop more adenomas compared to females [51] and AOM injection at a younger age increase the tumorigenic response [52, 53]. Beyond mouse strain, DSS concentrations and frequency of administration, responses to DSS are highly affected by housing facility, molecular weight of DSS, and mouse microbiota composition [18]. Gut microbiota in laboratory mice vary across facilities, and has been shown to alter the outcomes in several disease models [54, 55]. Thus, pilot testing of the present experimental setup is encouraged for each individual laboratory, in accord with good practice when introducing new protocols.

## Conclusions

In summary, we show that an AOM/DSS model with a low dose of DSS can be used to reliably induce colorectal carcinogenesis measured as preneoplastic lesions in both B6 and A/J mouse strains while limiting severe symptoms. This study highlights the importance of adjusting the treatment regimen according to mouse strain and study purposes in future studies employing the AOM/DSS model.

## Methods

### Ethical considerations

The experiment was approved by the Norwegian Animal Research Authority (FOTS ID 15446). The study was conducted at the Section for Experimental Biomedicine, Faculty of Veterinary Medicine, NMBU, Oslo, in accordance with local and national regulations for laboratory animal experiments. The animal facility is licensed by the Norwegian Food Safety Authority, and the health of the animals were monitored following a program recommended by the Federation of European Laboratory Animal Science Association (FELASA).

### Animals and husbandry

Wild-type A/J mice were bred at the Department of Experimental Biomedicine at NMBU, Norway as previously described [36]. A total of 15 purchased female inbred C57BL/6J (B6; Janvier Labs, Saint-Berthevin Cedex, France) mice aged 7 weeks, and 15 female inbred A/J wild-type mice aged 7–9 weeks were randomized to six groups based on strain. The groups were administered either NaCl injection combined with distilled H<sub>2</sub>O administration (control treatment), AOM injection, or AOM injection combined with DSS treatment (Fig. 1). The mice were maintained in closed type III individually ventilated cages (Allentown Inc., USA) under standard conditions (12 h light/dark cycle, 21 ± 2 °C, 20 air

changes per hour, and 45 ± 5% relative humidity). All cages contained standard aspen bedding, cellulose nesting material and red polycarbonate houses (Tecniplast, Buguggiate, Italy). Tap water and standard chow diet (RM1(E), SDS; Special Diet Services, Witham, United Kingdom) was provided ad libitum. The cages, bedding, nesting material and water bottles were changed minimum once a week.

### Experimental procedure and health monitoring

A 10 mg/mL stock solution of AOM in sterile H<sub>2</sub>O was prepared from 25 mg AOM (Sigma-Aldrich, #A5486). Fresh 1 mg/mL working solutions of AOM was prepared by addition of sterile NaCl (0.9%, B.Braun) prior to use. The animals were injected subcutaneously (s.c.) into the neck fold with 10 mg/kg AOM working solution, while animals were under transient anesthesia (sevoflurane, 3%, 200 mL/min). The control treatment entailed one single s.c. injection of sterile NaCl solution (10 mg/kg). Injection volume was rounded to nearest 10 µL. For DSS administration, DSS (36,000–50,000 M.Wt., Colitis Grade, MP Biomedicals) was dissolved in distilled H<sub>2</sub>O (1%, w/v) just prior to supply. Control treatment entailed the same regimen with fresh distilled H<sub>2</sub>O only. DSS or distilled H<sub>2</sub>O was administered in three 7-day cycles (day 7–14, 32–39, 56–63). Fresh DSS solution as well as distilled H<sub>2</sub>O was prepared and supplied every 2nd day throughout the 7-day cycles. For 16 days between the 1st and 2nd cycles, and 18 days between the 2nd and 3rd cycle, the animals were given regular tap water and allowed to recover. Animals were euthanized 18 days after the last cycle of DSS/control treatment.

Health monitoring was performed daily for all animals. For the AOM/DSS-treated animals, welfare was recorded every 2nd day during the DSS/control treatment regimen by use of a customized score sheet for body-weight, appearance and behavior, rectal bleeding and rectal prolapse (S1 dataset). Assessment of appearance and behavior included evaluation of overall condition, activity, movement and facial expression of pain. Blood in feces was recorded as rectal bleeding. Animals exhibiting any symptom was kept under close observation. Humane endpoints were defined as follows; body weight loss > 15%, rectal bleeding defined as blood around anus sustained over two subsequent days, a complete bulging of distal colon out of rectum, and severely under-conditioned appearance and behavior.

### Scoring of intestinal lesions

Colons and small intestines were harvested and briefly flushed with PBS. For scoring of intestinal lesions, colons were prepared as described previously [56]. Briefly, each intestinal segment was fixated flat between two filter papers in formalin solution (10%, neutral buffered; VWR

Chemicals) for 24 h prior to staining with methylene blue (MB) solution (Sigma-Aldrich; 0.1% in 10% neutral buffered formalin). The intestinal segments were stored refrigerated in 70% ethanol until analysis. The identification of intestinal lesions was performed by microscopy according to previously described procedure [57]. An inverted light microscope (CKX41, Olympus Inc., Hamburg, Germany) equipped with a digital color camera (DP25, Olympus Inc., Hamburg, Germany) was used to examine the colons for lesions.

Colonic lesions were classified in two categories; aberrant crypt foci (ACF) and tumor. ACFs can be recognized and distinguished from normal epithelia based on MB staining [8–10, 58]. In the current study, the lesions were not further distinguished. Diameters of lesions were measured using an eye piece graticule, and colonic lesion size ( $\text{mm}^2$ ) was calculated based on the measured diameters. All recorded lesions were grouped into lesion size classes ( $0.002\text{--}0.008\text{ mm}^2$ ,  $0.009\text{--}0.064\text{ mm}^2$ ,  $0.065\text{--}0.512\text{ mm}^2$ ,  $0.513\text{--}4.096\text{ mm}^2$  and  $\geq 4.097\text{ mm}^2$ ) as previously defined [36, 56]. Lesions were considered tumors if they contained  $\geq 30$  abnormal crypts per lesion ( $0.4\text{ mm}^2$ ). The total number of lesions, lesion load and distribution were measured and calculated per mouse in order to study lesion development in the intestines. Lesion load was defined as the sum of the area of all lesions (ACFs or tumors) observed in an intestine. For the small intestines, ACFs are not present and thus only lesions were recorded. Scoring of intestinal lesions are rendered in supplementary material (S2 dataset).

### Histopathology

Histopathological classification of colonic lesions was conducted on colons from all AOM/DSS-treated individuals and AOM-treated A/J mice. Following the scoring of lesions, swiss rolls were made of the colons, using a procedure first described by Moolenbeek and Ruitenberg [59] and further modified by Sodring et al. [36]. Briefly, colons were rolled lengthwise from proximal to distal, with the mucosa facing inwards, and embedded in paraffin blocks. For each paraffin-embedded colon, sections ( $3\text{ }\mu\text{m}$  thick) were made at three different depths (top, middle, bottom). The sections were stained with hematoxylin and eosin (HE) and examined blindly by a pathologist using a light microscope. Lesions were classified as hyperplasia/dysplasia, adenomas (tumors restricted to the mucosa) or carcinomas (tumors with distinct infiltrative growth through the mucosa into the submucosa).

### Statistical analyses

Statistical analyses were run in JMP® Pro 15 (SAS, NC, USA) or GraphPad Prism (v6.07 and v9.1.1; GraphPad Software, Inc., La Jolla, USA). Figures were created using

GraphPad Prism and Inkscape (v0.92.4; <http://www.inkscape.org/>). Applied statistical methods are specified in figure legends. Normality was controlled by Normal Quantile plot and D'Agostino-Pearson test. For non-normally distributed variables, including the ordinal data, Mann-Whitney U tests were conducted on non-transformed data.

### Abbreviations

ACF: Aberrant crypt foci; AOM: Azoxymethane; B6: C57BL/6J; CRC: Colorectal cancer; DSS: Dextran sulfate sodium

### Supplementary Information

The online version contains supplementary material available at <https://doi.org/10.1186/s42826-021-00096-y>.

**Additional file 1 S1 Dataset.** Records of bodyweight, health monitoring and DSS consumption (XLSX).

**Additional file 2 S2 Dataset.** Identification and classification of intestinal lesions (XLSX).

### Acknowledgements

The authors would like to thank Christer Wiggen Johnsen and the veterinary technicians at NMBU for caretaking of the animals and support in carrying out the trial. A great thank to Silje Modahl Johanson, Sergio D. C. Rocha and Dimitrios Papoutsis at NMBU for valuable advice on methodology.

### Authors' contributions

Conceptualization: HA, MHBM, JEP, HC, PB were responsible for the study concept and design. HA and MHBM conducted the experiment. MA, GCØ, HA, MHBM contributed to data acquisition, analysis, and interpretation. HA and MHBM wrote the manuscript. All authors read and approved the final manuscript.

### Funding

This work was funded internally at NMBU.

### Availability of data and materials

The datasets used and/or analyzed in this study is available within the provided supplementary material.

### Declarations

#### Competing interests

The authors declare that they have no competing interests.

#### Author details

<sup>1</sup>Department of Preclinical Sciences and Pathology, Faculty of Veterinary Medicine, Norwegian University of Life Sciences (NMBU), Oslo, Norway. <sup>2</sup>Faculty of Chemistry, Biotechnology and Food Science, Norwegian University of Life Sciences (NMBU), Ås, Norway. <sup>3</sup>Department of Paraclinical Sciences, Faculty of Veterinary Medicine, Norwegian University of Life Sciences (NMBU), Oslo, Norway. <sup>4</sup>Department of Production Animal Clinical Sciences, Faculty of Veterinary Medicine, Norwegian University of Life Sciences (NMBU), Oslo, Norway.

Received: 25 February 2021 Accepted: 1 July 2021

Published online: 27 July 2021

### References

- Dekker E, Tanis PJ, Vleugels JLA, Kasi PM, Wallace MB. Colorectal cancer. *Lancet*. 2019;394(10207):1467–80. [https://doi.org/10.1016/S0140-6736\(19\)32319-0](https://doi.org/10.1016/S0140-6736(19)32319-0).
- World Health Organization (WHO): International Agency for Research on Cancer. Globocan 2020: Cancer Fact Sheets — Colorectal Cancer. Available from: [https://gco.iarc.fr/today/data/factsheets/cancers/10\\_8\\_9-Colorectum-fact-sheet.pdf](https://gco.iarc.fr/today/data/factsheets/cancers/10_8_9-Colorectum-fact-sheet.pdf).

3. Jaspersen KW, Tuohy TM, Neklaus DW, Burt RW. Hereditary and familial colon cancer. *Gastroenterology*. 2010;138(6):2044–58. <https://doi.org/10.1053/j.gastro.2010.01.054>.
4. Jess T, Rungoe C, Peyrin-Biroulet L. Risk of colorectal cancer in patients with ulcerative colitis: a meta-analysis of population-based cohort studies. *Clin Gastroenterol Hepatol*. 2012;10(6):639–45. <https://doi.org/10.1016/j.cgh.2012.01.010>.
5. Terzić J, Grivninkov S, Karin E, Karin M. Inflammation and Colon Cancer. *Gastroenterology*. 2010;138(6):2101–14.e5.
6. Testa U, Pelosi E, Castelli G. Colorectal cancer: genetic abnormalities, tumor progression, tumor heterogeneity, clonal evolution and tumor-initiating cells. *Med Sci (Basel)*. 2018;6(2):31.
7. Srivastava S, Verma M, Henson DE. Biomarkers for early detection of colon cancer. *Clin Cancer Res*. 2001;7(5):1118–26.
8. Bird RP. Observation and quantification of aberrant crypts in the murine colon treated with a colon carcinogen: preliminary findings. *Cancer Lett*. 1987;37(2):147–51. [https://doi.org/10.1016/0304-3835\(87\)90157-1](https://doi.org/10.1016/0304-3835(87)90157-1).
9. Paulsen JE, Namork E, Steffensen IL, Eide TJ, Alexander J. Identification and quantification of aberrant crypt foci in the colon of min mice—a murine model of familial adenomatous polyposis. *Scand J Gastroenterol*. 2000;35(5):534–9. <https://doi.org/10.1080/003655200750023813>.
10. Paulsen JE, Loberg EM, Olstørn HB, Knutsen H, Steffensen IL, Alexander J. Flat dysplastic aberrant crypt foci are related to tumorigenesis in the colon of azoxymethane-treated rat. *Cancer Res*. 2005;65(11):121–9.
11. Caderni G, Femia AP, Giannini A, Favuzza A, Luceri C, Salvadori M, et al. Identification of mucin-depleted foci in the unsectioned colon of azoxymethane-treated rats: correlation with carcinogenesis. *Cancer Res*. 2003;63(10):2388–92.
12. Yamada Y, Yoshimi N, Hirose Y, Kawabata K, Matsunaga K, Shimizu M, et al. Frequent  $\beta$ -catenin gene mutations and accumulations of the protein in the putative preneoplastic lesions lacking macroscopic aberrant crypt foci appearance, in rat colon carcinogenesis. *Cancer Res*. 2000;60(13):3323–7.
13. Femia AP, Paulsen JE, Dolara P, Alexander J, Caderni G. Correspondence between flat aberrant crypt foci and mucin-depleted foci in rodent colon carcinogenesis. *Anticancer Res*. 2008;28(6a):3771–5.
14. Rosenberg DW, Giardina C, Tanaka T. Mouse models for the study of colon carcinogenesis. *Carcinogenesis*. 2009;30(2):183–96. <https://doi.org/10.1093/carcin/bgn267>.
15. Sohn OS, Fiala ES, Requejo SP, Weisburger JH, Gonzalez FJ. Differential effects of CYP2E1 status on the metabolic activation of the colon carcinogens azoxymethane and methylazoxymethanol. *Cancer Res*. 2001;61(23):8435–40.
16. Perse M, Cerar A. Morphological and molecular alterations in 1,2 dimethylhydrazine and azoxymethane induced colon carcinogenesis in rats. *J Biomed Biotechnol*. 2011;2011:473964.
17. Tanaka T, Kohno H, Suzuki R, Yamada Y, Sugie S, Mori H. A novel inflammation-related mouse colon carcinogenesis model induced by azoxymethane and dextran sodium sulfate. *Cancer Sci*. 2003;94(11):965–73. <https://doi.org/10.1111/j.1349-7006.2003.tb01386.x>.
18. Eichele DD, Kharbanda KK. Dextran sodium sulfate colitis murine model: an indispensable tool for advancing our understanding of inflammatory bowel diseases pathogenesis. *World J Gastroenterol*. 2017;23(33):6016–29. <https://doi.org/10.3748/wjg.v23.i33.6016>.
19. Araki Y, Mukaiyoshi K, Sugihara H, Fujiyama Y, Hattori T. Increased apoptosis and decreased proliferation of colonic epithelium in dextran sulfate sodium-induced colitis in mice. *Oncol Rep*. 2010;24(4):869–74. <https://doi.org/10.3892/or.2010.869>.
20. Melgar S, Karlsson A, Michaëlsson E. Acute colitis induced by dextran sulfate sodium progresses to chronicity in C57BL/6 but not in BALB/c mice: correlation between symptoms and inflammation. *Am J Physiol Gastrointest Liver Physiol*. 2005;288(6):G1328–38. <https://doi.org/10.1152/ajpgi.00467.2004>.
21. Thaker AJ, Shaker A, Rao MS, Ciorba MA. Modeling colitis-associated Cancer with Azoxymethane (AOM) and dextran sulfate sodium (DSS). *J Vis Exp*. 2012;67:4100.
22. De Robertis M, Massi E, Poeta ML, Carotti S, Morini S, Cecchetelli L, et al. The AOM/DSS murine model for the study of colon carcinogenesis: from pathways to diagnosis and therapy studies. *J Carcinog*. 2011;10:9.
23. Tanaka T. Development of an inflammation-associated colorectal cancer model and its application for research on carcinogenesis and chemoprevention. 2012;2012:658786.
24. Suzuki R, Kohno H, Sugie S, Tanaka T. Dose-dependent promoting effect of dextran sodium sulfate on mouse colon carcinogenesis initiated with azoxymethane. *Histol Histopathol*. 2005;20(2):483–92. <https://doi.org/10.14670/HH-20.483>.
25. Suzuki R, Kohno H, Sugie S, Nakagama H, Tanaka T. Strain differences in the susceptibility to azoxymethane and dextran sodium sulfate-induced colon carcinogenesis in mice. *Carcinogenesis*. 2006;27(1):162–9. <https://doi.org/10.1093/carcin/bgi205>.
26. Bader JE, Enos RT, Velázquez KT, Carson MS, Nagarkatti M, Nagarkatti PS, et al. Macrophage depletion using clodronate liposomes decreases tumorigenesis and alters gut microbiota in the AOM/DSS mouse model of colon cancer. *Am J Physiol Gastrointest Liver Physiol*. 2018;314(1):G22–31. <https://doi.org/10.1152/ajpgi.00229.2017>.
27. Guo Y, Wu R, Gaspar JM, Sargsyan D, Su ZY, Zhang C, et al. DNA methylome and transcriptome alterations and cancer prevention by curcumin in colitis-accelerated colon cancer in mice. *Carcinogenesis*. 2018;39(5):669–80. <https://doi.org/10.1093/carcin/bgy043>.
28. Kohno H, Suzuki R, Curini M, Epifano F, Maltese F, Gonzales SP, et al. Dietary administration with prenyloxycoumarins, auroaptene and collinin, inhibits colitis-related colon carcinogenesis in mice. *Int J Cancer*. 2006;118(12):2936–42. <https://doi.org/10.1002/ijc.21719>.
29. Zhan Y, Chen PJ, Sadler WD, Wang F, Poe S, Nunez G, et al. Gut microbiota protects against gastrointestinal tumorigenesis caused by epithelial injury. *Cancer Res*. 2013;73(24):7199–210. <https://doi.org/10.1158/0008-5472.CA-13-0827>.
30. Nambiar PR, Girmun G, Lillo NA, Guda K, Whiteley HE, Rosenberg DW. Preliminary analysis of azoxymethane induced colon tumors in inbred mice commonly used as transgenic/knockout progenitors. *Int J Oncol*. 2003;22(1):145–50.
31. Bissahoyo A, Pearsall RS, Hanlon K, Amann V, Hicks D, Godfrey VL, et al. Azoxymethane is a genetic background-dependent colorectal tumor initiator and promoter in mice: effects of dose, route, and diet. *Toxicol Sci*. 2005;88(2):340–5. <https://doi.org/10.1093/toxsci/kfi313>.
32. Perse M, Cerar A. Dextran sodium sulphate colitis mouse model: traps and tricks. *J Biomed Biotechnol*. 2012;2012:718617.
33. Zheng H, Lu Z, Wang R, Chen N, Zheng P. Establishing the colitis-associated cancer progression mouse models. *Int J Immunopathol Pharmacol*. 2016;29(4):759–63. <https://doi.org/10.1177/0394632016670919>.
34. Suzui M, Morioka T, Yoshimi N. Colon preneoplastic lesions in animal models. *J Toxicol Pathol*. 2013;26(4):335–41. <https://doi.org/10.1293/tox.2013-0028>.
35. European Parliament and Council of the European Union. Directive 2010/63/EU of the European Parliament and of the council of 22 September 2010 on the protection of animals used for scientific purposes. Strasbourg: Council of Europe; 2010.
36. Sodring M, Gunnes G, Paulsen JE. Spontaneous initiation, promotion and progression of colorectal cancer in the novel a/J min/+ mouse. *Int J Cancer*. 2016;138(8):1936–46. <https://doi.org/10.1002/ijc.29928>.
37. Halberg RB, Waggoner J, Rasmussen K, White A, Clipson L, Prunuske AJ, et al. Long-lived min mice develop advanced intestinal cancers through a genetically conservative pathway. *Cancer Res*. 2009;69(14):5768–75. <https://doi.org/10.1158/0008-5472.CAN-09-0446>.
38. Suzuki R, Kohno H, Sugie S, Tanaka T. Sequential observations on the occurrence of preneoplastic and neoplastic lesions in mouse colon treated with azoxymethane and dextran sodium sulfate. *Cancer Sci*. 2004;95(9):721–7. <https://doi.org/10.1111/j.1349-7006.2004.tb03252.x>.
39. Angelou A, Andreatos N, Antoniou E, Zacharioudaki A, Theodoropoulos G, Damaskos C, et al. A novel modification of the AOM/DSS model for inducing intestinal adenomas in mice. *Anticancer Res*. 2018;38(6):3467–70. <https://doi.org/10.21873/anticancer.12616>.
40. Paulsen JE, Knutsen H, Olstørn HB, Loberg EM, Alexander J. Identification of flat dysplastic aberrant crypt foci in the colon of azoxymethane-treated a/J mice. *Int J Cancer*. 2006;118(3):540–6. <https://doi.org/10.1002/ijc.21416>.
41. Chartier LC, Hebart ML, Howarth GS, Whittaker AL, Mashtoub S. Affective state determination in a mouse model of colitis-associated colorectal cancer. *PLoS One*. 2020;15(1):e0228413. <https://doi.org/10.1371/journal.pone.0228413>.
42. Papanikolaou A, Wang QS, Delker DA, Rosenberg DW. Azoxymethane-induced colon tumors and aberrant crypt foci in mice of different genetic susceptibility. *Cancer Lett*. 1998;130(1–2):29–34. [https://doi.org/10.1016/S0304-3835\(98\)00101-3](https://doi.org/10.1016/S0304-3835(98)00101-3).

43. Papanikolaou A, Wang Q-S, Papanikolaou D, Whiteley HE, Rosenberg DW. Sequential and morphological analyses of aberrant crypt foci formation in mice of differing susceptibility to azoxymethane-induced colon carcinogenesis. *Carcinogenesis*. 2000;21(8):1567–72. <https://doi.org/10.1093/carcin/21.8.1567>.
44. Van Der Kraak L, Meunier C, Turbide C, Jothy S, Gaboury L, Marcus V, et al. A two-locus system controls susceptibility to colitis-associated colon cancer in mice. *Oncotarget*. 2010;1(6):436–46. <https://doi.org/10.18632/oncotarget.177>.
45. Keane TM, Goodstadt L, Danecek P, White MA, Wong K, Yalcin B, et al. Mouse genomic variation and its effect on phenotypes and gene regulation. *Nature*. 2011;477(7364):289–94.
46. Ishikawa H, Li Y, Abeliovich A, Yamamoto S, Kaufmann SH, Tonegawa S. Cytotoxic and interferon gamma-producing activities of gamma delta T cells in the mouse intestinal epithelium are strain dependent. *Proc Natl Acad Sci U S A*. 1993;90(17):8204–8. <https://doi.org/10.1073/pnas.90.17.8204>.
47. Elderman M, Hugenholtz F, Belzer C, Boekschoten M, van Beek A, de Haan B, et al. Sex and strain dependent differences in mucosal immunology and microbiota composition in mice. *Biol Sex Differ*. 2018;9(1):26. <https://doi.org/10.1186/s13293-018-0186-6>.
48. Hensel JA, Khattar V, Ashton R, Ponnazhagan S. Characterization of immune cell subtypes in three commonly used mouse strains reveals gender and strain-specific variations. *Lab Invest*. 2019;99(1):93–106. <https://doi.org/10.1038/s41374-018-0137-1>.
49. Yang F, Wang D, Li Y, Sang L, Zhu J, Wang J, et al. Th1/Th2 balance and Th17/Treg-mediated immunity in relation to murine resistance to dextran sulfate-induced colitis. *J Immunol Res*. 2017;2017:7047201.
50. Rudeck J, Bert B, Marx-Stoelting P, Schönfelder G, Vogl S. Liver lobe and strain differences in the activity of murine cytochrome P450 enzymes. *Toxicology*. 2018;404–405:76–85.
51. Lee SM, Kim N, Son HJ, Park JH, Nam RH, Ham MH, et al. The effect of sex on the Azoxymethane/dextran sulfate sodium-treated mice model of Colon Cancer. *J Cancer Prev*. 2016;21(4):271–8. <https://doi.org/10.15430/JCP.2016.21.4.271>.
52. Chung H, Wu D, Gay R, Han SN, Goldin B, Bronson R, et al. Effect of age on susceptibility to Azoxymethane-induced colonic aberrant crypt foci formation in C57BL/6JNIA mice. *J Gerontol A Biol Sci Med Sci*. 2003;58(5):B400–B5. <https://doi.org/10.1093/gerona/58.5.B400>.
53. Paulsen JE, Steffensen IL, Namork E, Eide TJ, Alexander J. Age-dependent susceptibility to azoxymethane-induced and spontaneous tumorigenesis in the min/+ mouse. *Anticancer Res*. 2003;23(1a):259–65.
54. Rausch P, Basic M, Batra A, Bischoff SC, Blaut M, Clavel T, et al. Analysis of factors contributing to variation in the C57BL/6J fecal microbiota across German animal facilities. *Int J Med Microbiol*. 2016;306(5):343–55. <https://doi.org/10.1016/j.ijmm.2016.03.004>.
55. Franklin CL, Ericsson AC. Microbiota and reproducibility of rodent models. *Lab Anim (NY)*. 2017;46(4):114–22. <https://doi.org/10.1038/labanim.1222>.
56. Steppeler C, Sædring M, Paulsen JE. Colorectal carcinogenesis in the a/J min/+ mouse model is inhibited by hemin, independently of dietary fat content and fecal lipid peroxidation rate. *BMC Cancer*. 2016;16(1):832. <https://doi.org/10.1186/s12885-016-2874-0>.
57. Sædring M, Gunnes G, Paulsen JE. Detection and characterization of flat aberrant crypt foci (flat ACF) in the novel a/J min/+ mouse. *Anticancer Res*. 2016;36(6):2745–50.
58. Paulsen JE, Steffensen IL, Loberg EM, Husoy T, Namork E, Alexander J. Qualitative and quantitative relationship between dysplastic aberrant crypt foci and tumorigenesis in the min/+ mouse colon. *Cancer Res*. 2001;61(13):5010–5.
59. Moolenbeek C, Ruitenberg EJ. The 'Swiss roll': a simple technique for histological studies of the rodent intestine. *Lab Anim*. 1981;15(1):57–9. <https://doi.org/10.1258/002367781780958577>.

## Publisher's Note

Springer Nature remains neutral with regard to jurisdictional claims in published maps and institutional affiliations.

Ready to submit your research? Choose BMC and benefit from:

- fast, convenient online submission
- thorough peer review by experienced researchers in your field
- rapid publication on acceptance
- support for research data, including large and complex data types
- gold Open Access which fosters wider collaboration and increased citations
- maximum visibility for your research: over 100M website views per year

At BMC, research is always in progress.

Learn more [biomedcentral.com/submissions](https://biomedcentral.com/submissions)







# Paper III

III



## Naturalizing laboratory mice by housing in a farmyard-type habitat confers protection against colorectal carcinogenesis

Henriette Arnesen <sup>a,b</sup>, Thomas C. A. Hitch <sup>c</sup>, Christina Steppeler<sup>d</sup>, Mette Helen Bjørge Müller<sup>d</sup>, Linn Emilie Knutsen<sup>a</sup>, Gjermund Gunnes<sup>a</sup>, Inga Leena Angell<sup>b</sup>, Ida Ormaasen<sup>b</sup>, Knut Rudi<sup>b</sup>, Jan Erik Paulsen<sup>d</sup>, Thomas Clavel <sup>c</sup>, Harald Carlsen <sup>b</sup>, and Preben Boysen <sup>a</sup>

<sup>a</sup>Department of Preclinical Sciences and Pathology, Faculty of Veterinary Medicine, Norwegian University of Life Sciences (NMBU), Aas, Norway;

<sup>b</sup>Faculty of Chemistry, Biotechnology and Food Science, Norwegian University of Life Sciences (NMBU), Norway; <sup>c</sup>Functional Microbiome Research Group, Institute of Medical Microbiology, University Hospital of RWTH Aachen, Aachen, Germany; <sup>d</sup>Department of Paraclinical Sciences, Faculty of Veterinary Medicine, Norwegian University of Life Sciences (NMBU), Aas, Oslo, Norway

### ABSTRACT

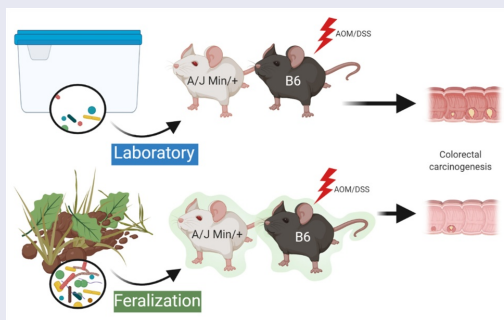
Living in a farm environment in proximity to animals is associated with reduced risk of developing allergies and asthma, and has been suggested to protect against other diseases, such as inflammatory bowel disease and cancer. Despite epidemiological evidence, experimental disease models that recapitulate such environments are needed to understand the underlying mechanisms. In this study, we show that feralizing conventional inbred mice by continuous exposure to a livestock farmyard-type environment conferred protection toward colorectal carcinogenesis. Two independent experimental approaches for colorectal cancer induction were used; spontaneous (Apc Min/+ mice on an A/J background) or chemical (AOM/DSS). In contrast to conventionally reared laboratory mice, the feralized mouse gut microbiota structure remained stable and resistant to mutagen- and colitis-induced neoplasia. Moreover, the feralized mice exhibited signs of a more mature immunophenotype, indicated by increased expression of NK and T-cell maturation markers, and a more potent IFN- $\gamma$  response to stimuli. In our study, hygienically born and raised mice subsequently feralized post-weaning were protected to a similar level as life-long exposed mice, although the greatest effect was seen upon neonatal exposure. Collectively, we show protective implications of a farmyard-type environment on colorectal cancer development and demonstrate the utility of a novel animal modeling approach that recapitulates realistic disease responses in a naturalized mammal.

### ARTICLE HISTORY

Received 20 May 2021  
Revised 27 September 2021  
Accepted 8 October 2021

### KEYWORDS



Gut microbiota; feralized mice; colorectal cancer; farmyard-like habitat; animal model; naturalized mice; short-chain fatty acids; immunity




## Introduction

The mammalian gut hosts a complex and diverse ecosystem, which has co-evolved with the host to form a symbiotic relationship fundamental for host fitness. The gut microbiota has been shown to

shape host immunity during development, ensuring adequate defense toward potentially harmful pathogens and tolerance to commensal species.<sup>1, 2</sup> The gut microbiota is acquired and influenced by both vertical and horizontal transmission from

**CONTACT** Preben Boysen  [preben.boysen@nmbu.no](mailto:preben.boysen@nmbu.no)  Department of Preclinical Sciences and Pathology, Faculty of Veterinary Medicine, Norwegian University of Life Sciences (NMBU), Oslo, Norway

 Supplemental data for this article can be accessed on the [publisher's website](#).

© 2021 The Author(s). Published with license by Taylor & Francis Group, LLC.

This is an Open Access article distributed under the terms of the Creative Commons Attribution License (<http://creativecommons.org/licenses/by/4.0/>), which permits unrestricted use, distribution, and reproduction in any medium, provided the original work is properly cited.

maternal and environmental sources.<sup>3,4</sup> Epidemiological studies have demonstrated that children exposed to high microbial biodiversity environments harbor different microbiomes and enhanced immune regulation than urban children,<sup>5</sup> and are less susceptible to diseases, such as asthma and allergies.<sup>6–8</sup> Moreover, farmers have reduced risk of certain types of cancer.<sup>9</sup> A connection between decreased environmental biodiversity accompanying an urban living and increased risk for inflammatory bowel diseases (IBDs) has also been suggested.<sup>10,11</sup> Given that individuals with IBDs have substantially increased risk for colorectal cancer (CRC),<sup>12,13</sup> it can be hypothesized that exposure to environmental microbes and previous infections may also influence the risk for CRC.

CRC is the second most diagnosed cancer in women, and the third most common malignancy in men worldwide.<sup>14,15</sup> A minority of CRC cases are attributed to hereditary factors, such as germline mutations in susceptibility genes, while most CRCs arise sporadically and can be influenced by various environmental components, with gut microbiota as a unifying factor.<sup>16,17</sup> Both genetic and inducible CRC mouse models are commonly used to study the multifaceted mechanisms behind CRC. *Apc* *Min*/<sup>+</sup> mice harbor a mutant allele of the adenomatous polyposis coli (*Apc*) gene and spontaneously develop adenomatous polyps.<sup>18,19</sup> CRC can also be induced chemically by e.g. a combinatory treatment of the pro-carcinogen azoxymethane (AOM) and the inflammatory agent dextran sodium sulfate (DSS). The AOM/DSS model is considered robust and has emerged to become one of the most frequently used models to study inflammation-associated CRC. In this model, carcinogenesis is induced by AOM metabolism to alkylating species generating DNA mutations, while the subsequent colonic epithelial damage inflicted by DSS promotes the carcinogenic process.<sup>18</sup>

To decipher the role of gut microbiota in health and disease, engraftment of minimal or specific microbial communities in gnotobiotic and germ-free mice have been widely employed, allowing for controlled composition of gut commensals.<sup>20</sup> However, increased awareness of the tandem function of gut microbes and host immune system has engendered concerns over the potential bias

introduced by hygienic housing on the microbiota and its downstream effect on disease modeling in mice.<sup>21,22</sup> Moreover, while lab mice are known to have less microbiota variation than wild mice, the between-lab/vendor variability has been shown to alter the outcomes in disease models.<sup>23,24</sup> In essence, a growing body of research highlights that conventional lab mice are too far removed from their natural, usually microbially rich, habitat to accurately reflect the immunological responses of free-living mammals and humans.<sup>25–32</sup> In recent years, several approaches to study the implications of naturalized lab mice have been presented.<sup>26,27,29,30,33</sup> These studies show that naturalization of lab mice result in clear shifts in gut microbiota and more mature immunophenotypes, as well as protection against various diseases, including that a wild mouse microbiota mitigate CRC outcome.<sup>29</sup>

We have established a simulated natural indoor housing facility in which lab mice could be feralized in a farmyard-type setting with feral mice cohabitants, leading to distinct changes in immune parameters and gut microbiota.<sup>34</sup> In the current study, we employed this feralization model and found that a farmyard-type habitat itself, in the absence of feral mice, effectively dampened CRC development in the AOM/DSS as well as the A/J *Min*/<sup>+</sup> models of CRC. We characterized the gut microbiota and immune parameters as potential drivers of differential disease outcomes in the feralized mice.

## Results

### ***Genetically susceptible *Min*/<sup>+</sup> mice feralized in a naturalistic environment showed reduced rate of colonic lesion formation***

Young adult male A/J *Min*/<sup>+</sup> and A/J wild-type (WT) mice were either feralized (Fer) in a simulated natural environment or housed in clean conventional cages (Lab) for 7–9 weeks (Figure 1a). Changes in bodyweight were similar in all A/J *Min*/<sup>+</sup> mice independent of the housing conditions (Figure S1A). In the feralized A/J *Min*/<sup>+</sup> mice (FerMin), the number of observed colonic lesions were significantly reduced compared to the Lab mice (LabMin) (Figure 1b). The mean lesion size or load (sum of lesion area) between the



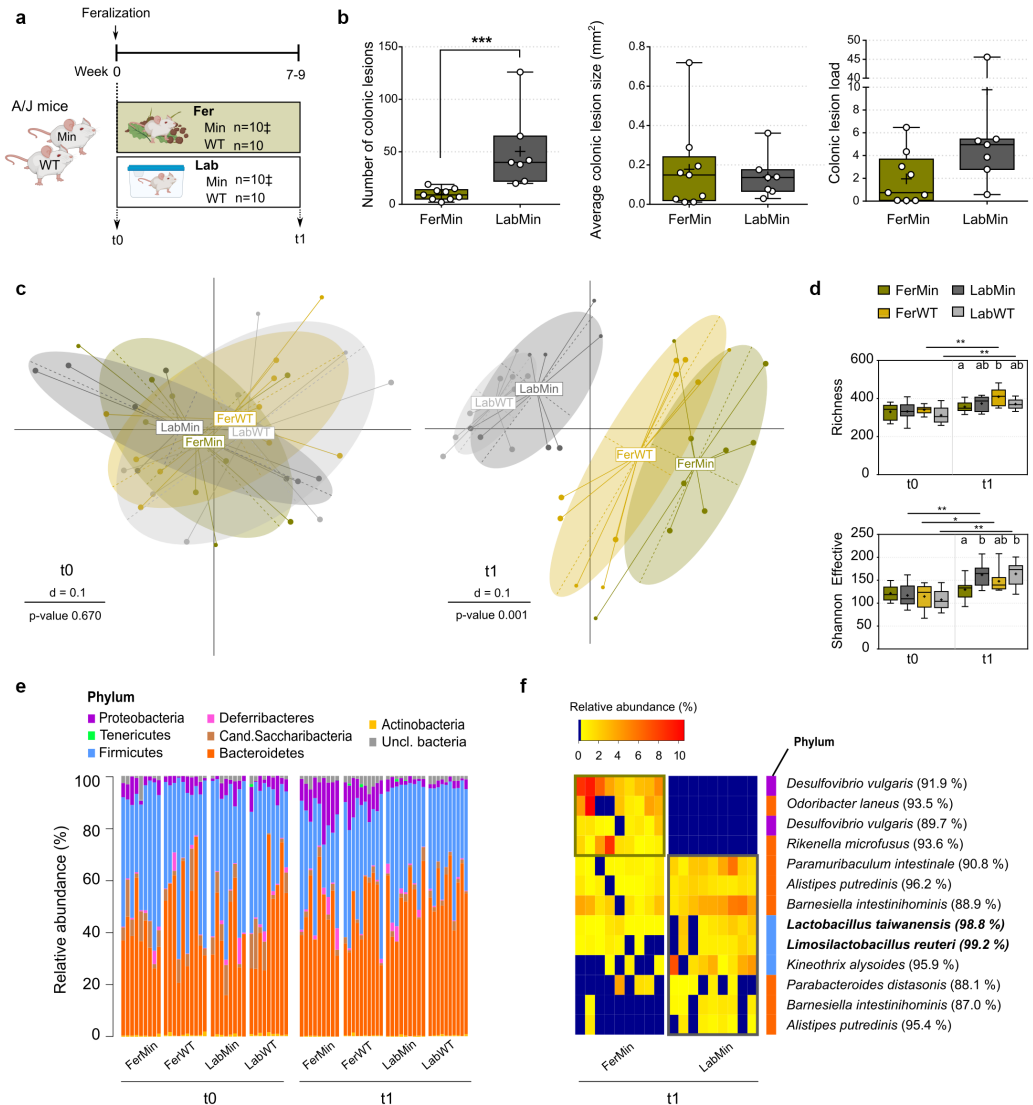


**Figure 1.** Feralization of A/J Min/+ mice led to diminished spontaneous colonic lesion formation, accompanied by altered microbiota profile. (a) Scheme of the experimental setup showing timeline and grouping. 6-8-week-old female mice were enrolled. Samples were collected at baseline (t0; week 0) and endpoint (t1; week 7-9). † one mouse deceased before endpoint and were consequently excluded from endpoint analyses. (b) Assessment of colonic lesions in Fer and Lab A/J Min/+ (FerMin and LabMin) mice at endpoint. The occurrence of lesions is presented as total number, mean size (mm<sup>2</sup>), and load (total mm<sup>2</sup>). Box plots show median (line), mean (+), IQR (box) and minimum to maximum (whiskers). Asterisks designate significant (\*\*\*) differences between the groups determined by Mann-Whitney tests. (c) Multi-dimensional scaling (MDS) plot of fecal microbiota profiles (generalized UniFrac distances) for Fer and Lab A/J Min/+ (FerMin, LabMin) and WT (FerWT, LabWT) mice at baseline (t0) and endpoint (t1). Significance of separation was determined by PERMANOVA. d = distance scale. (d) Observed number of OTUs (Richness) and Shannon Effective counts for all groups. Box plots show median (line), mean (+), IQR (box) and minimum to maximum (whiskers). Asterisks designate significant over-time differences determined by Wilcoxon Signed Rank Sum tests, whilst letters designate significant (p ≤ 0.05) differences between groups at each timepoint determined by Kruskal-Wallis tests followed by Wilcoxon Rank Sum tests. The Benjamini-Hochberg method was used to correct for multiple testing. (e) Taxonomic binning at phylum level, presented as relative abundance for Fer and Lab A/J Min/+ (FerMin, LabMin) and WT (FerWT, LabWT) mice at baseline (t0) and endpoint (t1). (f) Heatmap of relative abundance of specific OTUs enriched in Fer and Lab A/J Min/+ (FerMin, LabMin) mice at endpoint (t1). The occurrence of OTUs for which the relative abundance or prevalence differed significantly between the groups (determined by Wilcoxon Rank Sum tests and

groups were not significantly different, reflecting that the increased number of lesions in LabMin mice were small-sized lesions. The small intestines (SI) were also examined and scored, as A/J Min/+ mice have been previously shown to also develop SI lesions.<sup>19</sup> We observed a substantial number of SI lesions in both FerMin and LabMin mice. However, no significant differences in number, size or load between the two groups were observed (Figure S1B).

### **Feralization of A/J Min/+ mice led to altered gut microbiota profile with enrichment of Proteobacteria**

To characterize the influence of feralization on the gut microbiota, stool samples were collected for high-throughput 16S rRNA gene (V3-V4) amplicon analysis. This resulted in 1,002,551 high-quality and chimera-checked sequences (6,780 to 29,032 per sample), which represented a total of 670 OTUs. Sequencing depth was evaluated by rarefaction curves to confirm each sample's suitability for further analysis (Figure S2A).

Before separating the A/J Min/+ or A/J WT mice into Fer or Lab conditions, gut microbiota profiles were similar in all groups, but separated substantially following their introduction into the different housing conditions, confirming that the two environments differentially influenced gut microbiota structure (Figure 1c). *Alpha*-diversity measures showed that the number of detected molecular species (OTUs) (richness) and Shannon effective counts were similar in all groups at the starting point. At endpoint, the FerMin mice had significantly lower richness compared to the feralized WT mice (FerWT) ( $p = .012$ ), and significantly lower Shannon effective compared to both of the conventionally housed groups (i.e. LabMin and corresponding WT mice; LabWT) ( $p = .043$  and  $p = .024$ , respectively) (Figure 1d).

The changes in gut microbiota conferred by feralization were apparent at the taxonomic rank of phylum, where we detected significantly

higher relative abundances of Proteobacteria in both FerMin and FerWT mice than in the LabMin and LabWT (all comparisons  $p \leq 0.001$ ) (Figure 1e). No differences at the phylum level were detected at baseline, indicating that the Proteobacteria colonization was a result of the environmental influence rather than genotypic differences or disease state.

To further characterize the differences in the Fer and Lab gut microbiotas at endpoint, we conducted analysis at the level of specific OTUs (figure 1f). Two OTUs with closest sequence similarity to a member of the Proteobacteria, *Desulfovibrio vulgaris*, were detected in nearly all (9/9 and 8/9) FerMin mice and were completely absent in LabMin mice. In contrast, OTUs showing closest sequence similarities to members of the phylum Firmicutes, including two species assigned to *Lactobacillus* and *Limosilactobacillus* were enriched in the LabMin mice. Similar results were seen for the FerWT and LabWT mice, indicating that environmental influence rather than disease state was a major driver for the microbial differences (Figure S1C).

### **Feralization alleviated mutagen- and colitis-induced carcinogenesis in B6 mice**

We proceeded to employ a chemical induction (AOM/DSS) model of CRC using female C57BL/6 JRj (B6) mice to evaluate the influence of feralization independent of genetic susceptibility. The B6 mice were separated into Fer and Lab groups prior to the chemical induction (Figure 2a). To investigate the influence of early-life versus later-in-life colonization, we included second generation feralized animals born by feralized mothers, which had been feralized from birth onwards (Feralized Early; FerE), and animals born in the lab setting by lab mothers and feralized after weaning, at 5 weeks of age (Feralized Late; FerL). The groups were administered AOM/DSS (+) or control treatment (-).

The AOM/DSS-treated Lab+ mice lost significantly more weight than both FerE+ and FerL+ mice during the second and third cycles of DSS

Fisher's exact tests, respectively) are plotted. Blue color indicates the OTUs were absent or below cutoffs for analyses. The bacterial species with a valid name closest to the corresponding OTUs is indicated along with its sequence similarity; those OTUs identifiable at the species level ( $\geq 97\%$  similarity) are written in bold letters. Phyla to which the OTUs belong are designated with colored squares as specified in E. Frames indicate significant increased abundance or prevalence in FerMin (brown) and LabMin (gray). See also Figures S1 and S2A.

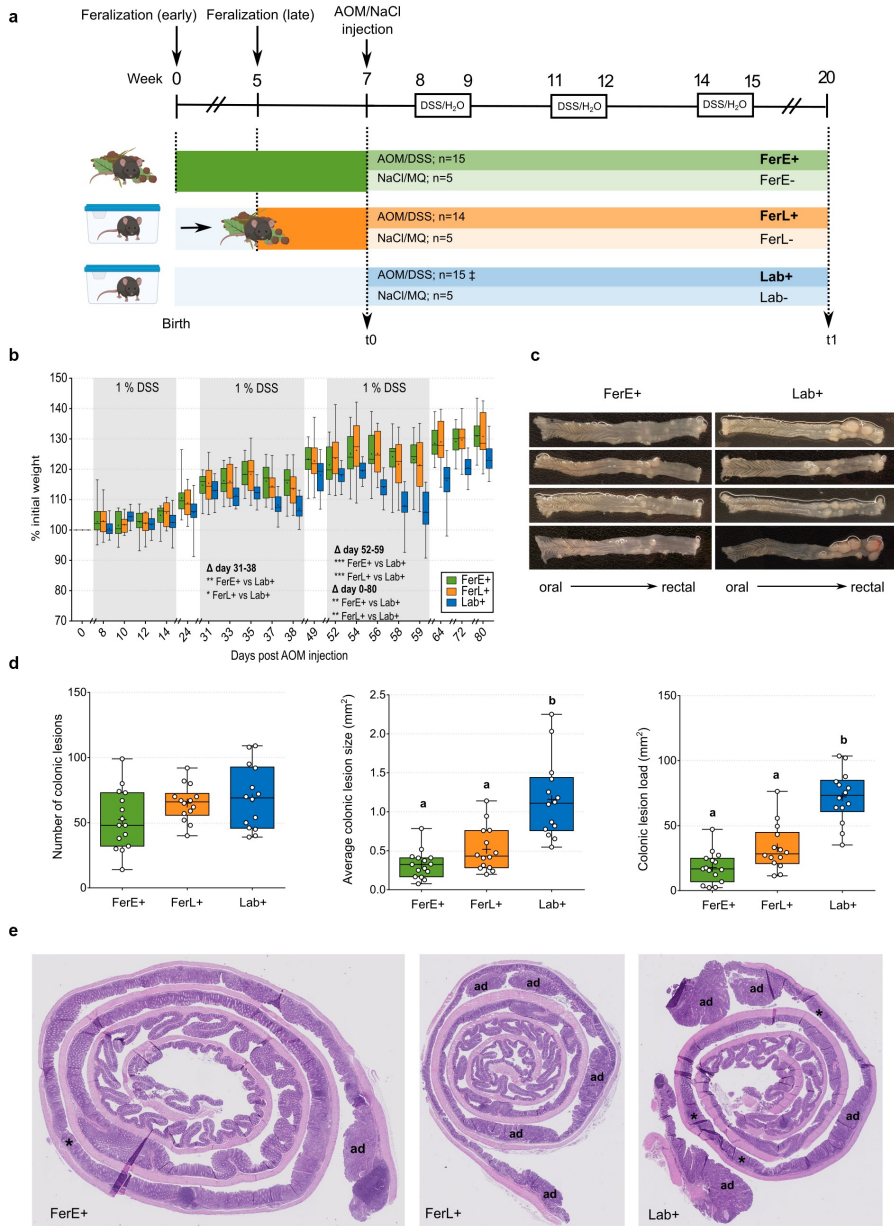


**Figure 2.** Feralization conferred protection toward mutagen- and colitis-induced carcinogenesis in B6 mice. (a) Chart showing timeline of the AOM/DSS trial and the grouping of animals. Timeline start at birth (week 0). Animals born in the mouse pens by feralized mothers compose the early feralized (FerE) groups, whilst animals born in the laboratory by non-feralized mothers compose the Lab groups. At week 5, feralization of a subset of Lab animals gave rise to the late feralized (FerL) groups. At week 7, CRC was induced by AOM injection followed by DSS administration. Control groups were given NaCl injection and H<sub>2</sub>O. Samples were collected prior to AOM or NaCl injection (t<sub>0</sub>; week 7) and at trial termination (t<sub>1</sub>; week 20). † one mouse deceased before endpoint and were consequently excluded from endpoint and over-time analyses. (b) Bodyweight curves for AOM/DSS-treated animals, presented as per cent of initial body weight. Box plots show median (line), mean (+), IQR (box) and minimum to maximum (whiskers). Significant changes in bodyweight from first to last day of the trial (0 to 80), and first to last day of each cycle (8–14, 31–38, 51–59), were

**Table 1.** Histopathological classification of colonic lesions. Presented are numbers of individual mice in which at least one lesion within the class was detected, and mean numbers of lesions detected within each class and in total in the given groups. SDs are presented in brackets. \* $p \leq 0.05$ , significant difference between groups (determined by Kruskal–Wallis test followed by Dunn's multiple comparisons tests).

	FerE+		FerL+		Lab+	
Hyperplasia	5/6	1.33 (1.03)	6/6	2.17 (1.17)	6/6	3.83 (3.06)
Adenoma	6/6	1.50 (0.84)	5/6	4.50 (3.62)	6/6	5.00 (3.46)
Carcinoma	0/6	-	0/6	-	0/6	-
Total	6/6	2.83 (1.33)*	6/6	6.67 (3.67)	6/6	8.83 (5.04)*

treatment, as well as over the whole trial (Figure 2b). Colonic lesions formed from the AOM/DSS treatment were macroscopically different between FerE+ and Lab+ mice, with more prominent tumors in the latter group, as depicted in Figure 2c. The total number of lesions in AOM/DSS-treated mice detected by surface microscopy were, not different between Fer and Lab groups, yet the mean lesion size and load were significantly lower in FerE+ and FerL+ mice than in Lab+ mice (Figure 2d). Neither lesion numbers, size nor load were significantly different between FerE+ and FerL+ animals, although the latter group did show a phenotype in between FerE+ and Lab+ (Figure 2d).

Following lesion scoring by surface microscopy, histopathological assessment was conducted of the colons (Figure 2e, Figure S8B). Hyperplasia, adenomas, and carcinomas were classified and counted in the six colons with the highest mean lesion sizes in each group. The numbers of adenomas ranged from 1–3 in the FerE+, 0–10 in FerL+ and 2–11 in Lab+ groups, while the number of hyperplastic lesions ranged 0–3 in FerE+, 1–4 in FerL+ and 1–7 in Lab+. No carcinomas were diagnosed in any of the colons (Table 1). Statistical comparisons of the total numbers of lesions diagnosed by histopathology showed significant difference between the groups ( $p = .016$ ) with pairwise comparisons revealing significantly lower numbers in FerE+ compared to Lab+ ( $p = .030$ ) yet no significant differences between FerL and the other groups.

In the control-treated groups, we detected no bodyweight loss. The bodyweight of both FerE- and FerL-mice increased compared to Lab-mice, as indicated by significantly different weight change from first to last day of the trial (Figure S3A). As would be expected, hardly any colonic lesions were observed in the control-treated groups (Figure S3B).

Because an inverse relationship between physical exercise and CRC outcome in mice has been reported,<sup>35,36</sup> we wished to assess whether the larger area of the naturalistic environment compared to the conventional lab cages could be responsible for the differences observed between feralized and lab mice. Thus, at week 7, five mice from both the FerE+ and FerL+ groups were placed into cages, along with environmental samples from their respective pens, to retain the environment, while otherwise treated with AOM/DSS (Figure S3C). Comparisons of bodyweight curves between the cage- and pen-housed Fer mice showed that FerE+ gained more weight than FerE<sup>cage+</sup> over the whole trial period (Figure S3D). The FerL<sup>cage+</sup> group lost significantly more weight than the corresponding FerL+ group during second cycle of DSS treatment, but apart from this the bodyweight curves for the two groups were comparable during the trial (Figure S3E). However, the lesion assessment data for FerE<sup>cage+</sup> and FerL<sup>cage+</sup> matched the findings from FerE+ and FerL+ mice, and no significant effects of the cage housing were detected for any of the lesion measurements (Figure S3F). Fluid intake was similar in all groups (Figure S3G), confirming that the phenotypic features were not due to unequal DSS consumption.

Taken together, these findings demonstrate that feralization in a naturalistic environment confers traits that limit the impact of mutagen- and colitis-induced carcinogenesis. Feralization from birth and from later in life both mitigated CRC outcome, yet the protection was most pronounced in the early feralized group. The protective effect of feralization was shown to be largely independent of the enlarged space in the mouse pens.

determined using repeated measures ANOVA with Tukey multiple comparison tests and indicated in the figure. \* $p \leq 0.05$ , \*\* $p \leq 0.01$ , \*\*\* $p \leq 0.001$ . (c) Representative macroscopic pictures of colons from four AOM/DSS-treated FerE (left) and Lab (right) mice. Colons were cut longitudinally and are presented with luminal side facing up, from oral to rectal end, as indicated. Pictures are taken at termination (day 80), prior to formalin fixation. (d) The occurrence of colonic lesions following AOM/DSS treatment measured by total number of colonic lesions, mean size of lesions, and lesion load. Box plots show median (line), mean (+), IQR (box) and minimum to maximum (whiskers). Significance was determined using Kruskal Wallis followed by Dunn's multiple comparison test. Different letters designate statistical significance with alpha level 0.05. (e) Images of H&E-stained colonic sections from FerE+, LabF+ and Lab+ groups. Presented are the most severely diagnosed sections per group. Ad, adenoma; \*, hyperplasia. See also Table 1, Figures S3 and S8.

### **The gut microbiota of feralized B6 mice was distinct from that of laboratory mice and unaffected by mutagen- and colitis-induced carcinogenesis**

Laboratory tests for common mouse pathogens were negative in fecal samples from mice representative for the Fer as well as the Lab groups (**Figure S4**). Likewise, standard examination (McMasters and immunofluorescent antibody testing for *Cryptosporidium* and *Giardia*) of mouse feces for parasites were negative. To unravel the influence of feralization on the gut microbiota structure in the chemical induction model, stool samples for all animals in the AOM/DSS trial were collected for high-throughput 16S rRNA gene amplicon sequencing. The analyzed 16S rRNA (V3-V4) amplicon dataset included 2,157,819 high-quality and chimera-checked sequences (8,266 to 26,531 per sample), which represented a total of 322 OTUs. Sequencing depth was evaluated by rarefaction curves to confirm the suitability of each sample for further analysis (**Figure S2B**).

Beta-diversity analysis identified significant clustering according to the environmental setting of AOM/DSS-treated animals (**Figure 3a**). The FerE+ and FerL+ groups formed distinct clusters from the Lab mice, both pre- (t0) and post-AOM/DSS treatment (t1). Pairwise comparisons confirmed that these observations were significant (**Figure S5A-C**). No significant difference was detected between FerE+ and FerL+ at baseline, demonstrating that the animals feralized at 5 weeks of age had approached a profile more similar to animals feralized from birth on than to Lab mice (**Figure S5A**). The richness was similar in the three groups at baseline, while effective Shannon counts were significantly lower in the FerE+ and FerL+ compared to Lab+ (both comparisons  $p = .003$ ), suggesting a microbiota dominated by fewer dominant bacterial species (**Figure 3b**).

The difference in gut microbiota elicited by the feralization was evident in the relative abundance of taxa at the level of phyla (**Figure 3c**). Prior to AOM/DSS treatment, both FerE+ and FerL+ had a significantly higher relative abundance of Bacteroidetes and lower relative abundance of Firmicutes compared to Lab+ (all comparisons  $p \leq 0.001$ ). Moreover, *Deferribacteres* was only

detected in the feralized mice. Analysis at the OTU level for timepoint 0 (t0) showed that the majority of molecular species enriched in the FerE+ and FerL+ mice are members of the Bacteroidetes, while OTUs belonging to Firmicutes were enriched in Lab+ mice (**Figure 3d**).

DSS treatment induces colitis accompanied by substantial changes in mice gut microbiota composition.<sup>37,38</sup> Thus, we expected significant shifts in gut microbiota profiles in response to the AOM/DSS treatment. Surprisingly, Fer mice responded minimally to the AOM/DSS treatment, in contrast to the Lab mice (**Figure 3a**) (**Figure S5B**). Alpha-diversity measures remained unchanged in both FerE+ and FerL+ over time, while the Lab+ mice were characterized by a substantial reduction in both richness and Shannon effective counts (both  $p \leq 0.001$ ) (**Figure 3b**). A marked shift from Firmicutes to Bacteroidetes domination was observed for the Lab+ mice following the AOM/DSS treatment (**Figure 3c**). In contrast, the effect of AOM/DSS treatment on the dominating phyla of the Fer animals was modest, with only a minor yet significant decrease in Firmicutes in the FerL+ group. Among the less abundant phyla, *Tenericutes* was only detected in the Fer mice and bloomed after AOM/DSS treatment. *Tenericutes* was represented by a single OTU with closest sequence similarity to *Anaeroplasmata bacteroides* (91.8%). All groups showed enrichment of *Verrucomicrobia* following AOM/DSS treatment, represented by a single OTU with closest sequence similarity to *Akkermansia muciniphila* (99.8%). This OTU was observed to be borderline more prevalent in Lab+ mice compared to FerE+ at endpoint ( $p = .051$ ) (**Figure S5D**). Moreover, a bloom of *Actinobacteria* were observed in Lab mice after AOM/DSS treatment, largely due to one OTU with closest sequence similarity to *Bifidobacterium animalis* (99.8%) (**Figure S5D**). These results support that the Fer and Lab mice responded differently to the AOM/DSS treatment and suggests that the microbiota of the Fer mice was more resistant to treatment, compared to the Lab mice microbiota, which showed substantial changes (**Figure 3e**, **Table S1**).

We also characterized the gut microbiota profiles and composition of the control-treated groups (**Figure S6A-C**) and the cage-housed feralized

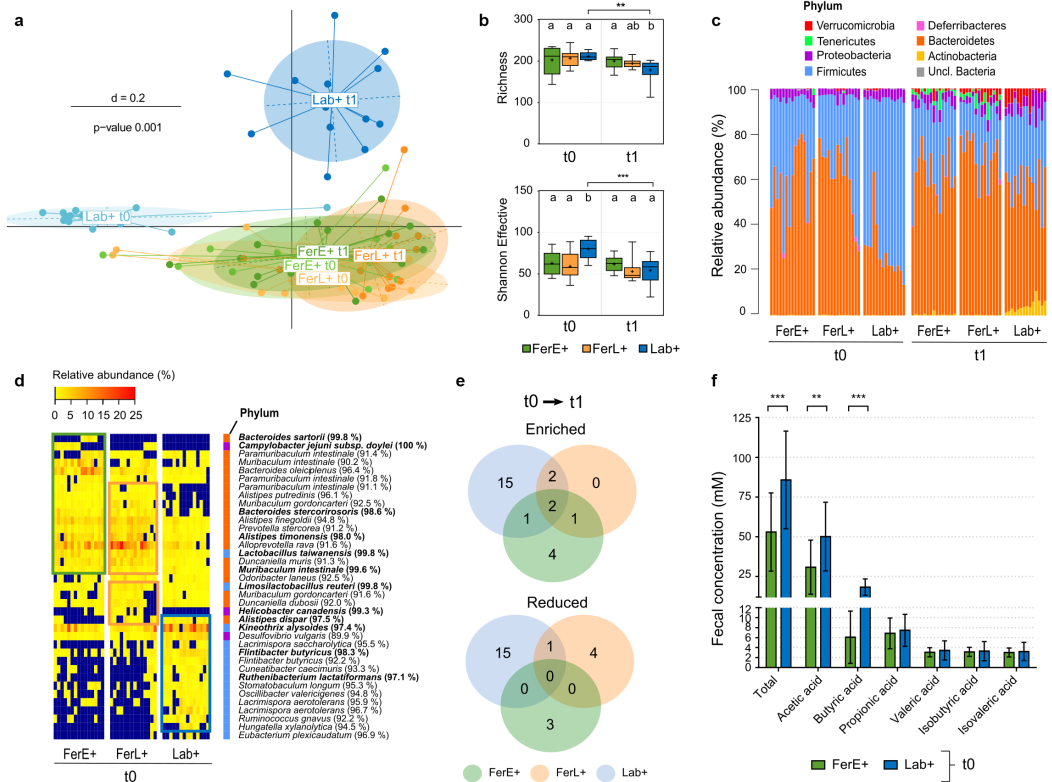


**Figure 3.** The gut microbiota of feralized and laboratory B6 mice significantly differed in composition and response to mutagen- and colitis-induced carcinogenesis. (a) Multi-dimensional scaling (MDS) plot of fecal microbiota profiles (generalized UniFrac distances) for AOM/DSS treated groups at baseline (t0) and endpoint (t1). Significance of separation was determined by PERMANOVA. d = distance scale. (b) Observed number of OTUs (Richness) and Shannon Effective counts for AOM/DSS treated groups. Box plots show median (line), mean (+), IQR (box) and minimum to maximum (whiskers). Asterisks designate significant (\*\* $p \leq 0.01$ , \*\*\* $p \leq 0.001$ ) over-time differences determined by Wilcoxon Signed Rank Sum tests, whilst letters designate significant ( $p \leq 0.05$ ) differences between groups at each timepoint determined by Kruskal-Wallis tests followed by pairwise Wilcoxon Rank Sum tests with Benjamini-Hochberg correction for multiple comparisons. (c) Taxonomic binning at the rank of phylum, presented as relative abundance for each individual. (d) Heatmap of relative abundance of specific OTUs enriched in Fer and Lab mice at baseline (t0). The occurrence of OTUs for which the relative abundance or prevalence differed significantly between the groups (determined by Kruskal-Wallis and Fisher's exact test, respectively) are plotted. Blue color indicates the OTUs were absent or below cutoffs for analyses. The bacterial species with a valid name closest to the corresponding OTUs is indicated along with its sequence similarity; those OTUs identifiable at the species level ( $\geq 97\%$  similarity) are written in bold letters. Phyla to which the OTUs belong are designated with colored squares as specified in c. Frames indicate significant increased relative abundance or prevalence in FerE (green), FerL (Orange) and Lab (blue) compared to one of the other groups determined by pairwise analyses (Wilcoxon Signed Rank Sum/Fisher's Exact tests with Benjamini-Hochberg correction for multiple comparisons). (e) Venn diagrams of shared enriched and reduced OTUs among the three groups in response to AOM/DSS treatment. Significant over-time (t0-t1) differences within each group at the OTU-level was determined by Wilcoxon Signed Rank Sum and Fisher's exact tests. Details are listed in Table S1. (f) Concentration of SCFAs in fecal samples obtained from Fer and Lab mice prior to AOM/DSS/control treatment, presented as mean with the standard deviation (SD) shown via the whiskers. Significance between groups was determined by Wilcoxon Rank Sum tests for each SCFA. \*\* $p \leq 0.01$ , \*\*\* $p \leq 0.001$ . Lab+ n = 13, FerE+, n = 15. See also **Figure S2B**, **Figures S4-S6** and **Table S1**.

groups (FerE<sup>cage+</sup> and FerL<sup>cage+</sup>) (**Figure S6D-F**). Comparisons of AOM/DSS-treated and control-treated groups showed that the gut microbiota profiles of feralized mice clustered independently of

treatment, while the Lab+ and Lab- were separate, particularly at endpoint (**Figure S6A**). The cage-housed Fer groups, FerE<sup>cage+</sup> and FerL<sup>cage+</sup>, showed gut microbiota profiles overlapping those

of FerE+ and FerL+ mice, respectively (**Figure S6D**). We found significant separation of gut microbiota profiles at endpoint yet pairwise comparisons showed no significant separation between FerL+ and FerL<sup>cafe</sup>+ ( $p = .137$ ) nor FerE+ and FerE<sup>cafe</sup>+ ( $p = .072$ ) groups. These data largely indicate that the farmyard-type environment rather than the enlarged space in the mouse pens influenced the gut microbiota profiles.

**The feralized gut microbiome is characterized by low fecal levels of SCFAs and relative abundance of short-chain fatty acid producers**

To investigate possible cancer protective mechanisms, fecal concentrations of short-chain fatty acids (SCFAs) were measured. SCFAs are microbially derived molecules known to have immunomodulatory effects in the gut.<sup>39,40</sup> A panel of SCFAs was analyzed in feces collected from FerE+ and Lab+ mice, before AOM/DSS treatment (t0; **Figure 2a**). In agreement with previous studies, we identified acetic acid as the dominant SCFA in our samples, followed by butyric acid and propionic acid.<sup>41</sup> Notably, the FerE+ mice had significantly lower amounts of butyric and acetic acid, as well as total SCFAs, compared to the Lab+ mice (**figure 3f**). This was reflected in the baseline microbiota, where Lab+ mice showed higher relative abundances or prevalence of species in the Firmicutes phylum, specifically OTUs showing the closest species similarity to known butyrate-producing bacteria such as *Flintibacter butyricus*<sup>42</sup> and *Kineothrix alysoides*<sup>43</sup> (**Figure 3d**). However, through the course of AOM/DSS treatment, these OTUs were reduced in Lab+ mice (**Figure 3e, Table S1**).

**Immune cells of feralized B6 mice displayed a mature phenotype and demonstrated enhanced IFN $\gamma$  T-cell response**

To identify possible immunological factors likely to be involved in cancer protection, we conducted immunophenotyping of cells based on previous findings in feralized mice<sup>34</sup> and of relevance in anti-tumor responses. Cells were harvested from spleen and mesenteric lymph nodes (mLNs) from all animals at endpoint (t1), and flow cytometry gating strategies are shown in **Figure S7**.

In spleens, we found comparable relative numbers of CD4<sup>+</sup> T-cells, but a significant effect of treatment on CD8<sup>+</sup> T-cells with lower relative numbers in AOM/DSS-treated mice (**Figure 4a**). We found significant effects of treatment, environment and their interaction on the relative number of memory (CD44<sup>+</sup>) type within CD4<sup>+</sup> T-cells in spleens. Pairwise comparisons showed significantly higher relative numbers of memory-type CD4<sup>+</sup> T-cells in FerE- and FerL- than in Lab-mice. The differences in treatment were largely driven by higher relative numbers in the AOM/DSS-treated FerL+ and Lab+ than FerL- and Lab-mice, respectively (**Figure 4a**). Moreover, we found that the effect of environments on relative numbers of memory (CD44<sup>+</sup>) phenotype in CD8<sup>+</sup> T-cells were driven by differences between the AOM/DSS-treated groups, where FerE+ and FerL+ showed higher numbers than Lab+ (**Figure 4a**).

In mLNs, we detected significant effects of treatment on both CD4<sup>+</sup> and CD8<sup>+</sup> T-cells, of which the CD4<sup>+</sup> T-cells were higher and CD8<sup>+</sup> T-cells lower in the AOM/DSS-treated mice (**Figure 4c**). The memory-type of CD4<sup>+</sup> T-cells in mLNs were higher in FerL- than in FerE- and Lab- (**Figure 4c**). We also found an effect of environment on memory-type CD8<sup>+</sup> T-cells in the mLNs of Fer mice compared to Lab mice (**Figure 4c**). Likewise, KLRG1 expressing T-cells (indicating antigenic experience) were increased in the Fer groups (**Figure 4c**).

Regulatory T-cells (Tregs) are important in conveying immunological tolerance to gut commensals.<sup>44</sup> Yet, in malignancies like cancer, Tregs have been shown to interfere with a proper anti-tumor immune response.<sup>45</sup> We observed no significant differences in relative numbers of splenic Tregs across environment or treatment (**Figure 4b**). In mLNs, we detected a significant interaction effect of environment and treatment on relative numbers of Tregs in mLNs driven by an increase in Lab+ mice compared to FerL+ mice (**Figure 4d**).

In the spleen, relative numbers of NK cells were similar across groups (**Figure 4e**). In mLNs, we found a significant effect of environment and treatment on relative number of NK cells, with pairwise comparisons showing significantly higher relative numbers in control-treated mice compared to AOM/DSS-treated mice, but no significant

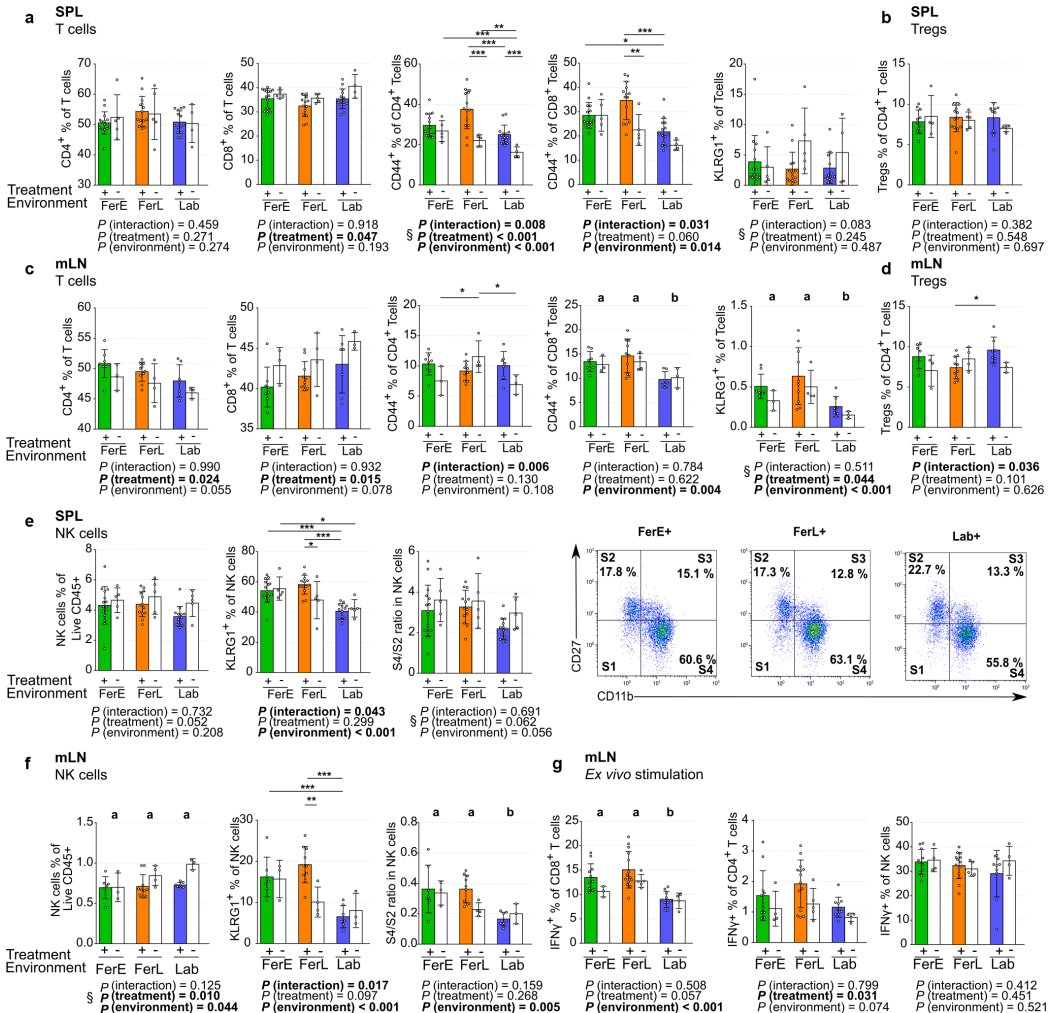


**Figure 4.** The feralized T and NK cells showed higher expression of maturation markers and increased IFN $\gamma$  response to *ex vivo* stimuli. Phenotypic markers of (a) T-cells in spleen (SPL), (b) Tregs in spleen, (c) T-cells in mesenteric lymph nodes (mLN), (d) Tregs in mLN, (e) NK cells in SPL and (f) NK cells in mLN of Fer and Lab mice treated with AOM/DSS (+) or NaCl/H<sub>2</sub>O (-). In C, representative flow cytometric plots of maturation stages S1-S4 based on CD27 and CD11b expression are shown for the AOM/DSS treated FF, LabF and Lab groups. **(E)** Cells expressing IFN $\gamma$  as % of CD4<sup>+</sup> T-cells, CD8<sup>+</sup> T-cells and NK cells. Cells were isolated from mLN, cultured with PMA and ionomycin (for T-cell activation) or IL-2+ IL-13 (for NK cell activation) for 4 hours prior to immunophenotyping. All graphs are presented as mean, with the standard deviation (SD) shown via the whiskers. Statistical differences were determined by two-way ANOVA, with the *P* values for the main effects written out below each plot (significant results at alpha level 0.05 in bold letters). Different letters designate only statistical significance (*p* ≤ 0.05) between environments (FerE; FerL; Lab) determined by post hoc Tukey's multiple comparison tests. Where interaction effects were detected, post hoc Bonferroni's multiple comparison tests were conducted, and asterisks designate statistical significance (\**p* < .05, \*\**p* < .01, \*\*\**p* < .001). The § symbol designates the statistical tests were conducted on Box Cox transformed data. See also **Figures S7 and Table S2**.

differences across environments (figure 4f). We detected significant interaction effects on KLRG1<sup>+</sup> NK cells in both the spleens and mLN, largely driven by higher numbers in FerE+ and FerL+

than in Lab+ mice (Figure 4(e,f)). Murine NK cells can be divided into maturation stages based on expression of CD11b and CD27, where the early (S1), mid (S2), late (S3) and fully mature (S4) stages



corresponds to CD27<sup>-</sup>CD11b<sup>-</sup>, CD27<sup>+</sup>CD11b<sup>-</sup>, CD27<sup>+</sup>CD11b<sup>+</sup> and CD27<sup>-</sup>CD11b<sup>+</sup>, respectively.<sup>28,46</sup> In mLNs, but not in spleens, we found a significant effect of environment on the S4/S2 ratio (the two dominating subsets), with pairwise comparisons showing a significant higher ratio in FerE+ and FerL+ mice compared to Lab mice (Figure 4(e,f)).

We addressed whether feralization influenced T-cells and NK cells potencies as effector cells by assessing the production of IFN $\gamma$ . Cells isolated from mLNs and incubated with PMA and Ionomycin, or IL-2 and IL-12, followed by flow cytometric evaluation of T- and NK cells with respect to IFN $\gamma$  expression. We found a significant effect of environment on the frequency of IFN $\gamma$  positive CD8<sup>+</sup> T-cells, which were higher in FerE and FerL mice compared to Lab mice (Figure 4g). Moreover, we found a significant effect of treatment on IFN $\gamma$ <sup>+</sup> CD4<sup>+</sup> T-cells, with higher relative numbers in AOM/DSS-treated mice than in control-treated mice. No significant effects of environment nor treatment were found for IFN $\gamma$ <sup>+</sup> NK cells (Figure 4g).

Taken together, the immunophenotyping data suggests that feralization in a farmyard-type environment promote immune maturation of the T and NK cell populations both locally (mLNs) and systemically (spleen).

## Discussion

Free-living mammals, including humans and mice, are exposed to a diverse range of microbes over their lifetime, which their immune system relies upon for development. Yet, disease modeling in mice usually take place under strictly hygienic conditions, far away from the typical lifestyle of the end goal for such studies, humans. To close the gap between the preclinical mouse model and human lifestyles, we have established a system where laboratory mice are raised under a full set of environmental conditions present in a naturalistic, farmyard-like habitat in indoor facilities.<sup>34</sup> In the current study, we addressed the effects of housing lab mice in a farmyard-type habitat on development of colorectal cancer (CRC). We demonstrate that feralization in this environment had prominent clinical consequences in conferring protection

toward colorectal carcinogenesis in the genetic (A/J Min/+ mice) as well as the chemical induction (AOM/DSS) models of CRC.

Our findings corroborate previous reports showing direct links between modulations of gut microbiotas and reduced colorectal carcinogenesis in AOM/DSS-treated mice<sup>29,47–49</sup> and Min/+ mice,<sup>50,51</sup> and indicate that the beneficial colorectal cancer-protective effects of the diverse farmyard-type habitat may be driven by the gut microbiota. We show that feralization led to shifts in gut microbiota profiles in both A/J and B6 mice, albeit differently in the two trials. Nevertheless, our study is not unique with respect to discrepancies in gut microbiota composition in naturalized mice, and this likely reflects differential sources for the natural microbes. Our A/J Min/+ mice were feralized in an environment containing farm material identical to those in our previous report of feral and feralized co-housed mice,<sup>34</sup> and the Proteobacteria enrichment and increased *alpha*-diversity in all feralized A/J mice corresponded to our findings in both feral and feralized B6 mice in that report. Moreover, the findings from the feralized A/J mice corresponded well with previous reports from lab mice housed or engrafted with material from free-living mice,<sup>29,34</sup> pet-store mice,<sup>32</sup> and lab mice exposed to natural soil.<sup>52</sup> In contrast, the B6 mice subjected to AOM/DSS treatment were feralized in an environment with components from a different farm source. In these feralized B6 mice, no changes in the relative abundance of Proteobacteria or in species richness was detected, corresponding to findings of re-wilded mice in outdoor facilities.<sup>33</sup> The higher relative abundance of Bacteroidetes detected in the feralized B6 mice also complements previous findings in re-wilded mice,<sup>33</sup> as well as lab mice engrafted with material from free-living mice,<sup>29</sup> yet contrasts with our previous report of feral and feralized mice.<sup>34</sup>

Gut microbes associated with CRC vary greatly between studies and experimental setups. Although a lower relative abundance of Firmicutes was observed in our feralized B6 mice, OTUs with closest sequence similarities to *Lactobacillus* and *Limosilactobacillus* species were enriched. *Lactobacillus* has been reported to be predictive of a light tumor burden in the AOM/DSS model and various *Lactobacillus* strains have been shown to

reduce gastrointestinal inflammation.<sup>48</sup> However, *Bifidobacterium* strains have also been shown to confer anticancer effects,<sup>53</sup> and we found higher relative abundance of this genus in lab B6 mice. Moreover, *Lachnospiraceae*, Clostridiales, Proteobacteria, *Alistipes* and *Aneroplasma* are all examples of taxa for which high baseline relative abundance has been associated with increased tumor burden in AOM/DSS model.<sup>48</sup> In our AOM/DSS experiment, several OTUs with highest similarity to *Lachnospiraceae* spp., such as *Lacrimispora* spp., *Ruminococcus gnavus*, *Cuneatibacter caecimuris*, and *Stomatobaculum longum*, were enriched in lab B6 mice. Yet, *Alistipes* spp. and Proteobacteria were enriched in feralized B6 mice. These findings were not consistent with observations from the A/J Min/+ trial, emphasizing that different community structures could confer beneficial effects in different models of carcinogenesis.

Microbiota-associated dysregulation of immune pathways and the epithelial barrier are known drivers of carcinogenesis.<sup>17</sup> Thus, a modulation of responses to inflammatory stimuli as previously implied in similar studies of a naturalized mouse microbiota<sup>29</sup> is a feasible rationale for protection seen in the feralized mice. However, assessment of the pathogenic pathways was beyond the scope of this study, and the inhibitory mechanisms associated with feralization require further investigation.

Interestingly, in comparison to lab B6 mice, the feralized B6 mice treated with AOM and DSS demonstrated a robustness of their gut microbiota. Generally, large microbial shifts are observed in mice subjected to AOM and/or DSS treatment,<sup>37,38,49</sup> and tumor burden has been associated with the magnitude of changes in gut microbiota community structure.<sup>54</sup> We found major changes in the microbiota profile of lab mice, but only minor in feralized mice, following AOM/DSS treatment. A recent study by Rosshart *et al.* showed that a wild mouse microbiota was stable and resilient against external disturbances.<sup>30</sup> Given the complex and diverse nature of gut microbes, it is feasible that the overall resilience of the gut microbiota, rather than single populations, is beneficial in preventing unhealthy states.<sup>55</sup> Accordingly, it is possible that the feralized B6 microbiota is resilient

to the perturbations inflicted by AOM and DSS, which may have contributed to the protective effects.

In the AOM/DSS trial, we assessed a panel of fecal SCFAs. As products of bacterial fermentation in the gut, SCFAs are known to play important roles in colonic energy metabolism, immune system, and gut barrier function. SCFAs, particularly butyrate, have been highly associated with colon health and anti-tumor properties,<sup>17,56</sup> albeit with disagreement between studies.<sup>57</sup> Previous studies have shown beneficial effects of SCFA administration on AOM- and DSS-induced carcinogenesis,<sup>58</sup> and exacerbated carcinogenesis in SCFA-receptor deficient mice.<sup>59</sup> However, we did not observe that feralization increased SCFA excretion, nor that protective mechanisms in our experiment were dependent of SCFAs. Nevertheless, analysis of the gut microbiota over-time indicated that known butyrate producers were reduced following AOM/DSS treatment in the lab mice. This suggests that SCFA levels may have been reduced which may have contributed to the exaggerated CRC development.

Immunophenotyping of T and NK cells showed increased expression of maturation markers, such as CD44 and KLRG1, in our feralized mice. The higher level of KLRG1<sup>+</sup> NK cells found in feralized mice is similar to our previous findings in feralized co-housed mice.<sup>34</sup> IFN $\gamma$ -mediated responses are important in anti-tumor immunity and have been positively associated with survival in CRC,<sup>60</sup> and the increased IFN $\gamma$  response to stimuli in CD8<sup>+</sup> T-cells in the feralized mice is also similar to our previous findings in feralized co-housed and feral mice.<sup>34</sup> While these findings add consistency to the observed impact by feralization on immunity, more elaborate studies are needed to conclude about causal relationships with CRC protection.

Currently, the presented feralization model is unique in its ability to continuously expose mice to diverse environmental components, while allowing for controlled conditions such as light, temperature, and humidity. Moreover, this model enables control of the timing of encounter of various environmental stimuli, among them microbes, that could be valuable for future investigating the dynamics of host-microbe interactions. We emphasized this concept by including the late

feralized mice in the AOM/DSS trial to investigate the potential role of feralization timing. Our late-feralized mice showed a disease phenotype in between the early-feralized and laboratory mice, yet closer to the former. Moreover, the gut microbiota composition was similar independently of feralization timing. These observations suggest that the transfer of maternal microbiota and early exposure to the farmyard environment had some effect yet was not essential in conferring protection against CRC.

While our study shows aspects of an original feralization approach, we do note some limitations. First, the two experiments reported here took place at two different sites with differences in the source of environmental material, mouse strain, age, gender, genotype, and use of different protocols in 16S rRNA sequencing. Hence, direct comparisons between the two trials presented within this manuscript should be made with caution. Nevertheless, it is noteworthy that similar disease outcomes were detected in both experiments. Second, the feralized mice described within this study are housed under a full set of complex environmental conditions. In the herein presented experiments, we have not assessed microbial components beyond the bacterial portion of the gut microbiota and certain pathogens and parasites, hence future studies should aim to unravel potential contributions of other communities such as fungi, viruses and bacteriophages. Moreover, the presence of a farmyard-type environment could offer other effects beyond modulations of the mouse microbiome. By testing the environmental material in both pens and in cages, we document limited effect of physiological and behavioral consequences of the enlarged space. Yet, nutritional elements, odors, tastes and other factors introduced through the farmyard-type environment remain uninvestigated. With studies of feralized mice, we are bringing the lab mice closer to a “real world” that has the potential to improve translational value to other mammals, including humans who rarely live in ultra-clean environments. The use of naturalized mouse studies is not intended to replace traditional reductionist studies, but rather complement them in search of both accuracy in reflecting true responses and precision in determining biological mechanisms.

In conclusion, we show that feralization of lab mice in a farmyard-type setting alleviate CRC development, and has considerable implications on gut microbiota and immunophenotype. We suggest that feralization of lab mice could complement traditional mice studies to improve our understanding of mechanisms underlying beneficial effects of diverse environments. The flexibility of choosing which factors to introduce, as well as the timing of their introduction, in the feralization model also provides novel opportunities to study dynamics of host interactions in various diverse environments.

## Materials and methods

### *Animals and environmental settings*

A microbially enriched, semi-naturalistic model was designed at the Norwegian University of Life Sciences. To resemble the common habitat of the house mouse (*Mus musculus*), indoor mouse pens containing natural environmental material were constructed. In the A/J Min/+ trial, pig pens (2.00 × 2.50 × 1.25 m) were adopted to house mice, containing sawdust, soil, compost, twigs, hay and fecal contents from pigs, cows and horses, as described previously.<sup>34</sup> For the AOM/DSS trial, refinements to the model were made, and the feralization took place in specially designed mouse pens constructed of galvanized steel plates (1.10 × 2.40 × 1.20 m) with mouse igloos, running wheels, as well as plastic boxes and tunnels allowing for sheltering and nesting (Figure 5; Video S1). A base layer of woodchip bedding was laid down and enriched with organic soil (Plantasjen, Norway), straw, and fecal content from farmed pigs, cows, horses, and poultry, originating from an organic farm located in Eastern Norway. Initially, about 50 liters of fecal material, 40 liters of soil, and 80 liters of bedding was added to each of the four mouse pens. Every two weeks during the experiments, fresh farm animal fecal content (approximately 50 liters/pen), always from the same farm within each experiment, was added to the pens to simulate a natural situation and sustain the microbial load. Simultaneously with the addition, a portion of the old material was removed. The environmental material was kept moist with fresh tap water.



**Figure 5.** Photographs of the mouse pens and feralized B6 mice. The photographs show the layout of the mouse pens (left) and feralized B6 mice (right). The upper right photograph shows a nest of second generation feralized B6 mice.

The mice were housed in either mouse pens (max 10/pen) or in individually ventilated cages (IVCs; Inovive Inc., San Diego, CA) (max 5/cage) with sterile bedding, mouse igloos and running wheels under standard conditions (12 h light/dark cycle, 23–25°C, 45–50% relative humidity). The non-feralized lab mice were kept under pathogen-free conditions. Water and standard chow diet (RM1(E), SDS; Special Diet Services, Witham, United Kingdom) were provided *ad libitum*. Throughout the trials, animal welfare was assessed by a health monitoring score sheet recording the animals' bodyweight, rectal prolapse, rectal bleeding, general appearance and behavior daily. Animals exhibiting any symptom was kept under close observation. Humane endpoints were defined as follows: body weight loss >15%, rectal bleeding defined as blood around anus sustained over two subsequent days, a complete bulging of distal colon out of rectum, and severely under-conditioned appearance and behavior.

Animal experiments were approved by the Norwegian Animal Research Authority (FOTS IDs 6799 and 18012).

### **A/J Min/+ model**

A/J Min/+ (Min; multiple intestinal neoplasia) mice harbor a mutant allele of the murine *Apc* gene (adenomatous polyposis coli) and are thus predisposed to intestinal adenoma formation. On an A/J background, Min/+ mice consistently develop

colonic adenomas, and are thus considered a relevant model of colorectal cancer in humans.<sup>19,61,62</sup> The A/J Min/+ were B6 Min/+ mice (The Jackson Laboratories) back-crossed with wild-type A/J mice (The Jackson Laboratories). Breeding of A/J Min/+ mice at the Department of Experimental Biomedicine at NMBU, campus Adamstuen, has previously been described.<sup>61</sup> Twenty male A/J Min/+ and twenty A/J wild-type (WT) aged 6–8 weeks were distributed to four age-matched groups (Figure 1a). The animals were either feralized in mouse pens or housed in conventional cages in a lab setting for 7–9 weeks before they were euthanized. One LabMin and one FerMin had bloody feces and altered behavior, and a tumor on the back, respectively, and were therefore euthanized earlier than the trial end. These two mice were excluded from all analyses, leaving  $n = 9$  in the LabMin and FerMin groups. The age of the remaining mice at euthanasia ranged between 18 and 23 weeks. Animals were randomized to four days of harvesting, where all groups were represented each day. Tissues were collected after cervical dislocation.

### **AOM/DSS model**

Thirty female C57BL/6 J (B6; Janvier Labs, Saint-Berthevin Cedex, France) mice aged 3 weeks were acclimatized for one week under conventional, pathogen-free conditions in individually ventilated cages (IVCs) before being distributed to the

different environments. The animals were feralized in mouse pens or housed in conventional cages in a lab setting for five weeks prior to breeding. The feralized females were mated with B6 males purchased from the same batch 2:1 in IVCs enriched with the same material as pens. After a 10-day breeding period, the females returned to the mouse pens to deliver. Additionally, 24 female mice from the same batch were housed and mated under pathogen-free conditions in IVCs.

Twenty-five female feralized offspring, and 45 female lab offspring, were included in the AOM/DSS trial. At 3 weeks of age, the offspring were weaned and randomly assigned to experimental groups (Figure 2a). At 7 weeks of age, colonic carcinogenesis was induced in the animals by use of a previously established protocol combining Azoxymethane (AOM; Sigma-Aldrich; 10 mg/kg) and repeated DSS (MP Biomedicals; 1% w/v, dissolved in distilled H<sub>2</sub>O) administration.<sup>63</sup> Under transient gas anesthesia (isoflurane 3–4%, 200 mL/min), mice were either injected with AOM or sterile NaCl (B.Braun; 0.9%) subcutaneously into the neck skin fold. DSS (36,000–50,000 M.Wt.) was dissolved in distilled water prior to supply. A 1% DSS solution was supplied in three 7-day cycles (day 8–14, 31–38, 52–59), with a 16-day recovery period between the cycles. Fresh DSS solution was prepared and supplied every second day throughout the 7-day cycles. Control treatment entailed the same regimen with fresh distilled water only.

Due to late removal of a male pup from one of the mouse pens, four mice were potentially impregnated prior to the AOM/DSS treatment. These mice (one individual in FerE+, two in FerE- and one in FerL+ groups) were quarantined in cages enriched with the same material as the mouse pens for 12 days (day 12–24), while provided the same treatment as their respective groups. Bodyweight registrations from these mice a week before and during the quarantine were excluded from analyses, but data from these mice were included in the other analyses as we did not observe any signs of influence on outputs. One Lab mouse was found dead at week 16 and excluded from all analyses, leaving 14 mice in this group. The animals were sacrificed between 25 and 40 days after the last cycle of DSS/water administration. Animals were randomized to five days of harvesting, and all

groups were represented each harvest day. Blood was collected by cardiac puncture while the animals were under terminal anesthesia induced by a single intraperitoneal (i.p.) injection of a cocktail consisting of Zoletil Forte (Virbac, Carros, France), Rompun (Bayer, Oslo, Norway), and Fentadon (Eurovet Animal Health, Bladel, The Netherlands) (0.1 mL/10 g body weight) with the following active ingredients: Zolezepam (32 mg/kg), Tiletamin (32 mg/kg), Xylazine (4.5 mg/kg) and Fentanyl 26 µg/kg. Tissues were collected after cervical dislocation.

### **Pathogen screening and parasitology**

For pathogen screening, blood was collected from three Lab mothers and six feralized mothers from the mouse pens by cardiac puncture while the animals were under terminal anesthesia induced by a single i.p. injection of a ZRF cocktail as described above. Serum was isolated by leaving blood samples clot at room temperature for 1–2 hours, followed by centrifugation at 1000–3000xg for 5–10 minutes. 100 µL serum from each animal was screened for common pathogens by BioDoc (Hannover, Germany).

For parasitology assessment, fecal pellets from a total of 12 female offspring housed in clean cages (3 animals from each of 4 cages), 6 animals housed in cages enriched with the natural environmental material also found in mouse pens (3 animals from each of 2 cages) and 24 animals housed in mouse pens (6 animals from each of 4 pens) was collected. Pellets were pooled, resulting in one sample per cage and two samples per pens. Feces were examined for parasites by standard methods including McMasters counting technique, and immunofluorescence antibody test (IFAT), for *Giardia spp.* and *Cryptosporidium spp.*

### **Scoring of intestinal lesions by surface microscopy**

The colons were prepared as described previously.<sup>61</sup> Briefly, each colon was fixated flat between two filter papers in formalin solution (VWR Chemicals; 10%, neutral buffered) for 24 hours prior to staining with Methylene blue solution (MB; Sigma-Aldrich; 0.1% in 10% formalin, neutral buffered). The colons were stored refrigerated in 70% ethanol until analysis. The

identification of intestinal lesions was performed by microscopy according to previously described procedure.<sup>19</sup> In short, an inverted light microscope (CKX41, Olympus Inc., Hamburg, Germany) equipped with a digital color camera (DP25, Olympus) was used to examine the colons for lesions. Aberrant crypt foci (ACF) stain bright blue/green and have enlarged crypts with compressed luminal openings, while normal crypts stain more subdued green/brown (**Figure S8A**). Thus, ACFs can be recognized and distinguished from normal epithelia. Diameters were measured using an eye piece graticule, and colonic lesion size (mm<sup>2</sup>) was calculated based on the measured diameters. The total number of lesions, lesion load and distribution were measured and calculated per mouse in order to study lesion development in the intestines. Lesion load (mm<sup>2</sup>) was defined as the sum of the area of all lesions observed in an intestine.

### **Histopathological classification of intestinal lesions**

Because scoring of ACFs by MB-staining is less characterized in B6 mice than A/J Min/+ mice, we subsequently conducted histopathological classification of lesions in colons from the AOM/DSS-treated FerE, FerL, and Lab groups. The six colons in each group with the largest mean lesion size determined by surface microscopy were selected for further examination. Swiss rolls of these colons were prepared by rolling lengthwise from oral to rectal end, with the mucosa facing inwards. The swiss rolls were embedded in paraffin, and for each paraffin-embedded colon, sections (2–3  $\mu$ m thick) were made at three different depths (top, middle, and bottom) to detect lesions over the width of the flattened intestine. For two individuals in the Lab+ group, only two sections were assessed. The sections were stained with hematoxylin and eosin (H&E) and examined blindly by a pathologist using high-resolution digitized slides scanned by a Philips UFS slide scanner. Lesions were classified as hyperplasia/dysplasia, adenomas (tumors restricted to the mucosa) or carcinomas (tumors with distinct infiltrative growth through the mucosa into the submucosa) (**Figure S8B**).

### **Microbial community analysis by 16S rRNA gene amplicon sequencing**

In the A/J Min/+ trial, fecal pellets were snap frozen in liquid nitrogen immediately after collection and stored at -80°C until DNA extraction. DNA extraction and library preparation of the V3-V4 regions of the 16S rRNA gene was conducted at NMBU according to a previously described procedure.<sup>64</sup> High-throughput amplicon sequencing was conducted on a MiSeq platform (Illumina Inc.) using V3 sequencing chemistry in a paired-end mode.

In the AOM/DSS trial, fecal pellets were collected in sterile tubes pre-filled with Zirconia-Silicate beads (0.1–0.15 mm, Cole-Palmer) and Stool DNA Stabilizer buffer (STRATEC Molecular GmbH). Samples were snap frozen in liquid nitrogen immediately after collection and stored at -80°C until DNA extraction. DNA was extracted as previously described,<sup>65</sup> including mechanical lysis by bead-beating. Amplicon libraries were prepared via a two-step PCR amplifying the V3-V4 regions, as described in detail previously.<sup>66</sup> Amplicons were purified with the AMPure XP system (Beckmann) before sequencing. High-throughput amplicon sequencing was performed at the ZIEL Institute for Food & Health, Technical University of Munich, according to previously described procedures.<sup>65</sup> Sequencing was carried out in a paired-end mode (PE300) using a MiSeq system (Illumina Inc.).

Raw reads were processed with the Integrated Microbial Next Generation Sequencing pipeline,<sup>67</sup> based on the UPARSE approach.<sup>68</sup> Briefly, sequences were demultiplexed, trimmed to the first base with a quality score >3, and assembled. Sequences with <300 and >600 nucleotides (AOM/DSS trial; paired-end analysis) or <200 and >300 nucleotides (A/J Min/+ trial; single-end analysis), as well as assembled sequences with expected error >3 were excluded from the analysis (USEARCH 8.1 (AOM/DSS trial) or 8.0 (A/J trial)).<sup>69</sup> Remaining reads were trimmed by 10 nucleotides at forward and reverse end to prevent analysis of regions with distorted base composition. The presence of chimeras was tested with UCHIME.<sup>70</sup> Operational taxonomic units (OTUs) were clustered at 97% sequence similarity (USEARCH 8.1),<sup>69</sup> and only those with a relative abundance >0.25% in at least

one sample were kept.<sup>71</sup> Taxonomies were assigned at 80% confidence level with the RDP classifier<sup>72</sup> (version 2.11, training set 15). Sequences were aligned with MUSCLE,<sup>73</sup> and tree generated with Fasttree.<sup>74</sup> Specific OTUs were identified using EzBioCloud.<sup>75</sup>

Raw sequence files were deposited to the Sequence Read Archive and are available under the accession number PRJNA669440.

### Short-chain fatty acid analysis

Analysis of short-chain fatty acids in stool samples was conducted using a Trace 1310 gas chromatograph (Thermo Scientific) equipped with an auto sampler, a flame ionization detector (FID), a split injector, and a Stabilwax DA column (Restek; 30 m, 0.25 mm ID, 0.25  $\mu\text{m}$ ), according to previously described procedures.<sup>76</sup> Briefly, thawed fecal samples were dissolved in water and homogenized in Fastprep (MP Biomedicals). Supernatant was collected and mixed 1:1 (vol/vol) with internal standard (solution of 0.4% formic acid and 2000  $\mu\text{M}$  2-methylvaleric acid). Samples were centrifuged, and supernatant was transferred into spin columns (VWR; 0.2  $\mu\text{m}$  filter) and centrifuged again. Eluates were transferred into GC vials and analyzed in the GC-FID instrument. The software Chromeleon (v. 7.2) was used for instrument control, quantification and data analysis. SCFA quantification was calculated based on a standard curve made from two-fold dilutions of SCFA standards.

### Immunophenotyping

Mesenteric lymph nodes (mLNs) and whole spleens were harvested and kept in RPMI-1640 medium (Sigma-Aldrich) with 2% FCS on ice until extraction of cells. Cells were extracted from tissues using GentleMACS dissociator. For splenic tissue, a collagenase/DNase solution was used for digestion. Splenic suspensions were briefly treated with  $\text{NH}_4\text{Cl}$  solution to lyse erythrocytes. Single-cell suspensions were prepared by running through a 70  $\mu\text{m}$  cell strainer (BD Biosciences) and concentrations standardized using Countess II automated cell counter (Thermo Fischer Scientific).

Immunophenotyping was carried out on ice by incubating single-cell suspensions in RPMI medium with 0.5% BSA. Following Fc blocking with anti-CD16

/CD32 antibody, cells were stained with Fixable Live/Dead Yellow (Thermo Fisher) and incubated with combinations of monoclonal antibodies listed in **Table S2**. For intracytoplasmic staining, surface staining was followed by additional steps of treatment with Intracellular Fixation & Permeabilization buffer or Foxp3 Staining buffer (eBioscience) according to manufacturer's manual. Cells were analyzed using a Gallios 3-laser flow cytometer and Kaluza 1.2 software (Beckman Coulter). Gating strategies are depicted in **Figure S7**.

### Ex vivo activation of immune cells

Cells isolated from mLNs were seeded on 96-well plates (500,000 cells/well) in triplicates. The cells were incubated with a cocktail of Brefeldin A (Sigma-Aldrich) in RPMI medium with PMA (phorbol 12-myristate-13-acetate; Sigma-Aldrich) and ionomycin for T-cell activation, and murine IL-2 and IL-12 for NK cell stimulation. Cells were incubated for 4 hours, spun down and stained for immunophenotyping of intracytoplasmic IFN $\gamma$  as described above.

### Statistical analyses

Microbial profiles and composition were analyzed in the R programming environment (R version 4.0.2)<sup>77</sup> using Rhea (available from: <https://github.com/Lagkouvardos/Rhea>).<sup>78</sup> OTU tables were normalized to account for differences in sequence depth by division to their sample size and then multiplication by the size of the smaller sample. *Beta*-diversity was computed based on generalized UniFrac distances,<sup>79</sup> and the significance of separation between groups was tested by permutational multivariate analysis of variance (PERMANOVA). *Alpha*-diversity was assessed based on species richness and Shannon effective diversity as explained in detail in Rhea. Only taxa with a prevalence of  $\geq 30\%$  (proportion of samples positive for the given taxa) in one given group, and relative abundance  $\geq 0.25\%$  were considered for statistical testing. Statistical differences in abundance and prevalence between two groups were determined by Wilcoxon Rank Sum test and Fisher's Exact test, respectively. Statistical differences in abundance and prevalence between  $\geq 3$  groups were determined by Kruskal-Wallis followed by Wilcoxon Rank Sum tests, and Fisher's Exact tests, respectively. *P*-values

were corrected for multiple comparisons by the Benjamini–Hochberg method. Analyses of over-time differences in abundance and prevalence (within groups) was assessed by Wilcoxon Signed Rank Sum test and Fisher’s test, respectively.

Statistical analyses were performed using the R programming environment, JMP Pro 15 (v15.2.1; SAS Institute Inc.; Cary, NC, USA) or GraphPad Prism 6 (v6.07; GraphPad Software Inc.; San Diego, CA, USA). All applied statistical methods are specified in figure legends. Prior to application of parametric statistics, normality and homogeneity of variance was tested on residuals by Shapiro–Wilk and Levene’s tests, respectively. Heatmaps were generated using the *heatmap.2* function from the *gplots* package<sup>80</sup> in R. Figures were created using GraphPad Prism 6 and Inkscape (v0.92.4; <http://www.inkscape.org/>).

## Acknowledgments

We are grateful to Sérgio Domingos Cardoso Da Rocha and Lars Fredrik Moen (NMBU) for assistance in conduction of the experiments; Sophie Campbell and Lucy Robertson (NMBU) for parasitological examinations and manuscript review; Soheir Chahine al Taoyl (NMBU) for preparation of histological sections; the Microbiome Core Facility at the ZIEL Institute for Food & Health (Technical University of Munich) for high-throughput sequencing; the staff and animals at Ramme Gaard (Hvitsten, Norway) and The Livestock Production Research Center (NMBU) for donation of materials for the mouse pens; Peter Olaf Hofgaard (University of Oslo, Department of Immunology, Oslo University Hospital) for advice on animal dissection; Grethe Marie Johansen (NMBU), Anne Mari Herfindal (NMBU), Hege Lund (NMBU), Leticia Monin, Anett Jandke and Adrian Hayday (The Francis Crick Institute, and King’s College, London, UK) for technical assistance and valuable discussions; Grete Ramsli Hauge (NMBU) for pioneering the mouse pens usage and workflow. The graphical abstract and illustrations in [Figure 1a](#), [Figure 2a](#) and [Figure S3A](#) were created with BioRender.com (<https://biorender.com/>).

## Disclosure statement

No potential conflict of interest was reported by the author(s).

## Funding

This research was funded internally at NMBU and the collaborators.

## ORCID

Henriette Arnesen  <http://orcid.org/0000-0003-1173-4010>  
 Thomas C. A. Hitch  <http://orcid.org/0000-0003-2244-7412>  
 Thomas Clavel  <http://orcid.org/0000-0002-7229-5595>  
 Harald Carlsen  <http://orcid.org/0000-0001-5123-5756>  
 Preben Boysen  <http://orcid.org/0000-0002-0084-1251>

## Data deposition

Raw sequence files can be found in NCBI’s Sequence read archive (SRA) under the accession number PRJNA669440.

## Author contributions

PB, HC, JEP, and HA designed the study and experiments. HA, PB, HC, MHB, CS, and LEK conducted the experiments. HA, PB, CS, KR, ILA, IO, and GG performed the laboratory procedures. HA, TCAH, and PB analyzed the data and wrote the manuscript. TC, HC, and MHB reviewed and edited the manuscript. All authors contributed to the article and approved the submitted version.

## References

1. Belkaid Y, Harrison OJ. Homeostatic immunity and the microbiota. *Immunity*. 2017;46:562–576. doi:10.1016/j.immuni.2017.04.008.
2. Rook G, Backhed F, Levin BR, McFall-Ngai MJ, McLean AR. Evolution, human-microbe interactions, and life history plasticity. *Lancet*. 2017;390:521–530. doi:10.1016/S0140-6736(17)30566-4.
3. Hornef MW, Torow N. ‘Layered immunity’ and the ‘neonatal window of opportunity’ - timed succession of non-redundant phases to establish mucosal host-microbial homeostasis after birth. *Immunology*. 2020;159:15–25. doi:10.1111/imm.13149.
4. Moeller AH, Suzuki TA, Phifer-Rixey M, Nachman MW. Transmission modes of the mammalian gut microbiota. *Science*. 2018;362:453–457.
5. Roslund MI, Puhakka R, Grönroos M, Nurminen N, Oikarinen S, Gazali AM, Cinek O, Kramná L, Siter N, Vari HK, et al. Biodiversity intervention enhances immune regulation and health-associated commensal microbiota among daycare children. *Sci Adv*. 2020;6:eaba2578. doi:10.1126/sciadv.aba2578.
6. Haahtela T. A biodiversity hypothesis. *Allergy*. 2019;74:1445–1456.
7. von Mutius E. The microbial environment and its influence on asthma prevention in early life. *J Allergy Clin Immunol*. 2016;137:680–689. doi:10.1016/j.jaci.2015.12.1301.



8. Birzele LT, Depner M, Ege MJ, Engel M, Kublik S, Bernau C, Loss GJ, Genuneit J, Horak E, Schloter M, et al. Environmental and mucosal microbiota and their role in childhood asthma. *Allergy*. 2017;72:109–119. doi:10.1111/all.13002.
9. Tual S, Lemarchand C, Boulanger M, Dalphin J-C, Racht B, Marcotullio E, Velten M, Guizard A-V, Clin B, Baldi I, et al. Exposure to farm animals and risk of lung cancer in the AGRICAN cohort. *Am J Epidemiol*. 2017;186:463–472. doi:10.1093/aje/kwx125.
10. Soon IS, Molodecky NA, Rabi DM, Ghali WA, Barkema HW, Kaplan GG. The relationship between urban environment and the inflammatory bowel diseases: a systematic review and meta-analysis. *BMC Gastroenterol*. 2012;12:51. doi:10.1186/1471-230X-12-51.
11. Mills JG, Brookes JD, Gellie NJC, Liddicoat C, Lowe AJ, Sydnor HR, Thomas T, Weinstein P, Weyrich LS, Breed MF, et al. Relating urban biodiversity to human health with the ‘Holobiont’ concept. *Front Microbiol*. 2019;10. doi:10.3389/fmicb.2019.00550
12. Jasperson KW, Tuohy TM, Neklason DW, Burt RW. Hereditary and familial colon cancer. *Gastroenterology*. 2010;138:2044–2058. doi:10.1053/j.gastro.2010.01.054.
13. Jess T, Rungoe C, Peyrin-Biroulet L. Risk of colorectal cancer in patients with ulcerative colitis: a meta-analysis of population-based cohort studies. *Clin Gastroenterol Hepatol*. 2012;10:639–645. doi:10.1016/j.cgh.2012.01.010.
14. Dekker E, Tanis PJ, Vleugels JLA, Kasi PM, Wallace MB. Colorectal cancer. *Lancet*. 2019;394:1467–1480. doi:10.1016/S0140-6736(19)32319-0.
15. World Health Organization (WHO). International Agency for Research on Cancer. *Globocan 2020: Cancer Fact Sheets — Colorectal Cancer*.
16. Tilg H, Adolph TE, Gerner RR, Moschen AR. The intestinal microbiota in colorectal cancer. *Cancer Cell*. 2018;33:954–964. doi:10.1016/j.ccell.2018.03.004.
17. Wong SH, Yu J. Gut microbiota in colorectal cancer: mechanisms of action and clinical applications. *Nat Rev Gastroenterol Hepatol*. 2019;16:690–704.
18. Rosenberg DW, Giardina C, Tanaka T. Mouse models for the study of colon carcinogenesis. *Carcinogenesis*. 2009;30:183–196. doi:10.1093/carcin/bgn267.
19. Sodring M, Gunnes G, Paulsen JE. Spontaneous initiation, promotion and progression of colorectal cancer in the novel A/J Min/+ mouse. *Int J Cancer*. 2016;138:1936–1946. doi:10.1002/ijc.29928.
20. Brugiroux S, Beutler M, Pfann C, Garzetti D, Ruscheweyh H-J, Ring D, Diehl M, Herp S, Lötscher Y, Hussain S, et al. Genome-guided design of a defined mouse microbiota that confers colonization resistance against *Salmonella enterica* serovar Typhimurium. *Nat Microbiol*. 2016;2:16215. doi:10.1038/nmicrobiol.2016.215.
21. Masopust D, Sivula CP, Jameson SC. Of mice, dirty mice, and men: using mice to understand human immunology. *J Immunol*. 2017;199:383–388. doi:10.4049/jimmunol.1700453.
22. Ericsson AC, Montonye DR, Smith CR, Franklin CL. Modeling a superorganism - Considerations regarding the use of “dirty” mice in biomedical research. *Yale J Biol Med*. 2017;90:361–371.
23. Roy U, Galvez EJC, Iljazovic A, Lesker TR, Blazejewski AJ, Pils MC, Heise U, Huber S, Flavell RA, Strowig T, et al. Distinct microbial communities trigger colitis development upon intestinal barrier damage via innate or adaptive immune cells. *Cell Rep*. 2017;21:994–1008. doi:10.1016/j.celrep.2017.09.097.
24. Rausch P, Basic M, Batra A, Bischoff SC, Blaut M, Clavel T, Gläsner J, Gopalakrishnan S, Grassl GA, Günther C, et al. Analysis of factors contributing to variation in the C57BL/6J fecal microbiota across German animal facilities. *Int J Med Microbiol*. 2016;306:343–355. doi:10.1016/j.ijmm.2016.03.004.
25. Seok J, Warren HS, Cuenca AG, Mindrinos MN, Baker HV, Xu W, Richards DR, McDonald-Smith GP, Gao H, Hennessy L, et al. Genomic responses in mouse models poorly mimic human inflammatory diseases. *Proc Natl Acad Sci U S A*. 2013;110:3507–3512.
26. Beura LK, Hamilton SE, Bi K, Schenkel JM, Odumade OA, Casey KA, Thompson EA, Fraser KA, Rosato PC, Filali-Mouhim A, et al. Normalizing the environment recapitulates adult human immune traits in laboratory mice. *Nature*. 2016;532:512–516. doi:10.1038/nature17655.
27. Reese TA, Bi K, Kambal A, Filali-Mouhim A, Beura LK, Burger MC, Pulendran B, Sekaly R-P, Jameson S, Masopust D, et al. Sequential infection with common pathogens promotes human-like immune gene expression and altered vaccine response. *Cell Host Microbe*. 2016;19:713–719. doi:10.1016/j.chom.2016.04.003.
28. Abolins S, King EC, Lazarou L, Weldon L, Hughes L, Drescher P, Raynes JG, Hafalla JCR, Viney ME, Riley EM, et al. The comparative immunology of wild and laboratory mice, *Mus musculus domesticus*. *Nat Commun*. 2017;8:14811. doi:10.1038/ncomms14811.
29. Rosshart SP, Vassallo BG, Angeletti D, Hutchinson DS, Morgan AP, Takeda K, Hickman HD, McCulloch JA, Badger JH, Ajami NJ, et al. Wild mouse gut microbiota promotes host fitness and improves disease resistance. *Cell*. 2017;171:1015–28.e13. doi:10.1016/j.cell.2017.09.016.
30. Rosshart SP, Herz J, Vassallo BG, Hunter A, Wall MK, Badger JH, McCulloch JA, Anastasakis DG, Sarshad AA, Leonardi I, et al. Laboratory mice born to wild mice have natural microbiota and model human immune responses. *Science*. 2019;365. doi:10.1126/science.aaw4361

31. Graham AL. Naturalizing mouse models for immunology. *Nat Immunol.* 2021;22:111–117. doi:10.1038/s41590-020-00857-2.
32. Huggins MA, Sjaastad FV, Pierson M, Kucaba TA, Swanson W, Staley C, Weingarden AR, Jensen IJ, Danahy DB, Badovinac VP, et al. Microbial exposure enhances immunity to pathogens recognized by TLR2 but increases susceptibility to cytokine storm through TLR4 sensitization. *Cell Rep.* 2019;28:1729–43.e5. doi:10.1016/j.celrep.2019.07.028.
33. Yeung F, Chen Y-H, Lin J-D, Leung JM, McCauley C, Devlin JC, Hansen C, Cronkite A, Stephens Z, Drake-Dunn C, et al. Altered immunity of laboratory mice in the natural environment is associated with fungal colonization. *Cell Host Microbe.* 2020;27:809–22.e6. doi:10.1016/j.chom.2020.02.015.
34. Arnesen H, Knutsen LE, Hognestad BW, Johansen GM, Bemark M, Pabst O, Storset AK, Boysen P. A model system for feralizing laboratory mice in large farmyard-like pens. *Front Microbiol.* 2021;11. doi:10.3389/fmicb.2020.615661.
35. Ju J, Nolan B, Cheh M, Bose M, Lin Y, Wagner GC, Yang CS. Voluntary exercise inhibits intestinal tumorigenesis in *Apc Min/+* mice and azoxymethane/dextran sulfate sodium-treated mice. *BMC Cancer.* 2008;8:316. doi:10.1186/1471-2407-8-316.
36. McClellan JL, Steiner JL, Day SD, Enos RT, Davis MJ, Singh UP, Murphy EA. Exercise effects on polyp burden and immune markers in the *ApcMin/+* mouse model of intestinal tumorigenesis. *Int J Oncol.* 2014;45:861–868. doi:10.3892/ijo.2014.2457.
37. Eichele DD, Kharbada KK. Dextran sodium sulfate colitis murine model: an indispensable tool for advancing our understanding of inflammatory bowel diseases pathogenesis. *World J Gastroenterol.* 2017;23:6016–6029. doi:10.3748/wjg.v23.i33.6016.
38. Nagalingam NA, Kao JY, Young VB. Microbial ecology of the murine gut associated with the development of dextran sodium sulfate-induced colitis. *Inflamm Bowel Dis.* 2011;17:917–926.
39. Luu M, Visekruna A. Short-chain fatty acids: bacterial messengers modulating the immunometabolism of T cells. *Eur J Immunol.* 2019;49:842–848. doi:10.1002/eji.201848009.
40. Parada Venegas D, De la Fuente MK, Landskron G, González MJ, Quera R, Dijkstra G, Harmsen HJM, Faber KN, Hermoso MA. Short chain fatty acids (SCFAs)-mediated gut epithelial and immune regulation and its relevance for inflammatory bowel diseases. *Front Immunol.* 2019;10:277. doi:10.3389/fimmu.2019.00277.
41. den Besten G, Van Eunen K, Groen AK, Venema K, Reijngoud D-J, Bakker BM. The role of short-chain fatty acids in the interplay between diet, gut microbiota, and host energy metabolism. *J Lipid Res.* 2013;54:2325–2340. doi:10.1194/jlr.R036012.
42. Lagkouvardos I, Pukall R, Abt B, Foessel BU, Meier-Kolthoff JP, Kumar N, Bresciani A, Martínez I, Just S, Ziegler C, et al. The mouse intestinal bacterial collection (miBC) provides host-specific insight into cultured diversity and functional potential of the gut microbiota. *Nat Microbiol.* 2016;1:16131. doi:10.1038/nmicrobiol.2016.131.
43. Haas KN, Blanchard JL. *Kineothrix alysoides*, gen. nov., sp. nov., a saccharolytic butyrate-producer within the family Lachnospiraceae. *Int J Syst Evol Microbiol.* 2017;67:402–410. doi:10.1099/ijsem.0.01643.
44. Sakaguchi S, Yamaguchi T, Nomura T, Ono M. Regulatory T cells and immune tolerance. *Cell.* 2008;133:775–787. doi:10.1016/j.cell.2008.05.009.
45. Togashi Y, Shitara K, Nishikawa H. Regulatory T cells in cancer immunosuppression — implications for anticancer therapy. *Nat Rev Clin Oncol.* 2019;16:356–371. doi:10.1038/s41571-019-0175-7.
46. Chiossone L, Chaix J, Fuseri N, Roth C, Vivier E, Walzer T. Maturation of mouse NK cells is a 4-stage developmental program. *Blood.* 2009;113:5488–5496. doi:10.1182/blood-2008-10-187179.
47. Zhu W, Miyata N, Winter MG, Arenales A, Hughes ER, Spiga L, Kim J, Sifuentes-Dominguez L, Starokadomskyy P, Gopal P, et al. Editing of the gut microbiota reduces carcinogenesis in mouse models of colitis-associated colorectal cancer. *J Exp Med.* 2019;216:2378–2393. doi:10.1084/jem.20181939.
48. Zackular JP, Baxter NT, Chen GY, Schloss PD, Tringe SG. Manipulation of the gut microbiota reveals role in colon tumorigenesis. *mSphere.* 2016;1:e00001–15. doi:10.1128/mSphere.00001-15.
49. Zackular JP, Baxter NT, Iverson KD, Sadler WD, Petrosino JF, Chen GY, Schloss PD. The gut microbiome modulates colon tumorigenesis. *MBio.* 2013;4:e00692–13. doi:10.1128/mBio.00692-13.
50. Kaur K, Saxena A, Debnath I, O'Brien JL, Ajami NJ, Auchtung TA, Petrosino JF, Sougiannis A-J, Depaep S, Chumanevich A, et al. Antibiotic-mediated bacteriome depletion in *Apc(Min/+)* mice is associated with reduction in mucus-producing goblet cells and increased colorectal cancer progression. *Cancer Med.* 2018;7:2003–2012. doi:10.1002/cam4.1460.
51. Li L, Li X, Zhong W, Yang M, Xu M, Sun Y, Ma J, Liu T, Song X, Dong W, et al. Gut microbiota from colorectal cancer patients enhances the progression of intestinal adenoma in *Apc min/+* mice. *EBioMedicine.* 2019;48:301–315. doi:10.1016/j.ebiom.2019.09.021.
52. Ottman N, Ruokolainen L, Suomalainen A, Sinkko H, Karisola P, Lehtimäki J, Lehto M, Hanski I, Alenius H, Fyhrquist N, et al. Soil exposure modifies the gut microbiota and supports immune tolerance in a mouse model. *J Allergy Clin Immunol.* 2019;143:1198–206.e12. doi:10.1016/j.jaci.2018.06.024.

53. Asadollahi P, Ghanavati R, Rohani M, Razavi S, Esghaei M, Talebi M. Anti-cancer effects of *Bifidobacterium* species in colon cancer cells and a mouse model of carcinogenesis. *PLoS One*. 2020;15:e0232930. doi:10.1371/journal.pone.0232930.
54. Baxter NT, Zackular JP, Chen GY, Schloss PD. Structure of the gut microbiome following colonization with human feces determines colonic tumor burden. *Microbiome*. 2014;2:20. doi:10.1186/2049-2618-2-20.
55. Fassarella M, Blaak EE, Penders J, Nauta A, Smidt H, Zoetendal EG. 2020. Gut microbiome stability and resilience: elucidating the response to perturbations in order to modulate gut health. *Gut*. 2021; 70:595-605. doi:10.1136/gutjnl-2020-321747
56. Corrêa-Oliveira R, Fachi JL, Vieira A, Sato FT, Vinolo MAR. Regulation of immune cell function by short-chain fatty acids. *Clin Transl Immunol*. 2016;5:e73-e. doi:10.1038/cti.2016.17.
57. Belcheva A, Irrazabal T, Robertson Susan J, Streutker C, Maughan H, Rubino S, Moriyama E, Copeland J, Surendra A, Kumar S, et al. Gut microbial metabolism drives transformation of *Msh2*-deficient colon epithelial cells. *Cell*. 2014;158:288-299. doi:10.1016/j.cell.2014.04.051.
58. Tian Y, Xu Q, Sun L, Ye Y, Ji G. Short-chain fatty acids administration is protective in colitis-associated colorectal cancer development. *J Nutr Biochem*. 2018;57:103-109. doi:10.1016/j.jnutbio.2018.03.007.
59. Kim M, Friesen L, Park J, Kim HM, Kim CH. Microbial metabolites, short-chain fatty acids, restrain tissue bacterial load, chronic inflammation, and associated cancer in the colon of mice. *Eur J Immunol*. 2018;48:1235-1247. doi:10.1002/eji.201747122.
60. Castro F, Cardoso AP, Gonçalves RM, Serre K, Oliveira MJ. Interferon-Gamma at the crossroads of tumor immune surveillance or evasion. *Front Immunol*. 2018;9:847.
61. Steppeler C, Sødring M, Paulsen JE. Colorectal carcinogenesis in the A/J Min/+ mouse model is inhibited by hemin, independently of dietary fat content and fecal lipid peroxidation rate. *BMC Cancer*. 2016;16:832. doi:10.1186/s12885-016-2874-0.
62. Johanson SM, Swann JR, Umu ÖCO, Aleksandersen M, Müller MHB, Berntsen HF, Zimmer KE, Østby GC, Paulsen JE, Ropstad E, et al. Maternal exposure to a human relevant mixture of persistent organic pollutants reduces colorectal carcinogenesis in A/J Min/+ mice. *Chemosphere*. 2020;252:126484. doi:10.1016/j.chemosphere.2020.126484.
63. Arnesen H, Müller MHB, Aleksandersen M, Østby GC, Carlsen H, Paulsen JE, Boysen P. Induction of colorectal carcinogenesis in the C57BL/6J and A/J mouse strains with a reduced DSS dose in the AOM/DSS model. *Lab Anim Res*. 2021;37:19. doi:10.1186/s42826-021-00096-y.
64. Angell IL, Hanssen JF, Rudi K. Prokaryote species richness is positively correlated with eukaryote abundance in wastewater treatment biofilms. *Lett Appl Microbiol*. 2017;65:66-72. doi:10.1111/lam.12746.
65. Reitmeier S, Kiessling S, Clavel T, List M, Almeida EL, Ghosh TS, Neuhaus K, Grallert H, Linseisen J, Skurk T, et al. Arrhythmic gut microbiome signatures predict risk of Type 2 diabetes. *Cell Host Microbe*. 2020;28:258-72.
66. Lagkouvardos I, Klaring K, Heinzmann SS, Platz S, Scholz B, Engel KH, Schmitt-Kopplin P, Haller D, Rohn S, Skurk T, et al. Gut metabolites and bacterial community networks during a pilot intervention study with flaxseeds in healthy adult men. *Mol Nutr Food Res*. 2015;59:1614-1628. doi:10.1002/mnfr.201500125.
67. Lagkouvardos I, Joseph D, Kapfhammer M, Giritli S, Horn M, Haller D, Clavel T. IMNGS: a comprehensive open resource of processed 16S rRNA microbial profiles for ecology and diversity studies. *Sci Rep*. 2016;6:33721. doi:10.1038/srep33721.
68. Edgar RC. UPARSE: highly accurate OTU sequences from microbial amplicon reads. *Nat Methods*. 2013;10:996-998. doi:10.1038/nmeth.2604.
69. Edgar RC. Search and clustering orders of magnitude faster than BLAST. *Bioinformatics*. 2010;26:2460-2461. doi:10.1093/bioinformatics/btq461.
70. Edgar RC, Haas BJ, Clemente JC, Quince C, Knight R. UCHIME improves sensitivity and speed of chimera detection. *Bioinformatics*. 2011;27:2194-2200. doi:10.1093/bioinformatics/btr381.
71. Reitmeier S, Hitch TCA, Fikas N, Hausmann B, Ramer-Tait AE, Neuhaus K, Berry D, Haller D, Lagkouvardos I, Clavel T. Handling of spurious sequences affects the outcome of high-throughput 16S rRNA gene amplicon profiling. *ISME COMM*. 2021;1:31. doi:10.1038/s43705-021-00033-z
72. Wang Q, Garrity GM, Tiedje JM, Cole JR. Naive Bayesian classifier for rapid assignment of rRNA sequences into the new bacterial taxonomy. *Appl Environ Microbiol*. 2007;73:5261-5267. doi:10.1128/AEM.00062-07.
73. Edgar RC. MUSCLE: multiple sequence alignment with high accuracy and high throughput. *Nucleic Acids Res*. 2004;32:1792-1797. doi:10.1093/nar/gkh340.
74. Price MN, Dehal PS, Arkin AP. FastTree 2—approximately maximum-likelihood trees for large alignments. *PLoS One*. 2010;5:e9490. doi:10.1371/journal.pone.0009490.
75. Yoon SH, Ha SM, Kwon S, Lim J, Kim Y, Seo H, Chun J. Introducing EzBioCloud: a taxonomically united database of 16S rRNA gene sequences and whole-genome assemblies. *Int J Syst Evol Microbiol*. 2017;67:1613-1617. doi:10.1099/ijsem.0.001755.
76. Andreassen M, Rudi K, Angell IL, Dirven H, Nygaard UC. Allergen immunization induces major changes in microbiota composition and short-chain

- fatty acid production in different gut segments in a mouse model of lupine food allergy. *Int Arch Allergy Immunol.* **2018**;177:311–323. doi:[10.1159/000492006](https://doi.org/10.1159/000492006).
77. R Core Team. R: a language and environment for statistical computing. Vienna (Austria): R Foundation for Statistical Computing; **2020**.
78. Lagkouvardos I, Fischer S, Kumar N, Clavel T. Rhea: a transparent and modular R pipeline for microbial profiling based on 16S rRNA gene amplicons. *PeerJ.* **2017**;5:e2836. doi:[10.7717/peerj.2836](https://doi.org/10.7717/peerj.2836).
79. Chen J, Bittinger K, Charlson ES, Hoffmann C, Lewis J, Wu GD, Collman RG, Bushman FD, Li H. Associating microbiome composition with environmental covariates using generalized UniFrac distances. *Bioinformatics.* **2012**;28:2106–2113. doi:[10.1093/bioinformatics/bts342](https://doi.org/10.1093/bioinformatics/bts342).
80. Warnes GR, Bolker B, Bonebakker L, Gentleman R, Huber W, Liaw A, Lumley T, Maechler M, Magnusson A, Moeller S, et al. gplots: various R programming tools for plotting data. R package version 3.0.3; **2020**.

# Paper IV

IV



1 ***Profiling of colonic mucosal tissue transcriptome and mucus layer properties in***  
2 ***mice feralized in a farmyard-like habitat***

3 Henriette Arnesen<sup>1,2</sup>, Turhan Markussen<sup>1</sup>, George Birchenough<sup>3</sup>, Gunnar C. Hansson<sup>3</sup>,  
4 Harald Carlsen<sup>2</sup> and Preben Boysen<sup>1\*</sup>

5 <sup>1</sup>Faculty of Veterinary Medicine, Norwegian University of Life Sciences (NMBU), Ås, Norway

6 <sup>2</sup>Faculty of Chemistry, Biotechnology and Food Science, Norwegian University of Life Sciences (NMBU),  
7 Ås, Norway

8 <sup>3</sup>Mucin Biology Group, Department of Medical Biochemistry & Cell Biology, University of Gothenburg,  
9 Sweden

10 \*Correspondence: [preben.boysen@nmbu.no](mailto:preben.boysen@nmbu.no)

11

12 **ABSTRACT**

13 To close the gap between the preclinical mouse model and human lifestyles, we have  
14 established a system where laboratory mice are raised under a full set of environmental  
15 conditions present in a naturalistic, farmyard-type habitat – a process we have called  
16 feralization. In previous studies we have shown that feralized (Fer) mice were protected  
17 against colorectal cancer when compared to conventionally reared laboratory mice (Lab).  
18 However, the protective mechanisms remain to be elucidated, and in the herein study we  
19 assessed colonic mucosal barrier function in healthy mice. We found similar mucus layer  
20 properties between Fer and Lab mice when measured as mucus penetrability. However,  
21 increased mRNA levels of the known mucus components Fcgbp and Clca1 still suggested  
22 that the mucus could be enforced. Other proteins like Itln1 is known to be involved in  
23 bacterial defense mechanisms, and upregulation of the Itln1-encoding gene further  
24 suggests that the Fer mice may have an enhanced bacterial defense. Future studies  
25 should address other areas of the intestine and employ targeted approaches to evaluate  
26 gene expression of specific cell populations.

27

## 28 INTRODUCTION

29 Throughout evolutionary history, mammals have co-evolved with the billions of microbes  
30 surrounding them and colonizing their bodies. The host and their microbiota have  
31 developed a symbiotic relationship fundamental for host fitness, emphasized by the major  
32 impact the microbiota have on host metabolism and development of organ systems,  
33 including the immune system (1-3). Yet, laboratory mice used to model human responses  
34 are usually studied under strictly hygienic conditions, deprived of the natural stimuli a  
35 microbially rich environment provides. The dogma for laboratory mouse studies have long  
36 been to create a highly standardized environment with emphasis on microbial control and  
37 strict surveillance of pathogen status. This has several advantages, but also creates a  
38 risk that laboratory mice are removed from their natural conditions, and also deviate from  
39 the organism they are aimed to model, humans, that rarely live under microbial isolation.  
40 Lately, an increased focus has been turned towards generating more naturalistic mice  
41 that can recapitulate realistic traits, aiming to improve the translatability from mouse  
42 models to human relevance (4). We have established a model system where laboratory  
43 mice are feralized in a farmyard-like habitat, producing a real-life adapted mammal (5). In  
44 our feralization system, we study the laboratory mice in a holistic fashion, where the mice  
45 are housed under a full set of natural environmental factors, also enabling species-  
46 specific behavior.

47 In two different mouse models of colorectal cancer (CRC), we have shown that the mice  
48 feralized in a farmyard-like habitat were protected against colorectal carcinogenesis when  
49 compared to conventionally housed lab mice (6). The intestinal barrier is the first line of  
50 defense and is thus interesting with respect to colorectal carcinogenesis. The intestinal  
51 barrier encompasses the mucus layer, a single layer of epithelium tied together by various  
52 junctions to prevent paracellular passage of luminal content. Specialized cells such as  
53 mucus-producing Goblet cells, and antimicrobial peptides-producing Paneth cells are  
54 also important components of the intestinal barrier. The organization of the mucus layer  
55 varies along the length of the intestine. The small intestine is lined with a single loosely  
56 organized layer allowing for movement of the loose mucus with bound bacteria to the  
57 colon, while the colon is lined by an inner, dense layer and an outer loose layer (7). The



58 mucus layer is continuously renewing and is crucial to hinder luminal contents coming in  
59 contact with the epithelial wall and underlying tissue as well as prevent bacterial  
60 overgrowth. The gut microbiota composition has been shown to shape the mucus layer  
61 in mouse colons (8), and wild-caught feral mice have been shown to have a thicker and  
62 less penetrable mucus layer than conventional laboratory mice (9). That fecal transfer of  
63 wild mouse microbiota has been shown to ameliorate CRC in lab mice (10), could point  
64 towards an enhanced mucosal barrier conveying CRC protective effects.

65 With the current study we aimed to address how feralization in a farmyard-like habitat  
66 influenced colonic mucosa in healthy wild-type mice by assessing the intestinal mucus  
67 layer properties and mucosal gene expression. To evaluate if potential effects of  
68 feralization on the mucosal barrier could be enlightened by differences in gut microbiota,  
69 we also characterized the cecal microbiota.

70

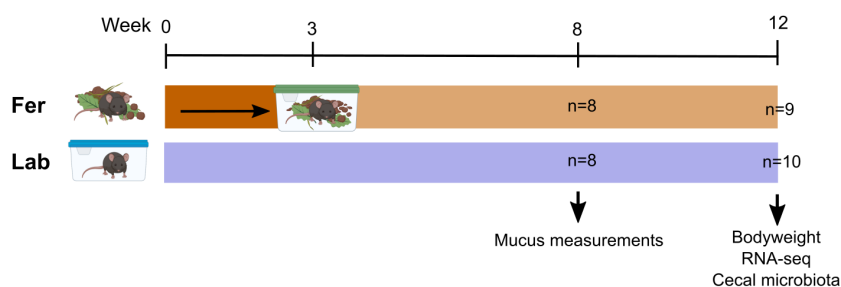
## 71 MATERIALS AND METHODS

### 72 **Animals and housing conditions**

73 A microbially enriched, semi-naturalistic model was designed at the Norwegian  
74 University of Life Sciences (NMBU) as previously described (6). Briefly, to resemble the  
75 common habitat of the house mouse (*Mus musculus*), indoor pens were enriched with  
76 livestock bedding, ecological soil, straw and fecal content from ecologically farmed pigs,  
77 cows, horses and poultry.

78 Animal experiment were approved by the Norwegian Animal Research Authority. 30  
79 female C57BL/6JRj (Janvier Labs, Saint-Berthevin Cedex, France) mice aged 3 weeks  
80 were feralized for 7 weeks prior to breeding. Females were mated with males from the  
81 same batch 2:1 in individually ventilated cages (IVCs; Inovive Inc., San Diego, CA, USA)  
82 enriched with the same material as pens. After a 10-day breeding period, the females  
83 returned to the pens to deliver. As controls, 24 female mice from the same batch were  
84 housed and mated under pathogen-free conditions in IVC. Both feralized and laboratory  
85 mice were housed under standard conditions (12 h light/dark cycle, 23-25 °C, 45-50 %

86 relative humidity). Water and standard chow diet (RM1(E), SDS; Special Diet Services,  
 87 Essex, United Kingdom) was provided *ad libitum*. At 3 weeks of age, male offsprings  
 88 were weaned and then housed under the same conventional laboratory conditions  
 89 (Lab), or in cages enriched with environmental material from the mouse pens (feralized;  
 90 Fer) (**Figure 1A**). These male Lab and Fer mice were sacrificed at 8 weeks of age for  
 91 mucus measurements, or 12 weeks of age for RNA sequencing and cecal microbiota  
 92 profiling.



93

94 **Figure 1:** Experimental setup. Fer, feralized; Lab, laboratory.

95

### 96 **Mucus growth rate, thickness and penetrability**

97 Mucus growth rate was measured using needle over time in *ex vivo* perfusion system as  
 98 previously described (11). Mucus growth rate (representing secretion and proteolytic  
 99 expansion) was expressed as  $\mu\text{m}$  mucus growth/minute. Mucus thickness and  
 100 penetrability to fluorescent microbeads was assessed according to previously described  
 101 procedures (12). Briefly, the tissue was stained, and microbeads were allowed to  
 102 sediment onto the mucus for 5 minutes before the surface was gently washed to remove  
 103 excess microbeads. The tissue and microbeads were visualized with confocal  
 104 microscopy. Mucus penetrability was quantified by analyzing the distribution of  
 105 microbeads within the mucus layer and generate area under the curve for normalized  
 106 distribution curves. Baseline (pre-treatment; n=8) growth rate was established for all  
 107 samples before 50 % (n=4) were then treated with EDTA (metalloprotease inhibitor) and

108 50 % (n=4) with complete protease inhibitor cocktail (serine+cysteine protease inhibitor  
109 mixture). The inhibitor treatment was conducted to assess potential differences between  
110 the groups in involvement of endogenous proteases in controlling mucus expansion (13).

111 Colon and ileum mucus barrier properties were measured by assessing penetration of  
112 bacteria-sized beads via confocal microscopy according to previously established  
113 methodology (14). Barrier function were expressed as normalized penetrability (bead  
114 distribution within mucus) and mucus thickness (average tissue-bead distance). For  
115 ileum, mucus thickness was measured in relation to villus tips.

116

### 117 **Isolation of total RNA**

118 Upon collection, colons were flushed with ice-cold PBS and submerged in RNeasy<sup>TM</sup>  
119 stabilization solution (Qiagen<sup>TM</sup>) for 24 hours in room temperature before they were  
120 stored at -80 °C. For RNA extraction, colons in RNeasy<sup>TM</sup> were thawed on ice and cut  
121 open longitudinally. Colons were divided into three equally sized segments, of which the  
122 colonic mucosa of the distal segment was scraped using a microscope glass slide. The  
123 mucosal scrapings were transferred to Eppendorf tubes and kept on RNeasy<sup>TM</sup> at room  
124 temperature until RNA isolation. Total RNA was isolated from the colonic scrapings using  
125 the RNeasy<sup>TM</sup> RNA/Protein kit (Qiagen), following the manufacturer's  
126 instructions. Quantity and integrity of the isolated RNA was assessed by Nanodrop<sup>TM</sup>  
127 2000c (Thermo Scientific) and Agilent 2100 BioAnalyzer (Agilent Technologies).

128

### 129 **RNA-Seq and data processing**

130 The nineteen samples of total RNA subjected to RNA-Sequencing (RNA-Seq) had  
131 260/230 ratios ranging from 1.20 to 2.14. Moreover, electropherograms and gels  
132 produced by Bioanalyzer showed distinct peaks/bands corresponding to 18S and 28S  
133 ribosomal RNA (**Supplementary Figure S1**). Library preparation and sequencing were  
134 conducted by the Norwegian Sequencing Centre (NSC). Briefly, libraries were generated  
135 using the TruSeq Stranded mRNA Library Prep Kit (Illumina Inc.) according to

136 manufacturer's manual. Sequencing was performed on an Illumina NovaSeq 6000 SP  
137 system using a single end 100 bp run. The yielded number of reads per sample ranged  
138 from 39 092 586 to 87 826 915 (**Supplementary Table S1**).

139 The quality of the RNA-Seq data was assessed using FastQC (15) and MultiQC (16). The  
140 reads were adapter trimmed with Trim Galore (v. 0.6.5) and mapped to the mouse  
141 reference genome GRCm38.p6 using HISAT2 (v. 2.1.0) (17). The overall alignment rates  
142 were above 96 % for all samples (**Supplementary Table S1**). The BAM files generated  
143 by HISAT2 were then imported and visualized in SeqMonk v1.47.1<sup>1</sup>, specifying a minimal  
144 mapping quality of 20. The RNA-Seq quantitation pipeline implemented in SeqMonk was  
145 used to quantitate the read counts. Quantitation was conducted at the gene level by  
146 counting the merged transcripts over exons with 75-percentile normalization of all  
147 libraries. The final quantitated values were presented as log<sub>2</sub> transformed reads per  
148 million reads (RPM). Functional enrichment analysis was performed with g:Profiler  
149 (version e102\_eg49\_p15\_7a9b4d6) against a custom background list of expressed  
150 genes (at least one read detected in at least one sample), with Benjamini-Hochberg FDR  
151 correction applying significance threshold of 0.05 (18) (**Supplementary Tables S3-S4**).

152

### 153 **Microbial community analyses**

154 Caecums were snap frozen in liquid nitrogen immediately after collection and stored at -  
155 80°C until DNA extraction. DNA was extracted as previously described (19), including  
156 mechanical lysis by bead-beating. Amplicon libraries were prepared via a two-step PCR  
157 amplifying the V3-V4 regions, as described in detail previously (20). Amplicons were  
158 purified with the AMPure XP system (Beckmann) before sequencing. High-throughput  
159 amplicon sequencing was performed at the ZIEL Institute for Food & Health, Technical  
160 University of Munich, according to previously described procedures (19). Sequencing  
161 was carried out in a paired-end mode (PE300) using a MiSeq system (Illumina Inc.).

162 The analyzed 16S rRNA (V3-V4) amplicon dataset included 416,773 high-quality and  
163 chimera-checked sequences (7,956 to 45,498 per sample), which represented a total of

---

<sup>1</sup> Available from <https://www.bioinformatics.babraham.ac.uk/projects/seqmonk/>

164 183 OTUs. Raw reads were processed with the Integrated Microbial Next Generation  
165 Sequencing pipeline (21), based on the UPARSE approach (22). Briefly, sequences were  
166 demultiplexed, trimmed to the first base with a quality score >3, and assembled.  
167 Sequences with <300 and >600 nucleotides, as well as assembled sequences with  
168 expected error >3 were excluded from the analysis. Remaining reads were trimmed by  
169 10 nucleotides at forward and reverse end to prevent analysis of regions with distorted  
170 base composition. The presence of chimeras was tested with UCHIME (23). Operational  
171 taxonomic units (OTUs) were clustered at 97 % sequence similarity (USEARCH 11.0)  
172 (24), and only those with a relative abundance >0.25 % in at least one sample were kept.  
173 Non 16S sequences was removed by use of SortMeRNA (v4.2) (25) with SILVA release  
174 128<sup>2</sup> as reference. Sequence alignment and taxonomic classification at 80 % confidence  
175 level was conducted with SINA 1.6.1 (26) using the taxonomy of SILVA release 128.  
176 Phylogenetic tree was generated with Fasttree (27). Specific OTUs were identified using  
177 EzBioCloud (28).

178

## 179 **Statistical analyses**

180 Differentially expressed genes (DEGs) were identified from raw read counts using  
181 DESeq2 corrected for multiple testing (29) in the R programming language (R version  
182 4.0.2) (30) implemented in SeqMonk. Other statistical analyses were conducted in  
183 GraphPad Prism (v.6.07; GraphPad Software Inc.; Software Inc.; San Diego, CA, USA)  
184 and the applied statistical methods are specified in figure legends.

185 Microbial profiles and composition were analyzed in the R programming environment  
186 using Rhea (81) (available from: <https://github.com/Lagkouvardos/Rhea>). OTU tables  
187 were normalized to account for differences in sequence depth by division to their sample  
188 size and then multiplication by the size of the smaller sample. Beta-diversity was  
189 computed based on generalized UniFrac distances (82), and the significance of  
190 separation between groups was tested by permutational multivariate analysis of variance  
191 (PERMANOVA). Alpha-diversity was assessed based on species richness and Shannon

---

<sup>2</sup> <https://www.arb-silva.de/documentation/release-128/>

192 effective diversity as explained in detail in Rhea. Only taxa with a prevalence of  $\geq 30\%$   
193 (proportion of samples positive for the given taxa) in one given group, and relative  
194 abundance  $\geq 0.25\%$  were considered for statistical testing. Statistical differences in  
195 abundance and prevalence between two groups were determined by Wilcoxon Rank Sum  
196 test and Fisher's Exact test, respectively. Statistical differences in abundance and  
197 prevalence between the groups were determined by Wilcoxon Rank Sum tests, and  
198 Fisher's Exact tests, respectively.

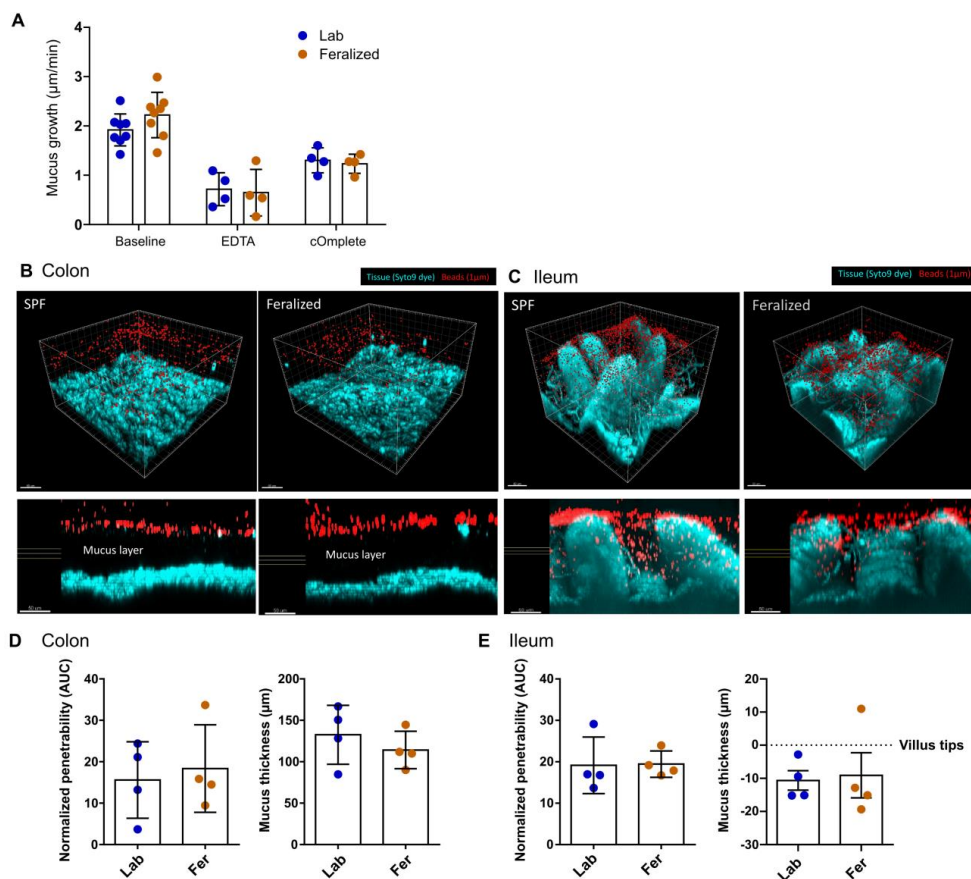
199 Statistical analyses were performed using the R programming environment or GraphPad  
200 Prism 6 (v6.07; GraphPad Software Inc.; San Diego, CA, USA). All applied statistical  
201 methods are specified in figure legends. Prior to application of parametric statistics,  
202 normality and homogeneity of variance was tested on residuals by Shapiro-Wilk and  
203 Levene's tests, respectively. Heatmap was created using the *heatmap.2* function from the  
204 *gplots* package<sup>81</sup> in R. Figures were created using GraphPad Prism 6 (v6.07; GraphPad  
205 Software Inc.; San Diego, CA, USA) and Inkscape (v0.92.4; <http://www.inkscape.org/>).

206

## 207 RESULTS

### 208 **Feralization did not significantly alter colonic nor ileal mucus layer properties**

209 Mice terminated after 8 weeks of feralization were subjected to assessment of intestinal  
210 mucus layer properties. We found no difference in baseline growth rate between Fer and  
211 Lab mice, and a significant decrease in growth in both groups in response to inhibitor  
212 treatment (**Figure 2A**). Barrier function expressed as normalized penetrability (bead  
213 distribution within mucus) and mucus thickness (average tissue-bead distance) were  
214 similar between the two groups in both colon and ileum (**Figure 2B-E**), suggesting that  
215 feralization in a farmyard-like habitat had no major influence on intestinal mucus layer  
216 properties. In ileum, segmented filamentous bacteria (SFB) could be seen as filaments  
217 between the villi (**Figure 2E**). These were present in both groups, although visual  
218 evaluation is suggestive of them being more abundant in the Fer group.



219

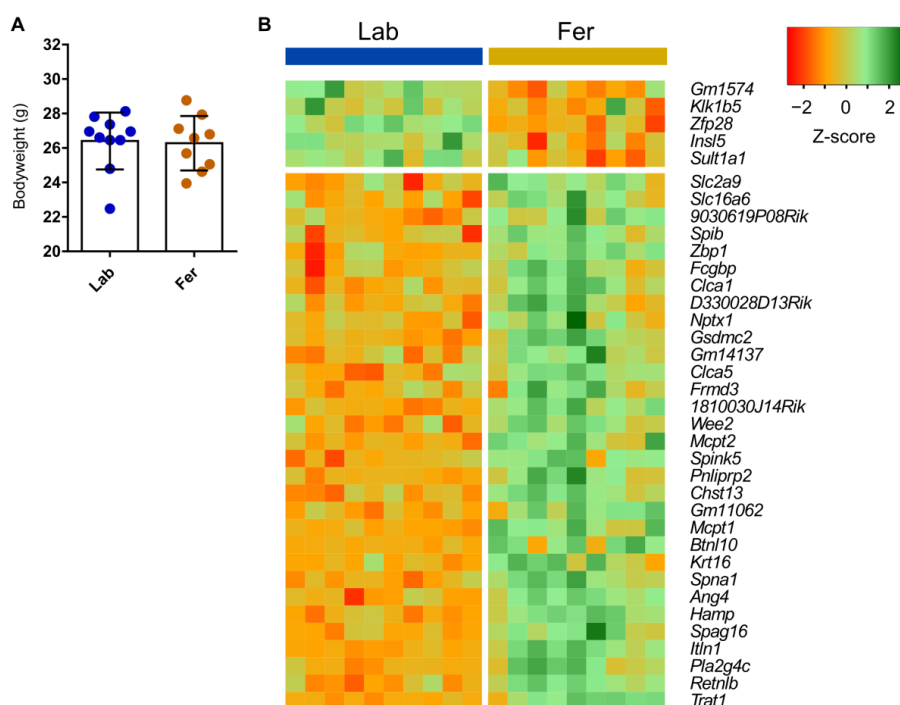
220 **Figure 2.** Assessment of intestinal barrier function in Fer and Lab mice by measurements of mucus layer  
 221 properties in colon and ileum. **(A)** Mucus thickness was measured using needle over time in an *ex vivo*  
 222 perfusion system. Mucus growth (representing secretion+ proteolytic expansion) was expressed as  $\mu\text{m}$   
 223 mucus growth/minute. **(B)** Thickness and penetrability of mucus layers in colon and ileum of Fer and Lab  
 224 mice. The mucus barrier properties were measured by assessing penetration of bacteria-sized beads via  
 225 confocal microscopy. Pictures show 3D overviews of confocal z-stacks (top) and cross-section view  
 226 (bottom) of colon (C), and ileum (D), with corresponding bar plots of results (E, F). Fer, feralized; Lab,  
 227 laboratory.

228

229 **Transcriptome profiling revealed few important genes differentially expressed in**  
 230 **colonic tissue of feralized and laboratory mice**

231 Mice feralized for 12 weeks exhibited no differences in bodyweight measurements  
 232 compared to Lab mice (**Figure 3A**). Mucosal scrapings from colon tissues collected from  
 233 Fer and Lab were subjected to RNA isolation and subsequent RNA-Seq. The RNA-Seq  
 234 identified 31 significantly upregulated and 5 significantly downregulated genes in Fer mice  
 235 compared to Lab mice (**Figure 3B; Supplementary figure S2**).

236



237

238 **Figure 3.** Bodyweight registration (**A**) and differentially expressed genes in the colonic mucosa of feralized  
 239 and lab mice (**B**) terminated at week 12. Heatmap showing significant ( $p < 0.05$ , FDR adjusted) differences  
 240 in gene expression between the two groups, displayed using log2 fold change values from DESeq2. The  
 241 log2 normalized counts are scaled to Z-score for each gene. Fer, feralized; Lab, laboratory. See also  
 242 Supplementary Figure S2.



243 To better explain the biological function of the differentially expressed genes (DEGs), we  
244 conducted a functional enrichment analysis. Functional enrichment analysis of the 31  
245 genes upregulated in Fer mice identified by DESeq2 were associated with GO terms such  
246 as: response to biotic stimulus (adj.  $P=0.007$ ), defense response to bacterium (adj.  
247  $P=0.017$ ), biological process involved in interspecies interaction between organisms (adj.  
248  $P=0.014$ ) and response to other organism (adj.  $P=0.007$ ) (**Supplementary Figure S3;**  
249 **Supplementary Table S2**). A similar GO analysis of the five genes upregulated in Lab  
250 mice associated with terms such as chemical carcinogenesis (adj.  $P=0.039$ ), estrogen  
251 metabolism (adj.  $P=0.011$ ) and retinol metabolism (adj.  $P=0.017$ ) (**Supplementary**  
252 **Figure S4; Supplementary Table S3**).

253 A few of the upregulated genes in the Fer mice (**Figure 3B**) are known goblet cell products  
254 involved in mucus layer organization and generation. These are the Fcgbp and Clca1  
255 proteins that are the major ones in colon mucus together with Muc2. The Intelectin1 (Itln1)  
256 is binding glycans and aggregate bacteria and is thus involved in bacterial defense.

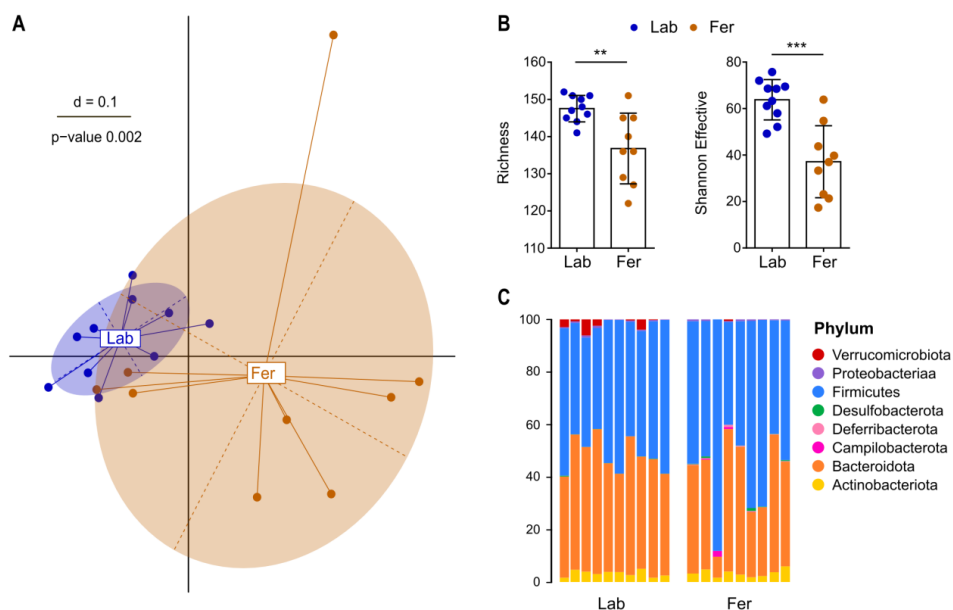
257

### 258 **Cecal microbiota profile of feralized mice differed significantly from laboratory** 259 **mice, while only minor compositional differences were discovered**

260 Laboratory tests for common mouse pathogens were negative in fecal samples from mice  
261 representative for the Fer as well as the Lab groups. Likewise, standard examination  
262 (McMasters and immunofluorescent antibody testing for Cryptosporidium and Giardia) of  
263 mouse feces for parasites were negative (6). Microbial community analysis was  
264 conducted on cecal samples from the mice terminated at week 12. *Beta*-diversity analysis  
265 identified significant clustering of the two groups, albeit the inter-individual variance in the  
266 Fer group was greater than the Lab group (**Figure 4A**). The richness and effective  
267 Shannon counts were significantly lower in the Fer group than the Lab group ( $P=0.004$   
268 and  $P<0.001$ , respectively) (**Figure 4B**)

269 No significant differences were detected at the phylum level (**Figure 4C**). However, the  
270 phylum Campilobacterota was only present in Fer mice (3/9). This phylum was  
271 represented by a single OTU showing the closest sequence similarity to *Helicobacter*

272 *equorum* (99.5 %). Moreover, Verrucomicrobiota was present in 6/10 Lab mice but only  
 273 1/9 Fer mice. This phylum was represented by a single OTU showing the closest  
 274 sequence similarity to *Akkermansia muciniphila* (99.5 %).



275

276 **Figure 4.** Cecal microbiota profiles and composition of Fer and Lab mice. **(A)** Multi-dimensional scaling  
 277 (MDS) plot of fecal microbiota profiles (generalized UniFrac distances) for Fer and Lab mice terminated at  
 278 week 12. Significance of separation was determined by PERMANOVA. **(B)** Observed number of OTUs  
 279 (Richness) and Shannon Effective counts for all groups. Plots show group mean (bars), SD (error bars) and  
 280 individual mice (dots). Significant differences between the groups were determined using unpaired t-test.  
 281 \*\* $P < 0.01$ ; \*\*\* $P < 0.001$ . **(C)** Taxonomic binning at the rank of phylum, presented as relative abundance for  
 282 each individual. Fer, feralized,  $n=9$ ; Lab, laboratory,  $n=10$ .

283

## 284 DISCUSSION

285 This study aimed to characterize the influence of feralization of research mice on intestinal  
 286 barrier function. We previously reported protective effects of feralization on colorectal  
 287 cancer development (6) and hypothesized this could be explained, at least in part, by

288 changes in the local barrier function prior to the induction of cancer-promoting agents.  
289 We have previously found that free-living feral mice have thick, impenetrable mucus  
290 layers (9). We hypothesized that the higher environmental microbial load invoked by  
291 feralization would strengthen the mucus layer similar to wild mice. However, in the current  
292 study, we observed no differences in mucus quality between Fer and Lab mice. Several  
293 notable differences remain between captured wild mice and Fer mice, such as unknown  
294 age, infectious history and ubiquitous presence of intestinal parasites, the latter which  
295 was not found in our feralized mice (6).

296 A higher presence of SFB was noted in the ileum of Fer mice by subjective confocal  
297 microscopical assessment. SFB are known as one of few non-pathogenic bacteria that  
298 penetrate the mucus layer. SFB adhere to intestinal epithelial cells and have been shown  
299 to activate non-inflammatory Th17 responses (31). Because of SFB adherence to  
300 intestinal epithelial cells, sequencing of the intimate microbiota must be conducted to  
301 detect them. This should be considered for future studies, to quantitatively determine if  
302 feralization leads to increased abundance or prevalence of SFB.

303 It is tempting to hypothesize that potential differences in the intestinal barriers of Fer and  
304 Lab mice could be associated with the microbial composition in the mouse gut. In our  
305 previous studies, feralization was accompanied by large shifts in fecal microbiota profiles,  
306 both when the mice were feralized in the presence (5) and absence (6) of wild-caught  
307 feral mice. In the current study, analysis of cecal microbiota profiles showed limited  
308 differences between Fer and Lab mice. However, direct comparisons between the current  
309 and previous studies should be avoided, as they differ both in the tissues sampled and  
310 gender of the mice. In the current study, male mice were assessed whereas females were  
311 used in our previous studies. Gender-bias has been described in mouse microbiota (32).  
312 However, an OTU with closest sequence similarity to *Helicobacter equorum* was only  
313 detected in our Fer mice. *Helicobacter spp.* is frequently detected in wild mice (33, 34),  
314 suggesting it is a natural component of a wild mouse microbiota. *Helicobacter spp.* has  
315 also been consistently detected in our previous feralization studies (5, 6). Albeit the  
316 sequencing was conducted on material from male mice and from a different intestinal  
317 region in the current study, it is an interesting note that *Helicobacter equorum* was

318 detected. This bacterial species is found in horses (35) and thus may derived from the  
319 horse fecal matter in the farmyard-type environment.

320 Although RNA-Seq of colonic mucosa revealed relatively few DEGs between the two  
321 groups, the functional enrichment analysis pointed in direction of immune responses and  
322 defense mechanisms for the genes significantly upregulated in Fer mice. A closer look at  
323 the genes upregulated in Fer revealed two out of three major colonic mucus proteins,  
324 Fcgbp and Clca1 (36, 37). These two proteins are reported to be present to similar levels  
325 as the Muc2 mucin. The functional role of the Fcgbp and Clca1 is poorly understood, but  
326 interestingly these proteins are not found in normal respiratory tract, but appear and  
327 become as high as in colon mucus upon the formation of an attached mucus layer (38).  
328 The Fcgbp (IgGFc-binding protein) does not bind immunoglobulins, but rather forms large  
329 polymers that are likely involved in mucus attachment (39, 40). The Clca1 (calcium-  
330 activated chloride channel regulator 1, previously named Clca3 in mouse) is an enzyme  
331 and likely a structural component in the formation of a mucus layer (41). We did not  
332 observe any differences in the mucus penetrability or growth of mucus, but this does not  
333 exclude that there are substantial differences in the Fer mucus. Such conclusions are  
334 also supported by the observation of less colon cancer development in the Fer mice as  
335 protection of the epithelium and suppression of inflammation is known to lower the risk  
336 for cancer. The mice subjected to RNA-Seq were feralized for a longer period than the  
337 mice subjected to mucus measurements, which may in part explain the discrepancies.

338 Another epithelial cell upregulated gene is Intelectin1 (*Itln1*), a protein that binds bacterial  
339 glycans and aggregates bacteria (42, 43). This is likely acting as another mucus protein,  
340 Zg16, that is also aggregating bacteria and by this moves bacteria in the mucus layer  
341 further away from the epithelium (44).

342 Expression of *Gsdmc2* encoding Gasdermin C, which is a known effector protein for  
343 pyroptosis, was also upregulated in Fer mice. Pyroptosis may play a role in antitumor  
344 immunity by facilitating the killing of tumor cells (45, 46). Gasdermin C has mostly been  
345 studied in the small intestine. In a recent article, *Gsdmc2* was identified as a target gene  
346 in small intestinal epithelial cells for the type 2 cytokines IL-4 and IL-13, and the authors  
347 suggested that the *Gsdmc* family of proteins could be important effectors for type 2

348 responses in the gut (47). *Zbp1* is another gene that was upregulated in Fer mice. This  
349 gene encodes Z-DNA-binding protein 1, identified as an innate sensor of viral infections  
350 that is induced by IFN with effects including regulation of cell death and inflammation (48).

351 However, the RNA-Seq was conducted on mucosal scrapings, something that could  
352 explain the low number of detected DEGs expressed in the epithelial cells and suggesting  
353 only minimal changes in the overall colonic mucosal gene expression following  
354 feralization. We did not determine gene expression in single cell populations and only few  
355 of the altered genes were from the epithelial cells (40). Further studies would be required  
356 in order to obtain more in-depth information on the differences between Fer and Lab mice,  
357 and this would also represent a natural continuation of the description of feralized mice.  
358 Future studies should include careful isolation of epithelium and lamina propria and, if  
359 possible, transcriptome sequencing of individual (single) cells to obtain more specific  
360 data. Finally, our transcriptome analyses covered only a limited part of the colon, and thus  
361 we recommend that other parts of the intestine are evaluated in future studies. Future  
362 studies should aim to include female mice, address other regions of the intestine, and  
363 employ targeted approaches to obtain transcriptomic data specific for various cell types.

364

## 365 ACKNOWLEDGEMENTS

366 The authors would like to thank Sergio Domingos Cardoso da Rocha, Lars Fredrik Moen  
367 and Grethe Marie Johansen at NMBU for valuable technical assistance; the staff and  
368 animals at Ramme Gaard and Centre for livestock production (SHF, NMBU) for donation  
369 of farm materials for the mouse pens; Torgeir R. Hvidsten for valuable advice related to  
370 sequencing data analyses; and the Microbiome Core Facility at the ZIEL Institute for Food  
371 & Health (Technical University of Munich) for conducting high-throughput sequencing.

372

## 373 FUNDING DETAILS

374 This work was funded internally at NMBU and the collaborators. The costs involved with  
375 RNA-Seq was supported by a grant from the Nansen Fund (Unifor, Norway).

376

## 377 DISCLOSURE OF INTEREST

378 The authors declare no conflict of interest regarding the publication of this article.

379

## 380 DATA AVAILABILITY STATEMENT

381 All data generated or analyzed during the current study are available from the  
382 corresponding author on reasonable request.

383

## 384 REFERENCES

- 385 1. Koren O, Ley RE. The human intestinal microbiota and microbiome. In: Podolsky DK, Camilleri M,  
386 Fitz JG, Kalloo AN, Shanahan F, Wang TC. *Yamada's Textbook of Gastroenterology*. 6th ed: John  
387 Wiley & Sons, Ltd.; 2016.
- 388 2. Foster KR, Schluter J, Coyte KZ, Rakoff-Nahoum S. The evolution of the host microbiome as an  
389 ecosystem on a leash. *Nature*. 2017;548(7665):43-51.
- 390 3. Rook G, Backhed F, Levin BR, McFall-Ngai MJ, McLean AR. Evolution, human-microbe  
391 interactions, and life history plasticity. *Lancet*. 2017;390(10093):521-30.
- 392 4. Graham AL. Naturalizing mouse models for immunology. *Nat Immunol*. 2021;22(2):111-7.
- 393 5. Arnesen H, Knutsen LE, Hognestad BW, Johansen GM, Bemark M, Pabst O, Storset AK, Boysen P.  
394 A Model System for Feralizing Laboratory Mice in Large Farmyard-Like Pens. *Front Microbiol*.  
395 2021;11(3413).
- 396 6. Arnesen H, Hitch TCA, Steppeler C, Müller MHB, Knutsen LE, Gunnes G, Angell IL, Ormaasen I,  
397 Rudi K, Paulsen JE, Clavel T, Carlsen H, Boysen P. Naturalizing laboratory mice by housing in a  
398 farmyard-type habitat confers protection against colorectal carcinogenesis. *Gut Microbes*.  
399 2021;13(1):1993581.
- 400 7. Johansson MEV, Sjövall H, Hansson GC. The gastrointestinal mucus system in health and disease.  
401 *Nat Rev Gastroenterol Hepatol*. 2013;10(6):352-61.
- 402 8. Johansson ME, Jakobsson HE, Holmén-Larsson J, Schütte A, Ermund A, Rodríguez-Piñeiro AM,  
403 Arike L, Wising C, Svensson F, Bäckhed F, Hansson GC. Normalization of Host Intestinal Mucus  
404 Layers Requires Long-Term Microbial Colonization. *Cell Host Microbe*. 2015;18(5):582-92.
- 405 9. Jakobsson HE, Rodríguez-Piñeiro AM, Schutte A, Ermund A, Boysen P, Bemark M, Sommer F,  
406 Backhed F, Hansson GC, Johansson ME. The composition of the gut microbiota shapes the colon  
407 mucus barrier. *EMBO Rep*. 2015;16(2):164-77.
- 408 10. Rosshart SP, Vassallo BG, Angeletti D, Hutchinson DS, Morgan AP, Takeda K, Hickman HD,  
409 McCulloch JA, Badger JH, Ajami NJ, Trinchieri G, Pardo-Manuel de Villena F, Yewdell JW,  
410 Rehmann B. Wild Mouse Gut Microbiota Promotes Host Fitness and Improves Disease  
411 Resistance. *Cell*. 2017;171(5):1015-28.e13.

- 412 11. Gustafsson JK, Ermund A, Johansson MEV, Schütte A, Hansson GC, Sjövall H. An ex vivo method  
413 for studying mucus formation, properties, and thickness in human colonic biopsies and mouse  
414 small and large intestinal explants. *Am J Physiol Gastrointest Liver Physiol*. 2012;302(4):G430-  
415 G8.
- 416 12. Volk JK, Nyström EEL, van der Post S, Abad BM, Schroeder BO, Johansson Å, Svensson F,  
417 Jäverfelt S, Johansson MEV, Hansson GC, Birchenough GMH. The Nlrp6 inflammasome is not  
418 required for baseline colonic inner mucus layer formation or function. *J Exp Med*.  
419 2019;216(11):2602-18.
- 420 13. Nyström EEL, Birchenough GMH, van der Post S, Arike L, Gruber AD, Hansson GC, Johansson  
421 MEV. Calcium-activated Chloride Channel Regulator 1 (CLCA1) Controls Mucus Expansion in  
422 Colon by Proteolytic Activity. *EBioMedicine*. 2018;33:134-43.
- 423 14. Volk JK, Nyström EEL, van der Post S, Abad BM, Schroeder BO, Johansson Å, Svensson F,  
424 Jäverfelt S, Johansson MEV, Hansson GC, Birchenough GMH. The Nlrp6 inflammasome is not  
425 required for baseline colonic inner mucus layer formation or function. *J Exp Med*.  
426 2019;216(11):2602-18.
- 427 15. Andrews S. FastQC: A Quality Control Tool for High Throughput Sequence Data [Online]. 2010.  
428 cited 16 Feb 2021]. Available from:  
429 <http://www.bioinformatics.babraham.ac.uk/projects/fastqc/>.
- 430 16. Ewels P, Magnusson M, Lundin S, Käller M. MultiQC: summarize analysis results for multiple  
431 tools and samples in a single report. *Bioinformatics*. 2016;32(19):3047-8.
- 432 17. Kim D, Paggi JM, Park C, Bennett C, Salzberg SL. Graph-based genome alignment and genotyping  
433 with HISAT2 and HISAT-genotype. *Nat Biotechnol*. 2019;37(8):907-15.
- 434 18. Raudvere U, Kolberg L, Kuzmin I, Arak T, Adler P, Peterson H, Vilo J. g:Profiler: a web server for  
435 functional enrichment analysis and conversions of gene lists (2019 update). *Nucleic Acids Res*.  
436 2019;47(W1):W191-W8.
- 437 19. Reitmeier S, Kiessling S, Clavel T, List M, Almeida EL, Ghosh TS, Neuhaus K, Grallert H, Linseisen J,  
438 Skurk T, Brandl B, Breuninger TA, Troll M, Rathmann W, Linkohr B, Hauner H, Laudes M, Franke  
439 A, Le Roy CI, Bell JT, Spector T, Baumbach J, O'Toole PW, Peters A, Haller D. Arrhythmic Gut  
440 Microbiome Signatures Predict Risk of Type 2 Diabetes. *Cell Host Microbe*. 2020;28:258–72.
- 441 20. Lagkouvardos I, Klaring K, Heinzmann SS, Platz S, Scholz B, Engel KH, Schmitt-Kopplin P, Haller D,  
442 Rohn S, Skurk T, Clavel T. Gut metabolites and bacterial community networks during a pilot  
443 intervention study with flaxseeds in healthy adult men. *Mol Nutr Food Res*. 2015;59(8):1614-28.
- 444 21. Lagkouvardos I, Joseph D, Kapfhammer M, Giritli S, Horn M, Haller D, Clavel T. IMNGS: A  
445 comprehensive open resource of processed 16S rRNA microbial profiles for ecology and  
446 diversity studies. *Sci Rep*. 2016;6:33721.
- 447 22. Edgar RC. UPARSE: highly accurate OTU sequences from microbial amplicon reads. *Nat Methods*.  
448 2013;10(10):996-8.
- 449 23. Edgar RC, Haas BJ, Clemente JC, Quince C, Knight R. UCHIME improves sensitivity and speed of  
450 chimera detection. *Bioinformatics*. 2011;27(16):2194-200.
- 451 24. Edgar RC. Search and clustering orders of magnitude faster than BLAST. *Bioinformatics*.  
452 2010;26(19):2460-1.
- 453 25. Kopylova E, Noé L, Touzet H. SortMeRNA: fast and accurate filtering of ribosomal RNAs in  
454 metatranscriptomic data. *Bioinformatics*. 2012;28(24):3211-7.
- 455 26. Pruesse E, Peplies J, Glöckner FO. SINA: Accurate high-throughput multiple sequence alignment  
456 of ribosomal RNA genes. *Bioinformatics*. 2012;28(14):1823-9.
- 457 27. Price MN, Dehal PS, Arkin AP. FastTree 2--approximately maximum-likelihood trees for large  
458 alignments. *PLoS One*. 2010;5(3):e9490.

- 459 28. Yoon SH, Ha SM, Kwon S, Lim J, Kim Y, Seo H, Chun J. Introducing EzBioCloud: a taxonomically  
460 united database of 16S rRNA gene sequences and whole-genome assemblies. *Int J Syst Evol*  
461 *Microbiol.* 2017;67(5):1613-7.
- 462 29. Love MI, Huber W, Anders S. Moderated estimation of fold change and dispersion for RNA-seq  
463 data with DESeq2. *Genome Biol.* 2014;15(12):550.
- 464 30. R Core Team. R: A language and environment for statistical computing. Vienna, Austria: R  
465 Foundation for Statistical Computing; 2020.
- 466 31. Omenetti S, Bussi C, Metidji A, Iseppon A, Lee S, Tolaini M, Li Y, Kelly G, Chakravarty P, Shoaie S,  
467 Gutierrez MG, Stockinger B. The Intestine Harbors Functionally Distinct Homeostatic Tissue-  
468 Resident and Inflammatory Th17 Cells. *Immunity.* 2019;51(1):77-89.e6.
- 469 32. Elderman M, Hugenholtz F, Belzer C, Boekschoten M, van Beek A, de Haan B, Savelkoul H, de  
470 Vos P, Faas M. Sex and strain dependent differences in mucosal immunology and microbiota  
471 composition in mice. *Biol Sex Differ.* 2018;9(1):26.
- 472 33. Rosshart SP, Herz J, Vassallo BG, Hunter A, Wall MK, Badger JH, McCulloch JA, Anastasakis DG,  
473 Sarshad AA, Leonardi I, Collins N, Blatter JA, Han SJ, Tamoutounour S, Potapova S, Foster St  
474 Claire MB, Yuan W, Sen SK, Dreier MS, Hild B, Hafner M, Wang D, Iliev ID, Belkaid Y, Trinchieri G,  
475 Rehmann B. Laboratory mice born to wild mice have natural microbiota and model human  
476 immune responses. *Science.* 2019;365(6452).
- 477 34. Linnenbrink M, Wang J, Hardouin EA, Künzel S, Metzler D, Baines JF. The role of biogeography in  
478 shaping diversity of the intestinal microbiota in house mice. *Molecular Ecology.*  
479 2013;22(7):1904-16.
- 480 35. Moyaert H, Pasmans F, Decostere A, Ducatelle R, Haesebrouck F. *Helicobacter equorum*:  
481 prevalence and significance for horses and humans. *FEMS Immunology & Medical Microbiology.*  
482 2009;57(1):14-6.
- 483 36. Johansson MEV, Phillipson M, Petersson J, Velcich A, Holm L, Hansson GC. The inner of the two  
484 Muc2 mucin-dependent mucus layers in colon is devoid of bacteria. *Proc Natl Acad Sci U S A.*  
485 2008;105(39):15064-9.
- 486 37. Johansson ME, Thomsson KA, Hansson GC. Proteomic analyses of the two mucus layers of the  
487 colon barrier reveal that their main component, the Muc2 mucin, is strongly bound to the Fcgbp  
488 protein. *J Proteome Res.* 2009;8(7):3549-57.
- 489 38. Fernández-Blanco JA, Fakh D, Arike L, Rodríguez-Piñeiro AM, Martínez-Abad B, Skansebo E,  
490 Jackson S, Root J, Singh D, McCrae C, Evans CM, Åstrand A, Ermund A, Hansson GC. Attached  
491 stratified mucus separates bacteria from the epithelial cells in COPD lungs. *JCI Insight.*  
492 2018;3(17).
- 493 39. Ehrencrona E, van der Post S, Gallego P, Recktenwald CV, Rodriguez-Pineiro AM, Garcia-Bonete  
494 M-J, Trillo-Muyo S, Bäckström M, Hansson GC, Johansson MEV. The IgGfC-binding protein  
495 FCGBP is secreted with all GDPH sequences cleaved but maintained by interfragment disulfide  
496 bonds. *J Biol Chem.* 2021;297(1):100871.
- 497 40. Nyström EEL, Martinez-Abad B, Arike L, Birchenough GMH, Nonnecke EB, Castillo PA, Svensson  
498 F, Bevins CL, Hansson GC, Johansson MEV. An intercrypt subpopulation of goblet cells is  
499 essential for colonic mucus barrier function. *Science.* 2021;372(6539):eabb1590.
- 500 41. Nyström EEL, Arike L, Ehrencrona E, Hansson GC, Johansson MEV. Calcium-activated chloride  
501 channel regulator 1 (CLCA1) forms non-covalent oligomers in colonic mucus and has mucin 2-  
502 processing properties. *J Biol Chem.* 2019;294(45):17075-89.
- 503 42. Almalki F, Nonnecke EB, Castillo PA, Bevin-Holder A, Ullrich KK, Lönnnerdal B, Odenthal-Hesse L,  
504 Bevins CL, Hollox EJ. Extensive variation in the intelectin gene family in laboratory and wild  
505 mouse strains. *Sci Rep.* 2021;11(1):15548.

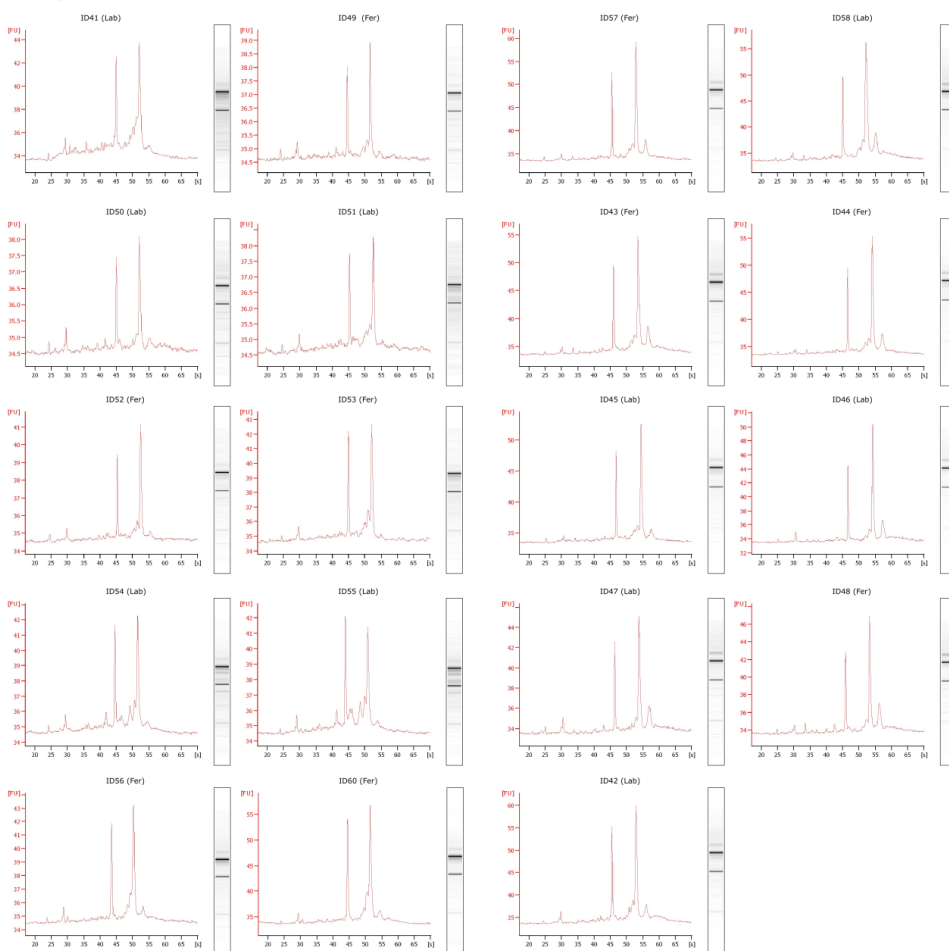


- 506 43. Nonnecke EB, Castillo PA, Dugan AE, Almalki F, Underwood MA, De La Motte CA, Yuan W, Lu W,  
507 Shen B, Johansson MEV, Kiessling LL, Hollox EJ, Lönnerdal B, Bevins CL. Human intelectin-1  
508 (ITLN1) genetic variation and intestinal expression. *Sci Rep.* 2021;11(1):12889.
- 509 44. Bergström JH, Birchenough GM, Katona G, Schroeder BO, Schütte A, Ermund A, Johansson ME,  
510 Hansson GC. Gram-positive bacteria are held at a distance in the colon mucus by the lectin-like  
511 protein ZG16. *Proc Natl Acad Sci U S A.* 2016;113(48):13833-8.
- 512 45. Tsuchiya K. Switching from Apoptosis to Pyroptosis: Gasdermin-Elicited Inflammation and  
513 Antitumor Immunity. *Int J Mol Sci.* 2021;22(1).
- 514 46. Hou J, Zhao R, Xia W, Chang C-W, You Y, Hsu J-M, Nie L, Chen Y, Wang Y-C, Liu C, Wang W-J, Wu  
515 Y, Ke B, Hsu JL, Huang K, Ye Z, Yang Y, Xia X, Li Y, Li C-W, Shao B, Tainer JA, Hung M-C. PD-L1-  
516 mediated gasdermin C expression switches apoptosis to pyroptosis in cancer cells and facilitates  
517 tumour necrosis. *Nature Cell Biology.* 2020;22(10):1264-75.
- 518 47. Xi R, Montague J, Lin X, Lu C, Lei W, Tanaka K, Zhang YV, Xu X, Zheng X, Zhou X, Urban JF,  
519 Iwatsuki K, Margolske RF, Matsumoto I, Tizzano M, Li J, Jiang P. Up-regulation of gasdermin C in  
520 mouse small intestine is associated with lytic cell death in enterocytes in worm-induced type 2  
521 immunity. *Proc Natl Acad Sci U S A.* 2021;118(30):e2026307118.
- 522 48. Kuriakose T, Kanneganti TD. ZBP1: Innate Sensor Regulating Cell Death and Inflammation.  
523 *Trends Immunol.* 2018;39(2):123-34.

524

## 525 SUPPLEMENTARY MATERIAL

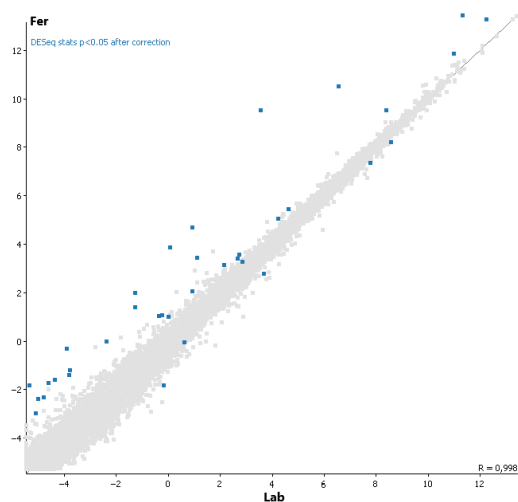
Electropherogram Summary



526

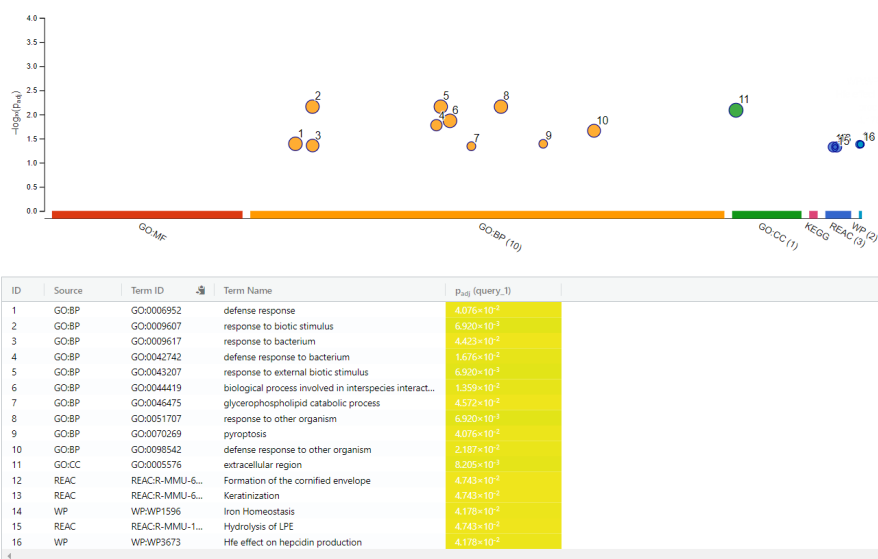
527 **Figure S1.** Electropherogram summary for samples subjected to RNA sequencing.

528



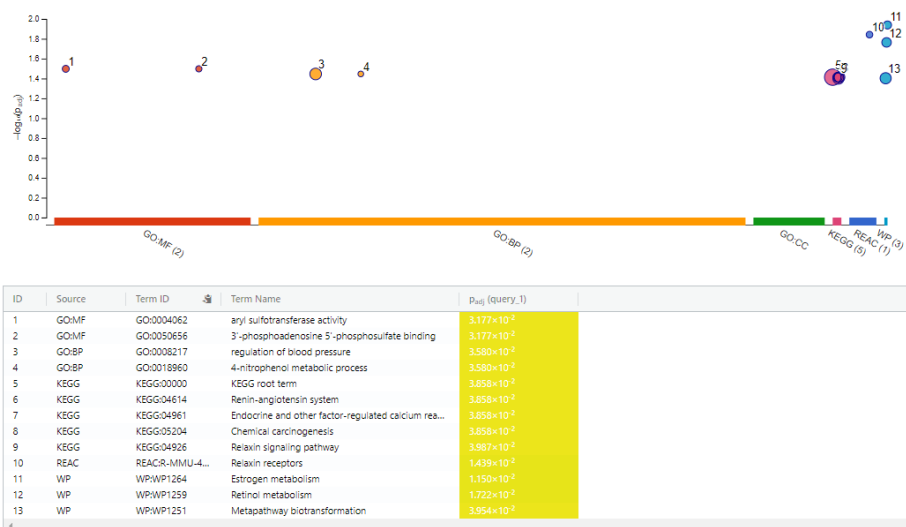
529  
 530 **Figure S2.** Scatterplot of relative expression levels as log<sub>2</sub> scale RPKM (reads per kilobase transcript per  
 531 million mapped reads) in Fer and Lab mice. Genes significantly up/down-regulated between the two  
 532 groups are highlighted in blue (DESeq2 test with FDR cutoff of 0.05).

533



534  
 535 **Figure S3.** Manhattan plot of the significantly enriched gene function annotations from the indicated  
 536 databases (cutoff  $P < 0.05$ ) for the genes significantly upregulated in Fer against a custom list of expressed  
 537 genes. See also Supplementary Table S2. GO: Gene Ontology, MF: Molecular Function, BP: Biological  
 538 Process, CC: Cellular Component, KEGG: KEGG Pathway, REAC: Reactome, WP: WikiPathways.

539



540

541 **Figure S4.** Manhattan plot of the significantly enriched gene function annotations from the indicated  
 542 databases (cutoff  $P < 0.05$ ) for the genes significantly upregulated in Lab against a custom list of  
 543 expressed genes. See also Supplementary Table S3. GO: Gene Ontology, MF: Molecular Function, BP:  
 544 Biological Process, CC: Cellular Component, KEGG: KEGG Pathway, REAC: Reactome, WP:  
 545 WikiPathways.

546

547 **Supplementary Table S1.** Total number of reads and overall results from alignment to the mouse  
 548 reference genome GRCm38.p6 by use of HISAT2.

Sample	Group	Total # reads	Unpaired reads	Aligned 0 times	Aligned exactly 1 time	Aligned >1 times	Overall alignment rate
1	Lab	49330089	49330089	1420377	38860131	9049581	97.12 %
2	Lab	46394358	46394358	1192355	37458804	7743199	97.43 %
3	Fer	45316186	45316186	869665	36788546	7657975	98.08 %
4	Fer	57191455	57191455	1228596	46636326	9326533	97.85 %
5	Lab	58635434	58635434	1736077	46486755	10412602	97.04 %
6	Lab	63742588	63742588	1519754	51942168	10280666	97.62 %
7	Lab	45500650	45500650	1087493	37093515	7319642	97.61 %
8	Fer	52698880	52698880	1246776	41931132	9520972	97.63 %
9	Fer	43487149	43487149	1095474	33847968	8543707	97.48 %
10	Lab	54730333	54730333	1607576	41514658	11608099	97.06 %
11	Lab	84939759	84939759	1858172	68071185	15010402	97.81 %
12	Fer	39092586	39092586	965914	32073569	6053103	97.53 %
13	Fer	57072934	57072934	1755611	45311472	10005851	96.92 %
14	Lab	48651763	48651763	1599099	38617720	8434944	96.71 %
15	Lab	87826915	87826915	2244022	69667739	15915154	97.44 %
16	Fer	55516274	55516274	1789777	43309845	10416652	96.78 %
17	Fer	45773292	45773292	1141916	36277936	8353440	97.51 %
18	Lab	48149835	48149835	1155817	38909424	8084594	97.60 %
20	Fer	45764994	45764994	1102933	37093133	7568928	97.59 %

549

550 **Supplementary Table S2.** Functional enrichment analysis of genes significantly upregulated in the Fer  
 551 group (xlsx). Available upon request.

552 **Supplementary Table S3.** Functional enrichment analysis of genes significantly upregulated in the Lab  
 553 group (xlsx). Available upon request.

554

ISBN: 978-82-575-1874-5

ISSN: 1894-6402



Norwegian University  
of Life Sciences

Postboks 5003  
NO-1432 Ås, Norway  
+47 67 23 00 00  
[www.nmbu.no](http://www.nmbu.no)